6-1-2016

Development of honey/chitosan nanofibrous scaffolds loaded with natural materials and bacteriophage: Evaluation of their antimicrobial and wound healing activities.

Wesam Awad Sarhan

THE AMERICAN UNIVERSITY IN CAIRO
الجامعة الأمريكية بالقاهرة

The American University in Cairo
School of Sciences and Engineering

Development of Honey/Chitosan Nanofibrous Scaffolds Loaded with Natural Materials and Bacteriophage: Evaluation of their Antimicrobial and Wound Healing Activities.

A Dissertation Submitted to

The Nanotechnology Graduate Program

in partial fulfillment of the requirements for
the degree of Doctor of Philosophy

By Wesam A. Sarhan

Under the supervision of
Prof. Hassan M. E. Azzazy

Spring 2016

To My Parents, Awad & Asmaa

To My Husband, Wael

To My Sons, Omar, Adam & Youssef

To my sister & brother, Basma & Ahmed

You Are my Heaven on Earth.

ACKNOWLEDGEMENTS

First and foremost I would like to thank Allah for His guidance, love, and support in every step of my life, for being always there, for lifting me up throughout my weakness, for guiding me throughout my hesitations and for giving me strength to go on throughout the difficulties.

I would like to express my sincere gratitude to my advisor Prof. Hassan Azazzy for his continuous support throughout my PhD, for giving me the freedom to explore on my own and at the same time the guidance when I lose the way. Dr. Azzazy has taught me the true meanings of hard work, accuracy and innovation and inspired me to dream big, take difficult challenges and work for them.

I would like to extend my thanks to my advisory committee: Prof. Adham Ramadan and Prof. Tarek Madkour for being always supportive, encouraging and helpful throughout the different steps of my PhD.

My deepest thanks is extended to Prof. Ibrahim Elsherbiny for giving me the opportunity to work in his labs at Zewil City for Science and Technology and for his encouraging comments and continuous support to me.

My deepest gratitude is also extended to Mr. Youssef Jameel, for it was because of the support I received through the Youssef Jameel fellowship, that I was able to complete my PhD and dedicate my full time to my PhD research.

My deepest thanks is extended to my friends Walaa Wahbi, Sara Omar, Israa Hussien, Asmaa Gamal, and Huda Makki for being always there, for their care, love and support and for making my PhD journey the most joyful one.

I would also like to thank my family for their continuous support, encouragement, and believe in me. Special thanks to: my parents, Awad Sarhan and Asmaa Elsherbiny, my mother in law, Fatma Elsherbiny and my sister, Basma Awad for each of them has helped me in every possible way to allow me to fulfill my goals and achieve my PhD.

No words could ever express my gratitude to: my husband, Wael Mansy and my sons, Omar, Adam and Youssef for enduring me through these past few years and allowing me to reach my goals through their overwhelming love and support.

Finally, I recognize that this research would not have been possible without the nurturing, friendly, inspiring and supportive environment of the American University in Cairo (AUC) as well as its highly advanced facilities, well equipped labs and its highly qualified staff members.

ABSTRACT

The American University in Cairo

Development of Honey/Chitosan Nanofibrous Scaffolds Loaded with Natural Materials and Bacteriophages: Evaluation of their Antimicrobial and Wound Healing Activities.

BY: Wesam Awad Ahmed Sarhan
Under the Supervision of Prof. Hassan M.E. Azzazy

Non-healing wounds represent a serious health care burden with major socioeconomic impacts. Bacterial infection of the wound site further complicates the healing process as it stimulates the immune system which in turn prolongs tissue inflammation thus further delaying the healing process. Moreover, wound associated bacterial contamination usually develops resistance to commonly used antibacterials leading to increased risk of systemic infections. Treatment of infected wounds is being achieved via different kinds of dressings in association with antibacterials, antiseptics and wound healing materials. Currently, however there has been a noticeable shift towards advanced antimicrobial wound care as a possible solution for the problem. Advanced antimicrobial wound care are dressings that can be loaded with either antibiotics or antiseptics and are able to reduce or eliminate the bacterial load at the wound site. However, one of the major challenges associated with such dressings is the continuous emergence of antibiotic resistant strains as well as the observed damage of healthy tissues in case of antiseptics. Moreover, it has been argued that the antimicrobial efficacy alone of an advanced dressing is insufficient and other properties that enhance the wound healing process are also required. To help provide a solution for this challenge, this study aims to investigate the development of a novel series of advanced antimicrobial wound dressings that are based on honey and chitosan and fabricated in the nanofibrous form. Honey and chitosan are well known for their wound healing and antibacterial properties. Moreover, developing the dressings in the nanofibrous structure allows enhancement of the wound healing process. Electrospinning technique was adopted to fabricate novel nanofibrous wound dressings based on high honey and chitosan concentrations (HPCS). Natural extracts namely: *Cleome droserifolia* (CE) and *Allium sativum* (AE) and apitherapeutics namely: bee venom (BV) and propolis (Pr) as well as bacteriophages (PS1) were loaded within the fabricated honey chitosan based nanofibrous dressings to enhance their antibacterial activity and extend it against resistant bacterial strains as well as increase their wound healing abilities. The fabricated series of nanofibrous dressings, HPCS, HPCS-AE, HPCS-CE, HPCS-AE/CE, HPCS-BV, HPCS-Pr and HPCS-BV/PS1 demonstrated enhanced wound healing abilities and variable antibacterial effects against the examined bacterial strains as compared to the commercial wound dressing Aquacel Ag. Most importantly, the developed series of nanofibrous dressings demonstrated enhanced biocompatibility as compared to the Aquacel Ag that demonstrated noticeable cytotoxicity. Thus, the developed series of nanofibrous wound dressings that are based on natural materials represent competitive candidates to be used as effective wound dressings.

TABLE OF CONTENTS

LIST OF ABBREVIATIONS

AE: Allium sativum aqueous extract

BV: Bee venom

CE: Cleome droserifolia aqueous extract

CS: Chitosan

ECM: Extracellular matrix

FTIR: Fourier Transform Infra-Red Spectroscopy

GA: Glutraldehyde

H: Honey

P: PVA

Pr: Propolis

SEM: Scanning Electron Microscopy

TEM: Transmission Electron Microscopy

TGA: Thermogravimetric analysis

XRD: X-Ray Diffraction

LIST OF TABLES

LIST OF FIGURES

1. BACKGROUND AND LITERATURE REVIEW

1.1Wounds; Serious Health Care Burden

Non-healing wounds represent a significant health care burden with a major socioeconomic impact of over $25 billion as the cost of complicated and delayed wound healing (Sen et al., 2009). That is in addition to the mortality and morbidity risk posed to mankind due to chronic wound complications (Kirketerp-Møller et al., 2011). Chronic non-healing wounds are those that do not follow the normal physiological process in healing staying opened for several weeks reaching to months. The most commonly encountered chronic wounds include diabetic foot ulcers, arterial leg ulcers, pressure ulcers, venous leg ulcers and burns (Siddiqui & Bernstein, 2010). Pressure ulcers were found to affect nearly one-third of the population undergoing treatment in a critical care unit with an annual total treatment cost reaching to $11 billion in the United States. Moreover, $2.3–$3.6 billion are spent by the National Health Service (NHS) for the treatment of pressure ulcers and the cost per each case of pressure ulcer treatment ranges from $5,000 to $65,000 per case. Diabetic foot ulcers which are a leading cause of foot amputations, are considered among the most commonly encountered complications with diabetes affecting nearly 15% of the diabetic population. The prevalence of diabetes is expected to reach 333 million by 2025, from which 10% are expected to suffer from diabetic ulcers according to the International Diabetes Federation. Diabetic foot ulcers are considered one of the most serious chronic wounds leading to major socioeconomic implications as it takes about 12 to 14 weeks for a diabetic wound to heal. It was concluded from a recent study conducted in Sweden that the costs per case for the treatment of diabetic foot-ulcer associated complications range from $16,500 for patients suffering from severely impaired circulations to nearly $63,000 with patients undergoing amputation (Abrigo et al., 2014).

Healing of normal or acute wounds proceeds via a series of physiological phases that end up in functional and anatomic skin restoration (Figure 1). Normally, the wound healing process follows four distinct phases: hemostasis, inflammation, proliferation and tissue remodeling (Werner & Gorse, 2003). The hemostasis phase involves an immediate vascular and cellular response to the disruption of the skin surface. The arterial vessels constrict rapidly under the effect of various vasoactive mediators (norepinephrine, epinephrine, prostaglandins, serotonin and thromboxane)

which lead to hypoxia and acidosis. Moreover, the exposed sub endothelium activates the aggregation of the platelets leading to clot formation. Platelet aggregation results in their activation which enables them to release growth and chemotactic factors as proteases, platelet-derived growth factor (PDGF) and other vasoactive agents (eg, histamine, serotonin). Consequently, this mediates a reflex vasodilation and increase in the vascular permeability which facilitates the entrance of the inflammatory cells and the beginning of the inflammatory phase in the healing process (Hunt, 1988). The cellular components of the inflammatory phase include macrophages, lymphocytes and neutrophils. Neutropills are the predominant cell type at the beginning of the inflammatory phase, and while it is not essential to the wound healing process, its importance originates in its ability to cleanse the wound site from bacteria and necrotic matter. Macrophages on the other hand, are essential components in the early phase of the process of wound healing as they phagocytose bacteria and debris and release elastases, collagenases and PDGF which stimulates proliferation and chemotaxis of fibroblasts and cells of the smooth muscle. Additionally, macrophages produce substances that attract endothelial cells and stimulate their proliferation at the wound site to mediate angiogenesis. T lymphocytes play an important role in production of antibodies as well as cellular immunity (Broughton et al., 2006).

The proliferation phase involves the formation of granulation tissue which includes fibroblasts, neovascular and inflammatory cells within a matrix of collagen, fibronectin, proteoglycans and glycosaminoglycans. Additionally, the proliferation phase involves epithelization, fibroplasia, angiogenesis and contraction. Epithelialization involves the formation of epithelium which acts as a seal between the environment and the wound. Moreover, the epidermal cells secrete collagenases which stimulate plasmin production that promotes the dissolution of the clot. Migrating epithelial cells promote the keratinocyte adhesion in order to guide such cells across the base of the wound. In the fibroplasia phase, fibroblast and mesenchymal cells differentiate, moreover fibroblasts produce collagen, fibronectin, elastin, proteases and glycosaminoglycans. Fibroblasts grow and proliferate with the reduction in the number of inflammatory cells. Angiogenesis which is promoted via the endothelial growth factor basic fibroblast growth factor, is important to sustain a blood supply to the formed tissue, which in turn lead to increased perfusion of various healing factors. As a final step in the proliferative phase the wound edge contract facilitating the closure of the skin defect at the wound site (Kirsner & Eaglstein, 1993).

Tissue remodeling represents the final phase of the wound healing process, during which collagen undergoes increased organization. This proceeds via gradual disappearance of fibronectin and replacement of hyaluronic acid and glycosaminoglycans with proteoglycans. Type I collagen replaces type III collagen and water resorbtion occurs from the scar. This allows collagen crosslinking and decreasing the thickness of the scar (Hunt, 1988).

Both acute and chronic wounds pass through the previously demonstrated phases, however chronic wounds exhibit delayed healing. In chronic wounds the normal series of physiological processes involved in healing is interrupted by the presence of persistent inflammatory stimuli. Such inflammatory stimuli result in increased production of metalloproteinases (MMPs) which lead to degradation of the extracellular matrix which in turn decreases the migration of cells and reduce the deposition of new connective tissue. Most importantly, such MMPs lead to the degradation of the growth factors, such growth factors that are essential and very important mediators for the normal series of mechanisms that are involved in all phases of the wound healing process. Thus, eventually leading to the disruption of the wound healing process (Bjarnsholt et al., 2008; Chen et al., 1999). This problem is overcomplicated by the increased level of contamination of chronic wounds by different kinds of bacteria. Such bacterial infection stimulates the immune system which in turn prolongs tissue inflammation thus further delaying the healing process. Moreover, chronic wound associated bacterial infection usually develops resistance to commonly used antibacterials showing great difficulty and resistance to be treated with common antibiotics and antibacterials, thus, leading to increased risk of systemic infections (James et al., 2008)

A bacterial wound infection demonstrates various clinical symptoms that include edema, pain, erythema and purulent exudates (Robson et al., 1990). The quantity of bacteria at the wound site has been correlated to infection, where it has been suggested that bacterial counts of more than 10^5 CFU/g may be indicative of infection at the wound site. However, this varies according to the type of the organism, its virulence and pathogenicity, as well as the interaction of the organism with the surrounding microflora and the hosts' immune response (Bowler, 2003). Generally, the wound microbiology could be described in different phases: contamination, colonization and infection which could spread and lead to invasive infection and septicemia (Figure 2). Contamination of the wound site means presence of bacteria that are not replicating, whereas, colonization is the presence of bacteria that are replicating at the wound site without associated tissue damage. An

infected wound is often associated with clinical signs of infection as well as tissue damage (Edwards & Harding, 2004). Therefore, wound infection results in delay in the process of wound healing.

Different kinds of bacteria are involved in the process of wound healing, and they may be present at the wound site either as single bacterial species or as a polymicrobial load of two or more bacterial species. It was observed that the most common bacterial isolates were *Staphylococcus aureus, Pseudomonas aeruginosa, Escherichia coli,* Corynebacterium spp and *Proteus mirabilis*. Whereas, the most common species that are found in a polymicrobial infection were S. *aureus,* P. *mirabilis,* and *P. aeruginosa* with the most predominant associated combination between *S. aureus/P. aeruginosa* (Bessa et al., 2015).

It was reported that *Staphylococcus aureus* was the most common Gram positive bacteria (40-60% of the total load of bacteria) isolated from variable kinds of wounds (Bowler, 2003; Brook & Frazier, 1998; Gjødsbølet al., 2006; Davies et al., 2004; Urbancic-Rovan et al., 2000; Korber et al., 2010). Whereas, *P. aeruginosa* was the most predominant Gram negative isolate (Gjødsbøl et al., 2006; Davies et al., 2004; Halbert, 1992; Madsen, 1996; Burmølle, 2010). It has been observed that both *P. aeruginosa* and *S.aureus* produce destructive virulence factors that were found responsible for infection prolongation and delay in the wound healing process (Bessa et al., 2015). The production of different virulence factors as clumping-factor A, coagulase, leuocidines and catalase by *S.aureus* has been linked to clinically significant wound infections (Dissemond, 2009). Similarly, *P.aerugionsa* elastase has been linked to its pathogenicity at the wound site (Schmidtchen, 2003). Additionally, it was observed that a relevant percentage of the isolated *S.aureus* (Bessa et al., 2015) were methicillin resistant *S.aureus* (MRAS), and that MRSA is becoming a more prevalent wound pathogen (Demling & Waterhouse, 2007) thus further complicating the problem of an infected wound. This is because a chronic wound infected with MRSA represents a source of a resistant nosocomial infection, additionally the presence of MRSA in a wound increases the risk further complication of the wound infection to septicemia (Demling & Waterhouse, 2007).

Thus, the success in managing bacteria in wounds is of outmost importance. Generally, treatment of chronic wound infections is achieved via antimicrobial therapeutics either systemic or topical (Lipsky & Hoey, 2009). It was observed that > 60% of chronic wound patients received antibiotic

treatments for a long periods of time (Howell-Jones et al., 2005; Tammelin et al., 1998). Although antibiotic therapy revolutionized wound care, the increased and continuous emergence of resistant bacterial strains together with the marked decrease in the discovery of new antibiotics has necessitated the need to discover alternative antimicrobials (Cooper, 2004). Thus, the use of topical antiseptic treatments has increased leading to reduction of antibiotic use in chronic wound treatments. The commonly used wound dressings in the treatment of chronic wound infections are traditional gauzes and bandages which are considered the most primitive and simple kinds of dressings that generally work only on achieving wound protection from trauma and bacterial contamination. Such traditional dressings are usually used in chronic wounds in association with other antibacterials, antiseptics and wound healing materials. Currently, chronic wound treatment is witnessing an increasing shift towards advanced wound dressings. Advanced wound dressings, are dressings that aid and accelerate the wound healing process via exudate management, the ability to control infections and providing essential growth factors that enhance the healing process (Frost & Sullivan, 2014).

Among the advanced wound dressings, antimicrobial wound dressings stand as an important sector that is most beneficial in the treatment of chronic wound infections (Abrigo et al., 2014). Such antimicrobial advanced wound dressings allow the sustained release of the loaded antimicrobials thus allowing the realization of their antibacterial activity while maintaining a healthy concentration to the healing tissues (Vowden et al., 2011).

The most commonly available antimicrobial wound dressings are dressings loaded with antiseptics such as, as silver and iodine. Silver-based dressings stand as one of the most common and effective antimicrobial dressings used. However, despite their enhanced broad spectrum of activity, development of resistance has unfortunately been reported together with some undesirable side effects of silver (Lansdown, 2002). Thus, research into development of effective antimicrobial wound dressings based on effective antimicrobials that are more biocompatible and able to be effective against resistant bacterial strains is of great necessity.

Among the advanced wound dressings nanofibrous advanced wound dressings stand as an important emerging sector (Zahedi et al., 2010). Nanofibrous based dressings allow pronounced wound healing ability as compared to other traditional dressings due to the high surface to volume ratio, morphological resemblance to the extracellular matrix (ECM) in the skin and thus promoting

cell adhesion, proliferation, and migration. Additionally, nanofibrous dressings exhibit haemostasis capability and increased ability to absorb exudates as well as enhanced cell respiration due to high porosity. Most importantly, nanofibrous based dressings are easily loaded with different materials as extracts, drugs, antiseptics or others thus allowing enhancement of their wound healing and antibacterial abilities (Zahedi et al., 2010; Zhang et al., 2005; Kanani & Bahrami, 2010).

1.2 Electrospun Nanofibers; Emerging Advanced Wound Dressings.

Nanofibers are a class of nanobased materials with different and broad applications in different fields including environmental engineering, optical electronics, nanocatalysis, defense and security as well as pharmaceutical and biomedical applications. Nanofibers demonstrate multiple advantages that allowed it to be of great interest in different applications. Nanofibers exhibit increased surface to volume ratio, increased porosity, in addition to the ease of fabrication of the nanofibers from multiple polymers either natural, synthetic or combination of both and the feasibility of loading the nanofibers with different materials alone or in combinations (Cui et al., 2006; Ramakrishna et al., 2006; Luu et al., 2003; Welle et al., 2007; Subbiah et al., 2005).

Electrospinning represents a facile, cost effective and versatile technique for fabrication of nanofibers compared to other nanofiber fabrication techniques (i.e. phase separation or self-assembly). In the electrospinning process, the polymeric solution is contained in a capillary, subsequently a droplet of the polymer solution forms at the capillary tip under a certain flow rate. A high voltage is then applied to the polymeric droplet and the droplet gets electrified leading to accumulation of charge at the droplet surface. At a certain applied voltage the electrostatic forces are able to overcome the polymeric solutions' surface tension and the accumulated charge at the droplet surface causing the deformation of the formed droplet into a cone (Taylor cone), from which an ultrafine polymer jet is produced from the tip. The polymeric solutions' charged jets travel towards the used collector and the solvent evaporates rapidly followed by the collection of ultra-fine dry fibers on the collector (Altstädt et al., 2008).The morphology of the collected fibers can be controlled via the adjustment of the different parameters of the electrospinning process (Teo & Ramakrishna., 2006). A detailed illustration of the electrospinning process as well as the different parameters affecting the fabricated nanofibers was provided via Bhardwaj and Kundu (Bhardwaj & Kundu., 2010). The basic setup for the electrospinner is shown in figure 3, whereas,

Sahay et al and Migliaresi et al provided a detailed review for more complex electrospinner set-ups (Sahay et al., 2011 & Migliaresi et al., 2012).

Currently, one of the main drivers in the wound dressing field is developing wound dressings in the nanofibrous form (Zhang et al., 2005). Nanofibrous wound dressings exhibit a number of intrinsic properties that make them of particular interest in wound healing applications. An ideal wound dressing should be capable of mimicking the natural extra-cellular matrix (ECM). The ECM is non-cellualar constituent present in all tissues, during wound healing it acts as a scaffold that allow cell attachment, differentiation and proliferation (Martins et al., 2007). Nanofibers due to their nanometer size in addition to their random alignment within the nanofibrous mesh mimic the architecture of the ECM. Thus, wound dressings in the nanofibrous form provide the cells with an artificial ECM (Figure 4) promoting healing by encouraging tissue growth and leading to reduction in scar tissue formation as well as the required time for healing (Bhattarai et al., 2005). Moreover, the nano-pore sizes also assist in protecting injured tissues from bacteria and the high porosity and surface area enhance the absorption of fluids and the hemostasis. The nanofibrous mats exhibit high interconnected porosity (60-90%) (Kanani & Bahrami, 2010) thus, allowing high-gas permeation and cell respiration which prevent the dehydration of wounds (Zhang et al., 2005). The high surface area provided by the nanofibrous structure enhance the delivery of wound healing and antimicrobial agents, thus, eventually encourages wound healing (Diegelmann & Evans, 2004; Bhardwaj & Kundu, 2010).

Electrospun nanofibers for wound healing applications have been fabricated from synthetic and natural polymers as well as combinations of both of them (Zahedi et al., 2010). Synthetic polymers facilitate the process of electrospinning and enhance the mechanical properties of the developed nanofibrous mats, whereas, natural polymers increase the biocompatibility of the resulting nanofibrous mats and enhance the ability of the nanofibers to interact with the biomolecules that are involved in the wound healing process (Gunn & Zhang, 2010).

Initially, research involving development of nanofibrous wound dressings focused on optimizing the parameters of the process of electrospinning for fabrication of wound dressings with suitable mechanical, morphological and physico-chemical properties for providing dressings with suitable barrier properties that allow tissue protection and maintain the moisture level of the wound bed, such dressings that were referred to as passive dressings according to Abrigo et al (Abrigo et al.,

2014). Within this context, different types of nanofibers were fabricated from poly (urethane) (Khil et al., 2003), poly (vinyl alchol) (Phachamud & Phiriyawirut, 2011) and hyaluronic acid (Uppal et al., 2011), and both the morphological characterization and the invivo testing demonstrated their potential application as wound dressings. The hyaluronic acid nanofibers were proved to be more beneficial in treating full thickness wounds as compared to commercial wound dressings (Uppal et al., 2011).

More recent developments in nanofibrous wound dressing research involved development of nanofibrous dressings that are capable of accelerating the wound healing process and treating or preventing bacterial infection. Abrigo et al., referred to such dressings as interactive dressings that are able to combine the optimal physical and morphological requirements needed for wound healing and the value-added ability to limit the proliferation of bacteria and address the optimal environment for cell proliferation and migration (Abrigo et al., 2014). Such dressings were achieved via developing the nanofibrous wound dressings from a combination of polymers of synthetic origin and biopolymers that have antibacterial ability and enhanced affinity towards the wound environment. A wide variety of reports could be found in literature addressing the use of synthetic and natural combinations in the fabrication of nanofibrous wound dressings. Kim et al, developed nanofibrous meshes from a combination of polyurethane and gelatin that demonstrated their potential effectiveness as wound dressings (Kim et al., 2009). Similarly, nanofibrous meshes from keratin and poly (hydroxybutylate-co-hydroxyvalerate) have been fabricated and were proved to enhance the process of wound healing (Yuan et al., 2015). Cheng et al., developed nanofibrous mats from the combination of poly (ethylene oxide), type I collagen and chitosan. Such dressings demonstrated enhanced wound healing ability invivo compared to traditional wound dressings (Chen et al., 2008). Additionally, different reports demonstrated fabrication of nanofibrous meshes as potential wound dressings from combinations of synthetic polymers and natural materials as honey, natural extracts and essential oils (Jin et al., 2013). Further development within the nanofibrous wound dressing research involves loading of such interactive dressings with antimicrobials, drugs and wound healing agents to further enhance the wound healing and antibacterial properties of the developed wound dressings, such dressings that were referred to as advanced interactive wound dressings (Abrigo et al., 2014) were reported in a detailed review via Meinel et al., (Meinel et al., 2012). Despite that advanced interactive wound dressings are able to control bacterial infection at the wound bed, initial burst release of the loaded antibiotics and drugs

causes toxic effects to the healing tissue (Sill & von Recum, 2008; Agarwal et al., 2008). Thus, development of advanced interactive wound dressings that demonstrate no toxic effects to the healing tissues as well as enhanced antimicrobial and wound healing ability is of great demand.

1.3 Honey and Chitosan; Powerful Wound Dressing Materials

Honey and chitosan, two natural materials that possess a variety of favorable effects and exhibit particular importance in pharmaceutical and medical applications. Chitosan [(1–4)-linked 2-amino-2-deoxy-D-glucopyranose], is a natural polymer that is derived from chitin which is considered as one of the most abundant polysaccharides found in nature (Ohkawa et al., 2004; Prashanth & Tharanathan, 2007; Sun & Li, 2011). Chitosan is a biocompatible, biodegradable polymer with wound healing and antibacterial capabilities (Schiffman & Schauer, 2007), that's in addition to its ability to promote tissue regeneration and help achieve hemostasis (Zhou et al., 2007). Such properties allowed chitosan to be the ideal polymer in different fields and industrial applications (Schiffman, & Schauer, 2007) as food (Tripathi et al., 2009), paper coatings (Vartiainen et al., 2004), textiles (Lim & Hudson, 2003), ophthalmology (Alonso & Sánchez, 2003), agriculture (Hanshou et al., 2000) as well as different biomedical applications (Jayakumar et al., 2010). Thus, numerous studies have electrospun chitosan into fibers with diameter of ~100 nm (Zhou et al., 2007). However, the main drawback with such fibers was the inability to electrospin chitosan from its aqueous solution because of its high viscosity in addition to the strong hydrogen bonds forming in 3D networks and thus preventing the movement of the polymeric chains of chitosan under the influence of the electrical field (Homayoni et al., 2009; Zhou et al., 2007). Such a character that forced either the use of toxic solvents to allow spinning of chitosan in considerable high concentrations reaching to 7% (Geng et al., 2005) upon using (90%) concentrated acetic acid, or reaching 3% upon using trifloroacetic acid and dichloromethane (Ohkawa et al., 2004). Residues of such solvents are not favorable especially in applications where totally biocompatible material is required as drug delivery, wound dressings and tissue engineering. To decrease the toxicity of the solvents (Charernsriwilaiwat et al. 2010, Charernsriwilaiwat et al., 2011) prepared chitosan in aqueous salt as CS–hydroxybenzotriazole

/PVA and CS–ethylenediaminetetraacetic acid /PVA, however the amount of incorporated chitosan did not exceed 1%.

Another approach for spinning chitosan was through co-spinning with other easily spun polymers in more biocompatible solvents. Among them, the composite Poly (vinyl alcohol)/chitosan has received great scientific interest either alone (Chuang et al., 1999; Paipitak et al., 2011; Zhang et al., 2007) or loaded/mixed with different materials to alter their characters to be suitable for different applications (Liao et al., 2011; Yan et al., 2012). Still such approach did not allow spinning of high chitosan concentrations.

Chitosan nanofibrous mats have demonstrated enhanced antibacterial and wound healing effects via different studies. Chen et al., demonstrated that electrospun chitosan, collagen type I and poly(ethylene oxide) nanofibrous mats exhibited enhanced wound healing activity as compared to traditional dressings (Chen et al., 2008). Spasova et al. utilized chitosan for coating poly(L-lactide) and composite poly L lactic acid/poly(ethylene glycol) nanofibrous mats which resulted in enhanced antibacterial activity against *S.aureus* and well observed hemostatic ability, thus demonstrating the developed nanofibrous mats as possible wound dressings (Spasova et al., 2008). Chitosan has also been electrospun with silk fibroin and presented a possible candidate for wound dressing due to the demonstrated antibacterial effects and the ability of the developed nanofibrous mat to enhance fibroblast proliferation (Cai et al., 2010). Chitosan is commonly chosen for fabrication of nanofibrous wound dressings because it accelerates the wound healing process via its activation to the polymorphonuclear cells, its hemostatic and antibacterial abilities, in addition to its ability to promote fibroblast proliferation (Li et al., 2012; Chen et al., 2008; Duan et al., 2006). .

Honey is another natural material of striking medical importance that has always played an important role in traditional medicine and is now seriously witnessing a revival in modern care medicine.

Honey is a viscous hypersaturated sugar liquid mainly composed of fructose and glucose in addition to other compounds, especially phenolic compounds. Honey is a natural source of micro- and macro-nutrients with profound medicinal and nutritional properties (Khan et al., 2007). Honeys' composition varies according to the floral source, season as well as other environmental factors. Honey exhibits anti-inflammatory, antioxidant and antimicrobial properties. Moreover, honey has strong wound healing activity (Molan, 2006) this is because of its debriding,

deodorizing, antioxidant, antimicrobial and anti-inflammatory properties (Vandamme et al., 2013). Additionally, honey exhibits acidic nature that provides the optimal environment for fibroblast cell proliferation (Bardy et al., 2008). Currently, the therapeutic protocols undertaken in wound care depend on the use of silver. Such therapeutic protocols are considered useful in limiting the bacterial infections, however, due to the presence of excessive concentrations of ionic silver at the wound site, undesirable side effects have been recorded. Thus, this has initiated a new approach in wound healing that depends on the use of natural antimicrobials in everyday clinical practice. Consequently, despite its traditional daily use, honey is now licensed as a medical device either combined with a sterile dressing or sterile tubes (Dai et al., 2014).

Unfortunately, electrospinning natural materials like honey is not possible as the process will result in either elctrospraying at low concentrations or spinneret occlusion at high concentrations of the electrospun materials (Lin et al., 2013). Such natural materials are only electrospun into nanofibers when they are blended with other polymers.

In 2013, Maleki et al. were able to fabricate honey/polyvinyl alcohol nanofibers. Unfortunately, the maximum concentration that could be incorporated within the electrospun nanofibers was 2.25% honey of the total weight of the nanofibrous mat (Maleki et al., 2013). Recently, Wang and He, worked on fabrication of high honey concentration nanofibers, however, the maximum concentration of included honey was 9% with 10% polyvinyl alcohol of the total weight of the nanofibrous mat (Wang & He, 2013). This is because of the decreased viscosity of the honey/PVA solution where increasing the concentration of honey results in remarkable decrease in viscosity, making it quite difficult to electrospin because the degree of chain entanglements is not high enough to tolerate the columbic stretching force that the charged jet is subjected to during electrospinning so results in bead formation and at higher honey concentrations inability for fiber formation (Maleki et al., 2013). Thus, there is a need to fabricate nanofibers composed primarily of high honey concentrations. Such concentrations will maximize the therapeutic and nutritional benefits of honey nanofibrous formulations in smaller dosage forms.

1.4 Poly (Vinyl Alcohol); Biocompatible Synthetic Polymer for Co-Electrospinning.

Poly (vinyl alcohol) (PVA) is an artificial polymer that has been widely used in commercial, food, medical and industrial sectors. PVA is made via the hydrolysis of polyvinyl acetate resulting in a biodegradable, biocompatible polymer (Gaaz et al., 2015). PVA is a semi crystalline, hydrophilic, nontoxic polymer that has acquired increased attention due to its enhanced thermal stability, good resistance to chemicals, cost effectiveness and biocompatibility. Additionally, PVA readily forms a three-dimensional networks in aqueous media due to its hydrophilic nature, thus increasing its swelling capabilities (Supaphol & Chuangchote, 2008).

PVA exhibits the extra advantage of excellent electrospinnability. Through the past few years, extensive literature have studied electrospinning PVA nanofibers and the different parameters that affect the electrospinning process (Zhang et al., 2005).

Due to its advantageous properties PVA has been extensively used in co-spinning natural polymers, synthetic polymers, natural materials and biomolecules. Recently, Li and Yang have fabricated wool keratin /PVA blend nanofibers, which exhibited good interactions and better mechanical properties (Li & Yang, 2014). Similarly, silk fibroin protein and curcumin were made into nanofibers via co-electrospinning with PVA (Lin et al., 2015). Chitosan is a polymer that exhibits difficulty in electrospinning, thus it was electrospun with PVA in different studies in different ratios that affected the properties of the fabricated nanofibrous mats. Alhosseni et al., electrospun (PVA)/chitosan nanofibrous mats that exhibit large pore sizes for its application in nervous tissue engineering and observed that the fabricated mats exhibited the most optimum properties required to meet the main requirements for nerve cell proliferation (Alhosseni et al., 2012).

1.5 Natural Materials for Enhancing the Wound Healing and Antibacterial Properties of the Nanofibrous Wound Dressings.

1.5.1 Natural Plant Extracts: *Cleome Droserifolia* and *Allium Sativum*.

Recent research has realized the extent of dependence of the developed world on medicinal plants, where quarter of the prescriptions dispensed in the USA usually contains one or more ingredients

derived from medicinal plants (Lewington, 1993). Plants exhibit a broad spectrum of activities making them useful in the treatment of different kinds of diseases. According to the WHO 80% of the health problems of worlds' population could be treated by herbal medicinal drugs (Etkin 1981; WHO, 2003).

Cleome droserifolia (Forssk.)Del. is a plant belonging to the Cleomaceae family and is plant of striking medical importance and a long history of ethnomedecinal use (Rahman et al., 2004; Muhaidat et al., 2015). Different species of this family are of considerable interest for the human health and nutrition (Jeruto et al., 2008; Gupta & Rao, 2012). Cleome L. (Cleomaceae), is a genus of ca. 200 perennial and annual herbs (Simpson, 2010) among them nine species are found in Egypt (Ezzat & Motaal, 2012). *Cleome droserifolia* which is an aromatic herb having orbicular sticky leaves, is the most famous member of the Cleome genus in Egypt (Boulos, 1999). *Cleome droserifolia* is traditionally widely used in Egypt by the Bedouins in the treatment of diabetes. The antihyperglycemic effects of the plant has been proven through different studies (El-Khawaga et al., 2010; Abdel-Kawy et al., 2000). *Cleome droserifolia* is also traditionally used for treating rheumatism, scabies and inflammation (Hussein et al., 1994) that's in addition to its proven antioxidant activity (El-Shenawy & Abdel-Nabi, 2004). The phytochemical studies revealed enrichment of *Cleome droserifolia* with different beneficial compounds including phenolics, flavonoids, terpenoids and alkaloids (Aboushoer et al., 2010; Abdel-Monem, 2012; Jane and Patil, 2012). *Cleome droserifolia* has also demonstrated cytotoxic effects against different cancer cell lines (Ezzat & Motaal, 2012). However, studies regarding Cleome biological activity as well as its phytochemistry are still far from being complete (Muhaidat et al., 2015).

Cleome droserifolia has recently been characterized for its antibacterial activity, Muhaidat et al, demonstrated the antibacterial activity of *Cleome droserifolia* oil against a wide range of bacteria (Muhaidat et al., 2015). The wound healing ability of *Cleome droserifolia* has been realized and utilized by the Bedouins who use a decoction of the herb and apply it to the wound site. However, no research studies have yet been conducted to evaluate the wound healing ability of *Cleome droserifolia*.

Allium sativum (Garlic) is another medicinal plant that has been extensively explored and linked historically via different societies to its ability to treat different health problems (Durairaj et al., 2009). *Allium sativum* has been used for different medicinal uses since about 5000 years ago, and

was included in Chinese medicine from nearly 3,000 years. Moreover, *Allium sativums'* medicinal value was recognized by different civilizations as the Greeks, Egyptians, Babylonians and Romans. In 1858, *Allium sativums'* antibacterial activity was observed by Pasteur, additionally it was utilized as an antiseptic during World War I and II to prevent gangrene (Singh et al., 2008; Londhe, 2014). Allium is a genus that comprises more than 500 species that belong to family liliaceae (Pazyar & Feily, 2011). *Allium sativm* mainly contains enzymes, sulfur-containing compounds, minerals and amino acids. Other constituents as oligosaccharides, selenium, arginine and flavonoids are also found in *Allium sativum* (Aviello et al., 2009). The sulfur compounds found in *Allium sativum* are responsible for a large number of its medicinal properties (Pazyar & Feily, 2011).

Allium sativum is currently well known for its use in different medicinal purposes and these include lowering of the blood pressure and cholesterol, prevention and treatment of cardiovascular diseases, antimicrobial activity as well as protective agent from cancer. (Cutler & Wilson, 2004; Tsao & Yin, 2001; Bakri & Douglas, 2005; Iwalokun et al., 2004). Such therapeutic effect of *Allium sativum* is mainly attributed to the water soluble and oil soluble organosulfur compounds.

Allium sativums' antimicrobial activity has been addressed extensively in literature against wide range of bacteria (Benkeblia, 2004; Ankri & Mirelman, 1999; Cellini, 1996; Ekwenye & Elegalam, 2005). Such antibacterial activity is essentially important in wound healing due to the harmful effects of bacterial infection on the wound environment leading to delay in the process of wound healing.

Despite the huge literature on *Allium sativums'* different medicinal effects, its role as a topical treatment in wound healing was just recently investigated. In 2006, Sidik et al, have examined the effect of aqueous extracts of Allium and honey on the wound healing rate in rats. Their results demonstrated the enhanced wound healing rates upon application of the *Allium* and honey combination as compared to the use of honey only, thus elucidating the effect of *Allium sativum* on enhancing the wound healing rate. According to our knowledge this was the first investigation on the effect of *Allium sativum* on the wound healing process (Sidik et al., 2006). The effect of the concentration of the *Allium sativum* aqueous extract on the wound healing process was investigated via examination of the wound closure rate and subsequent histological examination of the wounds. The results demonstrated that 10% extract allowed enhanced wound healing rate compared to 5%

extract and the positive control solcoseryl jelly, whereas, the histopathological examination revealed that the 10% extract and the solcoseryl jelly allowed enhanced tissue regeneration (Rokik et al., 2009). Aged *Allium sativum* extract was also investigated for the mechanism of its wound healing activity on skin wound on chicken and it was observed that *Allium sativum* increases the re-epithelialization process and allows for a profuse dose-dependent neovascularization (Ejaz et al., 2009). Thus, scientific evidence is introducing *Alium sativum* as a new frontier in wound healing agents which exhibits enhanced wound healing ability in addition to well observed antibacterial ability against different kinds of bacteria.

It was observed that none of *Cleome droserifolia* and *Allium sativum*, have been co-spun into nanofibers. And with the enhanced medicinal properties of both materials such an approach should be investigated in different medicinal applications.

1.5.2 Apitherapeutics: Bee venom and Propolis.

Apitherapy involves the use of different bee products in the treatment of different human diseases. Apitherapeutics include honey, royal jelly, pollen, propolis, beeswax and bee venom. The use of apitherapeutics in human treatment dates back to thousands of years ago, and it was mentioned in different religious texts as the bible and the Quran, as well as several historical medical documents as the papyrus of Ebers (1550 BC) (Gupta et al., 2014). Propolis and beevenom stand as two of the most important apitherapeutics that have been used in the treatment of different diseases in traditional medicine and their biomedical value is now documented via different research studies. Bee venom is produced via the venom glands associating the sting apparatus of both the queens and the workers. Storing of the produced venom occurs in the reservoir of the bee venom and injection of the venom during the stinging process occurs through the sting apparatus (Schmidt & Buchmann., 1999). It was observed that approximately 0.15 – 0.30 mg of beevenom is injected via the bees' stinger (Schumacher et al., 1989). Bee venom was recognized as being safe for human therapies, where the median lethal dose (LD50) is 2.8mg of venom per Kg of body weight for the adult human (Ali, 2012).

Bee venom contains several pharmacologically and biochemically active compounds, with some of them well studied and their mechanism of action elucidated (Bellik, 2015). Beevenom is mainly a mixture of enzymes, peptides and amines. It was observed that bee venom stimulated the immune

system (Ali, 2012; Ram et al., 2014). Melittin represents the major component of beevenom and was found to block neutrophil superoxide production (Somerfield et al., 1986) and suppress the inflammation via inhibition of the activity of the phospholipase enzyme (Saini et al., 1997). Such enzyme that is extensively released in severe inflammatory disorders and was found to cause degradation of tissues and organs (Mihelich & Schevitz, 1999). Bee venom is utilized in the treatment of different diseases as rheumatoid arthritis, lupus, sciatica, arthritis, multiple sclerosis, cancerous tumors, low back pain and others (Ali, 2012; Kwon et al., 2002; Kim et al., 2013). Additionally, bee venom exhibits antimicrobial, analgesic and antioxidant effects, thus suggesting that it could be a successful candidate for enhancement of the wound healing process (Khatun & Mukhopadhyay, 2013). Amin et al., have observed accelerated wound healing rates due to application of chitosan blend film containing bee venom on wounds which was related to the anti-inflammatory activity of bee venom (Amin et al., 2008). Similar results were observed via Han et al., who compared the wound healing process in full thickness wounds after application of bee venom cream and the commercial silver sulfadiazine. The results demonstrated that the bee venom cream exhibited wound healing rates similar to that of the commercial silver sulfadiazine, moreover, the bee venom cream demonstrated enhanced anti-inflammatory effect (Han et al 2012). The wound healing effects of bee venom was also extended to diabetic foot infections. A hydrogel based on poly(vinyl alcohol) and chitosan and loaded with bee venom was tested on diabetic rats and the results showed accelerated rate of wound healing as compared to the negative control and similar anti-inflammatory effect to diclofenac gel (Amin & Abdel-Raheem, 2014). Despite the favorable effects observed for bee venom on the wound healing process, developing combination nanofibrous wound dressings loaded with bee venom was not yet explored.

Propolis is the generic name of a combination of resinous materials collected by the honey bees from plants, exudates and buds, then mixed with the bee enzymes and bee wax. The term propolis was coined by Aristotle from the Greek words pro meaning before and polis meaning city, which refers to before the city or defender of the city (Abu-Seida, 2015). Propolis is normally used by the bees to protect the bee hive via coating the inner walls, which provides a shelter against rain and wind and against the entrance of different intruders as insects, lizards and snakes and also prevents the bacterial and fungal growth. The amount of propoils collected via a bees's colony in one year ranges from 150 to 200 g of propolis (Martinotti & Ranzato, 2015). The major components of propolis include 50% resin, 30% bee wax, 10% aromatic and essential oils. 5%

pollen and 5% other substances (Burdock, 1998). With the realization of advanced identification techniques as high-performance liquid chromatography (HPLC), gas chromatography (GC), and mass spectroscopy (GC-MS) numerous compounds have been characterized in propolis (Huang et al., 2014) including aromatic and aliphatic acids, esters, aldehydes, ketones, carbohydrates, vitamins and others. Among the different compounds found in propolis flavonoids stand as one of the most important compounds that possess increasing research interest (Marcucci, 1995). However, the composition of propolis varies according to the phyto-geographic character of the surroundings of the bee hive (Alves de Souza, 2013).

Propolis exhibits different biological activities with respect to the human body that allowed it to be useful in the treatment of different diseases. Propolis is considered non-toxic to humans with safe concentration of approximately 1.4 mg/kg day or 70 mg/day (Wagh, 2013) Propolis content of polyphenols allowed it to exhibit strong antioxidant activity (Gulcin, 2012; Olczyk et al.,, 2013; Castaldo, 2002) as well as anti-inflammatory activity in both acute and chronic inflammatory processes (Kuropatnicki et al., 2013; Sawicka et al.,2012). Propolis demonstrated strong ability to inhibit the development of different kinds of cancer (Xuan et al., 2014; Szliszka et al., 2011). Moreover, anti-hyperglycemic effect of propolis was observed in different studies (Matsui et al., 2004; Fuliang et al., 2005). The antibacterial, antiviral, antifungal effects of propolis have also been documented (Tosi et al., 1996; Grange & Davey, 1990; Marcucci et al., 2001). Propolis also exhibits antiseptic, astringent, spasmolytic, anesthetic, antiulcer, and immunomodulatory effects (Kuropatnicki et al., 2013).

Propolis has also demonstrated strong wound healing abilities where it allows a favorable environment for re-epithelization (Olczyk et al., 2014) it enhances skin cell proliferation (Sehn et al., 2009) and it was recently observed to be able to quench free radicals, thus allowing its safe application in burn treatment (Olczyk et al., 2013). Propolis was also observed to speed up the repair of burned tissue via stimulating the remodeling of the wound bed matrix, which could be linked to propolis flavonoid content which reduces lipid peroxidation and prevents cell necrosis (Olczyk et al., 2014). Additionally, invitro immunomodulatory and immunostimulatory effects on macrophages has been observed (Toreti et al., 2013). Another important property of propolis that enhances the wound healing process is its antibacterial activity. Different studies revealed the strong antibacterial activity of propolis, especially against Gram positive bacterial strains (Grange

& Davey, 1990) Such antibacterial activities could be due to the synergistic activities of the different compounds found in propolis the most important of which is propolis flavonoid content (Abu-Seida, 2015).Thus, propolis role in enhancing the wound healing process could be attributed to its anti-inflammatory, antimicrobial and immumonodulatory properties (Castaldo., 2002). McLennan et al, demonstrated that a single topical application of propolis increases the wound healing rate of a full thickness cutaneous wound in a diabetic rodent model (McLennan et al., 2008). Abu-Seida et al, observed enhanced healing of full thickness skin wound in dogs after application of propolis (Abu-Seida, 2015).

Recently, propolis was electrospun into polymeric nanofibers via electrospinning polyurethane and propolis solution, and the results demonstrated that the inclusion of propolis within the nanofibrous mats allowed enhanced cell compatibility and increased hydrophilicity and antibacterial activities (Kim et al., 2014). Similarly, Sutjarittangtham et al fabricated nanofibers of polycaprolactone and ethanolic extracts of propolis via electrospinning (Sutjarittangtham et al., 2012). Propolis was also electrospun with polylactic acid forming nanofibers that exhibited bactericidal activity (Sutjarittangtham et al., 2014). Recently, Adomavičiūtė et al., combined propolis and silver nanoparticles in poly (vinyl pyrrolidone) nanofibers and demonstrated the enhanced antibacterial activities of the developed nanofibers against a wide range of bacteria (Adomavičiūtė et al., 2016). This illustrates that propolis has been electrospun into nanofibers with different polymers, however none of the developed nanofibers were tested for their wound healing activities despite the previously reported enhanced effect of propolis on wound healing.

1.5.3 Bacteriophages; Viruses Killing Bacteria

Bacteriophages (phages), (Figure 5) are viruses that infect and rapidly destroy bacteria (Brüssow & Hendrix, 2002). Phages are considered as the most abundant microorganisms with an average number of 10^{30}-10^{32} particles of bacteriophages. Humans are continuously exposed to phages via unprocessed food and water. Additionally, phages are found in the saliva, dental plaque and the intestinal tract. One milliliter of unpolluted water contains about 2 x 10^{8} bacteriohage particles (Endersen et al., 2014).

Felix d'Herelle introduced the term bacteriophage in 1917 and was the first to examine phage therapy. d'Herelle used phages against infections of livestock and even examined phages'

antibacterial therapeutic efficiency on himself. It was then noticed that Twort described the same phenomenon in 1915 and also Hankin in 1896 against *Vibrio cholerae* in the Ganges River (Twort, 1915). In the 1920s, d'Hérelle utilized bacteriophages to fight different bacterial infections introducing new discipline that was defined as "phage therapy".

Phage therapy was utilized in different countries as the major antibacterial. Additionally, different pharmaceutical companies including E.R. Squibb & Sons (Princeton, NJ, USA), Swan-Myers/Abbott laboratories, and Eli Lilly (Indianapolis, IN, USA) produced different bacteriophage commercial preparations (Monk et al., 2010). However, due to the poor understanding of phage properties in addition to the limited knowledge about different human diseases, variable outcomes were associated with phage therapy and thus their benefit was questioned via many specialists. It was in the 1940s when the utilization of bacteriophage ceased especially in Western countries with the introduction of the miracle antibiotics (Monk et al., 2010). However, with the alarming and continuous rise in bacterial resistance during the last two decades, together with the decrease in the introduction of new antibiotics, interest in phage therapy has been revived. An interest that has resulted in a number of companies in different countries for phage based products in food, diagnostics, agriculture, and therapeutics.

Bacteriophages were proved efficient antibacterials through numerous studies and against different kinds of bacteria, they were also proven to be more efficient than potent antibiotics in the market as vancomycin, linzolid, ampicillins and trimethoprim (Smith & Huggins, 1982; Smith & Huggins, 1983; Smith et al., 1987; Chibani-Chennoufi et al., 2004; Soothill, 1992). Additionally, the studies revealed that phages therapeutic efficiency is extended also against resistant bacterial strains as vancomycin-resistant *Enterococcus faecium* strain (Biswas et al., 2002) and methicillin- resistant *S. aureus* (MRSA) (Matsuzaki et al., 2005).

Bacteriophages were proved effective in enhancing the wound healing process via their ability to treat persistent bacterial infections in chronic wounds. Mendes et al., observed that the application of a topical bacteriophage cocktail to a wound in a diabetic animal model resulted in noticeable decrease in bacterial count and subsequent enhancement in the wound healing process (Mendes et al., 2013). Similar results were observed upon application of bacteriophages for the treatment of pseudomonas infections in burn wounds (Soothill, 1994; Ahmad, 2002). Bacteriophages were also efficient in eradication of bacterial biofilms in wound (Seth et al., 2013), this is considered very

important as biofilms represent communities of surface associated bacteria that are enveloped in a hydrated extracellular matrix. Thus, they are considered as a source of persistent infection to the wound site particularly because of their resistance to conventional antibiotics.

Due to the increased role of bacteriophages in human life there is a need for better storage techniques that will enable more stable and effective formulations for bacteriophage storage and transportation. Currently, freeze drying represents the most effective method for long term storage of bacteriophages (Miyamoto-Shinohara et al., 2000). However, freeze drying was found to be expensive and time consuming (Dai et al., 2014). Electrospinning of bio-composite nanofibers was utilized as a novel technique for storing bacteriophages (Korehei & Kadla, 2013; Salalha et al., 2006; Lee & Belcher, 2004). However, none of the electrospun bio-composite nanofibers loaded with bacteriophage was further tested in different biomedical applications.

Despite the promising research results of bacteriophages and despite the approval of the FDA for the utilization of phage in food preservation, different challenges are still facing the regulatory approval of bacteriophage based therapeutics. Among these challenges bacteriophages narrow host range stands as an important challenge that calls for innovative solutions. Each phage strain infects only one bacterial type (Sulakvelidze, 2011). In most situations cocktails of bacteriophages are utilized to broaden the host range and enhance the therapeutic efficiency. Nevertheless, approval of phage cocktails via the regulatory bodies is problematic, where they are more likely to approve a single phage strain thus other methods have also to be developed.

Thus, there is a need to develop broad spectrum bacteriophage formulations that are not based on phage cocktails. Within this context developing a broad spectrum bacteriophage wound dressing will satisfy an urgent need of developing bacteriophage preparations that could achieve approval of different regulatory bodies.

2. AIM & OBJECTIVES

The aim of this study is to develop biocompatible nanofibrous antimicrobial wound dressing based on natural materials and to load the developed nanofibrous wound dressing with different natural materials (natural extracts, apitherapeutics and bacteriophages) for the aim of achieving enhanced biocompatibility and wound healing activity as well as enhanced broad spectrum antimicrobial activity as compared to existing antimicrobial wound dressings. The objectives of the project are as follows:

1-Electrospinning of uniform nanofibers based on high concentrations of honey and chitosan via biocompatible solvents. Evaluation of the effect of changing the honey concentration on the properties of the developed nanofibers.

2-Fabrication of electrospun honey/chitosan based nanofibrous mats loaded with natural extracts to enhance the wound healing and antibacterial properties of the developed nanofibers.

3-Fabrication of electrospun honey/chitosan based nanofibrous mats loaded with apitherapeutics to enhance the wound healing and antibacterial properties of the developed nanofibers.

4-According to the results of objectives 2 and 3, one of the fabricated nanofibrous dressings will be further loaded with bacteriophages to achieve enhanced, broad spectrum antibacterial activity. At the same time, this will allow developing a broad spectrum bacteriophage formulation as a solution to one of the challenges of phage based therapeutics.

3. MATERIALS AND METHODS

3.1 Materials

Chitosan (Mw, 240 kDa and DDA of 84%, Chitoclear, cg110, TM 3728) was purchased from Primex, Siglufjordur, Iceland. Fresh bulbs of Allium sativum (AE) were purchased from a local vendor. Cleome droserifolia (CE) were collected from the mountains of Sinai, Egypt. Poly (vinyl alcohol) (85,000 Da Mwt), ethanol (absolute, ≥99.8%), gluteraldehyde (25% in H_2O) and Polyethylene glycol (6000 Da Mwt) were purchased from Sigma Aldrich (St. Louis, USA). Acetic acid (glacial, 99-100% purity) was supplied from Merck (Wadeville, South Africa). Muller Hinton broth, Nutrient broth, Nutrient agar, Luria-Bertani broth and agar-agar, were supplied from Oxoid (Basingstocke, UK). Aquacel ® Ag (ConvaTec Inc) was purchased from local pharmacy in Egypt. Fetal bovine serum (FBS), thiazolyl blue tetrazoliumbromide–MTT (M2128-1G), Phosphate buffered saline (PBS), Dulbecco's modified eagle medium (DMEM) and triton X were supplied from Sigma Aldrich (St. Louis, USA). Honey (clover) (H) *[viscosity: 15,300 mPas, total soluble solid content: 81%]*, Bee venom (BV) *[amino acid content (histidine; 12.6%, alanine; 7.9%, cysteine; 6.44%, glutamic; 3.81%, tyrosine; 3.28%, valine; 3.02%, leucine; 2.87%, and methionine; 2.69%) protein and peptide content (Milittin; 51.6%, phospholipase A2; 15.4%, mastocyte degranulating peptide; 3.5%, apamin; 3.3%, minimine; 3.2%, hyaluronidase; 2.5%, adolopin; 1.6% and unkowns; 18.9*)(Ahmed, 2006)*]* and propolis (Pr) *[Total flavonone and di hydroxyl flavonal; 1.330 ± 0.140, total flavones and flavonals; 3.200 ± 0.162, total phenolic content 30.847 ± 0.064, Phenolic content (mg/100g) (phenol; 37.57, parahydroxy benzoic acid 9.18, p.coumaric acid; 1.25, chrysin; 67.03, galangin; 70.13, daidzin; 42.97, acacetin; 48.32) total insoluble content (41.03 ± 0.16) and volatile substances content (4,10 ± 0.10)* (Aly, 2012)*]* were provided from the faculty of Agriculture, Cairo University (Egypt).

3.2 Methods

3.2.1 Preparation of Aqueous Extracts of Allium sativum (AE), Cleome droserifolia (CE), and propolis (Pr).

Bulbs of fresh AE were extracted according to the method of Al-Astal (Al-Astal, 2003). Fresh bulbs of AE (10 g) were peeled, washed with distilled water several times, then the AE was homogenized aseptically using a sterile mortar and a pestle. Subsequently, a Whatman No. 1 paper

was used to filter the homogenized mixture. The obtained filtrate was then directly used in the preparation of the electrospinning solutions. On the other hand, dried leaves of CE were extracted according to established protocols (Ezzat & Motaal, 2012). The air dried aerial parts of CE were powdered and extracted via boiling in distilled water for two minutes and then allowed to stand for ten minutes before filtration. Whatman No. 1 paper was used to filter the boiled mixture. Subsequently, a rotary evaporator was used to remove the water and the remaining extract was dried in a vacuum oven at 40°C (Jeiotech, OV-11, South Korea) until a dry powder of CE extract was obtained. The powder was weighed and stored until further use.

Aqueous extracts of propolis were prepared via covering propolis (500 g) with 1 liter of 20% aqueous ethanol solution as the solvent and placed in an amber glass container. The mixture was allowed to stand at room temperature for two weeks with periodic agitation. Subsequently, the mixture was filtered via Whatman No.1 filter paper. Dry propolis powder was achieved via incubating the filtrate at 70 °C. The dry powder achieved represents the water soluble propolis utilized in this study (Sosnowski, 1983).

3.2.2 Preparation of the electrospinning solutions

Different solutions were prepared with the aim of incorporation of the highest honey and chitosan concentrations using biocompatible solvents. Different weight ratios of PCS and HP as well as HPCS were prepared as follows: PCS (7%:1.5%, 7%:2.5% and 7%:3.5%); HP (20%:10%and 30%:10%), and HPCS (30%:7%:1.5%, 30%:7%:3.5%, 30%:5%:5.5%, 30%:5%:4.5%, 20%:7%:3.5%, and 40%:7%:3.5%). Solutions were prepared in 1% acetic acid. The HPCS solutions incorporating high honey and chitosan concentrations exhibited very high viscosity at the time of preparation thus they were aged at room temperature for different time intervals.

Subsequently, HPCS solutions with different honey concentrations were prepared for studying the effect of changing the honey concentration on the prepared nanofibers. The solutions were prepared using the following weight% ratios; (10:7:3.5), (20:7:3.5), and (30:7:3.5) of honey, poly(vinyl alcohol), and chitosan, respectively dissolved in 1% acetic acid. Then, the as-prepared solutions were allowed to age at room temperature.

For enhancing the antibacterial and wound healing activities of the fabricated nanofibers, natural extracts, namely *Allium sativum* (AE) and *Cleome droserifolia* (CE) and apitherapeutics, namely bee venom and propolis were loaded within HPCS nanofibers.

Blend solutions of honey/poly (vinyl alcohol)/ chitosan/bee venom (HPCS-BV) and honey/poly (vinyl alcohol)/ chitosan/ aqueous propolis extract (HPCS-Pr) were prepared in the following concentrations weight % ratios (30:7:3.5:0.01) and (30:7:3.5:10) respectively. The HPCS-BV and HPCS-Pr blend solutions were prepared in 1% acetic acid. Solutions were allowed to age at room temperature.

Various blend solutions of honey/poly (vinyl alcohol)/ chitosan/ *Allium sativum* extract (HPCS-AE), honey/poly (vinyl alcohol)/ chitosan/ *Cleome droserifolia* extract (HPCS-CE), and honey/poly (vinyl alcohol)/ chitosan/*Allium sativum* extract/ *Cleome droserifolia* extract (HPCS-AE/CE) were prepared. In the preparation of the blend solution of (HPCS-AE), AE was used as 50% of the solvent to which honey (30 w/v), chitosan (3.5 w/v) and poly (vinyl alcohol) (7 w/v) were dissolved. Both the blend solutions of HPCS and HPCS-AE were prepared in 1% of aqueous acetic acid. Both solutions were allowed to age at room temperature for 1 week. *Cleome droserifolia* dry powder extract (CE) (10 w/v) was added to both the as-prepared HPCS and HPCS-AE blend solutions before electrospinning and stirred for 1h to form the blend solutions of HPCS-CE (30:7:3.5:10 w%) and HPCS-AE/CE(30:7:3.5:10 w%) in 50% AE as the solvent, respectively. During preparation of all blend solutions, poly(vinyl alcohol) was dissolved separately in half the volume of the solvent at 100°C with stirring followed by addition of the remaining volume of the solvent with the other constituents to the cooled solutions to avoid any degradation of the active constituents due to exposure to elevated temperatures.

3.2.3 Viscosity measurements.

The viscosity of the poly(vinyl alcohol) (7%), PCS (7%:3.5%), HP (30%:7%), and HPCS (30%:7%:3.5% and 10%:7%:3.5%) samples were determined. The aqueous AE extract replaced 50% of the solvent of the HPCS blend solution, thus, its effect on the viscosity of the blend solution had to be examined. The viscosity of the HPCS-AE (30%:7%:3.5%:50%) blend solution was determined using a viscometer (Myr; VR-3000, Viscotech Hispania, Tarragona, Spain). The solutions were aged for a week and the viscosity was determined at different time intervals (0, 24, 48 h and 1 week). The average value of three measurements was reported as mean ± SD.

3.2.4 Electrospinning of the as-prepared solutions

The as-prepared solutions were loaded in a 5ml plastic syringe attached to a stainless steel needle (22 gauge) as the nozzle for electrospinning (E-spin, NanoTech, Kalyan-pur, India). Two electrospinners were utilized (NANON-O1A, MECC, Japan & E-spin, NanoTech, Kalyanpur, India). The nozzle was connected at a high electric potential and the distance between the nozzle and the collector, the flow rate and the voltage that allowed the most uniform nanofiber deposition were selected. A ground collector wrapped with aluminum foil and cotton gauze were used for collection of the samples.

3.2.5 Cross-linking of fiber mats

Physical and chemical methods were used to crosslink the nanofibrous mats of HPCS. Glutaraldehyde (GA) was used for chemical crosslinking. The fiber mats were placed in a closed desiccator that was saturated with GA vapors (40 ml). Exposure of the nanofibrous mats to the GA vapors was done for different time intervals (30, 60,120 and 180 min as well as 48 h and 72 h). Subsequently, enhancement of the crosslinking reaction and removal of unreacted (GA) were done via heating the nanofibrous mats in an oven under vacuum at 40◦C for 24 h. Physical crosslinking was performed by freezing/thawing and heating techniques. Freezing and thawing was performed via freezing the fiber mats for 15 min in liquid nitrogen followed by thawing at room temperature for 15 min for three successive cycles. Heating was carried out under vacuum in an oven (Jeiotech, OV-11, South Korea) at both 110◦C, 100◦C for 15 min and 80◦C for 25 min as well as at 70◦C for 24 h.

3.2.6 Characterization and measurements

The morphologies of the electrospun nanofibers were observed using scanning electron microscopy (FESEM, Leo Supra 55, Zeiss Inc., Oberkochen, Germany) and transmission electron microscopy (Jeol, Musashino, Akishima, Tokyo, Japan). Image-J software was used for measurement of the diameters of the collected nanofibers. From three different images 100 fibers were measured for each of the developed nanofibrous mats. Subsequently, the average diameter and diameter distribution were determined. Fourier transform infrared spectroscopy (FTIR) was performed for the raw poly(vinyl alcohol) and chitosan and the HPCS nanofibrous mats (30%:7%:3.5%) using FTIR (Thermoscientific, Nicolet 380, USA). The transmission mode with KBr pellets was used for bulk chitosan and poly(vinyl alcohol) as well as and HPCS nanofibrous

mats. The X-ray diffraction patterns of the HPCS nanofibers (30%:7%:3.5%) with increasing honey concentrations (10%H, 20%H & 30% H) were obtained using an XRD diffractometer (Bruker 4040, Karlsruhe, Germany) with a wavelength, λ=0.154 nm at 40 kV, 150 mA, and at a scan speed of 4° per minute in the 2θ range of 5°–80°. Moreover, thermogravimetric analysis of the nanofibers was performed with a TGA analyzer (TGA Q50, TA Instruments). Samples were heated in a platinum pan under nitrogen atmosphere (60ml/min) up to 700 ºC, at a heating rate of 10ºC/min. The stability of the nanofibrous structure was evaluated via SEM examination of the morphology of the crosslinked and non-crosslinked samples after storage for 1 year on shelf. Crosslinking of the stored samples was performed via exposure of the nanofibers to GA vapours for 1h and 3h followed by heating at 40ºC under vacuum.

3.2.7 Evaluation of swelling and weight loss capabilities of the HPCS nanofibers

The swelling and weight loss abilities of the developed HPCS nanofibrous mats with increasing honey concentrations; 10:7:3.5, 20:7:3.5, and 30:7:3.5 (W%) as well as the HPCS nanofibers loaded with the natural extracts and apitherapeutics were evaluated. The mats were placed in phosphate buffered saline, PBS of a pH 7.4 at 37°C. The following relationships were used for determination of the swelling ability of the nanofibrous mats at 1, 4 and 24 h, and their weight loss at 24 h:

$$\textit{Degree of swelling (\%)} = [M\text{-}M_i / M_i] \times 100 \qquad (1)$$

$$\textit{Weight loss (\%)} = [M_i\text{-}M_d / M_i] \times 100 \qquad (2)$$

Where M is the weight of the swollen nanofibrous mats after plotting their surface with filter paper, M_d is the weight of the dried nanofibrous mats after being removed from the phosphate buffer saline. The swollen nanofibrous mats were dried in an oven at 40°C until constant weight was achieved. M_i is the initial dry weight of the electrospun nanofibrous mats.

3.2.8 Evaluation of the Antibacterial activity

The viable cell count technique was used for the evaluation of the antibacterial properties of the developed nanofibrous mats. The collected nanofibrous mats were sterilized via exposure to the UV for 20 minutes except for the bacteriophage loaded nanofibers that were aseptically collected and stored. Both of the developed nanofibrous mats and the Aquacel Ag (0.05 gm) were added to 3ml sterile Muller Hinton broth. Subsequently an overnight bacterial suspension (30 ul) from each

of the tested bacteria that was adjusted to 0.5 McFarland standard (1x 10^8 c.f.u. /ml) was added to them. The tubes and a negative control were incubated at 37°C with agitation at 100 rpm for 24 h. Following the 2h incubation 10 ul from each treated bacterial suspension as well as the positive and negative controls were subjected to serial dilution. From every dilution 50 ul were added to nutrient agar plates and incubated for 24 h at 37°C. The surviving colonies on the nutrient agar plates were then recorded in plates that allowed counting from 10 to 150 CFU. The experiment was repeated three times and the mean value of CFU was determined (Gallant-Behm et al., 2005). Aquacel Ag (ConvaTec Inc) was evaluated for its antibacterial activity and utilized as the positive control.

The antibacterial activity of the developed HPCS nanofibers with different honey concentrations were evaluated against *Escherichia coli, Staphylococcus aureus* at two different bacterial counts *(*1x 10^8 cfu /ml & 1x 10^7 cfu /ml). Upon loading the HPCS nanofibers with natural extracts, apitherapeutics and bacteriophages, the antibacterial activity was evaluated against *Escherichia coli, Staphylococcus aureus,* and resistant bacterial strains: Methicillin resistant *Staphylococcus aureus* (MRSA) and Multi drug resistant (MDR) *Pseudomonas aeruginosa* at the bacterial count of (1x 10^8 cfu /ml).

3.2.9 In vivo wound healing studies

The wound healing abilities of the developed nanofibrous mats were evaluated invivo on male mice weighing 25g. All animals were anaesthetized with a mixture of ketamin HCl (50mg/kg) and xylene HCl (20mg/kg) and their backs shaved followed by creating a 9 mm wound on the back of every mice using a biopsy puncher. The tested nanofibrous mats were UV sterilized for 20 min before placing them on the wound site except for the bacteriophage loaded nanofibers that were aseptically collected. Aquacel Ag (ConvaTec Inc) was utilized as a positive control, whereas untreated wounds covered with a cotton gauze were utilized as a negative control. The change in the wound size was evaluated at 3, 5, 7, 10 and 12 days. The wound area (%) that remained exposed represented the ability of wound healing for each of the examined samples. Three mice were evaluated for each of sample and the controls and the mean value for three measurements was recorded.

Wound area (%) = [W (3, 5, 7, 10, 12)/W (0)] × 100

Where W (0) and W (3, 5, 7, 10, 12) represents the exposed wound areas of the wounds on days 0 and 3, 5, 7, 10 and 12 respectively.

3.2. 10 Histological examination and the scoring system used for the histologic outcomes

The wound site and the surrounding skin and muscle were cut and fixed with buffered formalin (10%) then the samples were put in paraffin followed by sectioning. Five mice were treated with each sample and the positive control as well as five mice untreated. Tissue samples were taken from each mice at eaxh time interval. The collected samples were subsequently stained via Hematoxylin and Eosin (H&E) staining and Masson's Trichrome staining (MT). Samples collected on days 3, 5,7,10 and 12 were subjected to H&E staining whereas the MT staining was performed for samples collected on day 10. The stained tissue sections were evaluated according to the following histological outcomes: necrosis, hemorrhage, granulation tissue, amount of inflammatory infiltrates, epithelization and thickness of the epidermis and collagen deposition. A histologic scoring system was utilized to evaluate every parameter and a 0-3 score was assigned for every sample. Necrosis, inflammatory infiltrates, hemorrhage, epithelization, epidermis thickness and collagen deposition were graded as 0 (none), 1 (scant), 2 (moderate) and 3 (abundant). Inflammation severity was scored as follows: 0 – (no inflammatory cells) no inflammation; 1– (scant inflammatory cells) 2 – (moderate inflammatory cells) 3 – (abundant inflammatory cells). The maturation of the granulation tissue was graded as: 0 (immature), 1 (mild maturation), 2 (matured), 3 (fully matured with collagen deposition). Collagen distribution (based on the distribution of the collagen fibers in the microscopic fields) was graded as: 0 (no collagen distributed), 1(non-uniform distribution), 2 (mild uniformity in distribution), 3 (uniform distribution) (Xie et al., 2013)

3.2.11 Cell viability assay

The developed nanofibrous mats as well as the commercial dressing Aquacel Ag as a positive control were evaluated for their cytotoxicity. The nanofibrous samples were sterilized for 30 min using the UV and then washed and soaked in PBS solution. The extract solutions of the tested samples were then filtered via sterile disposable filters (0.20 mm, Merck, Darmstadt, Germany). DMEM media was then used to make several dilutions of the extract (0, 25, 50 and 100%). Human fibroblast cells (HFD4, ATCC; crl-2522) ($1x10^4$ cells per well) were incubated for 24 h in a 96 well plate. The different dilutions of the extract solutions were added to the plate followed by incubation at 37°C in a CO_2 incubator. After 24h, the human fibroblast cells were incubated with

the extract solution for 48 h. Subsequently, 20 µl of the MTT [MTT: 3-(4, 5-dimethylthiazol-2-yl)-2, 5-diphenyltetrazolium bromide)] solution was added to every well and incubated for 4h. To evaluate the viability of the cells, the formazan crystals formed were dissolved in 200 µl DMSO and the optical density was recorded (595 nm). The results of the examined samples and the positive control were compared to those of an untreated control (Son et al., 2016).

3.2.12 Cell proliferation.

The effect of the developed nanofibrous mats as well as Aquacel Ag (positive control) on cell proliferation ability was evaluated. The human fibroblast cells (HFD4, ATCC; crl-2522) ($1x10^4$ cells/well) were seeded on the examined samples followed by incubation for 1 and 3 days. At every time point the examined samples were taken from the original plate to another 24 culture plate containing 1 ml fresh media and 100 µl MTT solution per well and then incubated for 4h. The formed dark blue formazan crystals were dissolved in DMSO and the optical density was measured at wave length 595 nm (Son et al., 2016).

3.2.13 Bacteriophage isolation, purification and characterization

According to the previous antibacterial evaluation one of the examined bacteria was selected and used for enriching and isolating a virulent bacteriophage. Briefly, sewage samples were collected from different Egyptian hospitals and used for bacteriophage isolation. Samples (5 gm) were suspended in Luria-Bertani broth (30 ml) and 30 ul from an overnight culture of the selected bacteria was added and incubated with the mixture for 6h at 35°C with constant shaking in order to enrich the bacteria specific bacteriophage. Subsequently, choloroform drops were added to the mixture that was allowed to stand for 15 min and then filtered via Whatman No.1 filter paper to remove any solid particles. Bacterial cells and debris were removed via centrifugation of the filtrate for 5 min at 11,000 g. For amplification of the isolated bacteriophage, polyethylene glycol 6000 (PEG 6000) (10%) and sodium chloride (1M) were put on the supernatant followed by incubation of the solution overnight at 4 °C and then centrifugation at 11,000 g for 20 min. The pellet was dissolved in PBS (1ml) and then filtered via 0.22 µm filter for removal of the residual bacterial cells. Phage plaque assay was performed via mixing the amplified bacteriophage solution with exponential growth culture of the selected bacteria and allowing them to stand for 15 mins and then plating them with semi-solid agar medium (0.6%) followed by incubation at 35 °C for 4h. From the resulting plates a single plaque was selected and used for purification and amplification

(Stenholm et al., 2008; Carey-Smith et al., 2006). This resulted in the collection of a concentrated phage stock solution (10^9-10^{10} PFU mL $^{-1}$)

For characterization of the isolated bacteriophage, an aliquot of the amplified phage suspension was put on a copper EM grid (400 mesh size) having a nitrocellulose surface backed with carbon. After 10 s of incubation, the copper grid was blotted using filter paper and 2% uranyl acetate and lead-citrate were used for staining. Subsequently, the copper grid was blotted again and then dried in air. Samples were observed via a Plus Transmission Electron Microscope (Jeol, Musashino, Akishima, Tokyo, Japan).

3. 2.14 Electrospinning and antibacterial evaluation of the bacteriophage loaded nanofibers

According to the antibacterial results of the HPCS nanofibers loaded with natural extracts and apitherapeutics, one of the nanofiber solutions is selected for subsequent loading with the isolated bacteriophage. The bacteriophage stock solution (1ml) was added to the selected nanofiber solution (9 ml) and agitated at 70 rpm for 1h. Subsequently, the mixture was subjected to electrospinning. The applied voltage, flow rate as well as the distance between the needle and the collector were selected based on the values that allowed the most uniform nanofiber deposition.

The collected nanofibres were then subjected to antibacterial evaluation together with the nanofibers without the bacteriophage and Aquacel Ag as a positive control. The viable cell count technique was utilized to evaluate the antibacterial activity. The same steps followed in the previous antibacterial evaluation were undertaken.

2.2.15 Statistical Analysis

The results of the quantitative data are presented as mean ± standard deviation (SD). For in vitro experiments, average values were reported from three independently prepared samples. Results were evaluated statistically using students t-test was and a p-value of less than 0.05 was considered significant.

4. RESULTS & DISCUSSION

4.1 Fabrication of Uniform Electrospun Nanofibers Based on High Concentrations of Honey and Chitosan (Sarhan & Azazzy, 2015a).

4.1.1 Preparation of the electrospinning solutions

Solutions of poly(vinyl alcohol)/chitosan (PCS), honey/poly(vinyl alcohol) (HP) and honey/poly(vinyl alcohol)/chitosan (HPCS) were prepared and tested for viscosity at different time intervals as shown in table 1. At zero time, the (HP; 30%:7%) exhibited very low viscosity (175 mpas) and the (PCS; 7%:3.5%) exhibited extremely high viscosity (85,440 mpas) making both solutions impossible to spin. Whereas, the combination of (HPCS; 30%:7%:3.5%) exhibited at day zero 34,000 mpas. However, such viscosity value was still above the optimum viscosity needed for electrospinning. Consequently, the HPCS solutions were allowed to age for one week at room temperature.

Interestingly, it was observed that the viscosity of the HPCS solutions decreased noticeably upon aging. This was unlike the PCS and the HP solutions that demonstrated increased viscosities after aging (Table 1). The decrease in viscosity with time that was observed with the HPCS solutions could be attributed to enzymatic degradation of chitosan by the enzymes that are found in honey. Honey contains small amounts of enzymes, including enzymes that are able to transform polysaccharides into smaller products as amylase. Such enzymes most likely degrade chitosan into its oligosaccharides (Xie et al., 2011). Additionally, hydrogen peroxide, which is a major component of honey, may have contributed to the enzymatic degradation of the chitosan backbone (Brudzynski, 2006). Interestingly, it was observed that increasing the honey concentration within the HPCS mixtures allowed further reduction in the viscosity of the solutions as demonstrated in table 1.

4.1.2 ***Electrospinning and characterization of the morphology and functional groups of the developed nanofibers.***

Different concentrations of the PCS, HP and HPCS were electrospun (E-spin, NanoTech, Kalyan-pur, India). For the PCS combinations, the highest concentration of chitosan that could be electrospun with polyvinyl alchol using 1% acetic acid, was 1.5% at 20 kV, 10ul/min as the flow rate and 15 cm distance between the collector and the needle. On the other hand, for the combinations of HP, the highest honey concentration that could be electrospun with polyvinyl alcohol was 20% honey (Figure 6a) at 22 kV, 10ul/min as the flow rate and 15 cm distance between the collector and the needle. However, clusters were observed within the electrospun nanofibers, which are most probably honey clusters that could not be included within the HP nanofibers. Remarkably, upon addition of 3.5% chitosan to the same combination of HP, uniform nanofibers were achieved (Figure 6b). This is attributed to the favorable effect of chitosan on solution viscosity, allowing it to reach to the optimum degree required for chain entanglements needed to form uniform nanofibers. However, upon increasing the concentration of honey to 30% within the HP combination, the clusters of honey increased extensively even after changing the parameters of electrospinning (Figure 6c). This indicates that the poly(vinyl alcohol) polymer is incapable of incorporating higher honey concentrations even at increased concentrations of poly(vinyl alcohol), where the reduction in viscosity imparted by honey on the HP combinations could not be overcome by increasing the poly(vinyl alcohol) concentration. On the other hand, increasing the concentration of chitosan within the PCS combinations resulted in extremely viscous solution that was impossible to electrospin (Table 1). Interestingly, aging the combination of HPCS (30%:7%:3.5%) for more than 2 days allowed it to reach to the optimum viscosity required for easy electrospinning and collection of uniform nanofibers at 24 kV, 10ul/min as the flow rate and 15 cm distance between the collector and the needle (Figure 6d). The combination of HPCS allowed for the first time the fabrication of biocompatible nanofibers containing high honey and chitosan concentrations using biocompatible solvents.

Realizing the synergistic effect of the combination of chitosan and honey on the HPCS solutions' viscosity, attempts were made to increase incorporated honey and chitosan concentrations. Electrospinning 35% and 40% honey within the PCS (3.5%: 7%) combination was successful (Figures 7a and b). Moreover, electrospinning 4.5% and 5.5% chitosan within the HP combinations containing 30% honey was achieved (Figures 7c and d). However, the concentration of incorporated P was decreased to 5% because of the increased viscosity of the solution due to the increased concentration of incorporated chitosan.

In previous attempts to fabricate nanofibers with high concentration of honey, the maximum concentration of honey that was electrospun with poly(vinyl alcohol) was 9% (Wang & He, 2013). This is due to the remarkable decrease in the solution viscosity upon increasing the honey concentration, thus making it impossible to electropsin. This is the first report to fabricate nanofibers with concentrations of honey reaching to 40% of the weight of the nanofibrous mats. Furthermore, the favorable effect of honey on the chitosan solution viscosity upon aging allowed for incorporating higher chitosan concentrations reaching to 5.5% for the first time via biocompatible solvents.

Despite the success achieved in electrospinning HPCS nanofibers containing 35% and 40% honey, the electrsopinning rate of such nanofibers was very slow leading to an increase in the collection time of the nanofibrous mats, especially with the single needle prototype electrospinner utilized in this study. Thus, the HPCS nanofibers with 30% honey were selected for completing the study due to the feasibility of their collection with the current electrospinner. However, with the advancement witnessed with multi-needle, needless and large scale electrsopinners, collection of nanaofibers with 40% and more honey should be feasible. On the other hand, HPCS nanofibers with 3.5% chitosan were selected for completing the study, because of the longtime of aging required for the 5.5% chitosan solution to allow it to reach to the viscosity optimum for electrospinning, in addition to the slow electrospinning rate.

The FTIR spectra of the powders of CS and P as well as the HPCS nanofibers were analyzed. Chitosan showed characteristic bands at 3429 cm−1and 1655 cm−1corresponding to both the OH and the amide O C NH2 groups. The CH3and CH3O groups showed bands between 1000 and 2000 cm−1 (Paipitak et al., 2011). Poly(vinyl alcohol) exhibited bands at 3429 cm−1, 2923 cm−1,and 1444 cm−1 corresponding to the characteristic bands of OH, CH2, and CH OH groups (Yan et al., 2012).

The previous characteristic bands observed for both P and CS were preserved in the resulting HPCS nanofibers. However, it was realized that the absorption peak at 3429 cm−1and 1655 cm-1 corresponding to both the OH and amide O C NH2 groups shifted to a lower wave number in the hybrid HPCS nanofibers. The characteristic peak observed in the HPCS nanofibers at 1058 cm−1

could be attributed to the C O C symmetric stretching and C O H bending vibrations of the proteins found in honey. Whereas, the amide band of the protein found in honey could be realized at 1641 cm−1 (Philip, 2009). Moreover, the peaks observed between 900 cm−1 and 750 cm−1 were attributed to the anomeric region, which is characteristic of the saccharide configuration of honey (Jaganathan & Mandal, 2009; Philip, 2010).

4.1.3 Crosslinking and characterization of the morphology of the nanofibers before and after cross-linking treatment.

It was observed that the HPCS nanofibrous mats lost their nanofibrous structure upon being in contact with aqueous media. Thus, different crosslinking techniques were undertaken, in order to achieve sufficient crosslinking degree without jeopardizing the nanofibers' biocompatibility. During crosslinking care was taken not to expose the nanofibers to temperatures exceeding 110◦ C to avoid the reduction in the quality of honey with increase in the hydroxymethylfurfural content upon exposure to elevated temperatures (Tosi et al., 2004). It was reported that exposure of honey to 40◦C for up to 96h does not affect any of the biomolecules found in honey (Molan, 1992).

The fabricated nanofibers were chemically crosslinked via exposure to the GA vapors for different time intervals followed by heating at 40◦C for 24 h under vacuum to enhance the crosslinking efficiency and remove any unreacted residues of the GA. Figure 9 illustrates the images of the nanofibers that were chemically cross-linked after being immersed in PBS for 15 min. It was observed that the nanofibers subjected for three days to GA vapors demonstrated superior crosslinking (Figure 9a) where their original shapes were maintained with no swelling observed. Whereas, the nanofibers exposed for two days to GA vapors demonstrated similar results, however slight swelling was noticed (Figure 9b). Interestingly, it was realized that the nanofibrous structure could still be maintained with some swelling observed after exposure to GA vapors to three hours (Figure 9c). Meanwhile, upon reduction of the exposure time to GA vapors for 1 h (Figure 9d) lower crosslinking efficiency could be realized (Figure 9d), where partial degradation of the surface layers of the nanofibers began together with noticeable swelling of the nanofibers. It is worth mentioning, that the crosslinking efficiency noticeably decreased upon reducing the exposure time to the GA vapors for thirty minutes, where the nanofibrous morphology of the surface layers was nearly lost, probably because of the increased percentage of degraded fibers.

The different physical crosslinking procedures undertaken were heating at different temperatures for different periods of time and different cycles of freezing and thawing in liquid nitrogen for different time intervals. It was observed that crosslinked nanofibers were achieved upon heating the nanofibrous mats at 110◦C for15 min (Figure 9e), with noticeable swelling realized. Meanwhile, heating for 24 h at 70◦C demonstrated partial degradation of the swollen nanofibers (Figure 9f). Heating causes induction of the crystallization of the polymers forming the nanofibers (Kang et al., 2010). On the other hand, freezing and thawing did not allow maintaining of the nanofibrous structure. It is worth noting that the physical crosslinking techniques employed made the nanofibrous mats brittle and easily liable to cracking. Moreover, heating resulted in a color change from white to light brown. The same effect was realized upon storage of the nanofibrous mats for several month. Such change in color may be attributed to possible interactions between the amino groups in chitosan and the GA aldehyde group.

4.1.4 Evaluation of the stability of the nanofibrous structure of the crosslinked and noncrosslinked nanofibers.

The developed HPCS (30%:7%:3.5%) were evaluated for the stability of their nanofibrous morphology before and after crosslinking. Samples were crosslinked via exposure to GA vapors for 1h and 3h followed by heating at 40ºC for 24h. The crosslinked and non-crosslinked samples were placed in petri dishes closed with parafilm and stored on shelf at room temperature for 1 year and then the stability of the nanofibrous structure was examined via SEM.

As seen in figure 10, the nanofibrous structure could still be realized in both the crosslinked and non-crosslinked samples after 1 year, however, the crosslinked samples allowed better preservation of the nanofibrous structure. In the non-crosslinked samples the outer layer of the nanofibrous mat seem to have degraded and the nanofibrous structure of the underlying layers could be observed beneath the upper degraded layer (Figure 10a & 10b). In the crosslinked samples, degradation of the outermost layer was not observed, however, significant swelling of the nanofibers could be observed. The degradation of the outermost layer in the non-crosslinked sample and the swelling observed in the crosslinked sample could be attributed to the adsorption of moisture from the surrounding environment.

It is of note that the increase in the crosslinking time from 1h to 3h exposure to GA vapours did not result in a noticeable change in the morphology of the stored nanofibers.

4.2 Evaluation of the effect of changing the honey concentration on the properties of the developed HPCS nanofibers (Sarhan et al., 2016a).

Novel honey/chitosan/ poly(vinyl alcohol) (HPCS) electrospun nanofibers based on high concentrations of honey reaching to 40% were successfully fabricated. Thus, honey is considered the major component of the developed HPCS nanofibers. Consequently, the effect of changing the honey concentration on the properties of the developed nanofibers was studied. Increasing concentrations of honey (10%, 20% & 30%) were included within the PCS (7%:3.5%) nanofibers and examined for the effect of changing the honey concentrations on the morphology, crystallinity, thermal behavior, swelling, degradation and antibacterial abilities of the developed HPCS nanofibers.

4.2.1 Effect of changing the honey concentration on the morphology of the electrospun HPCS nanofibers.

As apparent from Figure 11, it was noted that increasing the honey concentration led to increasing the diameter of the nanofibers. For instance, the HPCS nanofibers with 10% honey exhibited a mean fibre diameter of 284 ± 97 nm (Figures 11a & 11b) which increased to 371 ± 110 nm, and 464 ± 185 nm upon increasing the honey concentration to 20% (Figures11c &11d), and 30% (Figures 11e & 11f), respectively.

The increase in the fiber diameter is a direct consequence for increasing the amount of honey loaded within the nanofibers as can be observed from Figure 12a & 12b, where it is apparent that honey is embedded within the chitosan/poly(vinyl alcohol) nanofibers. It was also observed that the amount of honey loaded within the nanofibers influences the fiber diameter distribution. As seen in Figure 11d, addition of 20% honey to the chitosan/poly(vinyl alcohol) nanofibers allowed for the most focused fiber diameter distribution, as most of the nanofibers exhibited diameters between 300 nm and 450 nm (Figure 11d). Whereas, the addition of 10% and 30% honey to the

chitosan/polyvinyl alcohol nanofibers resulted in broad distribution of the diameters of the fibers (Figures 11b & 11f).

4.2.2 Evaluation of the effect of changing the honey concentration on the crystallization of the HPCS nanofibers

The XRD diffraction patterns of pure poly(vinyl alcohol) and chitosan have been previously reported (Nakane et al., 1999; Samuels, 1981). Moreover, the XRD patterns of polyvinyl alcohol/chitosan (PCS) nanofibers and films were reported by Jia et al., who observed that nanofibers of the PCS exhibited deteriorated crystalline structure compared to the films (Jia et al., 2007).

Figure 13, illustrates the XRD diffraction patterns of the prepared HPCS nanofibers with increasing honey concentrations. The HPCS nanofibers exhibited an amorphous microstructure with a single broad peek around $2\theta = 20°$. Such XRD patterns are in coherence with those observed for the previously prepared poly(vinyl alcohol)/chitosan nanofibers (Jia et al., 2007). Thus the addition of honey did not affect the diffraction model of the poly(vinyl alcohol)/chitosan nanofibers and consequently the increase in the honey concentration within the HPCS nanofibers had no effect on their diffraction pattern. The deterioration of the crystalline structure of the electrospun nanofibers was previously reported (Deitzel et al., 2001; Zong et al., 2002). Such deterioration could be attributed to the fast deposition and drying of the elongated electrospun nanofibers thus hindering the crystallization (Jia et al., 2007).

4.2.3 Evaluation of the effect of changing the honey concentration on the thermal stability of the HPCS nanofibers

Thermogravimetric analysis (TGA) analysis of the HPCS nanofibers with increasing honey concentrations (10%, 20% and 30%) was performed. As observed in figure 14, the examined samples demonstrated similar thermal degradation process that takes place in several steps. The first step of weight loss is attributed to moisture elimination which resulted in loss of less than 10% of the weight of the examined nanofibers below 120 ºC.

It is of note that at 120 ºC the HPCS nanofibers having 10% honey exhibited the highest weight loss of ~8% whereas the weight loss decreased by increasing the amount of honey within the HPCS

nanofibers to ~6% and ~3% with the 20% and 30% honey, respectively. This indicates that the HPCS nanofibers with higher honey concentrations exhibited higher initial moisture content, which is result of the hygroscopic nature of honey. The second and major weight loss of approximately 50% of the weight occurred after 120 ºC till 400ºCand is mainly attributed to the thermal decomposition of the polymer structure as well as degradation of the honey components followed by carbonization of the honey content (Figure 14). In the final step of the thermal decomposition at temperatures above 500ºC, the polymer backbone has been ruptured in addition to the oxidation of the organic matter found in honey. Similar observations have been previously reported (Chauhan et al., 2014; Felsner et al., 2004). The thermogravimetric analysis clearly demonstrates that the fabricated HPCS nanofibers with different honey concentrations exhibit good thermal stability below 120ºC.

4.2.4 Evaluation of the effect of changing the honey concentration on the swelling and weight loss abilities of the nanofibers.

Honey and chitosan nanofibrous mats represent top candidates for wound dressing applications and determining their swelling capabilities would allow prediction of their exudate management ability (Li et al., 2013). The effect of changing the honey concentration was studied at two mild crosslinking degrees. These include exposing the nanofibers to GA vapours for 1h and 3h with subsequent heating at 40°C to enhance the crosslinking and remove any residual GA.

As observed in figure 15, increasing the honey concentration within the nanofibers decreased its swelling ability at both the tested crosslinking degrees (Figures 15a & 15b). It could be observed from the figures that the HPCS nanofibers with 10% honey and 1h of crosslinking with the GA vapours exhibited superior swelling capabilities reaching to 520% at 1h and 300% after 24 h (Figure 15a).

On the other hand, the effect of the crosslinking time on the swelling capabilities of the HPCS nanofibers varied according to their incorporated honey concentration. For the HPCS nanofibers with 10% honey, increasing the crosslinking time from 1h to 3h decreased their swelling capabilities noticeably from 520% to 273%. Whereas, HPCS nanofibers with 20% honey exhibited increased swelling ability with the increase in the crosslinking time from 1h to 3h. Noticeably, the HPCS nanofibers with 30 % honey demonstrated the lowest swelling ability at both crosslinking times. Although honey is known for its high water uptake ability (MohdZohdi et al., 2011), it also

has high water solubility. Such high water solubility results in increasing the degradation rates of the nanofibers and consequently losing their compact porous structure that can hold in water (Wang et al., 2012). Thus, this eventually results in massive decrease in swelling ability. This was observed by the very low swelling abilities of the HPCS nanofibers with 30% honey. Interestingly, the increase in the crosslinking efficiency by increasing the exposure time to the GA vapours allows the nanofibers to maintain a more compact nanofibrous structure (Li et al., 2013; Kim et al., 1992) thus, the percent of released and solubilized honey decreases. This allows the honey to be maintained within the nanofibers for longer periods of time, and thus its water uptake capabilities could be realised.

On the other hand, the increase in the crosslinking degree decreases the swelling ability as it hinders the intermolecular motion and chain disentanglements within the nanofibrous scaffold. These two opposite effects on the swelling abilities of the nanofibrous scaffolds could be observed in the results presented in figures 15a & 15b.

In the HPCS nanofibers with 10% honey, the amount of honey within the nanofibers is small thus the effect of the swelling hindering due to crosslinking was more pronounced than the water uptake ability of the maintained honey. Whereas, when the concentration of honey increased to 20%, the water uptake ability of the maintained honey in this case exceeded the hindering effect of crosslinking on swelling which allowed the HPCS nanofibers with 20% honey to exhibit a noticeable increase in swelling ability even at 24 h by increasing the crosslinking time to 3h. The HPCS nanofibers with 30% honey however showed slight decrease in the swelling ability with increasing the crosslinking time after 24h. This is because at such high concentration of honey such crosslinking treatments could not overcome the increased solubility of the HPCS nanofibers with 30% honey which affects the compact structure of the nanofibrous scaffold. Such results were confirmed with the weight loss results of the HPCS nanofibers with increasing honey concentrations (Figure 15c), where the increase in the honey concentration within the nanofibers resulted in increased weight loss at both the tested crosslinking degrees.

These results reveal the importance of optimization of the crosslinking degree as well as the honey concentrations within the developed HPCS nanofibers to adjust the water uptake ability as well as the weight loss according to the desired application.

4.2.5 Effect of increasing the honey concentration on the antibacterial activity of the developed HPCS nanofibers

It is the aim of the current study to develop nanofibers that could be utilized as effective antimicrobial wound dressings, thus, the antibacterial activity of the fabricated HPCS nanofibers was screened against Gram positive; *S.aureus* and Gram negative; *E.coli* as they are two of the most common pathogens found in infected wounds (Bessa et al., 2015). Moreover, two different bacterial counts were utilized to study the efficacy of the developed nanofibrous mats in inhibition of high bacterial loads.

Both honey and chitosan exhibit antibacterial activity. Honey exerts its antibacterial activity via its acidity, high sugar content as well as its ability for hydrogen peroxide production (Vandamme et al., 2013). Whereas, the polycationic nature of chitosan allows it to interact with the negatively charged membranes of bacteria leading to loss in the permeability of the membrane with subsequent cell leakage and death (Muzzarelli et al., 1990).

The effect of changing the honey concentration within the HPCS nanofibers on the antibacterial activity of the developed nanofibers was investigated as shown in figure 16 The increase in the honey concentration within the HPCS nanofibers enhanced their antibacterial activities against both *S.aureus* and *E.coli* at 1×10^7 CFU/ml (Figures 16a & 16b). However, upon increasing the bacterial count to 1×10^8 CFU/ml the increase in the honey concentration resulted in an increase in the antibacterial activity against *S.aureus*, whereas nearly no antibacterial effect was realized against *E.coli*. These results are in agreement with No, et al (2002) who demonstrated the weak antibacterial activity exhibited by chitosan against Gram negative bacteria (No et al., 2002). The nanofibrous structure allowed enhancement in the antibacterial activity of the components included within the nanofibers. The examined samples (0.05 g) contain chitosan less than 10 ppm and ~ 0.0875% honey and demonstrated pronounced antibacterial effect against *S. aureus* compared to no antibacterial effect at the same concentrations for both chitosan and honey alone (Goy et al., 2009; Islam et al., 2011I; Liu et al., 2006; Mandal & Mandal, 2011).Such results could be due to the massive increase in the surface to volume ratio of the nanofibers.

Thus, due to the enhanced antibacterial activity of the HPCS nanofibers loaded with 30% honey they will be selected to be further loaded with other antimicrobials. Despite the increased swelling

ability of the 10% honey HPCS nanofibers, the main aim of the present study is to develop an efficient antimicrobial wound dressing. Consequently, the HPCS formula that was selected to be further loaded with natural materials and optimized as a nanofibrous antimicrobial wound dressing is 7% PVA, 3.5% Chitosan & 30% Honey.

4.3 Evaluation of HPCS Nanofibers Loaded with Natural Extracts as Antimicrobial Wound Dressings (Sarhan et al., 2016b).

To enhance the antibacterial activity of the HPCS (30%:7%:3.5%) nanofibers, they were loaded with two natural extracts that have demonstrated antibacterial and potential wound healing capability through previous literature. Thus, the HPCS (30%:7%:3.5%) nanofibers were loaded with aqueous extracts of *Allium sativum* (AE) and *Cleome droserifolia* (CE) and the resulting nanofibrous mats were examined for their swelling, weight loss, antibacterial, cytotoxicity, wound healing abilities as well as their abilities to enhance cell proliferation.

4.3.1 Fabrication of the electrospun HPCS, HPCS-AE, HPCS-CE, and HPCS-AE/CE nanofibers.

As previously demonstrated, electrospinning HPCS nanofibers containing high concentrations of H and CS was only possible by aging the solution of PCS with 30% H for a week. *Allium sativum* aqueous extract was included in the HPCS combination via substituting 50% of the solvent in which the HPCS were prepared resulting in the formation of HPCS-AE solution that was subsequently electrospun into HPCS-AE nanofibers. Upon preparation of the HPCS-AE it was observed that the solution exhibited high viscosity that was inappropriate for electrospinning, thus the solution was aged for a week at room temperature while observing the viscosity of the solution at different time intervals.

It was observed that the substitution of 50% of the solvent of the HPCS with aqueous extract of AE resulted in a massive reduction in its viscosity as compared to the HPCS solution which was utilized as the control (table 2). The observed reduction in viscosity could be due to degradation of the CS polysaccharide into its lower molecular weight oligomers due to the addition of the AE aqueous extracts.

As demonstrated in table 2, the reduction in viscosity imparted by the addition of the aqueous AE extract was very sharp and was observed from the first two hours (1410 mPas) and reached maximum decrease in viscosity after 48 h reaching to 420 mPas as compared to 3660mPas in the case of the HPCS solution without the aqueous AE extract. This indicates the vital role played via

the AE aqueous extract in the CS degradation with the subsequent reduction in the solution viscosity.

Before electrospinning and after both the HPCS and HPCS-AE solutions have reached to the optimum viscosity required for electrospinning, the dry powder of CE (10%) was added as stirred for 1h. It should be noted that addition of the CE extract to both the HPCS and HPCS-AE solutions was not possible before aging because of the increased viscosities of the solutions that were difficult to be stirred. It was realized that the addition of the CE dry powder extract did not affect the required viscosity for electrospinning even after aging.

The as-prepared solutions of HPCS and HPCS-AE were electrospun (NANON-O1A, MECC, Japan) and collected as nanofibrous mats for further examinations. It was observed that the addition of AE aqueous extracts to the HPCS solution has facilitated the electrospinning process, which was attributed to the reduction in viscosity imparted by the AE on the solution. However, due to the massive decrease in viscosity undesirable dripping has occurred. The parameters used during the electrospining of the HPCS-AE nanofibers and that allowed for a continuous and steady jet were a voltage of 27 kV, a flow rate of 0.5 ml/h, and 13 cm as the distance between the needle and the collector. Collection of the nanofibrous mats continued for 4.5h and their surface morphology was observed using SEM (Figure 17). Both the HPCS and HPCS-AE demonstrated a compact, uniform, smooth, and bead-free morphology. Additionally, it was realized that the HPCS-AE exhibited the least nanofiber diameter and the most focused diameter distribution among the tested nanofibrous mats (145 ± 58nm).

Upon the addition of the dry powder of CE to both the HPCS-AE and the HPCS solutions, the process of electrospinning became more difficult until optimizing the parameters of electrospinning to be 28kv, 0.7 ml/h flow rate and 14 cm as the distance between the needle and the collector. The nanofibers were collected for 3.5 hours, however it was still critical to achieve a uniform nanofiber deposition. This may be due to the sticky nature of *Cleome droserifolia* (CE) as it exhibits glandular sticky leaves (Płachno et al., 2009).

Figure 17 demonstrates a bimodal diameter distribution of both the HPCS-AE/CE and HPCS-CE nanofibers, because of the addition of high CE concentration in addition to its sticky nature. Moreover, noticeable branching was observed with a noticeable formation of clusters at the

branching points within the collected nanofibers (Xu et al., 2011). This branching could be attributed to spinning highly concentrated solution (Reneker & Yarin., 2005) using a high voltage combined with the sticky nature of electrospun solution. Electrospinning high concentrated solutions results in a jet with large diameter, which could result in the formation of branches (Yarin et al., 2005). This in turn leads to large inter-fiber spaces, which proofed to be more beneficial in cell related applications such as tissue engineering and wound healing (Gu et al., 2013; Shokrgozar et al., 2011) taking into consideration the density of the electrospun nanofibrous mat.

4.3.2 Evaluation of the swelling and weight loss abilities of the fabricated nanofibers.

The fabricated nanofibers of HPCS-CE, HPCS-AE and HPCS-AE/CE were crosslinked and examined for their swelling capabilities after immersion in PBS (pH 7.4) for 1, 4, and 24 h. Crosslinking of the fabricated electrospun nanofibers was done by exposing the nanofibers to GA vapors for 1 hour and 3 hours with subsequent heating at 40°C in order to remove any residues of GA and enhance the crosslinking of the nanofibers.

As observed in figure 18, the HPCS-CE and the HPCS-AE at one hour crosslinking, demonstrated similar swelling capabilities with a slight decrease in the swelling (%) of both the HPCS-CE and HPCS-AE as compared to the previously examined HPCS (30%H) (Figure 15), especially after 24 hours of immersion in the PBS (Figure 18a). At three hours crosslinking noticeable decrease in the swelling ability of the HPCS-CE was observed. On the other hand, the low swelling (%) of the HPCS-AE/CE nanofibrous mats was observed at one and three hours crosslinking times, demonstrating values of less than 15% swelling as compared to ~90% swelling in the case of the HPCS-AE and previously examined HPCS (30%H) (Figure 15) after immersion in PBS buffer for 24 h (Figure 18b). Such results illustrate that the swelling abilities of both the HPCS and the HPCS-AE nanofibers greatly decreased upon addition of the CE. This could be attributed to the CE sticky nature which hinders the chain disentanglements and intermolecular motion of the fabricated nanofibers and thus hinders their swelling abilities (Plachno et al., 2009).

Increasing the time of crosslinking permits maintaining a more compact nanofibrous structure that allows the water uptake ability of the porous structure of the nanofibers to be realized. At the same time, the extent of crosslinking should not be increased to the point that hinders the chain entanglements and intermolecular motion within the nanofibers (Li et al., 2013; Kim et al., 1992).

Upon increasing the time of crosslinking to 3 h, the swelling ability of both the HPCS-AE and HPCS-AE/CE increased, whereas, nearly no effect was realized on the HPCS-CE nanofibers, which demonstrated similar swelling (%) at both the crosslinking times (1 h and 3 h) examined. Such results illustrate that the increase in the time of crosslinking affected only the nanofibrous mats containing the aqueous AE. This could be due to the fact that the AE containing nanofibers demonstrated increased weight loss as compared to the HPCS-CE nanofibers (Figure 18c). Thus, upon crosslinking the AE containing nanofibers a more compact structure could be maintained for longer periods of time resulting in the enhancement observed in their swelling capabilities after three hours crosslinking.

According to the swelling results of the examined nanofibers (Figure 15 & 18), it is expected that the HPCS-AE/CE nanofibers would demonstrate nearly no capability for management of exudates. Whereas, the HPCS-CE, HPCS (30%H) and HPCS-AE nanofibrous wound dressings would demonstrate moderate capability for exudate management. The HPCS, HPCS-AE and HPCS-CE samples demonstrated moderate swelling capabilities as compared to nanofibers previously electrospun lacking honey (Jannesari et al., 2011). This could be due to honeys' high water solubility which results in increasing the weight loss of the electrospun nanofibers. Moreover, despite that chitosan enhances the water uptake capability of the electrospun nanofibers, increasing the chitosan concentration results in an opposite effect. This was previously illustrated by Son et al., who observed that in nanofibrous mats of chitosan/ poly(vinyl alcohol) having low chitosan concentration, polymeric hydrogels are easily formed via the hydrophilic poly(vinyl alcohol) in solutions thus leading to enhanced swelling. However, upon increasing the concentration of chitosan, the intermolecular forces between the amine groups and the side chains of chitosan increase and decrease the swelling capability (Son et al., 2009).

4.3.3 Evaluation of the antibacterial abilities of the fabricated nanofibers.

Research into development of effective antimicrobial wound dressings represents an increasing trend within the wound dressing market. This is because of the major complications associated with infected wounds that are resistant to current treatment protocols. Chronic non-healing wounds are usually treated with antimicrobial therapeutics either systemic or topical (Lipsky & Hoey., 2009). It was observed that > 60% of these patients received antibiotic treatments for a prolonged period of time (Howell-Jones et al., 2005; Tammelin et al., 1998). With the alarming rise in

antibiotic resistance alternative antibacterials are of great necessity. Silver-based dressings represent one of the most common alternative antibacterials now effectively used in wound treatment. Unfortunately, resistance against silver as well as undesirable side effects have been reported (Lansdown, 2002).

The developed HPCS nanofibrous mats exhibited mild antibacterial activity against *S. aureus* and weak antibacterial activity against *E. coli*. To enhance the antibacterial activity of the developed HPCS nanofibers, CE, AE and their combination were loaded within the HPCS nanofibers and examined for their antibacterial abilities against *S. aureus*, *E. coli* and two resistant strains; MDR *P. aeruginosa* and MRSA. The selected bacterial strains for the study are considered among the most common bacterial pathogens encountered at the wound site (Bessa et al., 2015). Aquacel Ag was examined for its antibacterial effect and compared to the antibacterial activities of the fabricated nanofibrous wound dressings. Recently, it was reported that the Aquacel Ag demonstrated the strongest antibacterial activity among other silver-based wound dressings in the market (Yunoki et al., 2015).

The antibacterial effect of *Allium sativum* has been attributed to its content of thiosulfinates including diallyl sulphide, allyl methyl sulphide, and diallyl disulphide, where they disrupt cell components and block the pathways of various bacterial enzymes (Elsom, 2000; Chen et al., 1999).Whereas Cleome's antibacterial activity has been attributed to its content of various terpenes including the β-eudesmol, sesquiterpenes carotol, and δ-cadinene (Muhaidat et al., 2015).

Figure 19 represents the antibacterial activities of the developed HPCS, HPCS-CE, HPCS-AE and HPCS-AE/CE nanofibrous wound dressings in comparison with the commercial Aquacel Ag wound dressing. It was observed that complete inhibition of *S.aureus* was achieved via both the HPCS-AE and HPCS-AE/CE nanofibrous mats compared to noticeable reduction in bacterial count with the Aquacel Ag wound dressing (Figure 19a). Such effect is mainly attributed to the inclusion of the AE aqueous extracts within the HPCS nanofibrous mats. Additionally, it was realized that among the fabricated nanofibrous mats, only the HPCS-AE/CE demonstrated mild antibacterial activity against MRSA, thus illustrating that the combined effects of both the CE and AE was needed to achieve antibacterial effect against MRSA (Figure 19b). It is of note that the achieved antibacterial effect against MRSA was not significant as compared to the negative control ($p < 0.05$) and less than that observed with the Aquacel Ag. On the other hand, no antibacterial

activity was demonstrated against both the *E. coli* and the *MDR P. aeruginosa,* whereas, the Aquacel Ag exhibited bactericidal activity against *E. coli* and enhanced bacterial inhibition against MDR *P. aeruginosa* (Figure 19 c & 19 d).

The antibacterial activities of the chitosan, honey, *Cleome droseifolia* and *Allium sativum* were reported against both Gram negative and Gram positive bacteria (Muhaidat et al., 2015; Muzzarelli et al., 1990; Gaherwal et al., 2004). Additionally, increased antibacterial effect against *S. aureus* compared to *E. coli* was observed for chitosan (No et al., 2002) and *Cleome droseifolia* oil (Muhaidat et al., 2015) as well as the honey and *Allium sativum* mixture (Andualem, 2013). This agrees with the results reported here regarding the enhanced antibacterial activity against the examined *S.aureus* and MRSA strains.

4.3.4 Evaluation of the wound healing abilities of the fabricated nanofibers.

The fabricated nanofibrous wound dressings and the commercial dressing Aquacel Ag were applied on a 9 mm excisional wound on the dorsal back of mice. For determination of the change in wound size over time, photographs of the wound area were taken on days 3, 5, 7, 10 and 12 (Figure 20). The wound healing ability of the examined nanofibrous wound dressings was determined via measurement of the percentage of the wound size remaining exposed at each time point as compared to the wound size on day 0 (Figure 20).

Honey and chitosan have well proven ability to enhance the wound healing process (Mandel & Mandel, 2011; Dai et al., 2011; Seckam & Cooper, 2013). Chitosan has been observed to beneficially influence every stage in the wound healing process (Dai et al., 2011). Chitosan indirectly enhances cell proliferation (Azuma et al., 2015) and stimulates migration of both the polymorphonuclear cells (PMN) and mononuclear cells (MN). Both of which showed the ability to degrade chitosan into its low molecular weight oligomers that exhibit profound capability to promote cell migration (Minami et al., 1997). Moreover, chitosan was observed for its stimulatory effects on macrophage nitric oxide production (Peluso et al., 1994). Honeys' wound healing ability has been historically recognized since ancient times. Such wound healing ability is related to honeys' ability to provide a moist wound healing environment, fast autolytic debridement and pro- as well as anti-inflammatory effects, in addition to honeys' antibacterial and antioxidant activities (Tonks et al., 2003, Majtan et al., 2006, Molan & Rhodes., 2015). *Allium sativum* have been recently studied for its effect on enhancing the wound healing process where it was reported that

it increases the re-epithelialization and neovascularization (Sidik et al., 2006). On the other hand, *Cleome droserifolia*, has not yet been evaluated for its effect on the wound healing process, however, Cleomes' antioxidant activity have been well observed (El-Khawaga et al., 2010; El-Shenawy & Abdel-Nabi, 2004) and antioxidants have been known for their ability to enhance the wound healing process via prevention of the overexposure of the wound site to oxidative stress which leads to delay in the wound healing process (Fitzmaurice et al., 2011).

As demonstrated in figure 20, the wound size decreased noticeably on day 3 as observed with the HPCS, HPCS-AE and HPCS-AE/CE nanofibrous dressings as compared to the wounds of the negative control. Additionally, all the examined wound dressings as well as the Aquacel Ag exhibited significant decrease in the wound size as well as the Aquacel Ag as compared to the negative control on days 5 and 7. At the same time there was nearly no reduction in the wound size of the negative control at day 5 (Figure 20).

It was observed that the rate of wound closure enhanced greatly with the HPCS nanofibrous mats and upon addition of aqueous extracts of AE in the HPCS-AE nanofibrous mats, the rate of wound closure increased. On the other hand, the rate of wound closure decreased upon addition of the dry extract of CE to the HPCS-CE nanofibrous mats. Whereas, the inclusion of the combination of both extracts within the nanofibrous mats of HPCS-AE/CE resulted in similar rates of wound closure to the HPCS nanofibrous dressings (Figure 20). Interestingly, it was observed that the HPCS-AE demonstrated enhanced wound closure rate as compared to the Aquacel Ag, whereas, both the HPCS and the HPCS-AE/CE demonstrated similar rates of wound closure to the commercial Aquacel Ag wound dressing.

The histopathology of the wound tissue was subsequently examined to observe the effect of the fabricated nanofibrous dressings on the different stages involved in the wound healing process. The wound tissues were H&E stained and their histopathology studied and scored at days 3, 5, 7, 10 and 12. Moreover, the collagen deposition in the wounded tissues was examined and scored at day 10 after staining the wound tissue with the MT stain (Figures 21 & 22, and Table 3). Necrotic tissue is usually accumulated in chronic wounds. Necrotic tissue is defined as dead tissue which most frequently results from inadequate blood supply. As observed in figure 21 and table 3, the application of all of the developed nanofibrous wound dressings as well as the positive control Aquacel Ag to the wound site reduced the necrosis as compared to the negative control, with the

most enhanced reduction in necrosis observed with the HPCS-CE since day 5. Additionally, the number of inflammatory cells reduced as compared to the negative control upon application of the developed nanofibrous wound dressings, where they completely disappeared at day 10 with the HPCS-AE/CE nanofibrous dressing. This indicates that the fabricated nanofibrous wound dressings prevented the prolongation of the inflammatory phase, which could be attributed to the anti-inflmmatory effects of the materials of the wound dressings as honey and Allium sativum. Moreover, it was realized that the number of macrophage cells was greater than the number of neutrophils in the treated wounds.

Early epithelization was observed in all the treated wounds as compared to the negative control with the AquacelAg, HPCS-AE/CE and HPCS-AE nanofibrous wound dressings demonstrating the earliest epithelization as well as formation of thicker epidermis (Figure 21 and Table 3). Additionally, both the HPCS-AE/CE and the Aquacel Ag allowed for earlier formation of granulation tissue. Moreover, the examined nanofibrous wound dressings as well as the Aquacel Ag allowed mature formation of granulation tissue together with dense collagen deposition (Figure 21 and Table 3). This was confirmed by the MT staining of the wound tissues at day 10 which showed that the regenerated collagen in the treated wounds was denser as compared to the negative control, and that both the nanofibrous mats of HPCS and the Aquacel Ag demonstrated the most dense deposition of collagen. It was also observed that the HPCS-AE, HPCS-AE/CE, HPCS, and the Aquacel Ag exhibited the most uniform distribution of collagen (Figure 22 and Table 3).
Overall, the scoring of the data of the histologic examination revealed that among the examined nanofibrous wound dressings, the HPCS-AE/CE exhibited the most enhanced effect on the wound healing process followed by the HPCS nanofibrous wound dressing having scores very similar to the Aquacel Ag. Both nanofibrous dressings allowed decrease in the inflammatory phase, and earlier formation of granulation tissue as well as earlier epithelization and deposition of thicker epidermis. Additionally, both nanofibrous wound dressing’s induced uniform and dense deposition of collagen.

4.3.5 Evaluation of the fibroblast cytotoxicity of the fabricated nanofibers and their effect on fibroblast cell proliferation.

The fabricated HPCS, HPCS-CE, HPCS-AE and HPCS-AE/CE nanofibrous mats as well as the commercial wound dressing Aquacel Ag were tested for their cytotoxicity using the MTT assay. Additionally, the effect of the fabricated nanofibrous dressings and the commercial wound dressing Aquacel Ag on fibroblast cell proliferation was evaluated via the MTT assay. Oxidoreductase cellular enzymes reflect the number of viable cells via reduction of the soluble tetrazolium dye (MTT; 3-(4, 5-dimethylthiazol-2-yl)-2, 5-diphenyltetrazolium bromide) to the insoluble purple formazan salt. The developed nanofibers were extracted and diluted to yield different extract concentrations; 100%, 75%, 50% and 25%, that were tested for their cytotoxicity. The fibroblast cells were cultured in the different dilutions of the extract and the cytotoxicity was determined via estimation of the viable cells after 48h (Figure 23a).

It was realized that both the HPCS-CE and the HPCS nanofibrous mats demonstrated the highest fibroblast cell viability of 90% and 87%, respectively in the 100% extract solution. Whereas, significant reduction in cell viability of 68% ($p < 0.05$) was observed with the HPCS-AE that increased to 75% upon adding CE to the HPCS-AE/CE nanofibers in the 100% extract solution (Figure 23a).On the other hand, it was observed that the commercial dressing Aquacel Ag at all tested dilutions exhibited increased cytotoxicity to the cultured fibroblasts ($p < 0.05$) and showed viable fibroblast cell counts of approximately 9% similar to the results observed with the cytotoxic control (Figure 23a).

Figure 23b demonstrates fibroblast cell proliferation results at 1 and 3 days as determined via the MTT assay. The OD values of the HPCS-AE/CE, HPCS-CE and HPCS nanofiber mats increased with the increase in culture time. Both the HPCS and the HPCS-CE nanofibrous mats exhibited the most significant enhancement ($p < 0.05$) in proliferation after 3 days of incubation (Figure 23b). Whereas the HPCS-AE nanofibrous mats exhibited nearly the same OD values at 1 & 3 days. On the other hand, the Aquacel Ag exhibited significant cytotoxic effect on the proliferation of the fibroblast cells as observed from the low OD values (Figure 23b). Such results confirm the previously reported cytotoxicity for the Aquacel Ag wound dressing in the previous evaluation of the cytotoxicity (Figure 23a). The observed cytotoxicity of the commercial wound dressing Aquacel Ag was previously reported in different studies (Yunoki et al., 2015; Burd et al., 2007).

Generally, the HPCS-CE and HPCS nanofibrous dressings exhibited the highest levels of cell proliferation and viability within the examined nanofibrous dressings. The addition of CE dry extract to the nanofibers of the HPCS-AE has increased their proliferation and cell viability results. Interestingly, all the fabricated nanofibrous mats exhibited major increase in cell proliferation and viability as compared to the Aquacel Ag commercial wound dressing (Figures 23a and 23b).

4.4 Evaluation of HPCS Nanofibers Loaded with Apitherapeutics and Bacteriophages as Antimicrobial Wound Dressings.

Apitherapeutics were loaded within the HPCS (30%:7%:3.5%) nanofibers as an alternative approach to enhance the antibacterial abilities of the developed nanofibers. Two apitherapeutics, namely: bee venom and propolis were loaded within the HPCS (30%:7%:3.5%) nanofibers and tested for their antibacterial abilities. Additionally, the nanofibrous mat that demonstrated the most enhanced antibacterial activity among the developed HPCS nanofibers loaded with natural extracts and apitherapeutics was selected and further loaded with bacteriophage. The bacteriophage was isolated against a bacteria resistant to the selected nanofibrous mat and electrospun with the selected combination of the nanofibrous mat, thus extending the spectrum of antibacterial activity of the selected nanofibrous mat. The developed apitherapeutic and bacteriophage loaded nanofibrous mats were examined for their swelling, weight loss, antibacterial, cytotoxicity, wound healing abilities as well as their abilities to enhance cell proliferation.

4.4.1Fabrication of the electrospun HPCS-Pr and HPCS-BV nanofibers.

Recently, propolis (Pr) has been co-spun into polymeric nanofibers and examined for its effect on the mechanical and antibacterial properties of the electrospun nanofibers. Ethanolic and aqueous propolis extracts have been loaded within the nanofibers in different concentrations ranging from 2 to 10% (Sutjarittangtham et al., 2012; Sutjarittangtham et al., 2014), however it was observed that at concentrations above 8% of ethanolic or aqueous propolis extract the solution could not be electrospun (Sutjarittangtham et al., 2014). Thus, in the current study the ability to fabricate uniform nanofibers loaded with 10% propolis was examined within the HPCS nanofibers.

Bee venom on the other hand has not yet been formulated in the nanofibrous form, however its diverse biomedical properties have been documented via different studies (Ali, 2012; Kwon et al., 2002; Kim et al., 2013). It was observed that bee venoms' antibacterial property was achieved via concentrations ranging from 12.5 to 25 ug/ml for Gram-positive bacteria and 1 to 10 mg/ml for Gram-negative bacteria (Lowenstein et al., 1997). Thus, bee venom was loaded within the HPCS nanofibers in the concentration of 1 mg/ml to be able to target both Gram positive and Gram negative bacteria.

The aqueous extracts of Pr and the dry powder of BV were added to the prepared solutions of HPCS prior to electrospinning. The electrospun mats were characterized via SEM (Figure 24) then subjected to analysis of the diameter of the nanofibers via image J. The HPCS solutions were previously spun into uniform bead free nanofibers of 464 ± 185 nm in diameter. As observed in figure 24, electrospinning of 10% Pr within the HPCS solution allowed for the collection of dense nanofibrous mats. However, due to the high concentration of Pr included within the nanofibers, noticeable branching was observed together with cluster formation within the nanofibers. Additionally, an increase in the diameter of the nanofibers over that of the previously spun HPCS was observed, where the average nanofiber diameter reached to 737 ± 260 nm with broad diameter distribution.

On the other hand, the inclusion of the BV within the HPCS nanofibers allowed for uniform deposition of the nanofibers with average diameter of 459 ± 140 nm and a focused diameter distribution (Figure 24). The inclusion of BV did not result in variation in the morphology of the nanofibers over the previously collected HPCS nanofibers. This could be attributed to the minute concentration of the included BV.

The parameters that were utilized in electrospinning both the HPCS-BV and HPCS-Pr solutions were a high electric potential of 27 kV (E-spin, NanoTech, Kalyan-pur, India) and a constant flow rate of 0.5 ml/h was maintained, whereas, the distance between the nozzle and the collector was maintained at 15 cm.

4.4.2 Evaluation of the swelling and weight loss abilities of the fabricated nanofibers.

The developed nanofibers of HPCS-Pr and HPCS-BV were examined for their swelling abilities after immersion in PBS (pH 7.4) for 1, 4, and 24 h. Crosslinking was performed by exposing the nanofibers to GA vapors for 1 & 3 hours with subsequent heating at 40°C.

As observed in figure 25, the HPCS-BV demonstrated enhanced swelling values as compared to the HPCS-Pr nanofibers at 1, 4 and 24h. The HPCS-BV exhibited swelling values similar to those previously reported for the HPCS nanofibers. This is because of the small concentration of BV

added to the HPCS nanofibers, thus, such low concentration did not result in variation of the swelling properties of the HPCS nanofibers.

The HPCS-Pr nanofibers exhibited very small swelling values, especially at 4h and 24h. This may be attributed to the high concentration of the included propolis (10%), which decreased the available void left for water uptake and swelling. Moreover, the observed increase in weight loss (Figure 25c) of the HPCS-Pr nanofibers is another reason for the decreased swelling values recorded for the HPCS-Pr due to the loss of the compact structure that allows the water uptake (Figure 25).

The increase in the crosslinking time resulted in slight effect on the swelling abilities of the HPCS-BV nanofibers, where a slight decrease in the swelling ability was observed at 24h. This could be attributed to the effect of crosslinking on hindering of the chain entanglements and intermolecular motion within the nanofibers (Kim et al., 1992).The effect of crosslinking was more pronounced on the HPCS-Pr nanofibers, where the swelling abilities of the HPCS-Pr nanofibers decreased noticeably. On the other hand, weight loss was slightly decreased upon increasing the crosslinking time to 3h.

4.4.3 Evaluation of the antibacterial abilities of the fabricated nanofibers.

Propolis and bee venom are two natural apitherapeutics that have demonstrated effective antibacterial activity against different kinds of bacteria (Hegazi et al., 2015; Popova et al., 2005; Kujumgiev et al., 1999). Bee venom's antibacterial activity is related to a number of peptides like melittin, adolapin, apamin and mast cell degranulating peptides as well as biologically active amines and non-peptide components (Kwon et al., 2002; Fennel., 1968). Whereas propolis antibacterial activity is mainly attributed to its content of flavonoids and cinnamic acid (Sharaf et al., 2013; Popova et al., 2005). It was observed that propolis prevents cell wall division, and causes disorganization of the cytoplasm, cell wall and the cytoplasmic membrane leading to inhibition of protein synthesis and bacteriolysis (Lotfy, 2006).

In this research propolis and bee venom have been loaded within the previously spun HPCS nanofibers and examined for their antibacterial activities against *S. aureus*, *E. coli* and two resistant strains; MDR *P. aeruginosa* and MRSA. The commercial wound dressing Aquacel Ag was used as a positive control, whereas untreated bacterial broth was utilized as a negative control.

As observed in figure 26, the inclusion of bee venom within the HPCS nanofibers in the HPCS-BV nanofibers allowed for noticeable enhancement in the antibacterial activity even against resistant bacterial strains. The HPCS-BV nanofibers allowed for complete bacterial inhibition of *E.coli* similar to the effect of the commercial Aquacel Ag. Such results agree with the previously reported enhanced antibacterial activity of bee venom against *E.coli* (Hegazi et al., 2014). Additionally the HPCS-BV nanofibers exhibited enhanced antibacterial activity over the commercial Aquacel Ag against the tested Gram positive strains where it demonstrated ~ 6 log and 5 log reduction in the bacterial count of *S.aureus* and MRSA respectively as compared to ~ 4 log and 2 log reduction in case of the Aquacel Ag. However, the HPCS-BV nanofibers exhibited no antibacterial activity against *P. aeruginosa,* whereas, the Aquacel Ag demonstrated enhanced antibacterial activity against it (Figure 26).

The HPCS-Pr nanofibers on the other hand exhibited weaker antibacterial activity than the HPCS-BV nanofibers. As compared to the Aquacel Ag, the HPCS-Pr demonstrated enhanced antibacterial activity against both *S.aureus* and MRSA, whereas against *E.coli* and MDR *P. aeruginosa* it exhibited nearly no antibacterial activity compared to enhanced antibacterial activity with the Aquacel Ag (Figure 26).

According to the antibacterial results of the HPCS nanofibers loaded with the natural extracts (Figure 19) and apitherapeutics (Figure 26), it was observed that the HPCS-BV nanofibers exhibited the most enhanced antibacterial activity among the developed nanofibers. The HPCS-BV nanofibers demonstrated enhanced antibacterial activity against *E.coli*, *S.aureus*, and MRSA, stronger than that observed with the commercial wound dressing Aquacel Ag. However, it exhibited nearly no antibacterial activity against *P. aeruginosa,* unlike the Aquacel Ag that demonstrated enhanced antibacterial activity against it. *P. aeruginosa* is considered the most commonly encountered Gram negative bacteria in wounds (Gjødsbøl et al., 2006; Burmølle, 2010). Thus, HPCS-BV was selected to be further loaded with a bacteriophage against P. *aeruginosa* in order to develop a nanofibrous wound dressing with broad spectrum antibacterial activity against the most common bacterial pathogens encountered at the wound site.

4.4.4 Isolation, electrospinning and antibacterial evaluation of the bacteriophage loaded nanofibers

The alarming rise in bacterial resistance has revived the interest in bacteriophage therapy. Bacteriophages are viruses that specifically infect and rapidly destroy bacteria. Although bacteriophages are now witnessing increased research and are applied in food preservation, integration of phage therapy in human therapeutics is still facing many challenges among them is their narrow host range (Sarhan & Azazzy., 2015b). Utilization of bacteriophage in wound care has been examined in a number of studies (Rhoads et al., 2009; Seth et al., 2013), however, its integration into nanofibrous wound dressing with broad spectrum antibacterial activity has not yet been realized.

The phage plaque assay was utilized for the isolation of a bacteriophage against the MDR *P. aeruginosa* from the different sewage samples collected and then subsequently purified and amplified into a *P. aeruginosa* phage (PS1) suspension. The PS1 phage was then subjected to morphological characterization via TEM. The results of the TEM imaging revealed that the PS1 phage exhibits an icosahedral head of 71 nm in diameter and a contractile tail of 110–115 nm in length (Figure 27a). Thus, the bacterial virus was classified as a representative of the Myoviridae family (Soothill, 1992; Ackermann et al., 1994).

The PS1 phage stock solution (10^9-10^{10} PFU mL $^{-1}$) was loaded within the HPCS-BV solution and subjected to electrospinning at 27 kV, 0.5 ml/h as flow rate, whereas the distance between the needle and the collector was maintained at 13 cm. The fibers collected were characterized via SEM which revealed a dense and uniform bead free deposition of the HPCS-BV/PS1 nanofibers (Figure 27b). The analysis of the fiber diameter distribution illustrated that the diameter distribution of the collected nanofibers did not show a noticeable difference from that of the HPCS-BV nanofibers (Figure 26) with an average diameter of 498 ±145 nm (Figure 27c) and a focused fiber diameter distribution.

The HPCS-BV/PS1 nanofibers were examined for their antibacterial activity against MDR *P. aeruginosa*. Bacteriophages are characterized by their instant antibacterial activity, where lysogenic phages are adsorbed on the surface of the bacterial cell followed by injection of the phages' genetic material into the bacterial cell cytoplasm. The host cell machineries are then utilized for making new phages and then the host cell is killed at the end of the growth cycle

(Sulakvelidze, 2011). To observe the antibacterial activity of the phage loaded nanofibers, the examined nanofibers as well as the controls were tested for the antibacterial activity after 24h. The results revealed strong antibacterial activity against MDR *P. aeruginosa* for the HPCS-BV/PS1 nanofibers which exceeded that of the Aquacel Ag (Figure 27d). Complete bacterial inhibition of the MDR *P. aeruginosa* was achieved via the HPCS-BV/PS1 nanofibers whereas the Aquacel Ag still showed week bacterial growth (Figure 27d).

Loading of the HPCS-BV nanofibers with the PS1 bacteriophage allowed for extension of the antibacterial activity of HPCS-BV against MDR *P. aeruginosa*. At the same time, the developed HPCS-BV/PS1 represents a broad spectrum bacteriophage formulation, where the combination of the natural materials of the nanofiber and the bacteriophage allowed the nanofibrous formulation to exhibit broad spectrum antibacterial activity. The observed results (figures 26 & 27d) illustrate that the HPCS-BV/PS1 nanofibers exhibit enhanced antibacterial activity over the commercial Aquacel Ag even against resistant bacterial strains. Aquacel Ag was recently reported to exhibit the strongest antibacterial activity among other silver based wound dressings in the market (Yunoki et al., 2015). Thus, this indicates the enhanced efficacy of the developed HPCS-BV/PS1 as an antibacterial formulation.

4.4.5 Evaluation of the wound healing abilities of the fabricated nanofibers.

The developed nanofibrous mats were evaluated for their effect in enhancing the wound healing process. Propolis has well proven ability to enhance the wound healing process (Mandel & Mandel, 2011; Seckam & Cooper, 2013; Dai et al., 2011; McLennan et al., 2008), whereas the wound healing ability of bee venom is recently recognized (Amin & Abdel-Raheem, 2014). Propolis, an important component of the bee hive was observed to exhibit wound healing ability due to its antimicrobial, antioxidant, immunomodulatory, anti-inflammatory and analgesic effects (Sforcin, 2007; Cardoso et al., 2010; Ramos et al., 2012). It was demonstrated that both caffeic and phenethyl ester present in propolis exhibit immunosuppressive activities on T-cells which play a significant role in several inflammatory diseases (Lotfy, 2006). Bee venom exhibits anti-inflammatory and antimicrobial activities that were proven beneficial in enhancing the wound healing process (Hider, 1988; Seo et al., 2008). It was recently observed that bee venom limits the prolongation of inflammation via regulating the levels of inflammatory cytokines (Kwon et al., 2002; Abu-Seida, 2015).

A 9 mm excisional wound was performed on the dorsal back of mice upon which the developed nanofibrous mats were applied. The wound region was photographed on days 3, 5, 7, 10 and 12 to illustrate the variation in the wound over time (Figure 28). Additionally, to determine the ability of the nanofibrous mats to enhance the wound closure rate, the wound size remaining exposed (%) was determined by comparing the wound size at each time point with the wound size at day 0 (Figure 28). Aquacel Ag was utilized as the positive control in the wound healing study of the developed nanofibrous mats and the subsequent histopathological examination.

As observed in figure 28, the HPCS-Pr, HPCS-BV and HPCS-BV/PS1 nanofibers as well as the Aquacel Ag exhibited enhanced wound closure rate as compared to the negative control covered with a cotton gauze.

Interestingly, it was observed that the HPCS-Pr demonstrated enhanced wound closure rate as compared to the commercial Aquacel Ag wound dressing. The enhanced effect of HPCS-Pr on wound healing was realized from day 3, with significant reduction in the wound size as compared to both the negative control and the Aquacel Ag. The HPCS-BV nanofibers, on the other hand exhibited similar wound closure rate to the positive control Aquacel Ag, whereas upon addition of PS1 to the HPCS-BV nanofibers a slight enhancement in the wound closure rate was observed (Figure 28). This could be attributed to the change in the weight loss rate of the HPCS-BV/PS1 nanofibers as compared to the HPCS-BV nanofibers because of the dilution of the HPCS-BV polymeric solution with 10% of the phage stock solution while electrospinning the HPCS-BV/PS1 nanofibers. This allows for the presence of increased concentration of the materials of the nanofibers at the wound site which leads to enhancement of the wound healing process due to the beneficial effects of the materials of the nanofibers on the wound healing process.

The reduction in the healing time could be attributed to the presence of the apitherapeutics, honey, propolis and bee venom as well as chitosan in the developed nanofibers. This is due to the anti-inflammatory effect of these materials that prevent prolongation of the inflammatory response that delays the wound healing process (Alvarez-Suarez et al., 2014). Moreover, the antibacterial properties of the utilized materials; honey, bee venom, propolis and chitosan prevent the presence of persistent inflammatory stimuli due to the presence of bacteria at the wound site and thus prevent the prolongation of the inflammatory phase (Bjarnsholt et al., 2008).

It is worth mentioning that the fabricated nanofibrous wound dressings easily attached to the wound site, eliminating the need for biological adhesives. This could be attributed to the hydrophilic nature of the CS, P and H in addition to the increased water solubility of the high honey concentration included within the nanofibers. Thus, the fabricated nanofibrous wound dressings allow to keep the wound desirably hydrated.

Samples of the wound tissue were H&E stained and their histopathology evaluated and scored at days 3, 5, 7, 10 and 12 days. Moreover, samples at day 10 were MT stained and examined for collagen deposition (Figures 29 & 30 and Table 4).

It was observed from the histological data (Figure 29 and Table 4) that the HPCS-Pr allowed for the most enhanced reduction in necrosis since day 5. At the same time, all the examined nanofibrous dressing and the Aquacel Ag decreased the necrosis as compared to the negative control. Such effect could be attributed to the anti-inflammatory effect of honey, chitosan, bee venom, and propolis which reduces the damage caused by the free radicals resulting from inflammation thus preventing further necrosis (Alvarez-Suarez et al., 2014).

Additionally, the application of the developed nanofibrous dressings to the wound site prevented prolongation of the inflammatory phase, especially with the HPCS-Pr and the HPCS-BV/PS1 nanofibrous wound dressings, where the inflammatory cells were last observed at day 7, whereas in the case of the negative control they persisted till day 12. Consequently, this allowed for early epithelization as well as formation of thick epidermis in the wounds treated with the nanofibrous dressings as well as the Aquacel Ag (Figure 29 and Table 4). Such results agree with previously reported results for bee venom, honey and propolis regarding their anti-inflammatory effect and thus their ability to decrease inflammation (Kwon et al., 2002; Molan, 2006; Han et al., 2012; Castaldo, 2002; Peng et al., 2008).

Earlier formation of granulation tissue was observed in the wounds treated with the Aquacel Ag, HPCS-Pr, and HPCS-BV/PS1, thus, indicating accelerated wound healing rate. Dense collagen deposition was observed with all the tested nanofibrous dressings and was confirmed via staining of the wounds with MT stain at day 10 and comparing them to the commercial Aquacel Ag due it its documented effect on enhancing the wound healing process (Barnea et al., 2010) (Figure 30 and Table 4).

As seen in figure 30 all the examined nanofibrous dressings allowed for dense collagen deposition as well as uniform collagen distribution similar to that observed with the Aquacel Ag. Previously,

it was reported that the presence of large amounts of collagen is correlated to adequate wound healing (Drucker et al., 1998).

Overall, it was observed that the developed nanofibrous dressings demonstrated enhanced wound healing rates as compared to the Aquacel Ag. In Fact, the HPCS-Pr demonstrated enhanced effect on wound healing more than that observed via the Aquacel Ag according to the histopathological examination and the scoring of the histologic data (Table 4), whereas, the HPCS-BV and HPCS-BV/PS1 nanofibrous dressings demonstrated similar results to the Aquacel Ag. Such results are of significant importance due to the current focus on honey and natural products with antimicrobial activity to be used as advanced antimicrobial wound care products in clinical practice (Alvarez-Suarez et al., 2014; Frost & Sullivan, 2014). Especially, that the current therapeutic protocols rely on silver, and despite their efficacy as antimicrobial wound dressings the undesirable side effects associated with silver are generating increasing concern (Demling & DeSanti, 2001; Alvarez-Suarez et al., 2014).

4.4.6 Evaluation of the fibroblast cytotoxicity of the fabricated nanofibers and their effect on fibroblast cell proliferation.

The developed HPCS-Pr, HPCS-BV and HPCS-BV/PS1 nanofibers were evaluated for their cytotoxicity on human dermal fibroblasts as well as for their effect on the cell proliferation via the MTT assay. Additionally, the effect of the commercial wound dressing Aquacel Ag on cell cytotoxicity and proliferation was evaluated and used as a positive control in both tests.

The developed nanofibers were extracted and diluted to yield different extract concentrations; 100%, 75%, 50% and 25%), that were tested for their cytotoxicity. The fibroblast cells were cultured in the different dilutions of the extract and the cytotoxicity was determined via estimation of the no of viable cells after 48h (Figure 31a).

As observed in figure 31a, the HPCS-BV nanofibers exhibited the highest cell viability even at 100% extract concentration thus indicating that loading of HPCS nanofibers with BV did not affect the biocompatibility of the nanofibers. Whereas, the HPCS-BV/PS1 nanofibers demonstrated a minor decrease in the viability of the fibroblast cells compared to the HPCS-BV nanofibers. This may be attributed to the increase in weight loss of the HPCS-BV/PS1 compared to the HPCS/BV nanofibers due to the loading of the nanofibers with 10% phage stock solution, where the loaded

solution affected the degradation rate of the polymeric based nanofibers, resulting in an increase in weight loss of the nanofibers. Thus, the amount of the released components including BV from the HPCS-BV/PS1 nanofibers increased which resulted in a minor change in cell viability. However, despite the reduction in cell viability due to the HPCS-BV/PS1 nanofibers it still exhibited significant ($p < 0.05$) enhancement in cell viability compared to the commercial Aquacel Ag dressing that demonstrated noticeable cytotoxic effects.

On the other hand, the HPCS-Pr nanofibers demonstrated a noticeable reduction in cell viability in the 100% and 75% extract solutions (Figure 31a). This may be due to the increased concentration of propolis loaded within the nanofibers. Propolis has been proven to exert cytotoxic effects on different tumor cell lines, however, it also demonstrated some cytotoxicity for non-tumor cell lines (da Silva et al., 2013; Calhelha et al., 2014). Moreover, Kim et al studied the cytotoxic effects of polyurethane nanofibers loaded with 5, 10 and 30% of propolis solution and demonstrated that the 5% propolis solution loaded nanofibers allowed for the most enhanced cell proliferation even after 7 days, whereas increasing the concentration of the loaded propolis solution to 30% resulted in decreased proliferation rates, taking into consideration that loading with 10% propolis solution extract contains less amount of propolis than loading with the same percent of dry powder propolis extract as was performed in the current study (Kim et al., 2014). Despite the reduction in cell viability observed with the HPCS-Pr nanofibers it still demonstrated significant ($p < 0.05$) enhancement in cell viability compared to the Aquacel Ag commercial dressing (Figure 31a).

The effect of the developed nanofibers as well as the Aquacel Ag on fibroblast cell proliferation was studied at 1 and 3 days. Figure 26b demonstrates the proliferation results as determined via the MTT assay. It was observed that HPCS-Pr demonstrated the lowest OD values among the developed nanofibers, whereas the HPCS-BV nanofibers exhibited the highest OD values followed by the HPCS-BV/PS1 nanofibers at 24h. However, none of the developed nanofibers allowed an enhancement in the proliferation of the fibroblast cells after 3 days of incubation. This may be related to the increased concentration of the released BV and Pr in the medium following prolonged incubation, especially that recent evaluation of the HPCS nanofibers on the fibroblast cell proliferation revealed significant enhancement in proliferation at 3 days of incubation. Compared to the commercial Aquacel Ag dressing, both the HPCS-BV and HPCS-BV/PS1 demonstrated significant increase in cell viability at both 24 and 72h as observed via the OD

values. The observed cytotoxicity of the Aquacel Ag was previously reported in different studies (Yunoki et al., 2015; Burd et al., 2007).

It is of note that the swelling capabilities of the nanofibrous mats and their capabilities to enhance cell proliferation and viability could be increased by increasing the pore diameter. This could be achieved by changing of the parameters utilized during the electrospinning process (Kazemi Pilehrood et al., 2014) or by inclusion of some treatments as carbon nanotubes before electrospinning (Shokrgozar et al., 2011). Additionally, the nanofibrous mats density must be taken into consideration as an increase in the density will result in reduction in the breathability of the fabricated nanofibrous mats and thus, lead to restriction in nutrient and metabolic waste transportation and reduction in cell viability as well as decrease in the swelling capability of the fabricated nanofibrous mats. Within this context it was observed that ultrasonication of the fabricated nanofibrous mats could help overcome such limitation (Lee et al., 2011). Moreover, collection of nanofibrous mats of low density on a substrate could be another approach to be undertaken to overcome such limitation. Thus, future work on the fabricated nanofibrous mats will consider optimization of the breathability of the nanofibrous mats by different approaches with subsequent testing of the effect of each approach on the cell proliferation and viability as well as the swelling capability of the fabricated nanofibers.

5. CONCLUSION

Non-healing wounds represent a pressing health care problem with major socioeconomic impacts. The success in managing bacteria in wounds is of outmost importance, this is because bacterial infection stimulates the immune system which in turn prolongs tissue inflammation thus further delaying the healing process. Moreover, wound associated bacterial infection usually develops resistance to commonly used antibacterials, thus leading to increased risk of systemic infections. Antimicrobial advanced wound dressings stand as an important sector in the treatment of wound infections. Silver-based dressings stand as one of the most common and effective antimicrobial dressings used. However, despite their enhanced broad spectrum antibacterial activity, development of resistance has been reported together with some undesirable side effects of silver. Thus, through the current research different approaches have been undertaken to develop a series of effective antimicrobial wound dressings based on effective antimicrobials that are more biocompatible and able to achieve enhanced antibacterial and wound healing activity.

The first objective in this study was to develop nanofibrous wound dressing based on high honey concentration. Different concentrations of honey (H) and chitosan (CS) were electrospun with poly(vinyl alcohol) (P) resulting in HPCS nanofibers having H concentrations up to 40% and CS concentration up to 5.5%. The combination of H and CS had a synergistic effect on the solution viscosity causing it to reach to the viscosity optimum for electrospinning. Such effect allowed for the first time for the development of nanofibers comprising 40% honey of their actual weight as compared to only 9% in previous attempts without the use of toxic solvents. Chemical and physical crosslinking of the fabricated HPCS nanofibers allowed different degrees of crosslinking, thus extending their areas of application.

Subsequently, different honey concentrations (10%, 20% and 30%) were electrospun within the chitosan (3.5%) /poly (vinyl alcohol) (7%) nanofibers to study the effect of changing the honey concentration on the different properties of the electrospun nanofibers. It was observed that increasing the honey concentration resulted in an increase in the fibre diameter from 284 ± 97 nm with 10% honey to 464 ± 185 nm with 30% honey. The swelling of the nanofibers was greatly influenced by the concentration of incorporated honey and the degree of crosslinking. Highest swelling extent was observed with HPCS nanofibers having 10% honey, and the least swelling

was noted in the HPCS nanofibers having 30% honey. The crystallization and thermal stability of the nanofibers on the other hand were not affected by changing the honey concentration within the developed HPCS nanofibers. The antibacterial activities of the HPCS nanofibers with different honey concentrations was evaluated against *S.aureus* and *E.coli* at two different bacterial counts. It was observed that increasing the honey concentration within the HPCS nanofibers enhanced their antibacterial activity against both *S. aureus* and *E.coli* at 7×10^7 CFU/ml. Whereas, at 7×10^8 CFU/ml nearly no antibacterial effect was realized against *E.coli* at all honey concentrations included within the HPCS nanofibers. Due to the enhanced antibacterial activity of the HPCS nanofibers loaded with 30% honey they were selected to be further loaded with other antimicrobials.

The second objective was to load the developed HPCS nanofibers with natural extracts to enhance their antibacterial and wound healing abilities. *Allium sativum* (AE) and *Cleome droserifolia* (CE) were loaded within the selected HPCS nanofibers. Allium sativum aqueous extract substituted 50% of the solvent of the HPCS in the HPCS-AE nanofibers and 10% of dried aqueous extract of *Cleome droserifolia* were loaded within the HPCS in the HPCS-CE nanofibers whereas, the HPCS-AE/CE were loaded with both the AE and CE extracts. The HPCS, HPCS-CE, HPCS-AE and HPCS-AE/CE nanofibrous mats were characterized and examined for their weight loss, swelling, cytotoxicity and wound healing capabilities. Moreover, the antibacterial activities of the developed nanofibers were evaluated against *S. aureus, E.coli,* MRSA and MDR *P. aeruginosa*. The antibacterial, wound healing abilities and cytotoxicity results were compared to those of the commercial wound dressing Aquacel Ag. It was observed that substitution of 50% of the solvent with AE resulted in massive reduction in the HPCS solution viscosity. The HPCS-AE/CE nanofibrous mats demonstrated the lowest swelling capabilities and the highest weight loss among the fabricated nanofibers at two tested crosslinking degrees (1h and 3h exposure to GA vapours followed by heating at 40 ºC for 24h) showing values of less than 90% weight loss and 15% swelling as compared to 60-70% weight loss and ~ 90% swelling in the case of HPCS and HPCS-AE after immersion in PBS buffer for 24h. The antibacterial evaluation demonstrated that the fabricated nanofibers exhibited no antibacterial activities against *E.coli* and *MDR P. aeruginosa.* However, complete bacterial inhibition of *S. aureus* better than that produced with the commercial dressing Aquacel Ag was achieved with both the HPCS-AE and the HPCS-AE/CE nanofibrous dressings. Moreover, the bacterial count of MRSA decreased by 1.5 log with the HPCS-AE/CE as

compared to 3.5 log decrease in bacterial count with the Aquacel Ag. On evaluation of the wound healing capabilities of the fabricated nanofibrous dressings as compared to the Aquacel Ag, it was observed that the HPCS-AE/CE and the HPCS exhibited similar wound closure rates whereas the HPCS-AE allowed enhancement in the wound closure over that exhibited via the Aquacel Ag. The scoring of the histopathological data showed that both the HPCS and the HPCS-AE/CE nanofibrous wound dressings demonstrated the most enhanced effects on the different stages in the wound healing process with scores very close to the Aquacel Ag. Most importantly, it was observed that the HPCS-CE, HPCS-AE/CE and HPCS exhibited the highest levels of proliferation and cell viability as compared to the commercial Aquacel Ag that demonstrated noticeable cytotoxicity.

The third objective achieved in this study was to load the fabricated HPCS nanofibers with apitherapeutics as another approach to develop effective biocompatible antimicrobial wound dressings. The HPCS nanofibers were loaded with apitherapeutics; bee venom (0.01%) in the HPCS-BV nanofibers and propolis (10%) in the HPCS-Pr nanofibers. The developed nanofibers were characterized and examined for their swelling and weigh loss abilities as well as their antibacterial activities against *S. aureus, E. coli,* MRSA and MDR *P.aeruginosa*. It was observed that the diameter of the HPCS-Pr nanofibers was 737 ± 260 nm, whereas, the HPCS-BV exhibited nanofiber diameter of 459 ± 140 nm. Moreover, the lowest swelling values were observed with the HPCS-Pr nanofibers, showing values of 20% and 29% as compared to 76% and 90% with the HPCS-BV nanofibers at 1 and 3 h of crosslinking, respectively. Whereas, the lowest weight loss values 65-55% were exhibited by the HPCS-BV nanofibers after 24h in PBS at the two tested crosslinking degrees (1h and 3h exposure to GA vapours followed by heating at 40 ºC for 24h). The results of the antibacterial study demonstrated strong antibacterial activity of the HPCS-Pr nanofibers against the tested Gram positive strains *S.aureus* and MRSA as compared to the commercial Aquacel Ag wound dressing. However, the HPCS-BV demonstrated enhanced antimicrobial activity over the HPCS-Pr nanofibers where it exhibited enhanced antibacterial activity against *S.aureus*, MRSA and *E.coli* more than that observed with the Aquacel Ag. Nevertheless, no antibacterial activity was achieved against MDR *P. aeruginosa* whereas the Aquacel Ag exhibited strong antibacterial activity against it. Thus, the HPCS-BV was selected to be further loaded with a bacteriophage against *P. aeruginosa* and achieve the forth objective of the current study. The bacteriophage PS1 was isolated against the examined MDR *P. aeruginosa* and

loaded within the HPCS-BV nanofibers extending the spectrum of antibacterial activity of the HPCS-BV/PS1 to include *P.aeruginosa* causing nearly complete inhibition of it. The developed HPCS-Pr, HPCS-BV and HPCS-PV/PS1 were further tested for their cytotoxicity and wound healing abilities. The wound healing study results demonstrated that the HPCS-Pr exhibited wound closure rates and histopathological scores better than those demonstrated with the Aquacel Ag, whereas the HPCS-BV and HPCS-BV/PS1 exhibited similar wound healing results to the Aquacel Ag. Most importantly, it was observed that the developed HPCS-BV and HPCS-BV/PS1 nanofibers demonstrated enhanced biocompatibility as compared to the Aquacel Ag that exhibited strong cytotoxicity. Whereas, the HPCS-Pr demonstrated some cytotoxicity at 100% and 75% extract solutions however, they were significantly lower than those observed with the Aquacel Ag.

Through the current study, a series of nanofibrous wound dressings based on natural materials were fabricated. The fabricated nanofibrous dressings, HPCS, HPCS-AE, HPCS-CE, HPCS-AE/CE, HPCS-BV, HPCS-Pr and HPCS-BV/PS1demostrated enhanced wound healing abilities and variable antibacterial effects against the examined bacterial strains as compared to the commercial Aquacel Ag. Most importantly the Aquacel Ag was proved to exhibit noticeable cytotoxicity on fibroblasts, whereas the fabricated nanofibrous dressings demonstrated enhanced biocompatibility, with the HPCS demonstrating the most enhanced cell viability and proliferation results. The HPCS nanofibrous dressing comprising 10% H demonstrated the highest swelling capability and thus the highest ability to absorb exudates. Among the developed nanofibrous dressings the HPCS-Pr demonstrated the most enhanced effect on wound healing, more pronounced than Aquacel Ag. Whereas, the HPCS-BV/PS1 demonstrated the most enhanced antibacterial activities exceeding the commercial Aquacel Ag and at the same time demonstrating similar wound healing effects and enhanced biocompatibility. Overall, the fabricated series of nanofibrous dressings exhibited antibacterial and wound healing abilities as well as enhanced biocompatibility, thus they represent competitive candidates to be used as effective wound dressings.

6. RECOMMENDATIONS AND FUTURE DIRECTIONS

Recommendations for future work on the developed series of honey based nanofibrous dressings include examination of the mechanical properties of the developed nanofibrous dressing and optimization of the mechanical properties of the developed nanofibrous dressings to be suitable for wound healing applications via the use of different fillers or different levels of crosslinking as well as utilization of polymers with enhanced mechanical properties. Furthermore, evaluation and optimization of the breathability of the developed series of honey based dressings will be undertaken. Additionally, the effect of loading the nanofibrous dressings with different natural materials as well as growth factors on the wound healing and antibacterial abilities of the developed nanofibrous dressings will be further explored. That's in addition to evaluating the effect of co-spinning different kinds of polymers with honey and evaluating the effect of such combinations on the swelling, degradation, and mechanical properties of the developed nanofibers.

The possible effect of honey and *Allium sativum* aquous extracts on the degredation of chitosan will be investigated via determination of the molecular weight of the chitosan after treatment with honey and *Allium sativum* aquous extracts. Additionally, the kinetics of release of the natural componenets included within the nanofibers will be studied as well as the degredation rate of the developed nanofibrous mats. Moreover, more biocompatible methods of crosslinking will be investigated. Additionally, the wound healing abilities of the developed nanofibrous mats will be tested on chronic non-healing wounds as well as infected wounds.

7. TABLES

Table 1. Change in the viscosity (mPas) of the P, PCS and HPCS solutions upon aging (Sarhan & Azazzy, 2015).

Sample	**2h**	**24h**	**48h**	**168h**
P (7%)	300	328	385	404
HP (30%:7%)	175	214	245	319
PCS (7%:3.5%)	86120	162830	152020	122180
HPCS(10%:7%:3.5%)	41120	9770	6100	2787
HPCS(30%:7%:3.5%)	27500	6520	3830	1851

Table 2: Change in the viscosity (mPas) of the HPCS and HPCS-AE solutions upon aging (Sarhan et al., 2016).

Sample	**2h**	**24h**	**48h**	**168h**
HPCS	27610	6990	3660	1980
HPCS-AE	1410	640	420	420

Table 3. Histological scoring system for MT and H&E stained wound tissues for both the control and experimental groups (Sarhan et al., 2016).

Histopathological lesions	Control group					Aquacel Ag					HPCS-AE					HPCS					HPCS-AE/CE					HPCS-CE				
	3	5	7	10	12	3	5	7	10	12	3	5	7	10	12	3	5	7	10	12	3	5	7	10	12	3	5	7	10	12
Necrosis	+++	+++	++	+	-	++	++	+	-	-	++	++	+	-	-	++	++	+	-	-	++	++	+	-	-	++	++	-	-	-
Inflammatory cells	+++	+++	++	++	++	+++	+++	+++	+	+	++	++	++	+	+	+++	+++	++	-	-	+++	++	++	-	-	++	++	++	+	+
Hemorrhage	++	++	++	+	-	-	-	-	-	-	-	-	-	-	-	-	-	-	-	-	-	-	-	+	-	-	-	-	-	-
Granulation tissue maturation	-	-	++	++	++	-	++	++	+++	+++	-	-	++	++	+++	-	-	++	+++	+++	-	+	+++	+++	+++	-	+	+	+++	+++
Epithelization	-	-	-	-	+++	-	-	+	+++	+++	-	-	-	++	+++	-	-	-	+++	+++	-	-	-	+++	+++	-	-	-	+	+++
Epidermis Thickness	-	-	-	-	++	-	-	-	++	+	-	-	-	-	++	-	-	-	++	+	-	-	-	+	++	-	-	-	-	+
Collagen deposition				+	+				+++	+++				++	+++				+++	+++				++	+++				++	++
Collagen distribution				+	+				+++	+++				+++	+++				+++	+++				+++	+++				++	++

The number of the histopathological scores: 0:_; 1:+; 2:++; 3:+++.

Table 4. Histological scoring system for Masson's trichome and H&E stained wound tissues for both the control and experimental groups.

Histopathological lesions	Control group					Aquacel Ag					HPCS-Pr					HPCS-BV					HPCS-BV/PS1				
	3	5	7	10	12	3	5	7	10	12	3	5	7	10	12	3	5	7	10	12	3	5	7	10	12
Necrosis	+++	+++	++	+	--	++	++	+	--	--	++	++	+	--	--	++	++	+	--	--	++	++	+	--	--
Inflammatory cells	+++	+++	++	++	+	+++	+++	+++	+	+	++	++	++	--	--	+++	+++	++	+	--	+++	++	++	--	--
Hemorrhage	++	++	++	+	--	--	--	--	--	--	--	--	--	--	--	--	--	--	--	--	--	--	--	+	--
Granulation tissue maturation	--	--	++	++	++	--	++	++	+++	+++	--	+++	+++	+++	+++	--	--	++	+++	+++	--	+	+++	+++	+++
Epithelization	--	--	--	--	+++	--	--	+	+++	+++	--	--	--	+++	+++	--	--	--	+++	+++	--	--	--	+++	+++
Epidermis Thickness	--	--	--	--	++	--	--	--	++	+	--	--	--	++	+++	--	--	--	++	++	--	--	--	++	++
Collagen deposition					+				+++	+++				+++	+++				+++	+++				++	++
Collagen distribution					+				+++	+++				+++	+++				+++	+++				+++	+++

¶

The number of the histopathological scores: 0:--; 1:+; 2:++; 3:+++

8. FIGURES

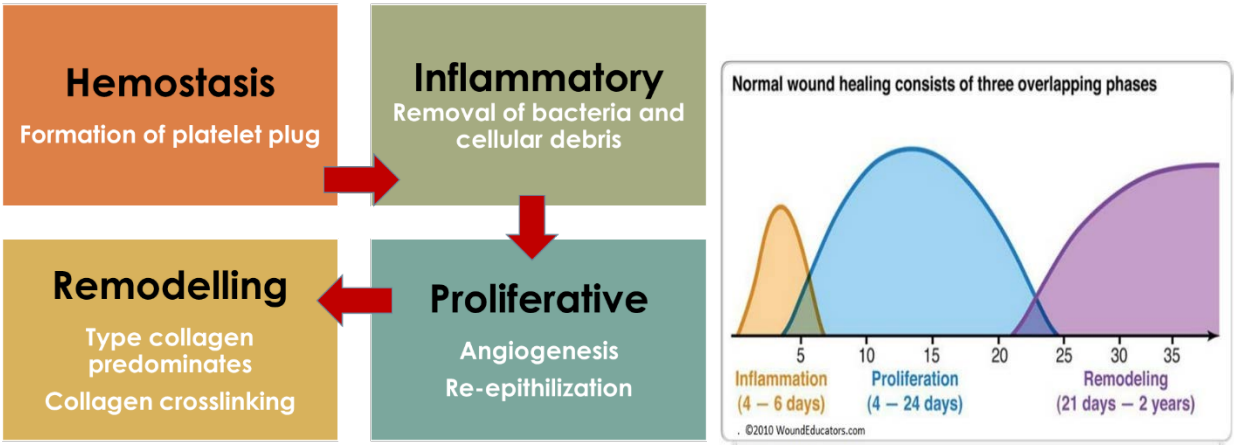

Fig 1: Schematic illustration of the different phases involved in the wound healing process.

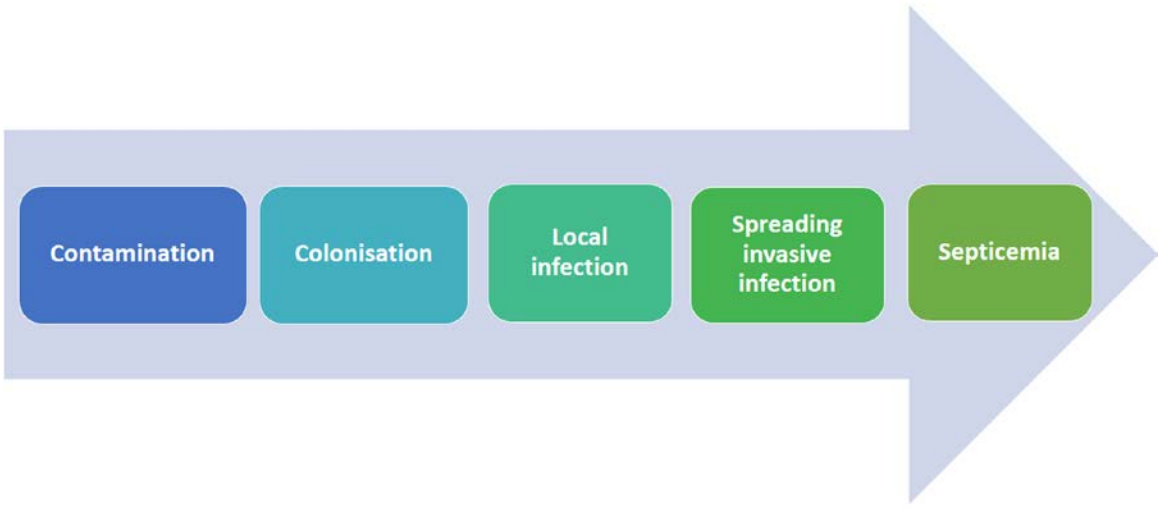

Fig 2. Schematic illustration of the wound bacterial microbiology.

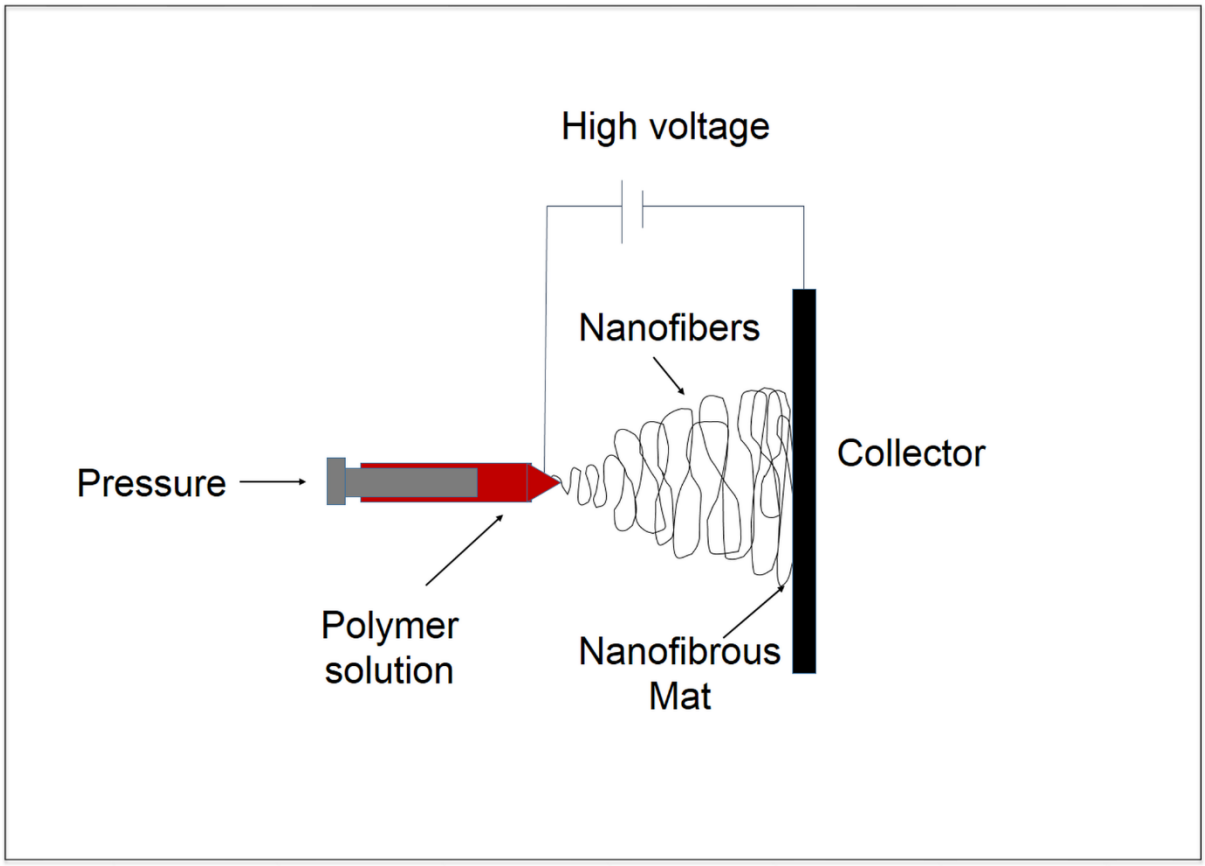

Fig 3. Schematic presentation of the electrospinnig process.

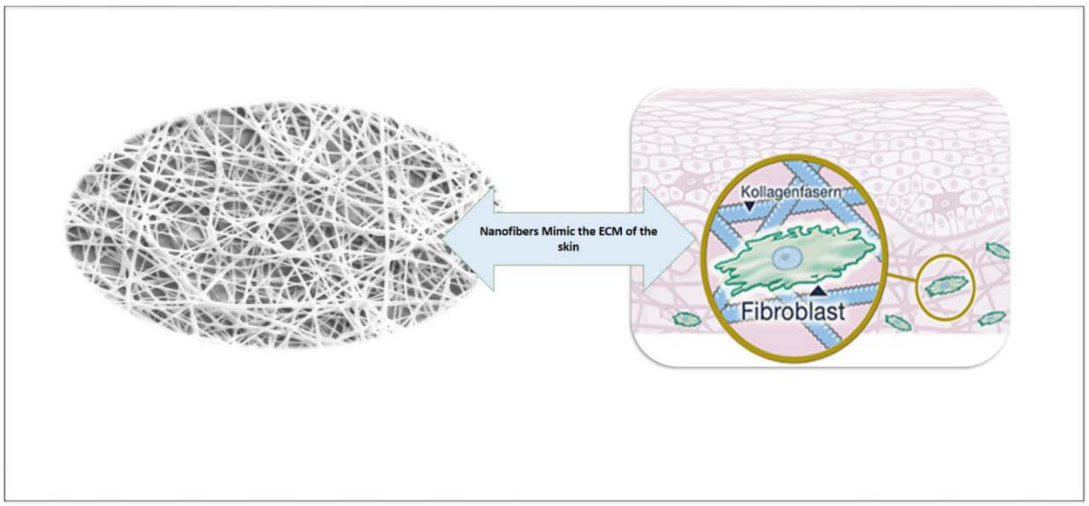

Fig 4. Schematic illustration of the resemblance of the nanofibrous structure to the extracellular matrix (ECM) of the skin

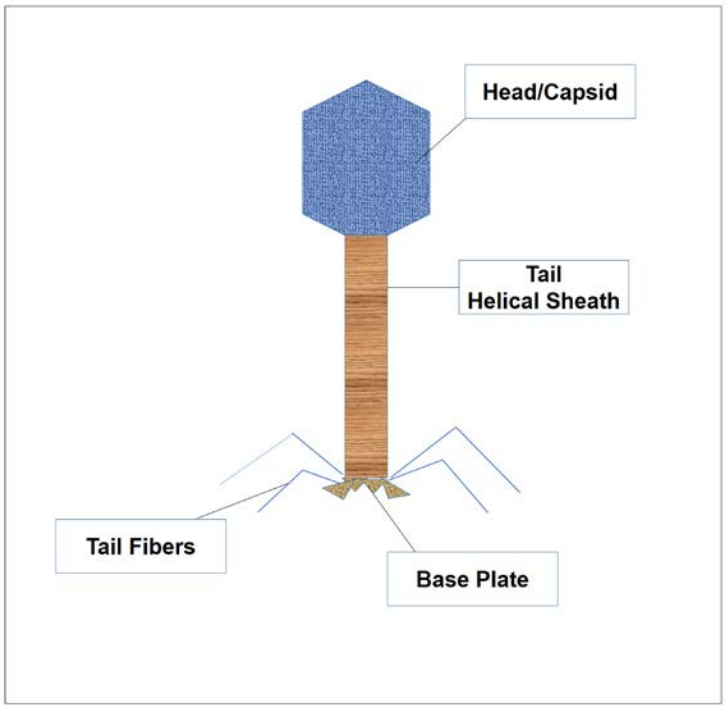

Fig 5. Schematic illustration of bacteriophage.

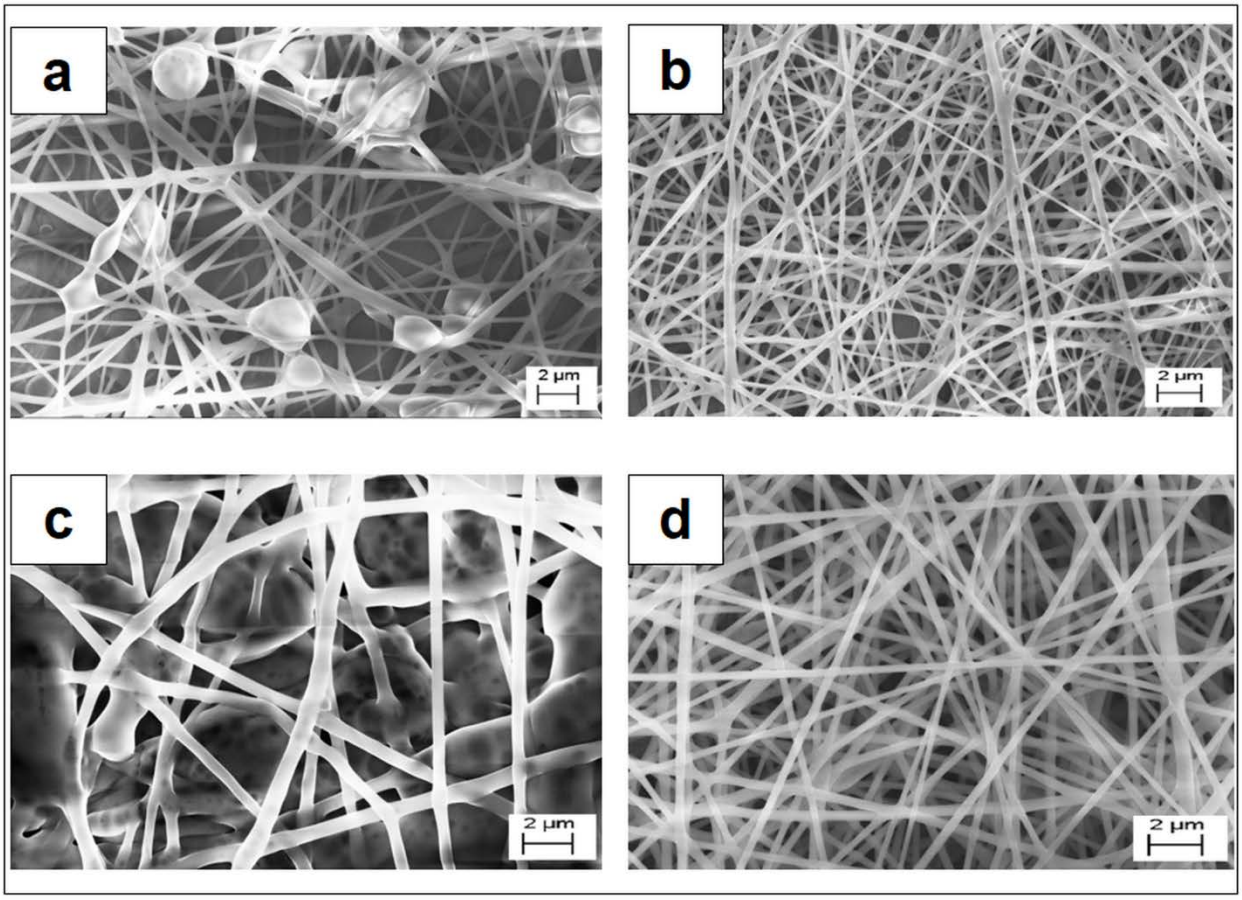

Fig 6. SEM images of the electrospun nanofibrous mats with the highest honey concentration within the HP and the HPCS nanofibers :(a) HP (20%:10%), (b) HPCS (20%:7%:3.5%) (c) HP (30%:10%), (d) HPCS (30%:7%:3.5%) (Sarhan & Azazzy, 2015a).

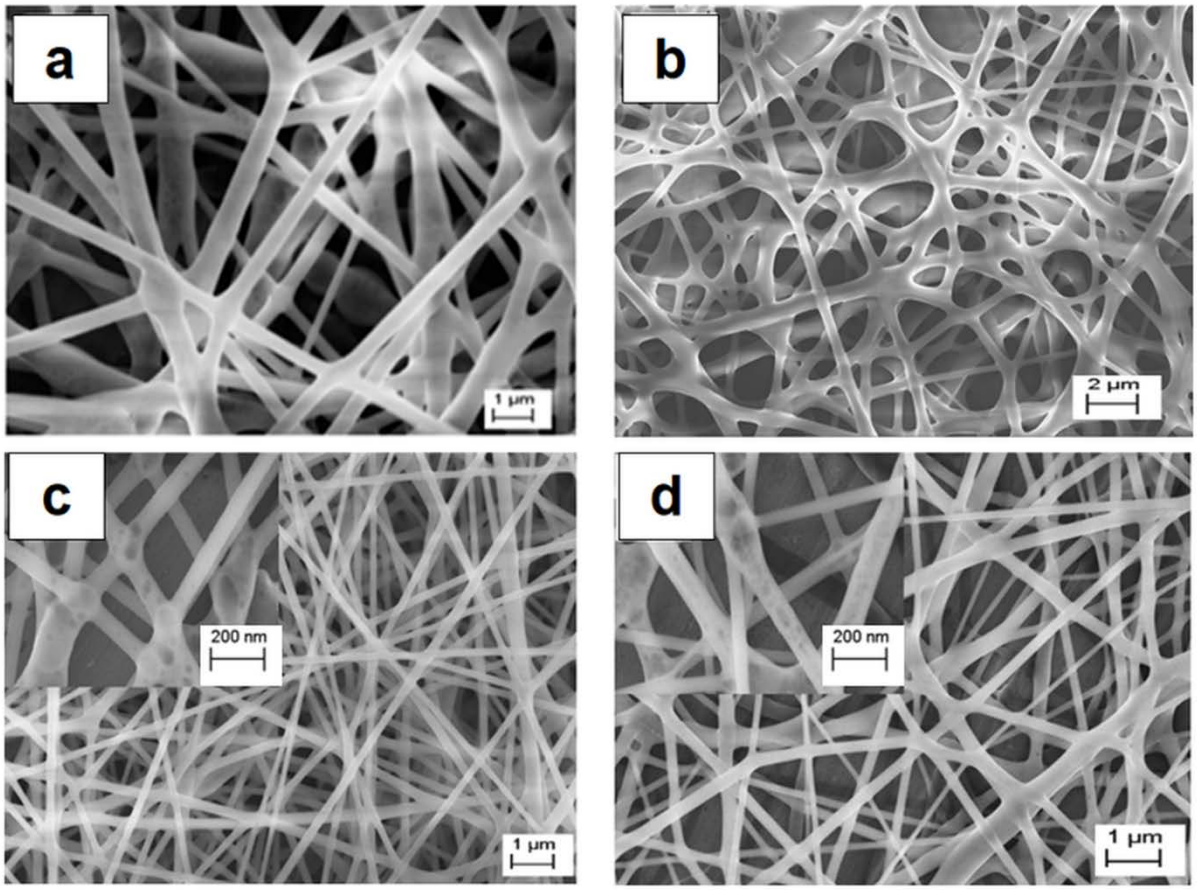

’;;’

Fig 7. SEM images of the electrospun nanofibers containing maximum concentration (%) of honey and chitosan within the HPCS nanofibers: (a) HPCS (35%:7%:3.5%), (b) HPCS (40%:7%:3.5%), (c) HPCS (30%:5%:4.5%), (d) HPCS (30%:5%:5.5%) (Sarhan & Azzazy., 2015a).

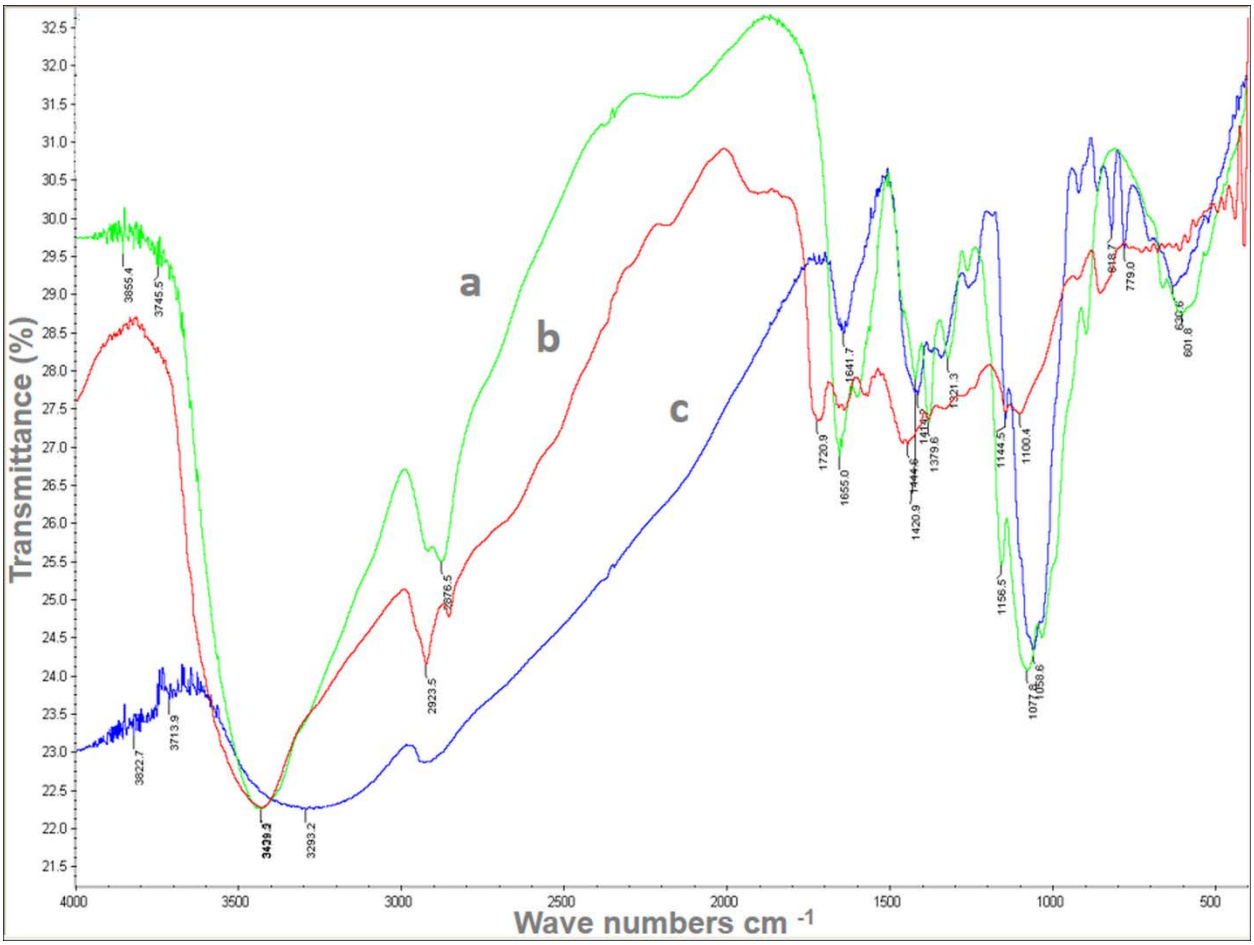

Fig 8. FTIR spectra for (a) chitosan (CS) (b) poly vinyl alcohol (P) and (C) HPCS nanofibers (30%:7%:3.5%).

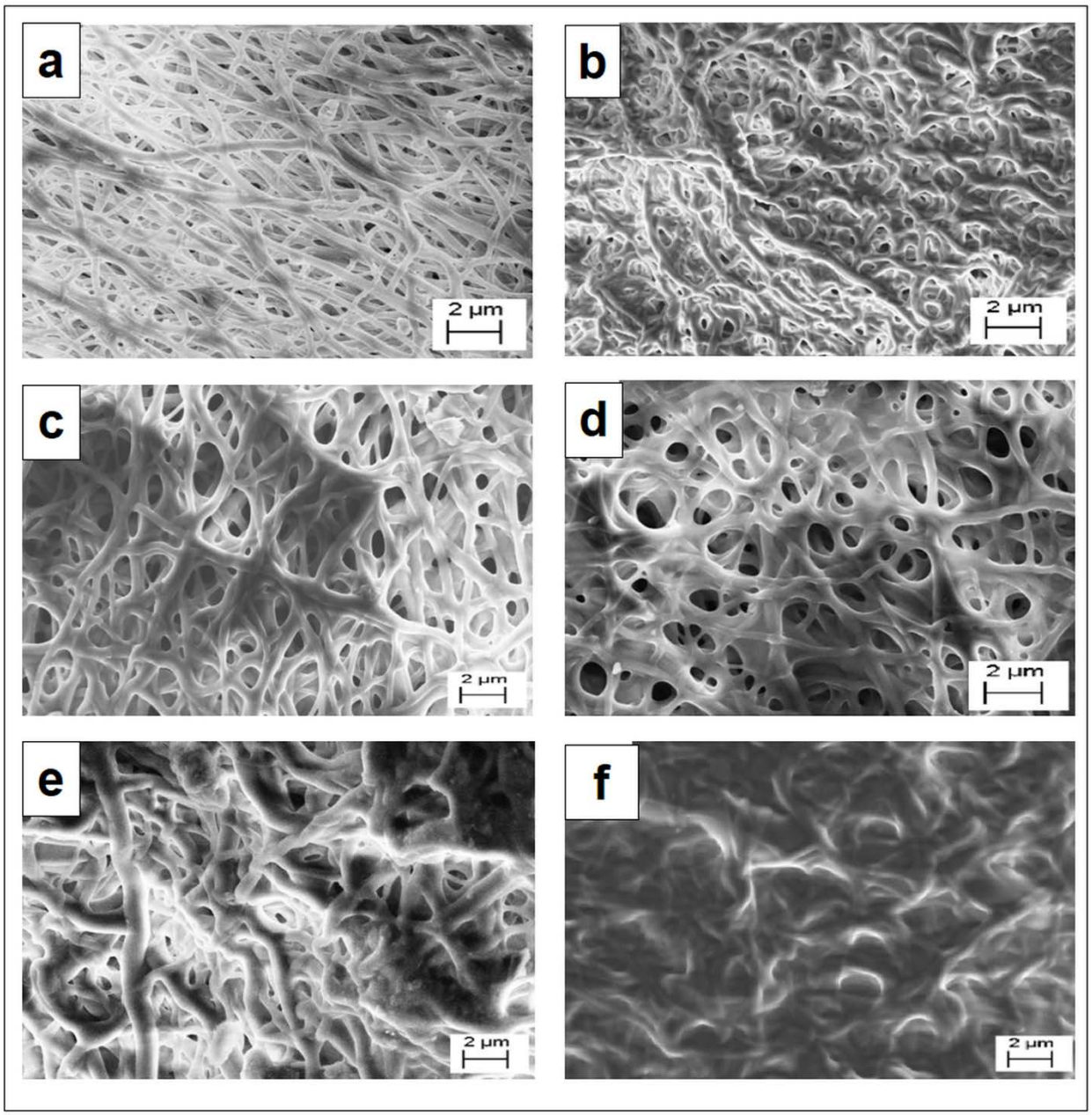

Fig 9. SEM images of the chemically (a, b, c, d) and physically (e, f) cross-linked HPCS (30%:7%:3.5%) nanofibrous mats. Cross-linking was performed by exposure to GA vapors with subsequent heating under vacuum at 40◦C for 24 h. Different mats were exposed to GA for different time intervals (a) 3 days, (b) 2 days, (c) 3 h, and (d) 1 h. Images (e) and (f) demonstrate the successful physical cross-linking attempts: (e) heating for 15 min at 110◦C under vacuum and (f) heating for 24h at 70◦C under vacuum (Sarhan & Azzazy., 2015a)

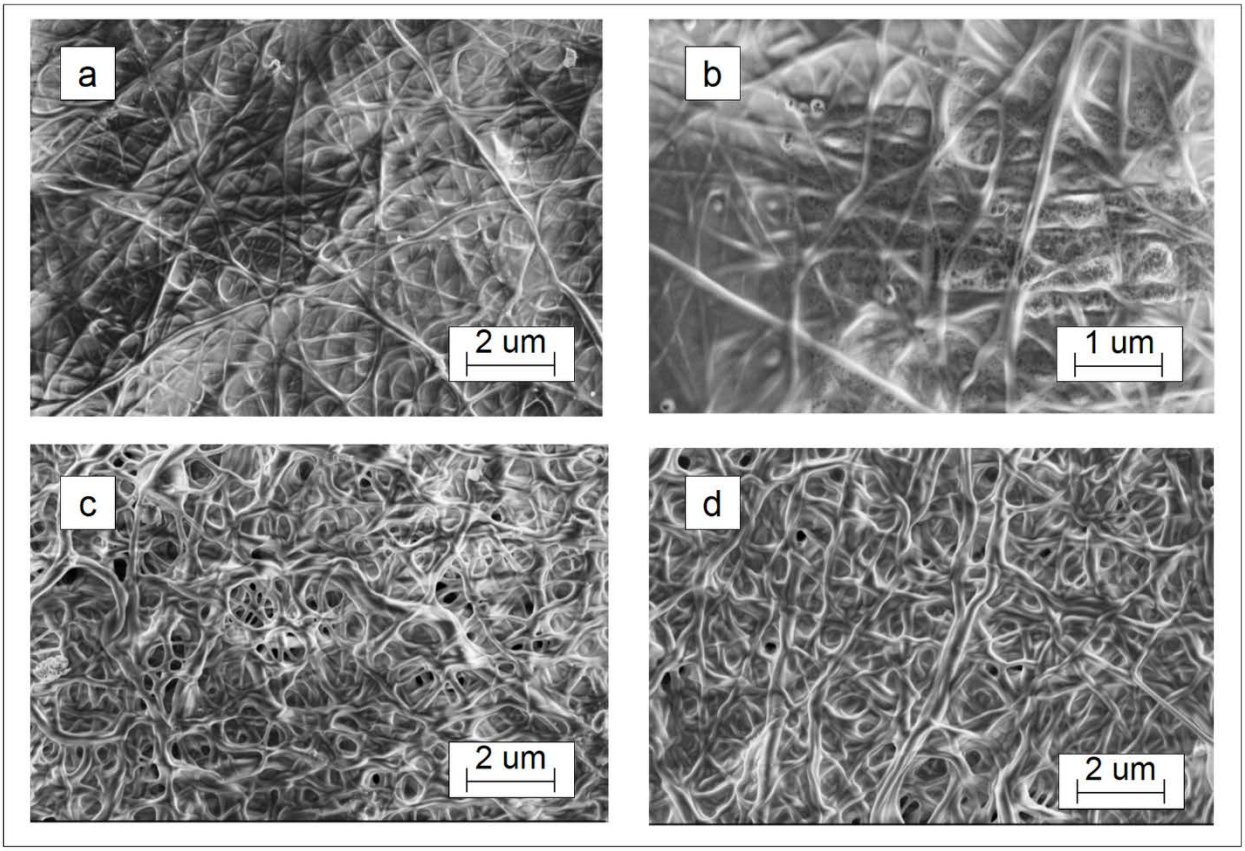

Fig 10. SEM images of the crosslinked and non-crosslinked electrospun HPCS nanofibers (30%:7%:3.5%), after 1 year of storage on shelf. (a, b) non-crosslinked HPCS (c) crosslinked HPCS via 1hr exposure to GA (d) crosslinked HPCS via 3hr exposure to GA.

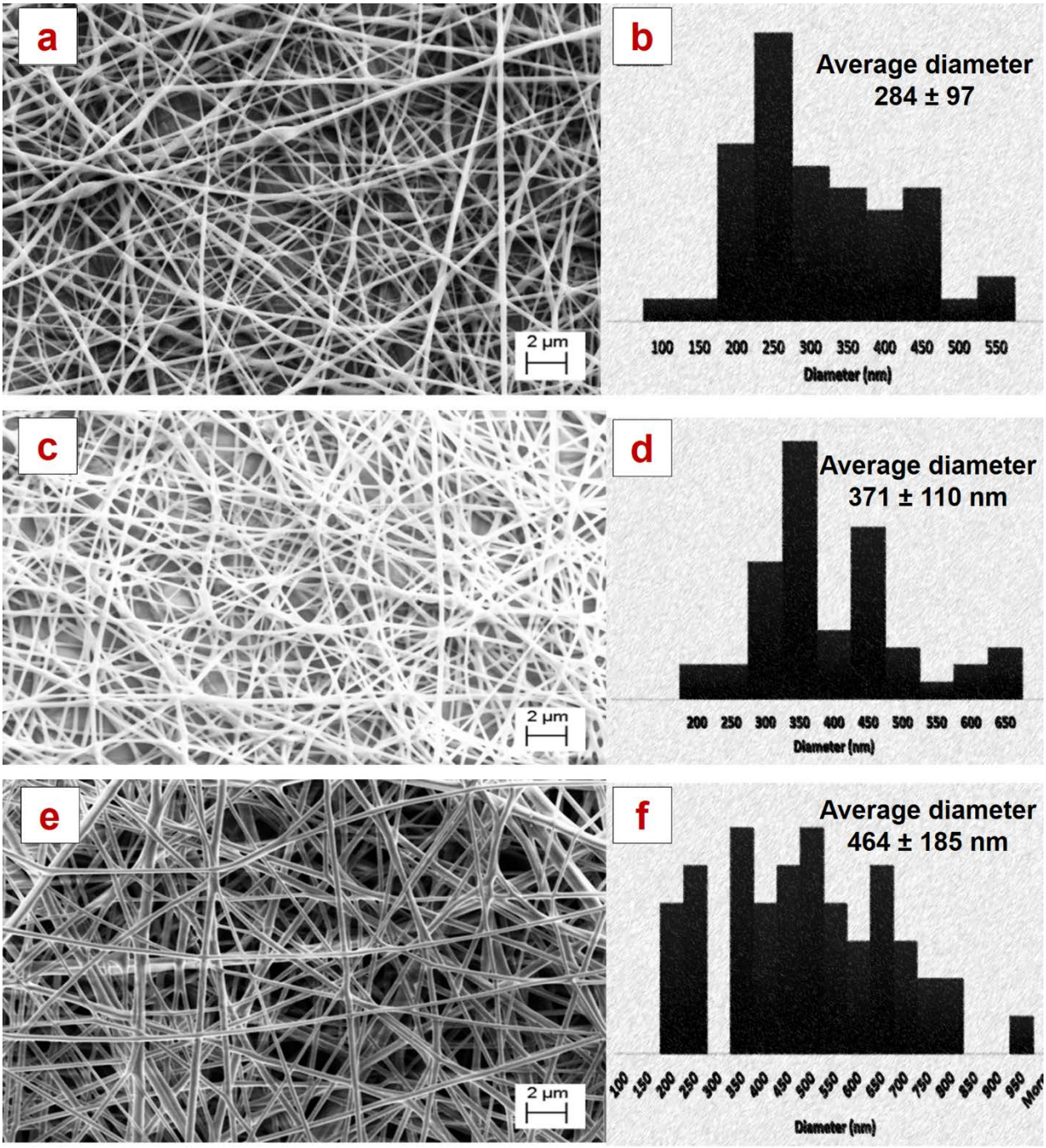

Fig 11. SEM images of the electrospun honey/polyvinyl alcohol/chitosan (HPCS) nanofibrousmats with increasing concentrations of honey (a, c, e) and their diameter distribution (b, d, f): (a, b) HPCS (10%:7%:3.5%), (c, d) HPCS (20%:7%:3.5%), and (e, f) HPCS (30%:7%:3.5%) (Sarhan et al., 2016a).

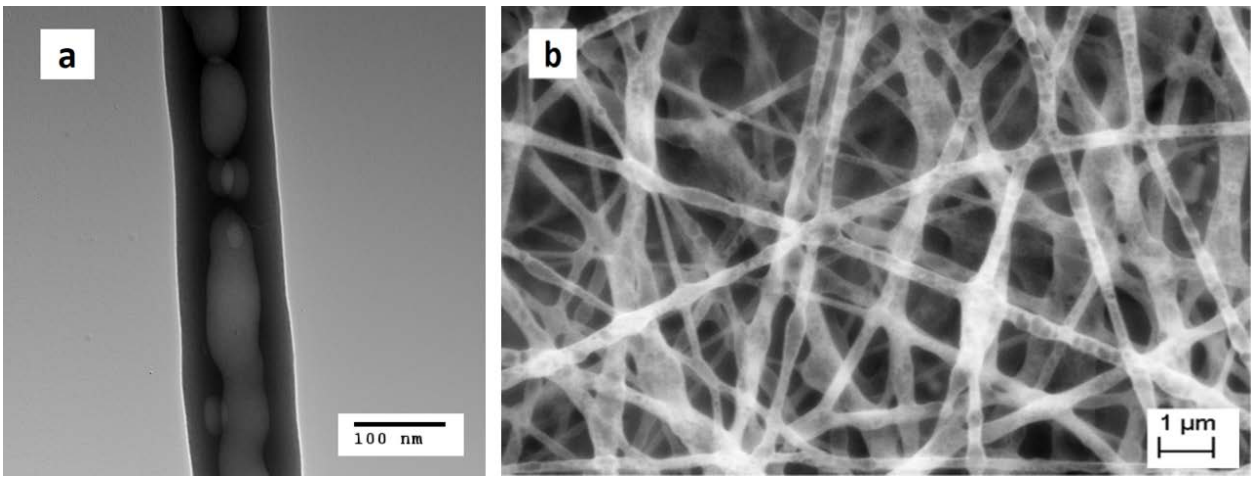

Fig 12. TEM (a) & SEM (b) images of honey/polyvinyl alcohol/chitosan (HPCS) nanofibers (30:7:3.5 w %) illustrating the inclusion of honey within the nanofibers (Sarhan et al., 2016a).

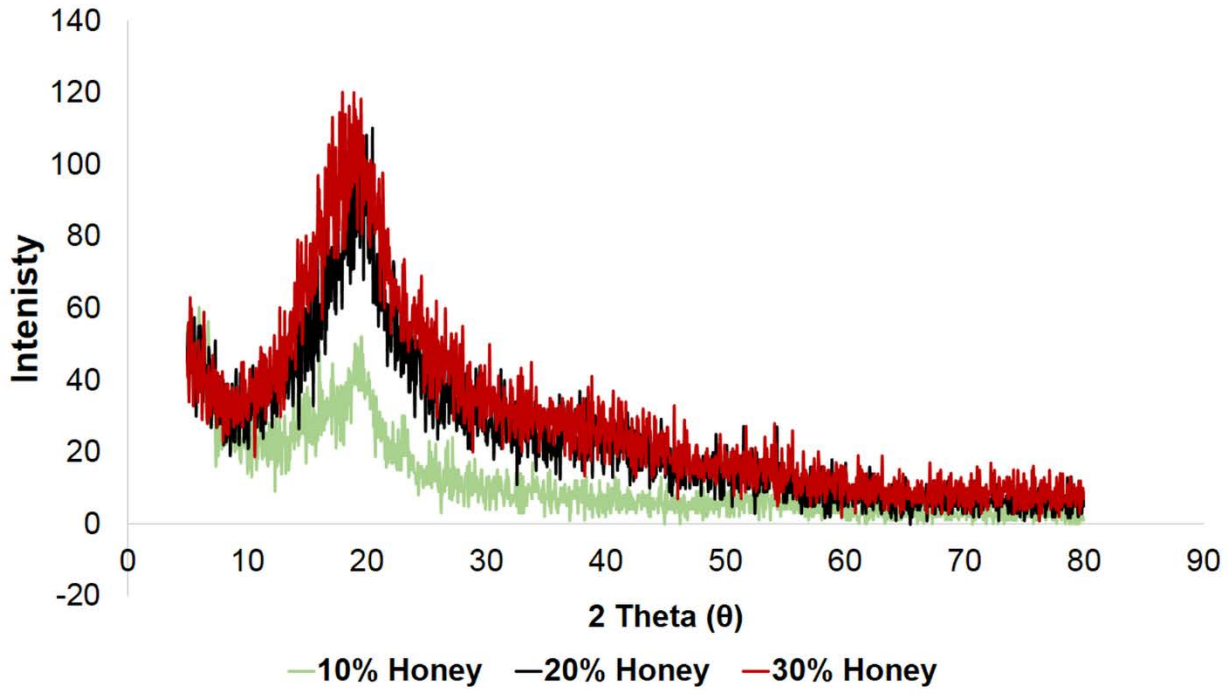

Fig 13. XRD diffraction patterns of the honey/polyvinyl alcohol/chitosan (HPCS) nanofibers with increasing honey concentrations. The weight blending ratios of the electrospun mats were 7% polyvinyl alcohol (P), 3.5% chitosan (CS), and increasing concentrations of honey (H): 10%, 20%, and 30% (Sarhan et al., 2016a).

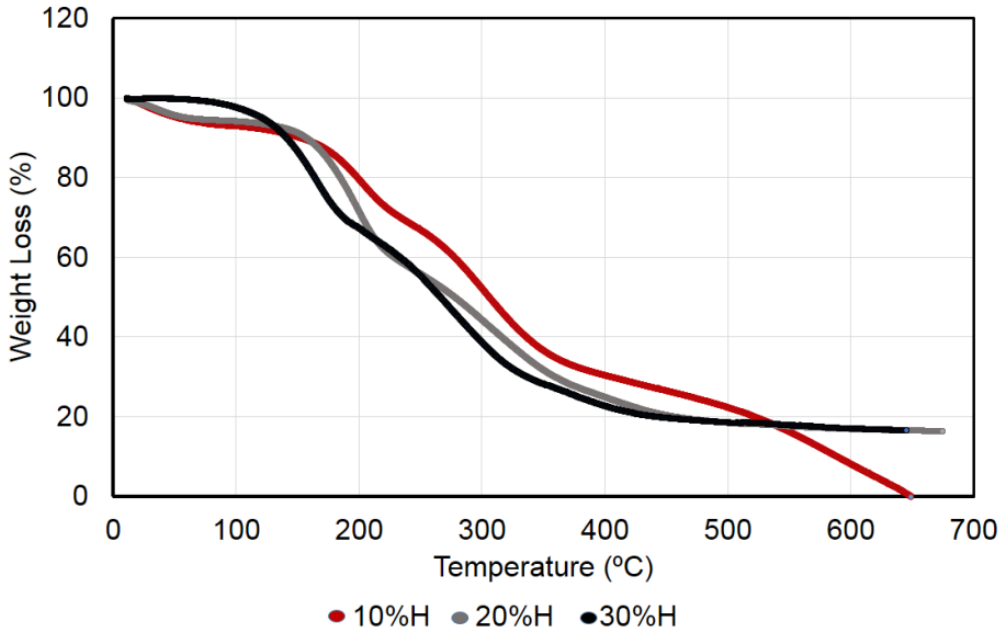

Fig 14. TGA of the honey/polyvinyl alcohol/chitosan (HPCS) nanofibers with increasing honey concentrations. The weight blending ratios of the electrospun mats were 7% polyvinyl alcohol (P), 3.5% chitosan (CS), and increasing concentrations of honey (H): 10%, 20%, and 30% (Sarhan et al., 2016a)

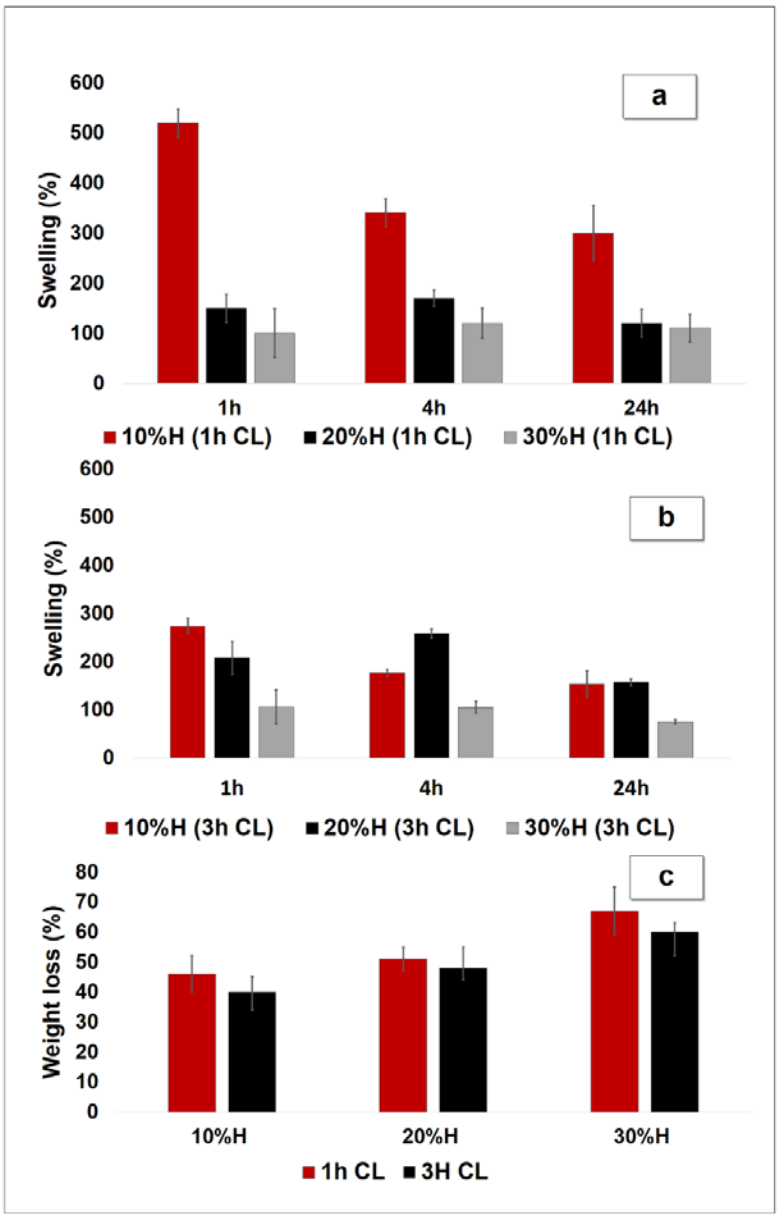

Fig 15. Swelling % (a & b), and weight loss % (c) of the honey/polyvinyl alcohol/chitosan (HPCS) nanofibers mats with increasing honey concentrations. The weight blending ratios of the electrospun mats were 7% polyvinyl alcohol (P), 3.5% chitosan (CS), and increasing concentrations of honey (H) 10%, 20%, and 30%. The swelling abilities of the nanofibers (a) 1 h crosslinked (1 h CL) (b) 3 h crosslinked (3 h CL) were tested after immersion in PBS (pH 7.4) for 1, 4, and 24 h. The weight loss of the 1 h and 3 h crosslinked nanofibers (c) were tested after immersion in PBS (pH 7.4) for 24 h (Sarhan et al., 2016a).

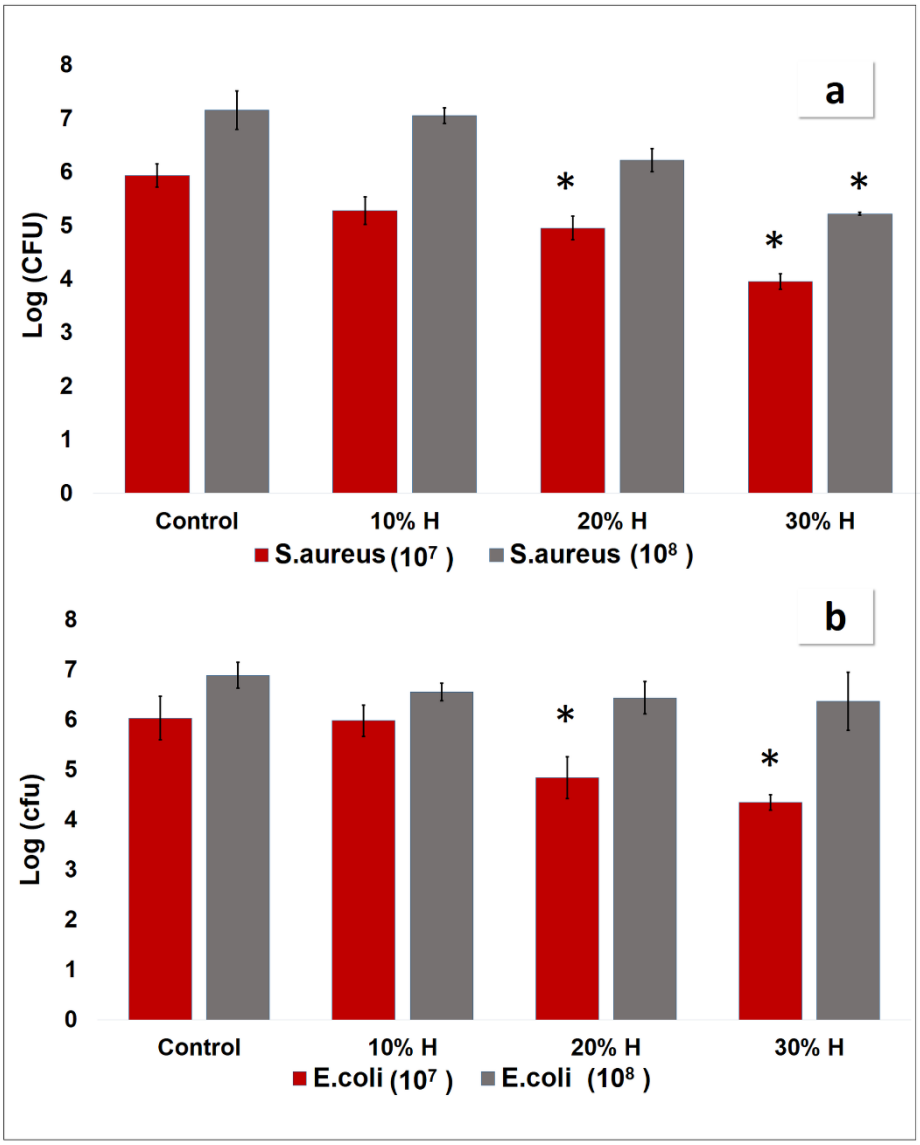

Fig 16. The antibacterial activity of the electrospun honey/polyvinyl alcohol/chitosan (HPCS) nanofibrous mats against 1×10^8 CFU/ml and 1×10^7 CFU/ml of *E. coli* (a) and *S. aureus* (b) represented by reduction in the log (CFU) after 24 h. The weight blending ratios of the electrospun mats were 7% polyvinyl alcohol (P), 3.5% chitosan (CS), and increasing concentrations of honey (H); 10%, 20%, and 30% (n = 3, Student's t-test, *$p < 0.05$ versus the negative control) (Sarhan et al., 2016a).

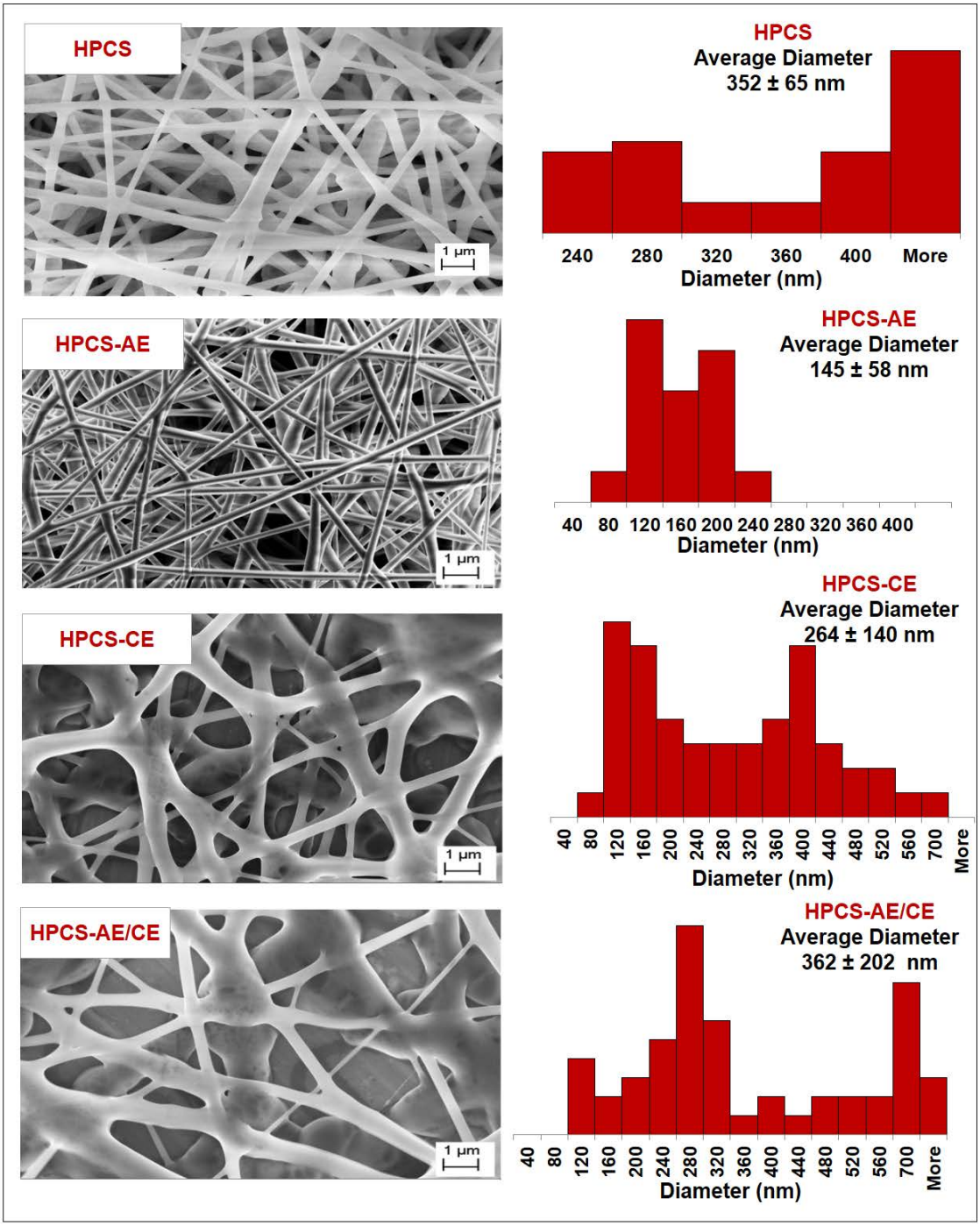

Fig 17. SEM images of the electrospun nanofibrous mats and their diameter distribution of HPCS, HPCS-AE, HPCS-CE, and HPCS-AE /CE (Sarhan et al., 2016b).

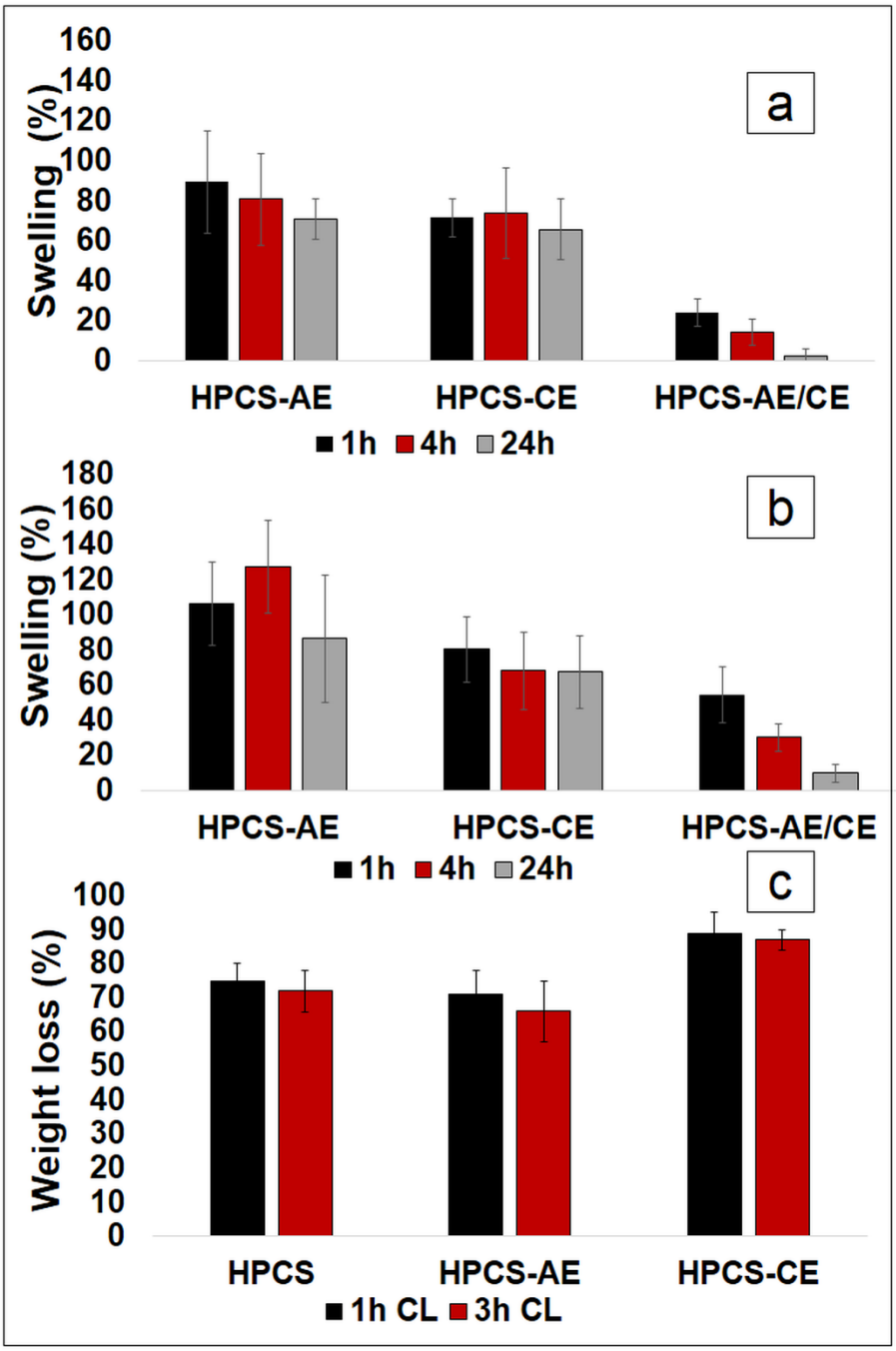

Fig 18. % Swelling (a & b) and % weight loss (c) of the HPCS-AE, HPCS-CE and HPCS-AE /CE. The swelling capabilities of the nanofibers (a) 1 h crosslinked (1h CL) (b) 3h crosslinked (3h CL) were examined after immersion in PBS (pH 7.4) for 1, 4, and 24 h. The weight loss of the 1h and 3h crosslinked nanofibers (c) were examined after immersion in PBS (pH 7.4) for 24h (Sarhan et al., 2016b).

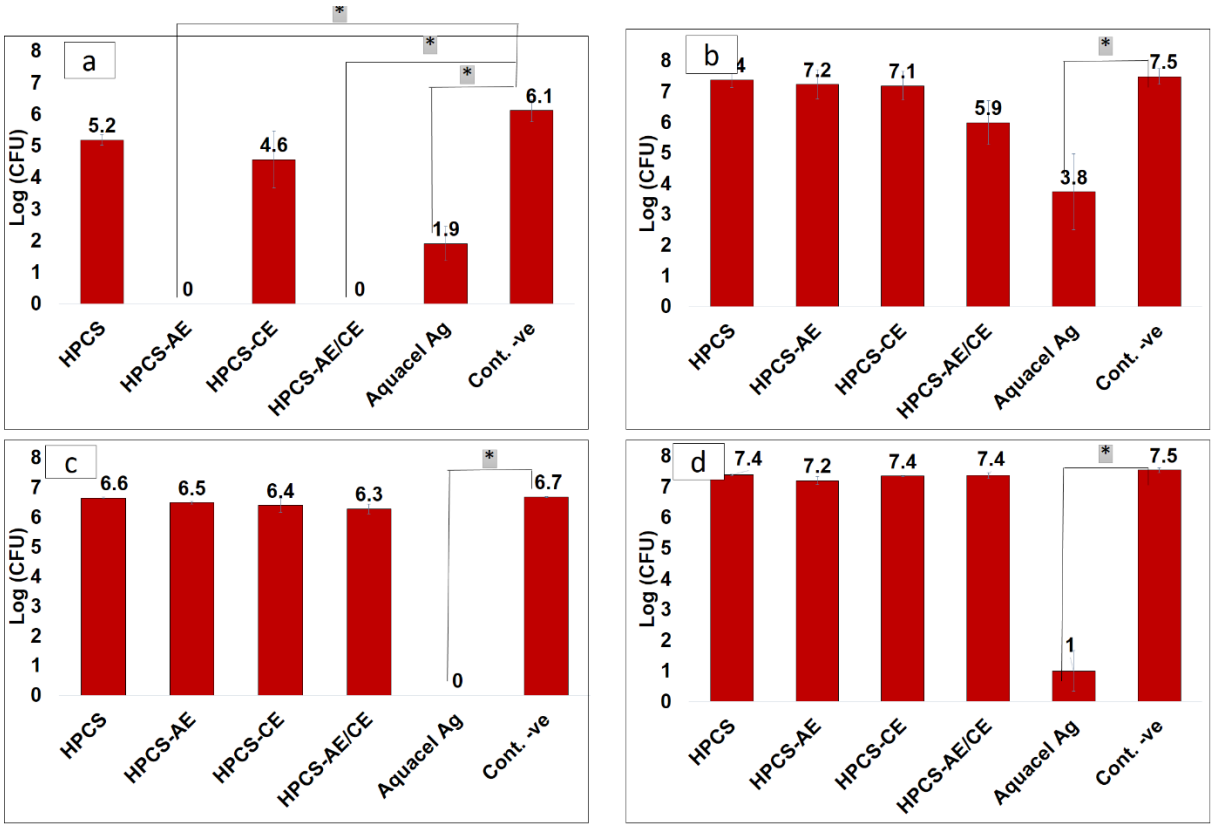

Fig 19. The antibacterial activity of the electrospun mats of HPCS, HPCS-AE, HPCS-CE, (HPCS-AE /CE and Aquacel Ag wound dressing against *S. aureus* (a) MRSA (b) *E. coli* (c) and MDR *P. aeruginosa* (d) at 24 h on 7×10^8 CFU/ml bacteria. Aquacel Ag was utilized as the positive control and the negative control was kept untreated. Data represents mean ± SD (n = 3, Student's t-test, *$p < 0.05$) (Sarhan et al., 2016b).

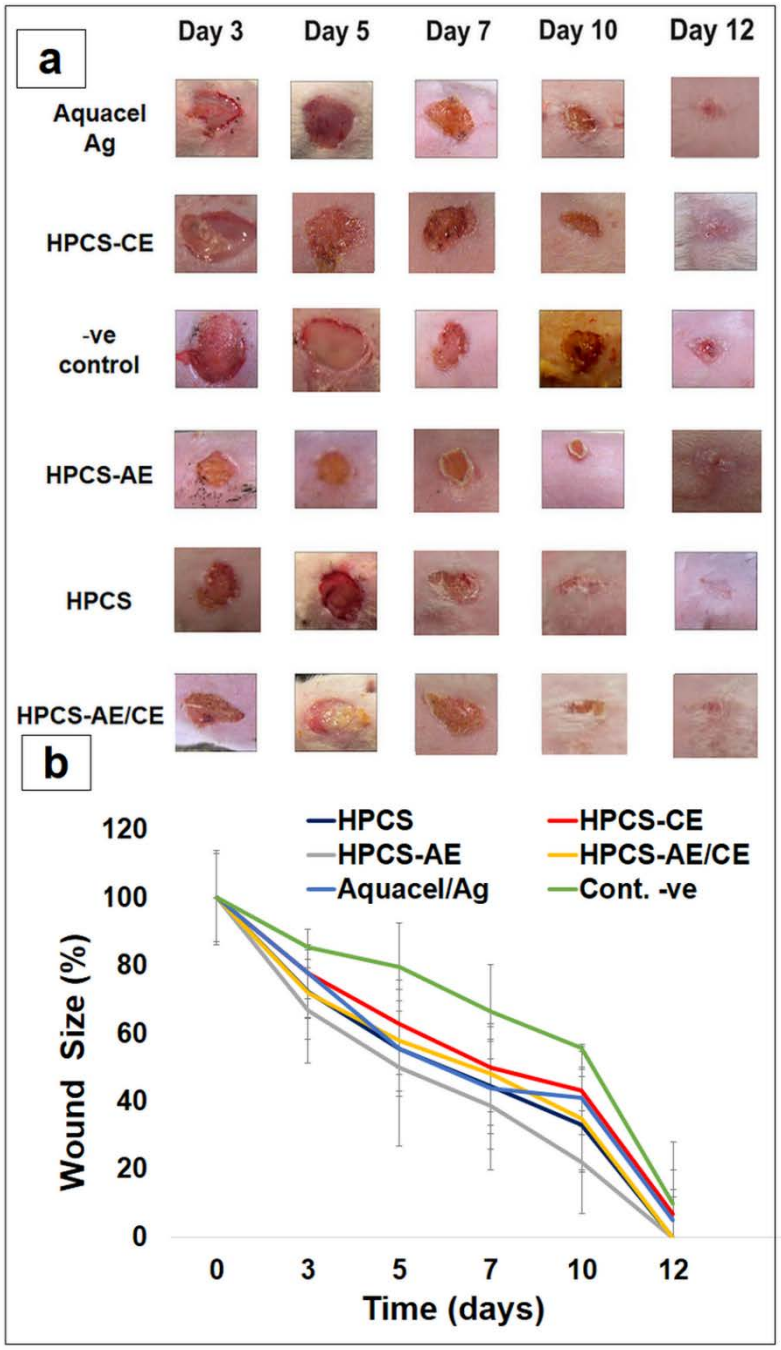

Fig 20. Photographic images of the extent of the wound closure (a) graphical demonstration of the changes in the size of wound (b) on days 3, 5, 7, 10 and 12 for the HPCS, HPCS-AE, HPCS-CE, HPCS-AE/CE nanofibrous mats and the Aquacel Ag wound dressing. The Aquacel Ag was utilized as the positive control and the negative control was kept untreated and covered with a cotton gauze (Sarhan et al., 2016b).

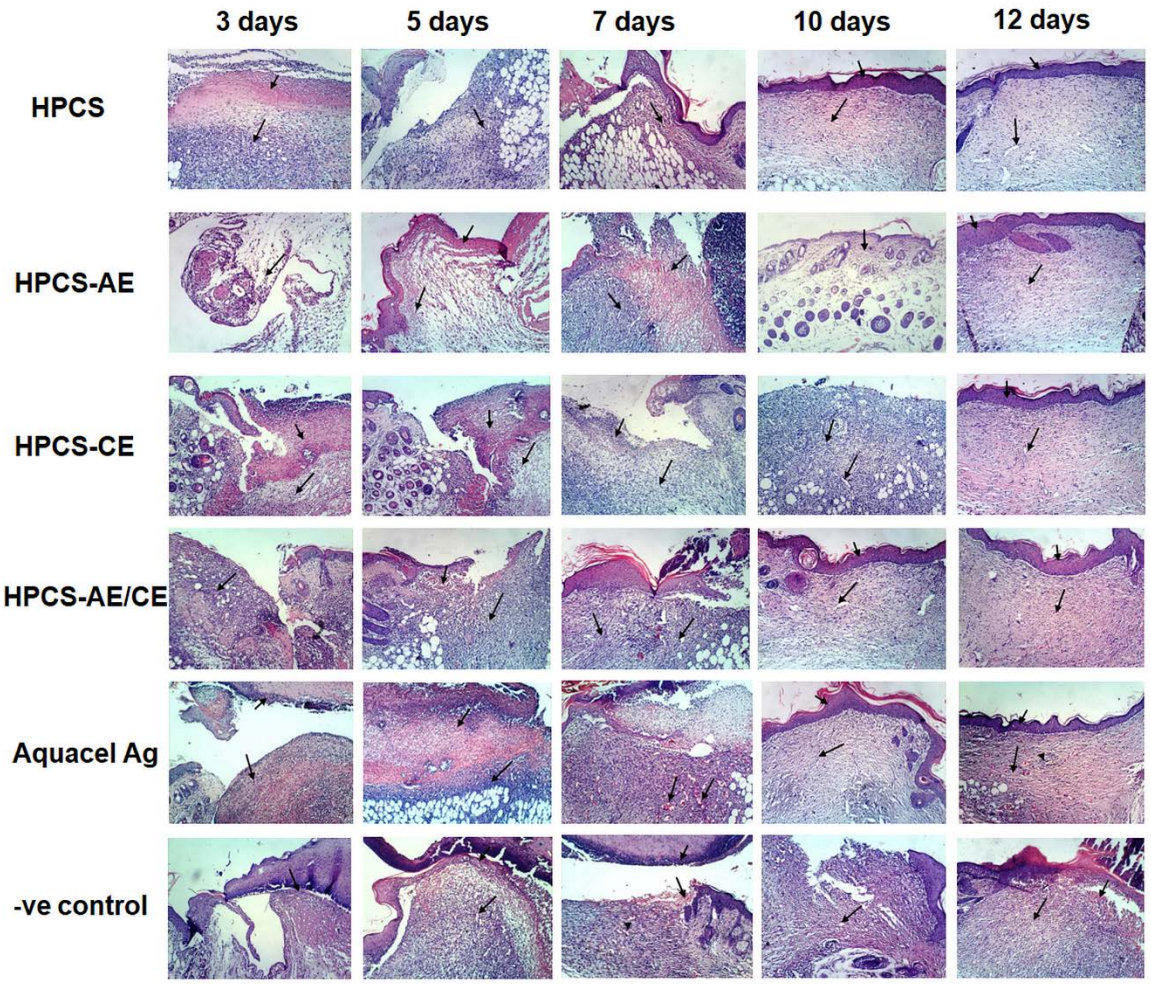

Fig 21. Histopathological evaluation of sections of the H&E stained wound tissue treated with the HPCS, HPCS-AE, HPCS-AE/CE, HPCS-CE nanofibrous mats and the Aquacel Ag wound dressing at days 3, 5, 7, 10 & 12 days (Original magnification 100). The Aquacel Ag was utilized as the positive control, and the negative control was untreated and covered with a cotton gauze. HPCS: Micrographs of the central area of the wound treated with the HPCS nanofibrous dressing. Note the increased infiltration of the inflammatory cells at 3 & 5 days and the formation of matured granulation tissue with well oriented deposition of collagen as well as thick layer of epidermis at days 10 & 12 and the near disappearance of the inflammatory cells. HPCS-AE: Micrographs of the central area of the wound treated with the HPCS-AE nanofiber dressing. Note the massive inflammatory cell infiltration at days 3, 5 & 7 and the exudate observed at 5 &7 days. Mature

granulation tissue that is well vascularized and with good oriented collagen deposition at day 10 was observed. HPCS-CE: Micrographs of the central area of the wound treated with the HPCS-CE nanofiber dressing. Note the massive infiltration of inflammatory cell at 3, 5, & 7 days and the enhanced vascularization (note the newly formed blood capillaries) within the matured formed granulation tissue. Well oriented deposition of collagen was observed since day 10. HPCS-AE/CE: Micrographs of the central area of wounds treated with the HPCS-AE/CE nanofibrous dressing. Note the massive inflammatory cell infiltration at 3, 5 & 7 days and the well vascularized granulation tissue formed with well oriented deposition of collagen since day 10. Notice the deposition of thick layer of epidermis since day 10 and that the inflammatory cells is nearly diminished. Aquacel Ag: Micrographs of the central area of wounds treated with the positive control Aquacel Ag dressing. Note the massive inflammatory cell infiltration at days 3 & 5 and the formation of mature granulation tissue that is highly vascularized and note the deposition of collagen since day 7. Notice the thick epidermal layer deposition since day 10 and that the inflammatory cells are greatly diminished. -ve control: Micrographs of central wound area of untreated controls: Note the massive inflammatory cell infiltration and the observed hemorrhage at days 7 & 12 as well as the disorganized granulation tissue. Notice the epithelial layer absence at day 10 and the deposition of thin epidermal layer at day 12 (Sarhan et al., 2016b).

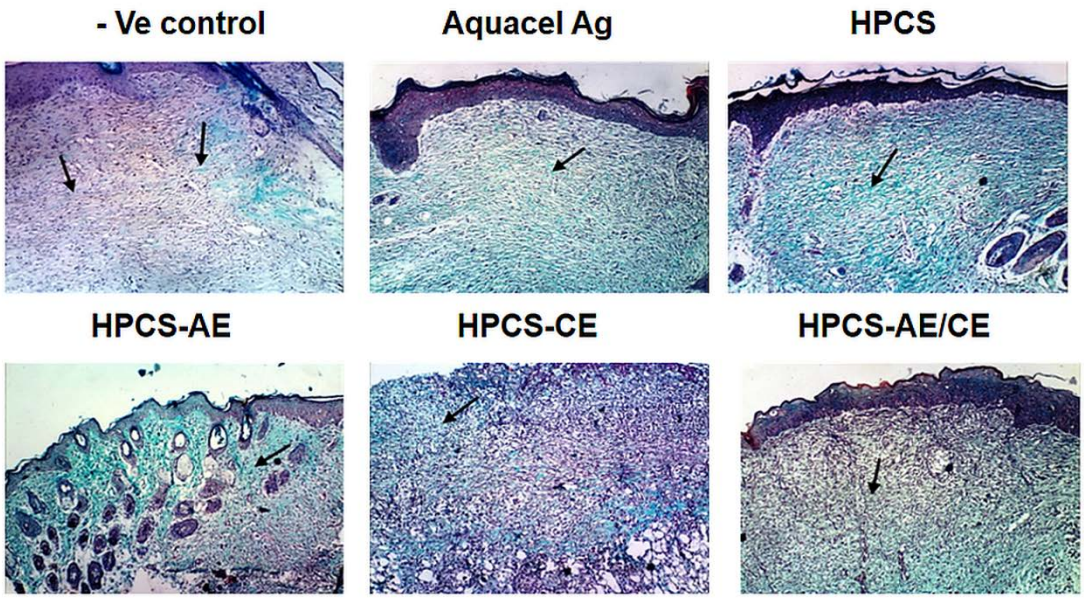

Fig 22. Histopathological evaluation of sections of the MT stained wound tissues treated with the HPCS, HPCS-AE, HPCS-AE/CE, HPCS-CE nanofibrous mats and the Aquacel Ag wound dressing at day 10 (Original magnification 100). The Aquacel Ag was utilized as the positive control and the negative control was kept untreated and covered with a cotton gauze. Notice deposition of dense collagen in the HPCS, HPCS-AE, HPCS-AE/CE, HPCS-CE nanofiber dressings and the Aquacel Ag as compared to the negative control (-ve control) (Sarhan et al., 2016b).

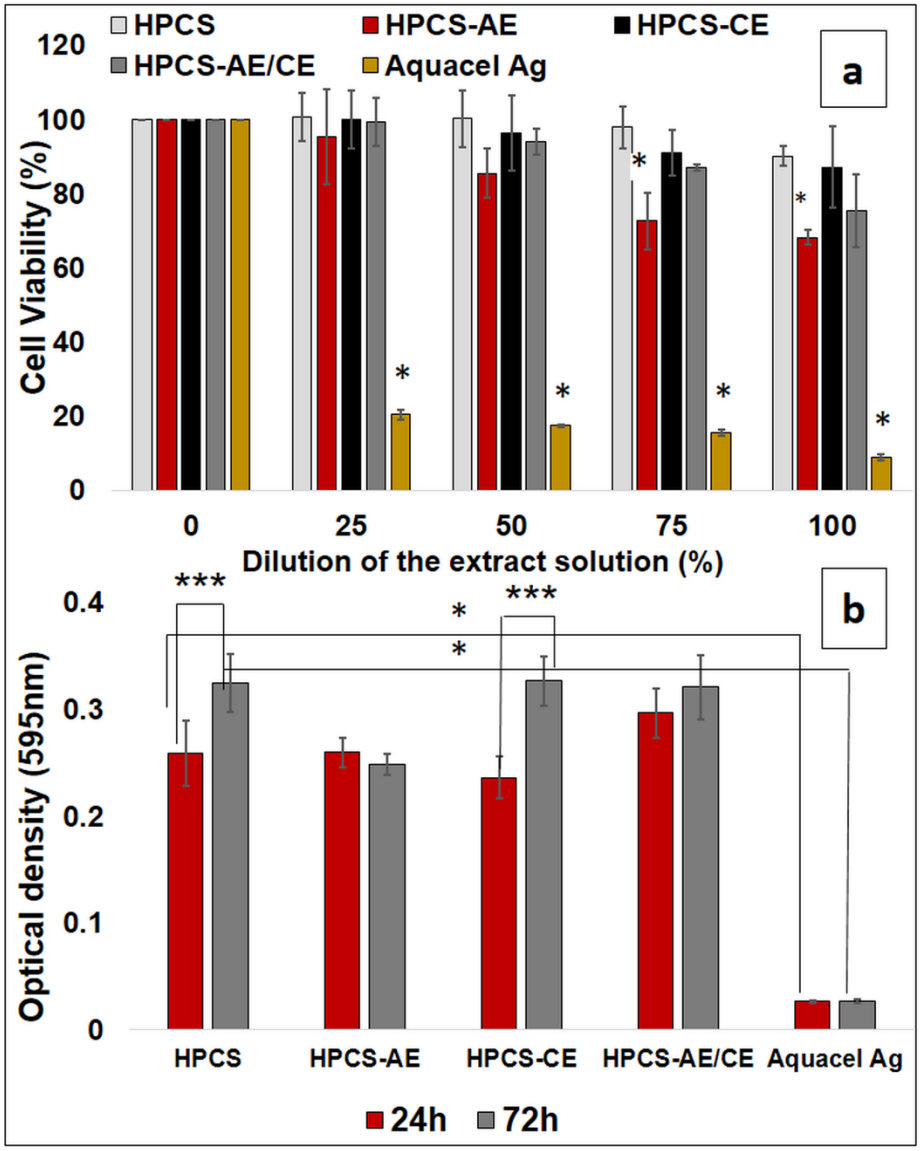

Fig 23. Fibroblast cell viability (a) and fibroblast cell proliferation (b) as determined via the MTT assay for the HPCS, HPCS-AE, HPCS-CE, HPCS-AE/CE and Aquacel Ag. Aquacel Ag was used as the positive control in the two assays. Data represents mean ± SD (n = 3, Student's t-test, *p < 0.05 versus the HPCS mats, ***p< 0.05 versus culture times 24h) (Sarhan et al., 2016b).

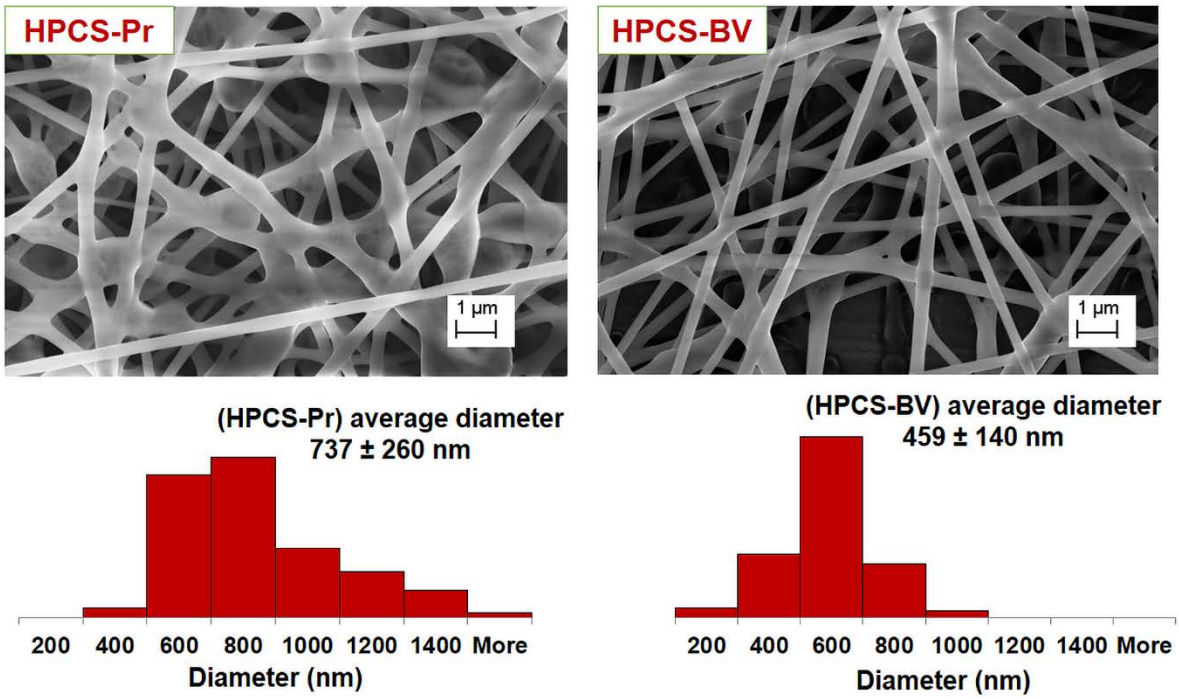

Fig 24. SEM images of the HPCS-Pr and HPCS-BV nanofibers and their corresponding diameter distribution.

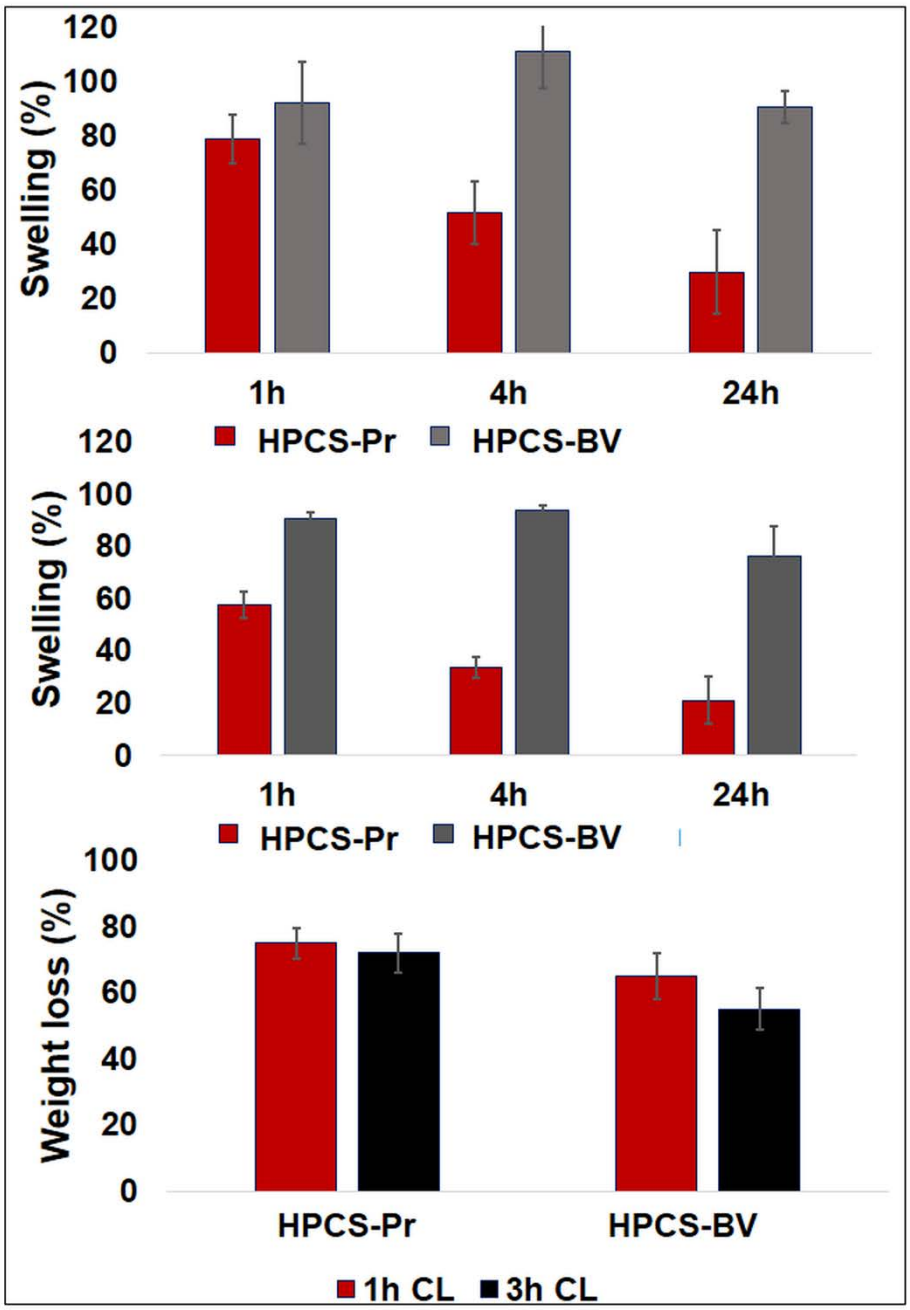

Fig 25. % Swelling (a & b) and % weight loss (c) of the HPCS-Pr and HPCS-BV nanofibrous mats. The swelling capabilities of the nanofibers (a) 1 h crosslinked (1h CL) (b) 3h crosslinked (3h CL) were examined after immersion in PBS (pH 7.4) for 1, 4, and 24 h. The weight loss of the 1h and 3h crosslinked nanofibers (c) were examined after immersion in PBS (pH 7.4) for 24h.

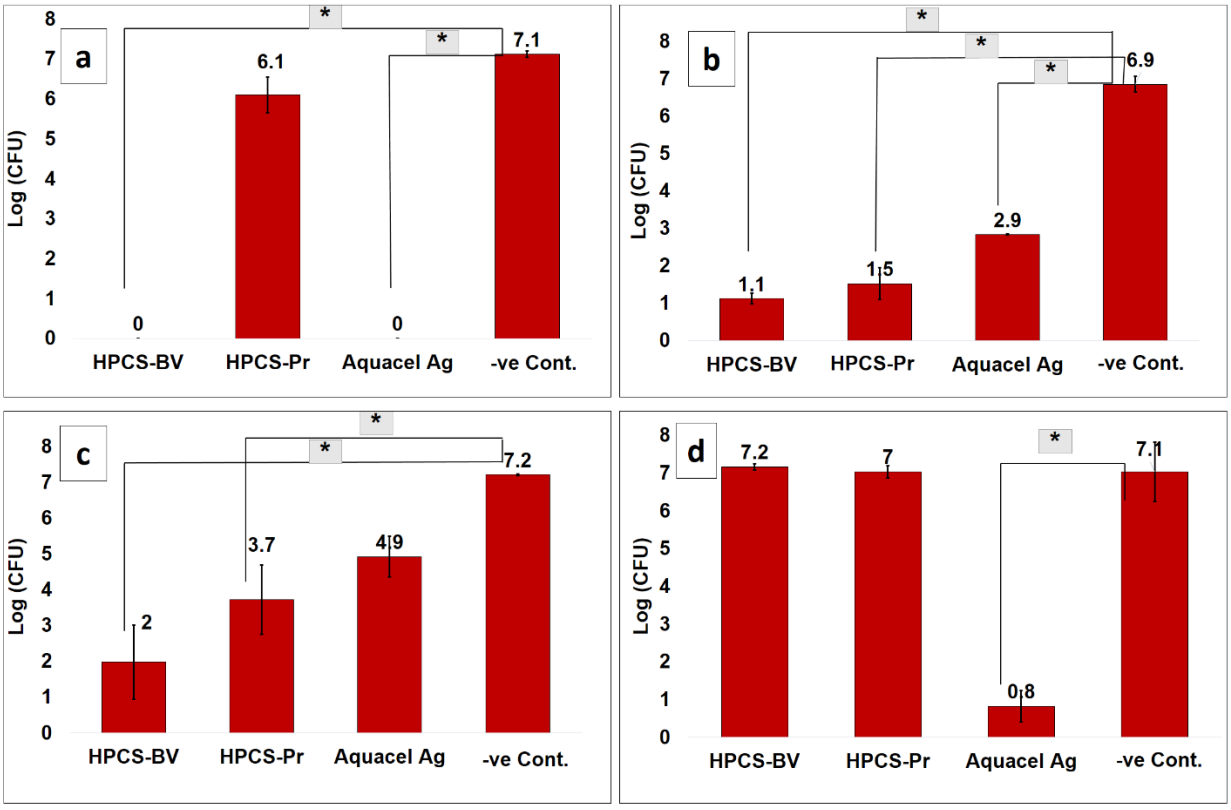

Fig 26. Illustration of the antibacterial activity of the HPCS-Pr, HPCS-BV nanofibrous mats and Aquacel Ag wound dressing. The antibacterial activity was tested against *E.coli* (a) *S. aureus* (b) MRSA (c) and MDR *P. aeruginosa* (d) at 24 h on 7×10^8 CFU/ml bacteria. Aquacel Ag was utilized as the positive control, whereas the negative control was kept untreated. Data represent mean ± SD (n = 3, Student's t-test, *$p < 0.05$).

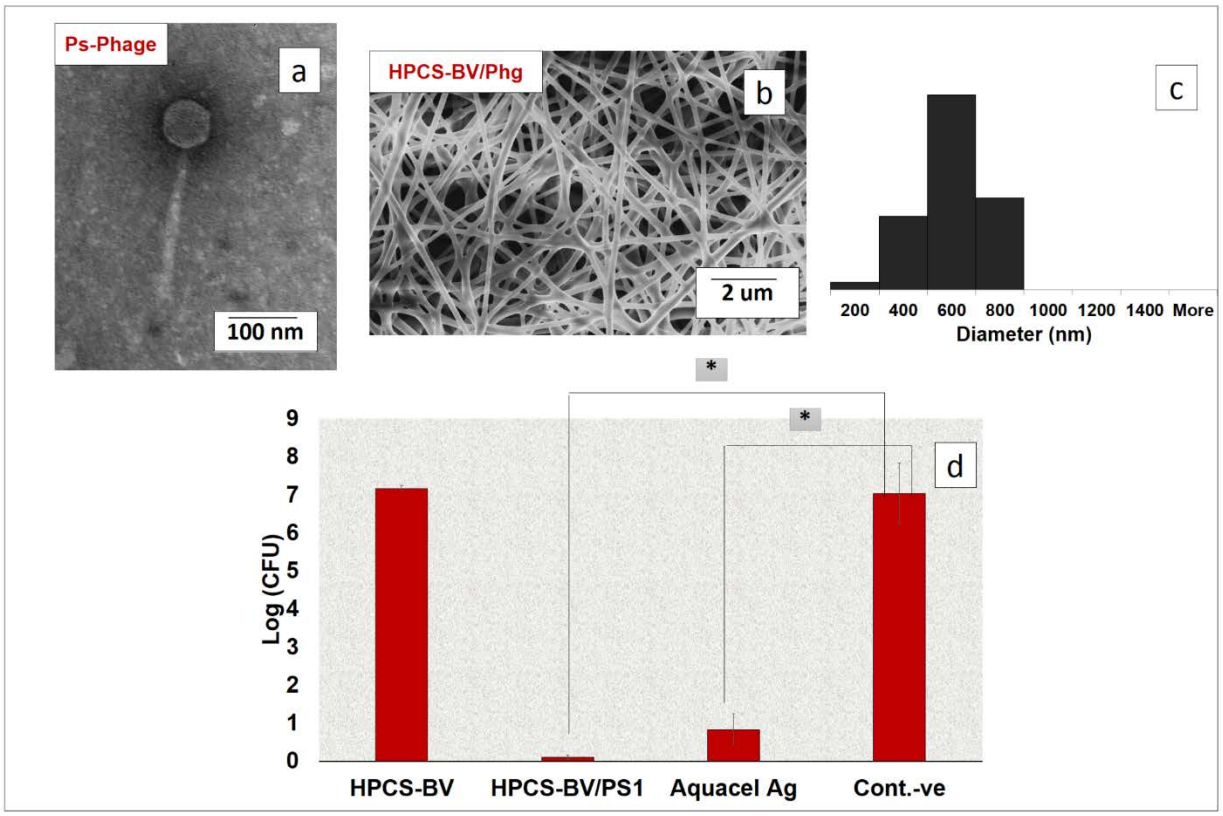

Fig 27. Illustration of the morphology of the isolated PS1 phage (a) and the electrospun HPCS-BV/PS1 nanofibers (b) and their diameter distribution (c). Illustration of the antibacterial activity of the HPCS-BV, HPCS-BV/PS1 nanofibers against MDR *P. aeruginosa* at 24 h on 7×10^8 CFU/ml bacteria (d). Aquacel Ag was utilized as the positive control, whereas the negative control was kept untreated. Data represent mean ± SD (n = 3, Student's t-test, *$p < 0.05$).

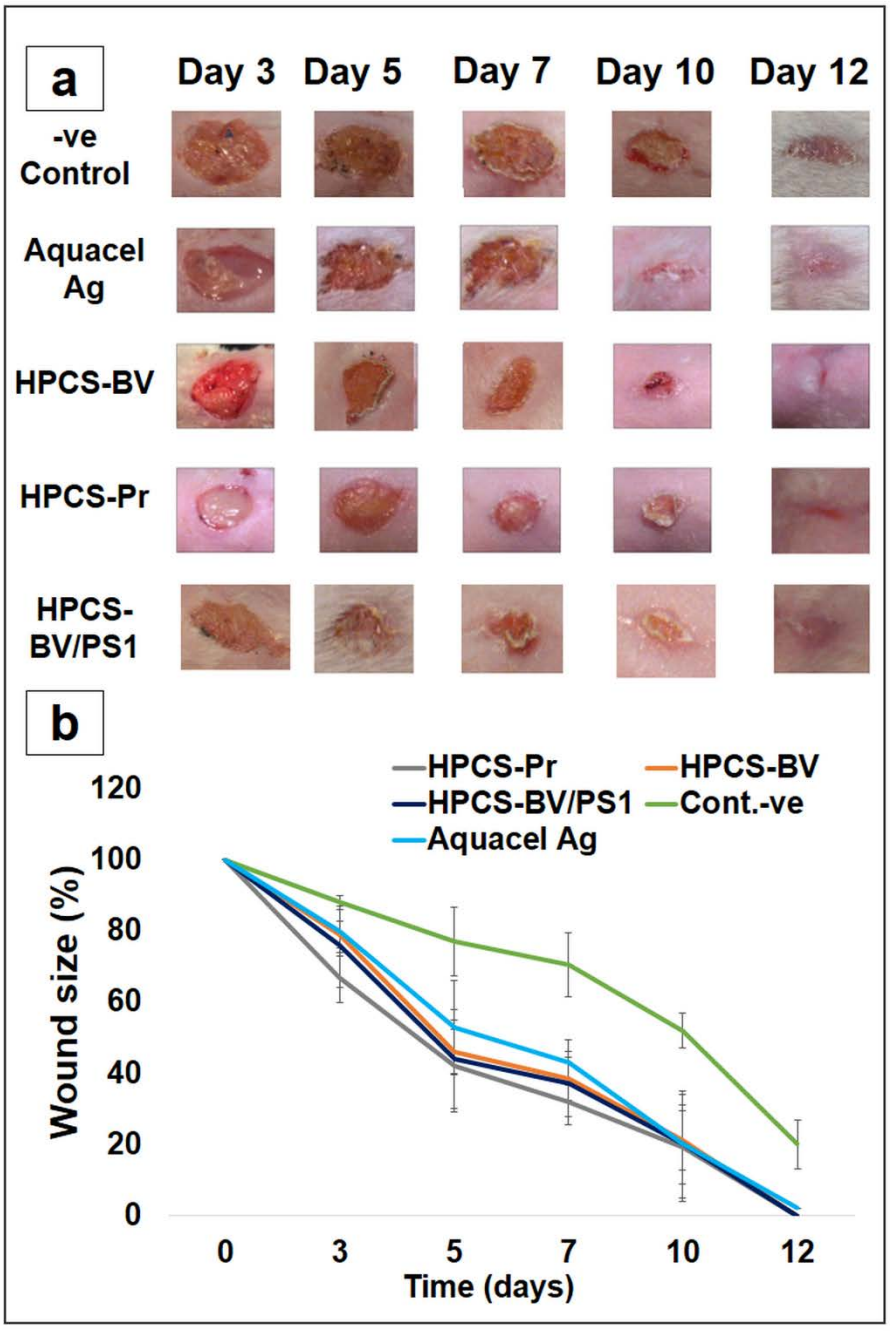

Fig 28. Photographic images of the wound healing process (a) graphical illustration of the variation in the size of the wound (b) on days 3, 5, 7, 10 and 12 for the nanofibrous dressings HPCS-Pr, HPCS-BV, HPCS-BV/PS1 and the untreated negative control (-ve control) as well as the positive control treated with the commercial wound dressing Aquacel Ag .

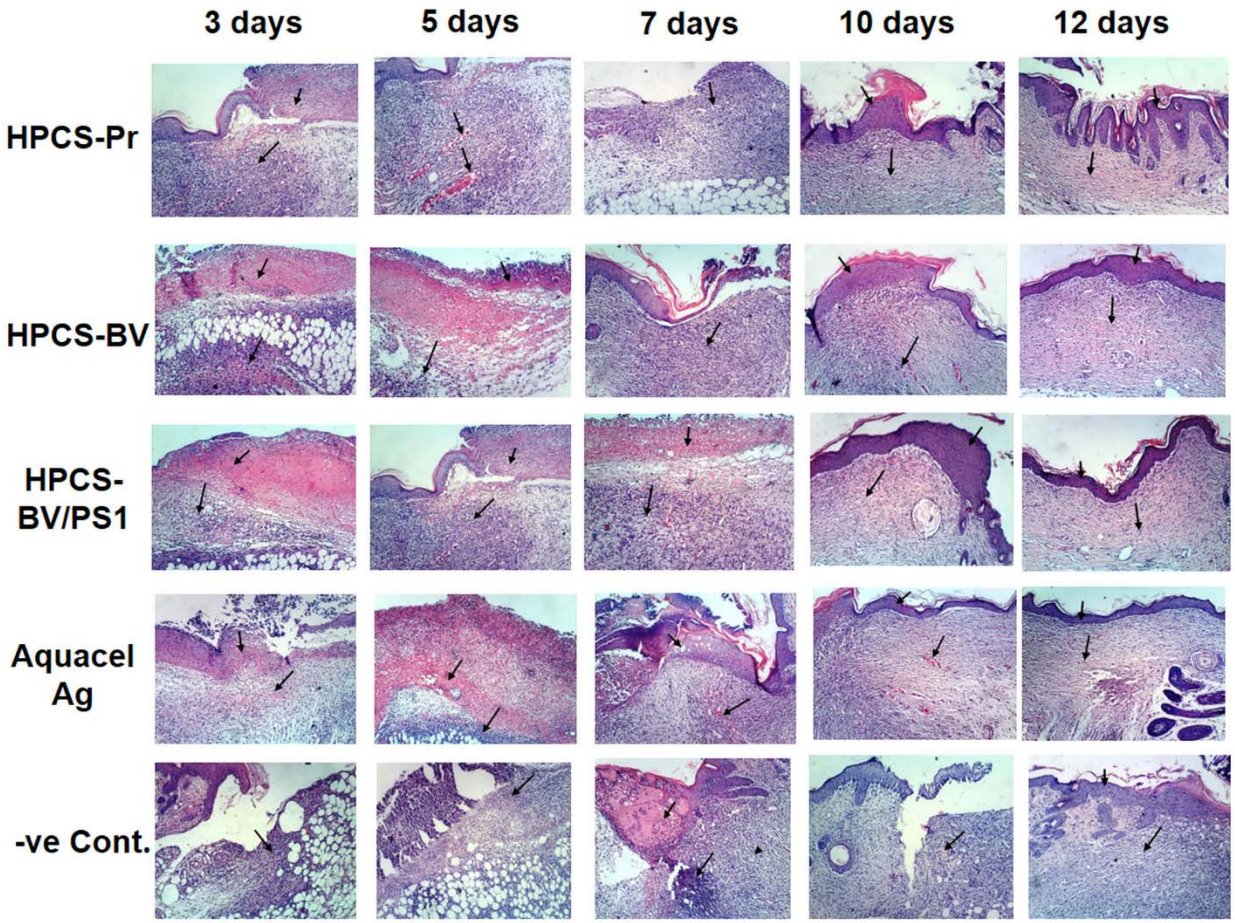

Fig 29. Histopathological evaluation of sections of the H&E stained wound tissue treated with the HPCS-Pr, HPCS-BV, HPCS-BV/PS1 nanofibrous mats and the Aquacel Ag wound dressing at different time intervals (3, 5, 7, 10 & 12 days) (Original magnification 100). The Aquacel Ag was utilized as the positive control and the negative control was kept untreated and covered with a cotton gauze. HPCS-Pr: Micrographs of the central area of the wound treated with the HPCS-Pr nanofibrous dressing. Note the necrosis at day 3, and the massive infiltration of inflammatory cells at days 3, 5, & 7. Highly vascularized granulation tissue was noticed since day 5. Notice the epithelization and thick epidermal layer at days 10 & 12.HPCS-BV and HPCS-BV/PS1: Micrographs of the central area of the wound treated with the HPCS-BV and HPCS-BV/PS1 nanofiber dressing, respectively. Note the massive inflammatory cell infiltration at days 3, 5, & 7, necrosis was observed at days 3 and 5. Note the well vascularized granulation tissue since day 7. Notice the epithelization since day 10 and formation of thick epidermal layer at 10 & 12 days.

Aquacel Ag: Micrographs of the central area of wounds treated with the positive control Aquacel Ag dressing. Note the necrosis at days 3 & 5 and the massive inflammatory cell infiltration. Notice the highly vascularized well oriented granulation tissue since day 7 and the epithelization and formation of thick epidermis at days 10 & 12. –ve cont.: Micrographs of central wound area of untreated controls covered with a cotton gauze. Note the massive inflammatory cell infiltration and necrosis till day 7 and deposition of thin epidermal layer at day 12.

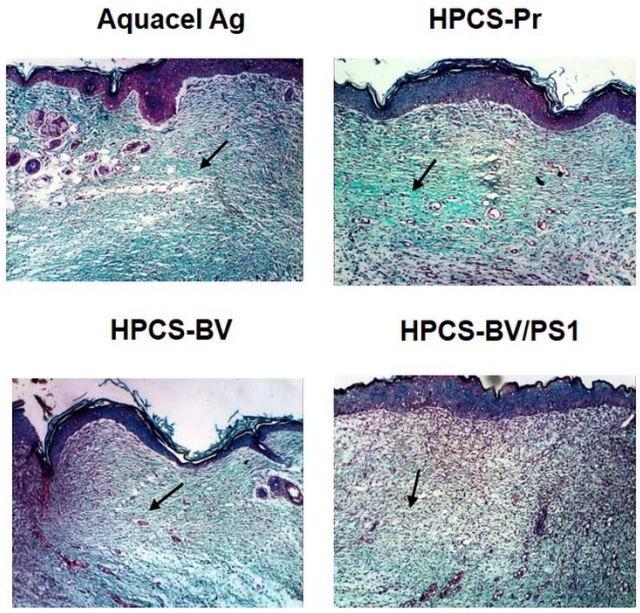

Fig 30. Histopathological evaluation of sections of the MT stained wounds treated with the HPCS-BV, HPCS-Pr, HPCS/BV/PS1 nanofibrous mats and Aquacel Ag wound dressing at day 10 (Original magnification 100). The Aquacel Ag was used as the positive control. Notice deposition of dense collagen in the wounds treated with the developed HPCS-Pr, HPCS-BV, HPCS-BV/PS1 nanofiber dressings similar to that observed with the positive control Aquacel Ag dressing. Note that the most uniform and dense collagen deposition was observed with the wound treated with the HPCS-Pr nanofibrous dressing.

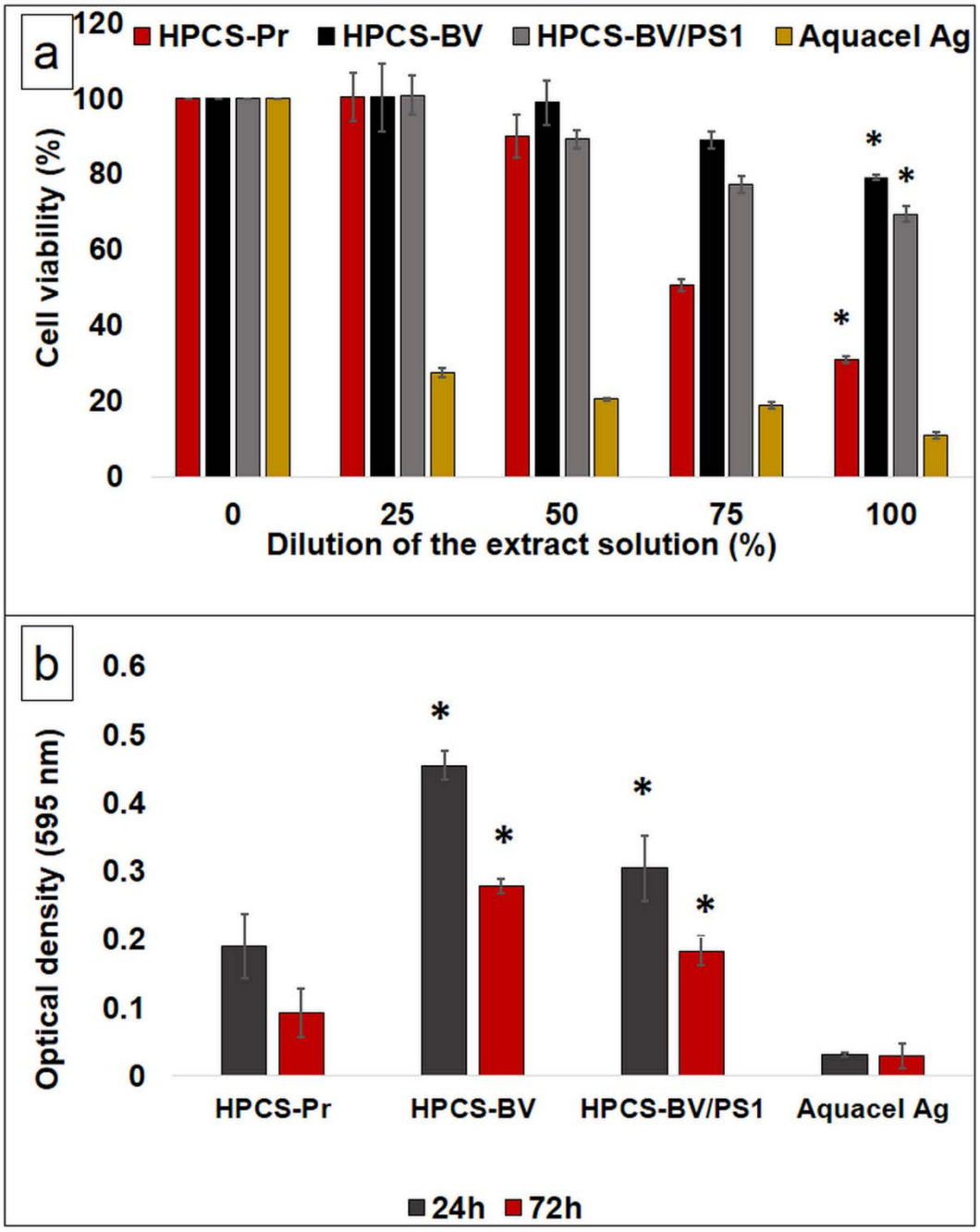

Fig 31. Illustration of results of the MTT assay for determination of the fibroblast cell (ATCC; crl-2522) viability (a) and proliferation (b) for the HPCS-Pr, HPCS-BV, HPCS-BV/PS1 nanofibrous mats and the Aquacel Ag wound dressing. Aquacel Ag was used as the positive control in both assays. Data represent mean ± SD (n = 3, Student's t-test, *p < 0.05 versus the Aquacel Ag dressings).

9. REFERENCES

Abdel-Kawy, M. A., El-Deib, S., El-Khyat, Z., & Mikhail, Y. A. (2000). Chemical and biological studies of Cleome droserifolia (Forssk.) Del. Part-I.*Egyptian Journal of Biomedical Science*, 6, 204.

Abdel-Monem, A. R. (2012). A new alkaloid and a new diterpene from Cleome paradoxa B. Br.(Cleomaceae). *Natural product research*, *26*(3), 264-269.

Aboushoer, M. I., Fathy, H. M., Abdel-Kader, M. S., Goetz, G., & Omar, A. A. (2010). Terpenes and flavonoids from an Egyptian collection of Cleome droserifolia. *Natural product research*, *24*(7), 687-696.

Abrigo, M., McArthur, S. L., & Kingshott, P. (2014). Electrospun Nanofibers as Dressings for Chronic Wound Care: Advances, Challenges, and Future Prospects. *Macromolecular bioscience*, *14*(6), 772-792.

Abu-Seida, A. M. (2015). Effect of Propolis on Experimental Cutaneous Wound Healing in Dogs. *Veterinary medicine international*, *2015*.

Ackermann, H. W., Brochu, G., & Emadi Konjin, H. P. (1994). Classification ofAcinetobacter phages. *Archives of virology*, 135(3), 345-354.

Adomavičiūtė, E., Stanys, S., Žilius, M., Juškaitė, V., Pavilonis, A., & Briedis, V. Formation and biopharmaceutical characterization of electrospun PVP mats with propolis and silver nanoparticles for fast releasing wound dressing. 2016., *BioMed Research International* Volume 2016 (2016), Article ID 4648287,

Agarwal, S., Wendorff, J. H., & Greiner, A. (2008). Use of electrospinning technique for biomedical applications. *Polymer*, *49*(26), 5603-5621.

Ahmad, S. I. (2002). Treatment of post-burns bacterial infections by bacteriophages, specifically ubiquitous Pseudomonas spp. notoriously resistant to antibiotics. *Medical hypotheses*, *58*(4), 327-331.

Ahmed, M. B. M (2006). Biochemical studies on some products of honey bee (masters' thesis). Retrieved from the library of Cairo University.

Al-Astal, Z. Y. (2003). Effect of storage and temperature of aqueous garlic extract on the growth of certain pathogenic bacteria. *Journal of Al Azhar Univeristy-Gaza*,*6*, 11-20.

Alhosseini, S. N., Moztarzadeh, F., Mozafari, M., Asgari, S., Dodel, M., Samadikuchaksaraei, A., ... & Jalali, N. (2012). Synthesis and characterization of electrospun polyvinyl alcohol nanofibrous scaffolds modified by blending with chitosan for neural tissue engineering. *International journal of nanomedicine*, 7, 25.

Ali, M. A. (2012). Studies on bee venom and its medical uses. *International Journal of Advanced Research and Technology*, *1*(2), 69-83.

Alonso, M. J., & Sánchez, A. (2003). The potential of chitosan in ocular drug delivery. *Journal of pharmacy and pharmacology*, *55*(11), 1451-1463.

Altstädt, V., Lovera, D., Schmidt, H., Schmidt, S., & Fery, A. (2008). Electrospun Polymeric Fine Fibres. *Imaging & Microscopy*, 10(2), 29-31.

Aly, A. K. A (2012). Biochemical studies on bee gum (Doctoral dissertation). Retrieved from the library of Cairo University.

Alvarez-Suarez, J. M., Gasparrini, M., Forbes-Hernández, T. Y., Mazzoni, L., & Giampieri, F. (2014). The composition and biological activity of honey: A focus on Manuka honey. *Foods*, *3*(3), 420-432.

Alves de Souza, S., Camara, C. A., Monica Sarmento da Silva, E., & Silva, T. M. S. (2013). Composition and antioxidant activity of geopropolis collected by Melipona subnitida (Jandaira) bees. *Evidence-Based Complementary and Alternative Medicine*, *2013*.

Amin, M. A., & Abdel-Raheem, I. T. (2014). Accelerated wound healing and anti-inflammatory effects of physically cross linked polyvinyl alcohol–chitosan hydrogel containing honey bee venom in diabetic rats. *Archives of pharmacal research*, 37(8), 1016-1031.

Amin, M. A., Abdel-Raheem, I. T., & Madkor, H. R. (2008). Wound healing and anti-inflammatory activities of bee venom-chitosan blend films. *Journal of Drug Delivery Science and Technology*, 18(6), 424-430.

Andualem, B. (2013). Combined antibacterial activity of stingless bee (Apis mellipodae) honey and garlic (Allium sativum) extracts against standard and clinical pathogenic bacteria. *Asian Pacific journal of tropical biomedicine*,*3*(9), 725-731.

Ankri, S., & Mirelman, D. (1999). Antimicrobial properties of allicin from garlic. *Microbes and infection*, 1(2), 125-129.

Aviello, G., Abenavoli, L., Borrelli, F., Capasso, R., Izzo, A. A., Lembo, F., ... & Capasso, F. (2009). Garlic: empiricism or science?. *Natural product communications*, 4(12), 1785-1796.

Azuma, K., Izumi, R., Osaki, T., Ifuku, S., Morimoto, M., Saimoto, H., ... & Okamoto, Y. (2015). Chitin, chitosan, and its derivatives for wound healing: Old and new materials. *Journal of functional biomaterials*, 6(1), 104-142.

Bakri, I. M., & Douglas, C. W. I. (2005). Inhibitory effect of garlic extract on oral bacteria. *Archives of Oral Biology*, 50(7), 645-651.

Bardy, J., Slevin, N. J., Mais, K. L., & Molassiotis, A. (2008). A systematic review of honey uses and its potential value within oncology care. *Journal of clinical nursing*, *17*(19), 2604-2623.

Barnea, Y., Weiss, J., & Gur, E. (2010). A review of the applications of the hydrofiber dressing with silver (Aquacel Ag) in wound care. *Journal of Therapeutics and Clinical Risk Management*, 6, 21-27.

Bellik, Y. (2015). Bee Venom: Its Potential Use in Alternative Medicine. *Anti-Infective Agents*, 13(1), 3-16.

Benkeblia, N. (2004). Antimicrobial activity of essential oil extracts of various onions (Allium cepa) and garlic (Allium sativum). *LWT-Food Science and Technology*, 37(2), 263-268.

Bessa, L. J., Fazii, P., Di Giulio, M., & Cellini, L. (2015). Bacterial isolates from infected wounds and their antibiotic susceptibility pattern: some remarks about wound infection. *International wound journal*, *12*(1), 47-52.

Bhardwaj, N., & Kundu, S. C. (2010). Electrospinning: a fascinating fiber fabrication technique. *Biotechnology advances*, *28*(3), 325-347.

Bhattarai, N., Edmondson, D., Veiseh, O., Matsen, F. A., & Zhang, M. (2005). Electrospun chitosan-based nanofibers and their cellular compatibility. *Biomaterials*, *26*(31), 6176-6184.

binti Rokik, R., & Ali, H. M. (2009, May). Sativum L. in Rats. In Annals of Medicine and Healthcare Research: Proceedings of the 2009 International Online Medical Conference (p. 412). Universal-Publishers.

Biswas, B., Adhya, S., Washart, P., Paul, B., Trostel, A. N., Powell, B., ... & Merril, C. R. (2002). Bacteriophage therapy rescues mice bacteremic from a clinical isolate of vancomycin-resistant Enterococcus faecium. *Infection and immunity*, 70(1), 204-210.

Bjarnsholt, T., Kirketerp-Møller, K., Jensen, P. Ø., Madsen, K. G., Phipps, R., Krogfelt, K., ... & Givskov, M. (2008). Why chronic wounds will not heal: a novel hypothesis. *Wound repair and regeneration*, *16*(1), 2-10.

Boulos L. (1999), Flora of Egypt, Vol. 1. Al-Hadara Publishing, Cairo, Egypt, pp. 177 – 179.

Bowler, P. G. (2003). The 10 (5) bacterial growth guideline: reassessing its clinical relevance in wound healing. *Ostomy/wound management*, *49*(1), 44-53.

Brook, I., & Frazier, E. H. (1998). Aerobic and anaerobic microbiology of chronic venous ulcers. *International journal of dermatology*, *37*(6), 426-428.

Broughton 2nd, G., Janis, J. E., & Attinger, C. E. (2006). The basic science of wound healing. *Plastic and reconstructive surgery*, 117(7 Suppl), 12S-34S.

Brudzynski, K. (2006). Effect of hydrogen peroxide on antibacterial activities ofCanadian honeys. *Canadian Journal of Microbiology*, 52(12), 1228–1237.

Brüssow, H., & Hendrix, R. W. (2002). Phage genomics: small is beautiful.*Cell*, 108(1), 13-16.

Burd, A., Kwok, C. H., Hung, S. C., Chan, H. S., Gu, H., Lam, W. K., & Huang, L. (2007). A comparative study of the cytotoxicity of silver-based dressings in monolayer cell, tissue explant, and animal models. *Wound repair and regeneration*, *15*(1), 94-104.

Burdock, G. A. (1998). Review of the biological properties and toxicity of bee propolis (propolis). *Food and Chemical toxicology*, *36*(4), 347-363.

Burmølle, M., Thomsen, T. R., Fazli, M., Dige, I., Christensen, L., Homøe, P., ... & Moser, C. (2010). Biofilms in chronic infections–a matter of opportunity–monospecies biofilms in multispecies infections. *FEMS Immunology & Medical Microbiology*, *59*(3), 324-336.

C. Migliaresi, G. A. Ruffo, F. Z. Volpato, D. Zeni, in Electrospinning for Advanced Biomedical Applications and Therapies (Ed., N. M. Neves), Smithers Rapra Technology, USA 2012, Ch. 2, p 23.

Cai, Z. X., Mo, X. M., Zhang, K. H., Fan, L. P., Yin, A. L., He, C. L., & Wang, H. S. (2010). Fabrication of chitosan/silk fibroin composite nanofibers for wound-dressing applications. *International journal of molecular sciences*,*11*(9), 3529-3539.

Calhelha, R. C., Falcão, S., Queiroz, M. J. R., Vilas-Boas, M., & Ferreira, I. C. (2014). Cytotoxicity of portuguese propolis: the proximity of the in vitro doses for tumor and normal cell lines. *BioMed research international*, *2014*.

Cardoso, R. L., Maboni, F., Machado, G., Alves, S. H., & de Vargas, A. C. (2010). Antimicrobial activity of propolis extract against Staphylococcus coagulase positive and Malassezia pachydermatis of canine otitis.*Veterinary microbiology*, 142(3), 432-434.

Carey-Smith, G. V., Billington, C., Cornelius, A. J., Hudson, J. A., & Heinemann, J. A. (2006). Isolation and characterization of bacteriophages infecting Salmonella spp. *FEMS microbiology letters*, *258*(2), 182-186.

Castaldo, S., & Capasso, F. (2002). Propolis, an old remedy used in modern medicine. *Fitoterapia*, 73, S1-S6.

Cellini, L., Di Campli, E., Masulli, M., Di Bartolomeo, S., & Allocati, N. (1996). Inhibition of Helicobacter pylori by garlic extract (Allium sativum). *FEMS Immunology & Medical Microbiology*, 13(4), 273-277.

Charernsriwilaiwat, N., Opanasopit, P., Rojanarata, T., & Ngawhirunpat, T. (2011). Fabrication and characterization of chitosan-ethylenediaminetetraacetic acid/polyvinyl alcohol blend electrospun nanofibers. *Advanced Materials Research*, *194*, 648-651.

Charernsriwilaiwat, N., Opanasopit, P., Rojanarata, T., Ngawhirunpat, T., & Supaphol, P. (2010). Preparation and characterization of chitosan-hydroxybenzotriazole/polyvinyl alcohol blend nanofibers by the electrospinning technique. *Carbohydrate Polymers*, *81*(3), 675-680.

Chauhan, D., Dwivedi, J., & Sankararamakrishnan, N. (2014). Novel chitosan/PVA/zerovalent iron biopolymeric nanofibers with enhanced arsenic removal applications. *Environmental Science and Pollution Research*,*21*(15), 9430-9442.

Chen, C., Schultz, G. S., Bloch, M., Edwards, P. D., Tebes, S., & Mast, B. A. (1999). Molecular and mechanistic validation of delayed healing rat wounds as a model for human chronic wounds. *Wound Repair and Regeneration*, *7*(6), 486-494.

Chen, G. W., Chung, J. G., Ho, H. C., & Lin, J. G. (1999). Effects of the garlic compounds diallyl sulphide and diallyl disulphide on arylamine N-acetyltransferase activity in Klebsiella pneumoniae. *Journal of Applied Toxicology*, *19*(2), 75-81.

Chen, J. P., Chang, G. Y., & Chen, J. K. (2008). Electrospun collagen/chitosan nanofibrous membrane as wound dressing. *Colloids and Surfaces A: Physicochemical and Engineering Aspects*, 313, 183-188.

Chibani-Chennoufi, S., Sidoti, J., Bruttin, A., Kutter, E., Sarker, S., & Brüssow, H. (2004). In vitro and in vivo bacteriolytic activities of Escherichia coli phages: implications for phage therapy. *Antimicrobial agents and chemotherapy*, 48(7), 2558-2569.

Chuang, W. Y., Young, T. H., Yao, C. H., & Chiu, W. Y. (1999). Properties of the poly (vinyl alcohol)/chitosan blend and its effect on the culture of fibroblast in vitro. *Biomaterials*, *20*(16), 1479-1487.

Cooper, R. (2004). A review of the evidence for the use of topical antimicrobial agents in wound care. *World wide wounds*, 1-11.

Cui, W., Zhou, S., Li, X., & Weng, J. (2006). Drug-loaded biodegradable polymeric nanofibers prepared by electrospinning. *Tissue Engineering*, 12, 1070- 1070.

Cutler, R. R., & Wilson, P. (2004). Antibacterial activity of a new, stable, aqueous extract of allicin against methicillin-resistant Staphylococcus aureus. *British journal of biomedical science*, 61(2), 71-74.

da Silva Frozza, C. O., Garcia, C. S. C., Gambato, G., de Souza, M. D. O., Salvador, M., Moura, S., ... & Dellagostin, O. A. (2013). Chemical characterization, antioxidant and cytotoxic activities of Brazilian red propolis.*Food and Chemical Toxicology*, 52, 137-142.

Dai, M., Senecal, A., & Nugen, S. R. (2014). Electrospun water-soluble polymer nanofibers for the dehydration and storage of sensitive reagents.*Nanotechnology*, 25(22), 225101.

Dai, T., Tanaka, M., Huang, Y. Y., & Hamblin, M. R. (2011). Chitosan preparations for wounds and burns: antimicrobial and wound-healing effects.*Expert review of anti-infective therapy*, 9(7), 857-879.

Davies, C. E., Hill, K. E., Wilson, M. J., Stephens, P., Hill, C. M., Harding, K. G., & Thomas, D. W. (2004). Use of 16S ribosomal DNA PCR and denaturing gradient gel electrophoresis for analysis of the microfloras of healing and nonhealing chronic venous leg ulcers. *Journal of clinical microbiology*, *42*(8), 3549-3557.

Deitzel, J. M., Kleinmeyer, J., Harris, D. E. A., & Tan, N. B. (2001). The effect of processing variables on the morphology of electrospun nanofibers and textiles. *Polymer*, *42*(1), 261-272.

Demling, R. H., & Waterhouse, B. (2007). The increasing problem of wound bacterial burden and infection in acute and chronic soft-tissue wounds caused by methicillin-resistant Staphylococcus aureus. *Journal of Burns and Wounds*,*7*(8).

Demling, R., & DeSanti, L. (2001). Effects of silver on wound management. *Wounds*, 13, 5–14

Diegelmann, R. F., & Evans, M. C. (2004). Wound healing: an overview of acute, fibrotic and delayed healing. *Frontiers Bioscience*, *9*(1), 283-289.

Dissemond, J. (2009). Methicillin resistant Staphylococcus aureus (MRSA): diagnostic, clinical relevance and therapy. *JDDG: Journal der Deutschen Dermatologischen Gesellschaft*, *7*(6), 544-553.

Drucker, M., Cardenas, E., Arizti, P., Valenzuela, A., & Gamboa, A. (1998). Experimental studies on the effect of lidocaine on wound healing. *World journal of surgery*, 22(4), 394-398.

Duan, B., Yuan, X., Zhu, Y., Zhang, Y., Li, X., Zhang, Y., & Yao, K. (2006). A nanofibrous composite membrane of PLGA–chitosan/PVA prepared by electrospinning. *European Polymer Journal*, *42*(9), 2013-2022.

Durairaj, S., Srinivasan, S., & Lakshmanaperumalsamy, P. (2009). In vitro antibacterial activity and stability of garlic extract at different pH and temperature. *Electronic Journal of Biology*, 5(1), 5-10.

Edwards, R., & Harding, K. G. (2004). Bacteria and wound healing. *Current opinion in infectious diseases*, 17(2), 91-96.

Ejaz, S., Chekarova, I., Cho, J. W., Lee, S. Y., Ashraf, S., & Lim, C. W. (2009). Effect of aged garlic extract on wound healing: a new frontier in wound management. *Drug and chemical toxicology*, 32(3), 191-203.

Ekwenye, U. N., & Elegalam, N. N. (2005). Antibacterial activity of Ginger (Zingiber officinale Roscoe and Garlic (Allium sativum L.) extracts on Escherichia coli and Salmonella typhi. *International Journal of Molecular Sciences*, 1, 411-416.

El-Khawaga, O. Y., Abou-Seif, M. A., El-Waseef, A., & Negm, A. A. (2010). Hypoglycemic, hypolipidemic and antioxidant activities of Cleome droserifolia in Streptozotocin-Diabetic Rats. *Journal of Stress Physiology & Biochemistry*, *6*(4).

El-Shenawy, N. S., & Abdel-Nabi, I. M. (2004). Comparative analysis of the protective effect of melatonin and Cleome droserifolia extract on antioxidant status of diabetic rats. *The Egyptian Journal of hospital medicine*, 14, 11-25.

Elsom, G. K. (2000). An antibacterial assay of aqueous extract of garlic against anaerobic/microaerophilic and aerobic bacteria. *Microbial ecology in health and disease*, *12*(2), 81-84.

Endersen, L., O'Mahony, J., Hill, C., Ross, R. P., McAuliffe, O., & Coffey, A. (2014). Phage therapy in the food industry. *Annual review of food science and technology*, 5, 327-349.

Etkin, N. L. (1981). A Hausa herbal pharmacopoeia: biomedical evaluation of commonly used plant medicines. *Journal of Ethnopharmacology*, 4(1), 75-98.

Ezzat, S. M., & Motaal, A. A. (2012). Isolation of new cytotoxic metabolites from Cleome droserifolia growing in Egypt. *Zeitschrift für Naturforschung C*,67 (5-6), 266-274.

Felsner, M. L., Cano, C. B., Matos, J. R., Almeida-Muradian, L. B. D., & Bruns, R. E. (2004). Optimization of thermogravimetric analysis of ash content in honey. *Journal of the Brazilian Chemical Society*, *15*(6), 797-802.

Fennell, J. E., W. H. Shipman and L. J. Cole (1968) Antibacterial action of melittin, a polypeptide from the venom. *Proceedings of the Society for Experimental Biology and Medicine*,127, 707-710.

Fitzmaurice, S. D., Sivamani, R. K., & Isseroff, R. R. (2011). Antioxidant therapies for wound healing: a clinical guide to currently commercially available products. *Skin pharmacology and physiology*, *24*(3), 113-126.

Frost & Sullivan. (2014, October 7). Global Wound Care Market Outlook, Analysis of Wound Care Technologies. Retrieved from http://www.frost.com/

Fuliang, H. U., Hepburn, H. R., Xuan, H., Chen, M., Daya, S., & Radloff, S. E. (2005). Effects of propolis on blood glucose, blood lipid and free radicals in rats with diabetes mellitus. *Pharmacological Research*, 51(2), 147-152.

Gaaz, T. S., Sulong, A. B., Akhtar, M. N., Kadhum, A. A. H., Mohamad, A. B., & Al-Amiery, A. A. (2015). Properties and Applications of Polyvinyl Alcohol, Halloysite Nanotubes and Their Nanocomposites. *Molecules*,20 (12), 22833-22847.

Gaherwal, S., Johar, F., Wast, N., & Prakash, M. M. (2014). Anti-Bacterial Activities of Allium sativum Against Escherichia coli, Salmonella Ser. Typhi and Staphylococcus aureus. *International Journal of Microbiological Research*, 5 (1): 19-22, 2014 *5*(1), 19-22.

Gallant-Behm, C. L., Yin, H. Q., Liu, S., Heggers, J. P., Langford, R. E., Olson, M. E., ... & Burrell, R. E. (2005). Comparison of in vitro disc diffusion and time kill-kinetic assays for the evaluation of antimicrobial wound dressing efficacy. *Wound repair and regeneration*, *13*(4), 412-421.

Geng, X., Kwon, O. H., & Jang, J. (2005). Electrospinning of chitosan dissolved in concentrated acetic acid solution. *Biomaterials*, *26*(27), 5427-5432.

Gjødsbøl, K., Christensen, J. J., Karlsmark, T., Jørgensen, B., Klein, B. M., & Krogfelt, K. A. (2006). Multiple bacterial species reside in chronic wounds: a longitudinal study. *International wound journal*, 3(3), 225-231.

Goy, R. C., Britto, D. D., & Assis, O. B. (2009). A review of the antimicrobial activity ofchitosan. *Polímeros*, 19(3), 241–247.

Grange, J. M., & Davey, R. W. (1990). Antibacterial properties of propolis (bee glue). *Journal of the Royal Society of Medicine*, 83(3), 159-160.

Gu, B. K., Park, S. J., Kim, M. S., Kang, C. M., Kim, J. I., & Kim, C. H. (2013). Fabrication of sonicated chitosan nanofiber mat with enlarged porosity for use as hemostatic materials. *Carbohydrate polymers*, *97*(1), 65-73.

Gülçin, I. (2012). Antioxidant activity of food constituents: an overview.*Archives of toxicology*, 86(3), 345-391.

Gunn, J., & Zhang, M. (2010). Polyblend nanofibers for biomedical applications: perspectives and challenges. *Trends in biotechnology*, *28*(4), 189-197.

Gupta, P. C., & Rao, C. V. (2012). Pharmacognostical studies of Cleome viscosa Linn. *Indian Journal of Natural Product Resources*, 3, 527-534.

Gupta, R. K., Reybroeck, W., van Veen, J. W., & Gupta, A. (2014).Beekeeping for Poverty Alleviation and Livelihood Security. Springer.

Halbert, A. R., Stacey, M. C., Rohr, J. B., & Jopp-Mckay, A. (1992). The effect of bacterial colonization on venous ulcer healing. *Australasian journal of dermatology*, *33*(2), 75-80.

Han, T. S., Sutradhar, B. C., Kim, J. M., Kim, M. H., Kim, G., & Choi, S. H. (2012). Healing Effect of Bee Venom Cream to Full-Thickness Skin Wound in Rabbits. *Journal of Biomedical Research*, 13(1), 47-52.

Hanshou, Y., Hanzhang, W., & Bing, Y. (2000). Recent advances of chitosan in suppression of plant diseases. *Natural Product Research and Development*, *3*, 018.

Hegazi, A. G., EL-Feel, M. A., Abdel-Rahman, E. H., & Al-Fattah, A. (2015). Antibacterial Activity of Bee Venom Collected from Apis mellifera Carniolan Pure and Hybrid Races by Two Collection Methods. *Int. J. Curr. Microbiol. App. Sci*, *4*(4), 141-149.

Hegazi, A., Abdou, A. M., Fyrouz, S. I. A. E. M., & Allah, A. (2014). Evaluation of the antibacterial activity of bee venom from different sources.*World Applied Sciences Journal*, 30(3), 266-270.

Hider, R. C. (1988). Honeybee venom: a rich source of pharmacologically active peptides. *Endeavour*, 12(2), 60-65.

Homayoni, H., Ravandi, S. A. H., & Valizadeh, M. (2009). Electrospinning of chitosan nanofibers: Processing optimization. *Carbohydrate Polymers*, *77*(3), 656-661.

Howell-Jones, R. S., Wilson, M. J., Hill, K. E., Howard, A. J., Price, P. E., & Thomas, D. W. (2005). A review of the microbiology, antibiotic usage and resistance in chronic skin wounds. *Journal of Antimicrobial Chemotherapy*,*55*(2), 143-149.

Huang, S., Zhang, C. P., Wang, K., Li, G. Q., & Hu, F. L. (2014). Recent advances in the chemical composition of propolis. *Molecules*, *19*(12), 19610-19632.

Hunt, T. K. (1988). The physiology of wound healing. *Annals of emergency medicine*, *17*(12), 1265-1273.

Hussein, N. S., Ahmed, A. A., & Darwish, F. M. K. (1994). Sesquiterpenes from cleome drosorifolia. *Pharmazie*, *49*(1), 76-77.

Islam, M., Masum, S. M., Mahbub, K. R., & Haque, M. (2011). Antibacterial activityof crab-chitosan against Staphylococcus aureus and Escherichia coli. *Journal ofAdvanced Scientific Research*, 2(4).

Iwalokun, B. A., Ogunledun, A., Ogbolu, D. O., Bamiro, S. B., & Jimi-Omojola, J. (2004). In vitro antimicrobial properties of aqueous garlic extract against multidrug-resistant bacteria and Candida species from Nigeria. *Journal of medicinal food*, 7(3), 327-333.

Jaganathan, S. K., & Mandal, M. (2009). Antiproliferative effects of honey and of itspolyphenols: A review. *Journal of Biomedicine and Biotechnology*, 2009. ArticleID: 830616, 13 pages.

James, G. A., Swogger, E., Wolcott, R., Secor, P., Sestrich, J., Costerton, J. W., & Stewart, P. S. (2008). Biofilms in chronic wounds. *Wound repair and regeneration*, *16*(1), 37-44.

Jane, R. R., & Patil, S. D. (2012). Cleome viscosa: an effective medicinal herb for otitis media. *Int J Sci Nat*, *3*(1), 153-158.

Jannesari, M., Varshosaz, J., Morshed, M., & Zamani, M. (2011). Composite poly (vinyl alcohol)/poly (vinyl acetate) electrospun nanofibrous mats as a novel wound dressing matrix for controlled release of drugs. *Int J Nanomedicine*, *6*, 993-1003.

Jayakumar, R., Menon, D., Manzoor, K., Nair, S. V., & Tamura, H. (2010). Biomedical applications of chitin and chitosan based nanomaterials—A short review. *Carbohydrate Polymers*, *82*(2), 227-232.

Jeruto, P., Lukhoba, C., Ouma, G., Otieno, D., & Mutai, C. (2008). An ethnobotanical study of medicinal plants used by the Nandi people in Kenya.*Journal of Ethnopharmacology*, *116*(2), 370-376.

Jia, Y. T., Gong, J., Gu, X. H., Kim, H. Y., Dong, J., & Shen, X. Y. (2007). Fabrication and characterization of poly (vinyl alcohol)/chitosan blend nanofibers produced by electrospinning method. *Carbohydrate Polymers*,*67*(3), 403-409.

Jin, G., Prabhakaran, M. P., Kai, D., Annamalai, S. K., Arunachalam, K. D., & Ramakrishna, S. (2013). Tissue engineered plant extracts as nanofibrous wound dressing. *Biomaterials*, *34*(3), 724-734.

Kanani, A. G., & Bahrami, S. H. (2010). Review on electrospun nanofibers scaffold and biomedical applications. *Trends Biomater Artif Organs*, *24*(2), 93-115.

Kang, Y. O., Yoon, I. S., Lee, S. Y., Kim, D. D., Lee, S. J., Park, W. H., et al. (2010). Chitosan-coated poly (vinyl alcohol) nanofibers for wound dressings. *Journal of Biomedical Materials Research Part B: Applied Biomaterials*, 92(2), 568–576.

Kazemi Pilehrood, M., Dilamian, M., Mirian, M., Sadeghi-Aliabadi, H., Maleknia, L., Nousiainen, P., & Harlin, A. (2014). Nanofibrous Chitosan-Polyethylene Oxide Engineered Scaffolds: A Comparative Study between Simulated Structural Characteristics and Cells Viability. *BioMed research international*, 2014. (59)

Khan, F. R., Abadin, Z. U., & Rauf, N. (2007). Honey: nutritional and medicinal value. *International journal of clinical practice*, *61*(10), 1705-1707.

Khatun, U. L., & Mukhopadhyay, C. (2013). Interaction of bee venom toxin melittin with ganglioside GM1 bicelle. *Biophysical chemistry*, 180, 66-75.

Khil, M. S., Cha, D. I., Kim, H. Y., Kim, I. S., & Bhattarai, N. (2003). Electrospun nanofibrous polyurethane membrane as wound dressing. *Journal of Biomedical Materials Research Part B: Applied Biomaterials*, *67*(2), 675-679.

Kim SH, Jung SY, Lee KW, Lee SH, Cai M, Choi SM, Yang EJ. 2013. Bee venom effects on ubiquitin proteasome system in hSOD1(G85R)-expressing NSC34 motor neuron cells. *BMC Complementary and Alternative Medicine*, 13,179–186.

Kim, J. H., Kim, J. Y., Lee, Y. M., & Kim, K. Y. (1992). Properties and swelling characteristics of cross-linked poly (vinyl alcohol)/chitosan blend membrane. *Journal of applied polymer science*, *45*(10), 1711-1717.

Kim, J. I., Pant, H. R., Sim, H. J., Lee, K. M., & Kim, C. S. (2014). Electrospun propolis/polyurethane composite nanofibers for biomedical applications. *Materials Science and Engineering: C*, *44*, 52-57.

Kim, S. E., Heo, D. N., Lee, J. B., Kim, J. R., Park, S. H., Jeon, S. H., & Kwon, I. K. (2009). Electrospun gelatin/polyurethane blended nanofibers for wound healing. *Biomedical Materials*, *4*(4), 044106.

Kim, S. H., Jung, S. Y., Lee, K. W., Lee, S. H., Cai, M., Choi, S. M., & Yang, E. J. (2013). Bee venom effects on ubiquitin proteasome system in hSOD1G85R-expressing NSC34 motor neuron cells. *BMC complementary and alternative medicine*, 13(1), 179.

Kirketerp-Møller, K., Zulkowski, K., & James, G. (2011). Chronic wound colonization, infection, and biofilms. In *Biofilm infections* (pp. 11-24). Springer New York.

Kirsner, R. S., & Eaglstein, W. H. (1993). The wound healing process.*Dermatologic clinics*, *11*(4), 629-640.

Körber, A., Schmid, E. N., Buer, J., Klode, J., Schadendorf, D., & Dissemond, J. (2010). Bacterial colonization of chronic leg ulcers: current results compared with data 5 years ago in a specialized dermatology department. *Journal of the European Academy of Dermatology and Venereology*, *24*(9), 1017-1025.

Korehei, R., & Kadla, J. (2013). Incorporation of T4 bacteriophage in electrospun fibres. *Journal of applied microbiology*, 114(5), 1425-1434.

Kujumgiev, A., Tsvetkova, I., Serkedjieva, Y., Bankova, V., Christov, R., & Popov, S. (1999). Antibacterial, antifungal and antiviral activity of propolis of different geographic origin. *Journal of ethnopharmacology*, 64(3), 235-240.,

Kuropatnicki, A. K., Szliszka, E., & Krol, W. (2013). Historical aspects of propolis research in modern times. *Evidence-Based Complementary and Alternative Medicine*, 2013.

Kwon, Y. B., Lee, H. J., Han, H. J., Mar, W. C., Kang, S. K., Yoon, O. B., ... & Lee, J. H. (2002). The water-soluble fraction of bee venom produces antinociceptive and anti-inflammatory effects on rheumatoid arthritis in rats.*Life sciences*, 71(2), 191-204.

Lansdown, A. B. G. (2002). Silver 2: toxicity in mammals and how its products aid wound repair. *Journal of wound care*, *11*(5), 173-177.

Lee, J. B., Jeong, S. I., Bae, M. S., Yang, D. H., Heo, D. N., Kim, C. H., ... & Kwon, I. K. (2011). Highly porous electrospun nanofibers enhanced by ultrasonication for improved cellular infiltration. *Tissue Engineering Part A*,17(21-22), 2695-2702.

Lee, S. W., & Belcher, A. M. (2004). Virus-based fabrication of micro-and nanofibers using electrospinning. *Nano letters*, 4(3), 387-390.

Lewington, A. (1993). A review of the importation of medicinal plants and extracts into Europe: species in danger. A traffic network report (No. 382.41388 L672). Traffic International, Cambridge (RU).

Li, B., Shan, C. L., Zhou, Q., Fang, Y., Wang, Y. L., Xu, F., ... & Sun, G. C. (2013). Synthesis, characterization, and antibacterial activity of cross-linked chitosan-glutaraldehyde. *Marine drugs*, *11*(5), 1534-1552.

Li, C., Fu, R., Yu, C., Li, Z., Guan, H., Hu, D., ... & Lu, L. (2013). Silver nanoparticle/chitosan oligosaccharide/poly (vinyl alcohol) nanofibers as wound dressings: a preclinical study. *International journal of nanomedicine,8*, 4131.

Li, S., & Yang, X. H. (2014). Fabrication and characterization of electrospun wool keratin/poly (vinyl alcohol) blend nanofibers. *Advances in Materials Science and Engineering*, 2014.

Li, X., Qin, J., & Ma, J. (2015). Silk fibroin/poly (vinyl alcohol) blend scaffolds for controlled delivery of curcumin. *Regenerative Biomaterials*,2 (2), 97-105.

Li, Y., Chen, F., Nie, J., & Yang, D. (2012). Electrospun poly (lactic acid)/chitosan core–shell structure nanofibers from homogeneous solution.*Carbohydrate polymers*, *90*(4), 1445-1451.

Liao, H., Qi, R., Shen, M., Cao, X., Guo, R., Zhang, Y., et al. (2011). Improved cellular response on multiwalled carbon nanotube-incorporated electrospun polyvinyl alcohol/chitosan nanofibrous scaffolds. *Colloids and Surfaces B: Biointerfaces*, *84*(2), 528-535.

Lim, S. H., & Hudson, S. M. (2003). Review of chitosan and its derivatives as antimicrobial agents and their uses as textile chemicals. *Journal of Macromolecular Science, Part C: Polymer Reviews*, *43*(2), 223-269.

Lin, L., Perets, A., Har-el, Y. E., Varma, D., Li, M., Lazarovici, P., ... & Lelkes, P. I. (2013). Alimentary 'green'proteins as electrospun scaffolds for skin regenerative engineering. *Journal of tissue engineering and regenerative medicine*, *7*(12), 994-1008.

Lipsky, B. A., & Hoey, C. (2009). Topical antimicrobial therapy for treating chronic wounds. *Clinical infectious diseases*, *49*(10), 1541-1549.

Liu, N., Chen, X. G., Park, H. J., Liu, C. G., Liu, C. S., Meng, X. H., et al. (2006). Effect of MW and concentration of chitosan on antibacterial activity of Escherichia coli.*Carbohydrate Polymers*, 64(1), 60–65.

Londhe, V. P. (2014). Role of garlic (allium sativum) in various diseases-an overview. *Journal of pharmaceutical research & opinion*, 1(4).

Lotfy, M. (2006). Biological activity of bee propolis in health and disease.*Asian Pac J Cancer Prev*, *7*(1), 22-31.

Lowenstein, Henning, and Lorraine M. Mulfinger. "Methods and compositions for the treatment of mammalian infections employing medicaments comprising hymenoptera venom, proteinageous or polypeptide components thereof, or analogues of such proteinaceous or polypeptide components." U.S. Patent Application 08/815,296, filed March 11, 1997.

Luu, Y. K., Kim, K., Hsiao, B. S., Chu, B., & Hadjiargyrou, M. (2003). Development of a nanostructured DNA delivery scaffold via electrospinning of PLGA and PLA–PEG block copolymers. *Journal of controlled release*,89 (2), 341-353.

Madsen, S. M., Westh, H., Danielsen, L., & Rosdahl, V. T. (1996). Bacterial colonization and healing of venous leg ulcers. *Apmis*, *104*(7-8), 895-899.

Majtán, J., Kováčová, E., Bíliková, K., & Šimúth, J. (2006). The immunostimulatory effect of the recombinant apalbumin 1–major honeybee royal jelly protein–on TNFα release. *International immunopharmacology*, 6(2), 269-278.

Maleki, H., Gharehaghaji, A. A., & Dijkstra, P. J. (2013). A novel honey-based nanofibrous scaffold for wound dressing application. *Journal of Applied Polymer Science*, *127*(5), 4086-4092.

Mandal, M. D., & Mandal, S. (2011). Honey: its medicinal property and antibacterial activity. *Asian Pacific Journal of Tropical Biomedicine*, 1(2), 154-160.

Marcucci, M. C. (1995). Propolis: chemical composition, biological properties and therapeutic activity. *Apidologie*, *26*(2), 83-99.

Marcucci, M. C., Ferreres, F., Garcıa-Viguera, C., Bankova, V. S., De Castro, S. L., Dantas, A. P., ... & Paulino, N. (2001). Phenolic compounds from Brazilian propolis with pharmacological activities. *Journal of ethnopharmacology*, 74(2), 105-112.

Martinotti, S., & Ranzato, E. (2015). Propolis: a new frontier for wound healing?. *Burns & Trauma*, 3(1), 1.

Martins, A., Araújo, J. V., Reis, R. L., & Neves, N. M. (2007). Electrospun nanostructured scaffolds for tissue engineering applications.*Future medicine*, 2, 924-942.

Matsui, T., Ebuchi, S., Fujise, T., Abesundara, K. J., Doi, S., Yamada, H., & Matsumoto, K. (2004). Strong antihyperglycemic effects of water-soluble fraction of Brazilian propolis and its bioactive constituent, 3, 4, 5-tri-O-caffeoylquinic acid. *Biological and Pharmaceutical Bulletin*, 27(11), 1797-1803.

Matsuzaki, S., Rashel, M., Uchiyama, J., Sakurai, S., Ujihara, T., Kuroda, M., ... & Imai, S. (2005). Bacteriophage therapy: a revitalized therapy against bacterial infectious diseases. *Journal of infection and chemotherapy*,11(5), 211-219.

McLennan, S. V., Bonner, J., Milne, S., Lo, L., Charlton, A., Kurup, S., ... & Twigg, S. M. (2008). The anti-inflammatory agent Propolis improves wound healing in a rodent model of experimental diabetes. *Wound Repair and Regeneration*, 16(5), 706-713.

Meinel, A. J., Germershaus, O., Luhmann, T., Merkle, H. P., & Meinel, L. (2012). Electrospun matrices for localized drug delivery: current technologies and selected biomedical applications. *European Journal of Pharmaceutics and Biopharmaceutics*, *81*(1), 1-13.

Mendes, J. J., Leandro, C., Corte-Real, S., Barbosa, R., Cavaco-Silva, P., Melo-Cristino, J., ... & Garcia, M. (2013). Wound healing potential of topical bacteriophage therapy on diabetic cutaneous wounds. *Wound Repair and Regeneration*, 21(4), 595-603.

Mihelich, E. D., & Schevitz, R. W. (1999). Structure-based design of a new class of anti-inflammatory drugs: secretory phospholipase A 2 inhibitors, SPI. *Biochimica et Biophysica Acta (BBA)-Molecular and Cell Biology of Lipids*, 1441(2), 223-228.

Minami, S. (1997). Mechanism of wound healing acceleration by chitin and chitosan. *Japanese Journal of Veterinary Research*, *44*(4), 218-219.

Miyamoto-Shinohara, Y., Imaizumi, T., Sukenobe, J., Murakami, Y., Kawamura, S., & Komatsu, Y. (2000). Survival rate of microbes after freeze-drying and long-term storage. *Cryobiology*, 41(3), 251-255.

Mohd Zohdi, R., Abu Bakar Zakaria, Z., Yusof, N., Mohamed Mustapha, N., & Abdullah, M. N. H. (2011). Gelam (Melaleuca spp.) honey-based hydrogel as burn wound dressing. *Evidence-Based Complementary and Alternative Medicine*, *2012*.

Molan, P. C. (1992). The antibacterial activity of honey. 2: Variation in the potencyof the antibacterial activity. *Bee World*, 73(2), 59–76.

Molan, P. C. (2006). The evidence supporting the use of honey as a wound dressing. *The International Journal of Lower Extremity Wounds*, *5*(1), 40-54.

Molan, P., & Rhodes, T. (2015). Honey: A Biologic Wound Dressing.*Wounds: a compendium of clinical research and practice*, 27(6), 141-151.

Monk, A. B., Rees, C. D., Barrow, P., Hagens, S., & Harper, D. R. (2010). Bacteriophage applications: where are we now?. *Letters in Applied Microbiology*, *51*(4), 363-369.

Muhaidat, R., Al-Qudah, M. A., Samir, O., Jacob, J. H., Hussein, E., Al-Tarawneh, I. N., ... & Orabi, S. T. A. (2015). Phytochemical investigation and in vitro antibacterial activity of essential oils from Cleome droserifolia (Forssk.) Delile and C. trinervia Fresen.(Cleomaceae). *South African Journal of Botany*, *99*, 21-28.

Muzzarelli, R., Tarsi, R., Filippini, O., Giovanetti, E., Biagini, G., & Varaldo, P. E. (1990). Antimicrobial properties of N-carboxybutyl chitosan.*Antimicrobial agents and chemotherapy*, *34*(10), 2019-2023.

Nakane, K., Yamashita, T., Iwakura, K., & Suzuki, F. (1999). Properties and structure of poly (vinyl alcohol)/silica composites. *Journal of Applied Polymer Science*, *74*(1), 133-138.

No, H. K., Park, N. Y., Lee, S. H., & Meyers, S. P. (2002). Antibacterial activity of chitosans and chitosan oligomers with different molecular weights.*International journal of food microbiology*, *74*(1), 65-72.

Ohkawa, K., Cha, D., Kim, H., Nishida, A., & Yamamoto, H. (2004). Electrospinning of chitosan. *Macromolecular Rapid Communications*, 25, 1600–1605.

Olczyk, P., Komosinska-Vassev, K., Winsz-Szczotka, K., Stojko, J., Klimek, K., & Kozma, E. M. (2013). Propolis induces chondroitin/dermatan sulphate and hyaluronic acid accumulation in the skin of burned wound. *Evidence-Based Complementary and Alternative Medicine*, 2013.

Olczyk, P., Wisowski, G., Komosinska-Vassev, K., Stojko, J., Klimek, K., Olczyk, M., & Kozma, E. M. (2013). Propolis modifies collagen types I and III accumulation in the matrix of burnt tissue. *Evidence-Based Complementary and Alternative Medicine*, 2013.

Paipitak, K., Pornpra, T., Mongkontalang, P., Techitdheer, W., & Pecharapa, W. (2011). Characterization of PVA-chitosan nanofibers prepared by electrospinning. *Procedia Engineering*, *8*, 101-105.

Pazyar, N., & Feily, A. (2011). Garlic in dermatology. Dermatology reports,3 (1).

Peluso, G., Petillo, O., Ranieri, M., Santin, M., Ambrosic, L., Calabró, D., ... & Balsamo, G. (1994). Chitosan-mediated stimulation of macrophage function. *Biomaterials*, *15*(15), 1215-1220.

Peng, C. C., Yang, M. H., Chiu, W. T., Chiu, C. H., Yang, C. S., Chen, Y. W., ... & Peng, R. Y. (2008). Composite Nano-Titanium Oxide–Chitosan Artificial Skin Exhibits Strong Wound-Healing Effect—An Approach with Anti-Inflammatory and Bactericidal Kinetics. *Macromolecular bioscience*, *8*(4), 316-327.

Percival, S. L., Woods, E., Nutekpor, M., Bowler, P., Radford, A., & Cochrane, C. (2008). Prevalence of silver resistance in bacteria isolated from diabetic foot ulcers and efficacy of silver-containing wound dressings.*Ostomy/wound management*, 54(3), 30-40.

Philip, D. (2009). Honey mediated green synthesis of gold nanoparticles. *Spec-trochimica Acta Part A: Molecular and Biomolecular Spectroscopy*, 73(4), 650–653.

Philip, D. (2010). Honey mediated green synthesis of silver nanoparticles.*Spectrochimica Acta Part A: Molecular and Biomolecular Spectroscopy*, 75(3),1078–1081.

Płachno, B. J., Adamec, L., & Huet, H. (2009). Mineral nutrient uptake from prey and glandular phosphatase activity as a dual test of carnivory in semi-desert plants with glandular leaves suspected of carnivory. *Annals of botany*,*104*(4), 649-654.

Popova, M., Silici, S., Kaftanoglu, O., & Bankova, V. (2005). Antibacterial activity of Turkish propolis and its qualitative and quantitative chemical composition. *Phytomedicine*, *12*(3), 221-228.

Prashanth` K. V. H., & Tharanathan, R. N. (2007). Chitin/chitosan: Modifications and their unlimited application potential. *Trends in Food Science & Technology*, 18, 117–131.

Rahman, M. A., Mossa, J. S., Al-Said, M. S., & Al-Yahya, M. A. (2004). Medicinal plant diversity in the flora of Saudi Arabia 1: a report on seven plant families. *Fitoterapia*, 75(2), 149-161.

Ram, S. K. M., Jayapal, N., Nanaiah, P., Aswal, G. S., Ramnarayan, B. K., & Taher, S. M. (2014). The therapeutic benefits of bee venom. *Int. J. Curr. Microbiol. App. Sci*, *3*(11), 377-381.

Ramakrishna, S., Fujihara, K., Teo, W. E., Yong, T., Ma, Z., & Ramaseshan, R. (2006). Electrospun nanofibers: solving global issues. *Materials today*,*9* (3), 40-50.

Ramos, I. F. D. A. S., Biz, M. T., Paulino, N., Scremin, A., Della Bona, Á., Barletta, F. B., & Figueiredo, J. A. P. D. (2012). Histopathological analysis of corticosteroid-antibiotic preparation and propolis paste formulation as intracanal medication after pulpectomy: an in vivo study. *Journal of applied oral science*, 20(1), 50-56.

Reneker, D. H., & Yarin, A. L. (2008). Electrospinning jets and polymer nanofibers. *Polymer*, *49*(10), 2387-2425.

Rhoads, D. D., Wolcott, R. D., Kuskowski, M. A., Wolcott, B. M., Ward, L. S., & Sulakvelidze, A. (2009). Bacteriophage therapy of venous leg ulcers in humans: results of a phase I safety trial. *Journal of wound care*, *18*(6).

Robson, M. C., Stenberg, B. D., & Heggers, J. P. (1990). Wound healing alterations caused by infection. *Clinics in plastic surgery*, 17(3), 485-492.

Sahay, R., Thavasi, V., & Ramakrishna, S. (2011). Design modifications in electrospinning setup for advanced applications. *Journal of Nanomaterials*,*2011*, 17.

Saini, S. S., Peterson, J. W., & Chopra, A. K. (1997). Melittin binds to secretory phospholipase A 2 and inhibits its enzymatic activity. *Biochemical and biophysical research communications*, 238(2), 436-442.

Salalha, W., Kuhn, J., Dror, Y., & Zussman, E. (2006). Encapsulation of bacteria and viruses in electrospun nanofibres. *Nanotechnology*, 17(18), 4675.

Samuels, R. J. (1981). Solid state characterization of the structure of chitosan films. Journal of *Polymer Science: Polymer Physics Edition*, 19(7), 1081-1105.

Sarhan, W. A., & Azzazy, H. M. (2015a). High concentration honey chitosan electrospun nanofibers: Biocompatibility and antibacterial effects. *Carbohydrate polymers*, *122*, 135-143.

Sarhan, W. A., & Azzazy, H. M. (2015b). Phage approved in food, why not as a therapeutic?.*Expert review of anti-infective therapy*, 13(1), 91-101.

Sarhan, W. A., El-Sherbiny I.M., Azzazy H.M.E (2016a). The Effect of Increasing Honey Concentration on the Properties of the Honey/ Polyvinyl Alcohol/ Chitosan Nanofibers**.** *Material Science and Engineering C.*

Sarhan, W. A., Azzazy, H. M., & El-Sherbiny, I. (2016b). Honey/Chitosan Nanofiber Wound Dressing Enriched with Allium sativum and Cleome droserifolia: Enhanced Antimicrobial and Wound Healing Activity. *ACS applied materials & interfaces*.

Sawicka, D., Car, H., Borawska, M. H., & Nikliński, J. (2012). The anticancer activity of propolis. *Folia Histochemica et Cytobiologica*, 50(1), 25-37.

Schiffman, J. D., & Schauer, C. L. (2007). Cross-linking chitosan nanofibers. *Biomacromolecules*, *8*(2), 594-601.

Schmidt, J. O., & Buchmann, S. L. (1992). Other products of the hive. The Hive and the Honey Bee, Hamilton, Illinois, 928-977.

Schmidtchen, A., Holst, E., Tapper, H., & Björck, L. (2003). Elastase-producing Pseudomonas aeruginosa degrade plasma proteins and extracellular products of human skin and fibroblasts, and inhibit fibroblast growth. *Microbial pathogenesis*, *34*(1), 47-55.

Schumacher, M. J., Schmidt, J. O., & Egen, N. B. (1989). Lethality of' killer'bee stings. *Nature*, 337(6206), 413-413.

Seckam, A., & Cooper, R. (2013). Understanding how honey impacts on wounds: an update on recent research findings. *Wounds International*, 4(1), 20-24.

Sehn, E., Hernandes, L., Franco, S. L., Gonçalves, C. C. M., & Baesso, M. L. (2009). Dynamics of reepithelialisation and penetration rate of a bee propolis formulation during cutaneous wounds healing. *Analytica Chimica Acta*, 635(1), 115-120.

Sen CK., Gayle M., Gordillo., Roy S., Kirsner R., Lambert L., et al (2009). Human Skin Wounds: A Major and Snowballing Threat to Public Health and the Economy. *Wound Repair Regeneration*, 17(6): 763–771.

Seo, S. W., Jung, W. S., Lee, S. E., Choi, C. M., Shin, B. C., Kim, E. K., ... & Shin, M. K. (2008). Effects of bee venom on cholecystokinin octapeptide-induced acute pancreatitis in rats. *Pancreas*, 36(2), e22-e29.

Seth, A. K., Geringer, M. R., Nguyen, K. T., Agnew, S. P., Dumanian, Z., Galiano, R. D., ... & Hong, S. J. (2013). Bacteriophage therapy for Staphylococcus aureus biofilm–infected wounds: a new approach to chronic wound care. *Plastic and reconstructive surgery*, *131*(2), 225-234.

Sforcin, J. M. (2007). Propolis and the immune system: a review. *Journal of ethnopharmacology*, 113(1), 1-14.

Sharaf, S., Higazy, A., & Hebeish, A. (2013). Propolis induced antibacterial activity and other technical properties of cotton textiles. *International journal of biological macromolecules*, *59*, 408-416.

Shokrgozar, M. A., Mottaghitalab, F., Mottaghitalab, V., & Farokhi, M. (2011). Fabrication of porous chitosan/poly (vinyl alcohol) reinforced single-walled carbon nanotube nanocomposites for neural tissue engineering. *Journal of biomedical nanotechnology*, *7*(2), 276-284.

Siddiqui, A. R., & Bernstein, J. M. (2010). Chronic wound infection: facts and controversies. *Clinics in dermatology*, *28*(5), 519-526.

Sidik, K., Mahmood, A. A., & Salmah, I. (2006). Acceleration of wound healing by aqueous extract of Allium sativum in combination with honey on cutaneous wound healing in rats. *International Journal of Molecular Medicine and Advance Sciences*, 2(2), 231-5.

Sill, T. J., & von Recum, H. A. (2008). Electrospinning: applications in drug delivery and tissue engineering. *Biomaterials*, *29*(13), 1989-2006.

Simpson, M. G. (2010). Plant systematics. Academic press.

Singh, V. K., & Singh, D. K. (2008). Pharmacological effects of garlic (Allium sativumL.). *Annual Reviews of Biomedical Science*, 10, 6-26.

Smith, H. W., & Huggins, M. B. (1982). Successful treatment of experimental Escherichia coli infections in mice using phage: its general superiority over antibiotics. *Microbiology*, 128(2), 307-318.

Smith, H. W., & Huggins, M. B. (1983). Effectiveness of phages in treating experimental Escherichia coli diarrhoea in calves, piglets and lambs. *Microbiology*, 129(8), 2659-2675.

Smith, H. W., Huggins, M. B., & Shaw, K. M. (1987). Factors influencing the survival and multiplication of bacteriophages in calves and in their environment. *Microbiology*, 133(5), 1127-1135.

Somerfield, S. D., Stach, J. L., Mraz, C., Gervais, F., & Skamene, E. (1986). Bee venom melittin blocks neutrophil O2− production. I*nflammation*,10(2), 175-182.

Son, B., Yeom, B. Y., Song, S. H., Lee, C. S., & Hwang, T. S. (2009). Antibacterial electrospun chitosan/poly (vinyl alcohol) nanofibers containing silver nitrate and titanium dioxide. *Journal of Applied Polymer Science*,*111*(6), 2892-2899.

Son, S. R., Linh, N. T. B., Yang, H. M., & Lee, B. T. (2016). In vitro and in vivo evaluation of electrospun PCL/PMMA fibrous scaffolds for bone regeneration. *Science and Technology of Advanced Materials*.

Soothill, J. S. (1992). Treatment of experimental infections of mice with bacteriophages. *Journal of medical microbiology*, 37(4), 258-261.

Soothill, J. S. (1994). Bacteriophage prevents destruction of skin grafts by Pseudomonas aeruginosa. *Burns*, 20(3), 209-211.

Sosnowski, Z. (1983). Method for extracting propolis and water soluble dry propolis powder. USA Patent, 4.

Spasova, M., Paneva, D., Manolova, N., Radenkov, P., & Rashkov, I. (2008). Electrospun Chitosan-Coated Fibers of Poly (L-lactide) and Poly (L-lactide)/Poly (ethylene glycol): Preparation and Characterization.*Macromolecular bioscience*, *8*(2), 153-162.

Stenholm, A. R., Dalsgaard, I., & Middelboe, M. (2008). Isolation and characterization of bacteriophages infecting the fish pathogen Flavobacterium psychrophilum. *Applied and environmental microbiology*,*74*(13), 4070-4078.

Subbiah, T., Bhat, G. S., Tock, R. W., Parameswaran, S., & Ramkumar, S. S. (2005). Electrospinning of nanofibers. *Journal of Applied Polymer Science*, *96*(2), 557-569.

Sulakvelidze, A. (2011). The challenges of bacteriophage therapy. *European Industerial Pharmacy*, 10, 14-18.

Sun, K., & Li, Z. H. (2011). Preparations, properties and applications of chitosan based nanofibers fabricated by electrospinning. *Express Polymer Letters*, *5*(4), 342-361.

Supaphol, P., & Chuangchote, S. (2008). On the electrospinning of poly (vinyl alcohol) nanofiber mats: a revisit. *Journal of Applied Polymer Science*,108(2), 969-978.

Sutjarittangtham, K., Sanpa, S., Tunkasiri, T., Rachtanapun, P., Chantawannakul, P., Intatha, U., ... & Eitssayeam, S. (2012, April). Preparation of polycaprolactone/ethanolic extract propolis nanofibers films. In *Advanced Materials Research* (Vol. 506, pp. 226-229). Trans Tech Publications.

Sutjarittangtham, Krit, Sirikarn Sanpa, Tawee Tunkasiri, Panuwan Chantawannakul, Uraiwan Intatha, and Sukum Eitssayeam. "Bactericidal effects of propolis/polylactic acid (PLA) nanofibres obtained via electrospinning." *Journal of Apicultural Research* 53, no. 1 (2014): 109-115

Szliszka, E., Zydowicz, G., Janoszka, B., Dobosz, C., Kowalczyk-Ziomek, G., & Krol, W. (2011). Ethanolic extract of Brazilian green propolis sensitizes prostate cancer cells to TRAIL-induced apoptosis. *International Journal of Oncology*, 38(4), 941-953.

Phachamud, T., & Phiriyawirut, M. (2011). In vitro cytotoxicity and degradability tests of gallic acid-loaded cellulose acetate electrospun fiber.*Research Journal of Pharmaceutical Biological and Chemical Sciences*, *2*(3), 85-98.

Tammelin, A., Lindholm, C., & Hambraeus, A. (1998). Chronic ulcers and antibiotic treatment. *Journal of wound care*, *7*(9), 435-437.

Teo, W. E., & Ramakrishna, S. (2006). A review on electrospinning design and nanofibre assemblies. *Nanotechnology*, 17(14), R89.

Tonks, A. J., Cooper, R. A., Jones, K. P., Blair, S., Parton, J., & Tonks, A. (2003). Honey stimulates inflammatory cytokine production from monocytes.*Cytokine*, 21(5), 242-247.

Toreti, V. C., Sato, H. H., Pastore, G. M., & Park, Y. K. (2013). Recent progress of propolis for its biological and chemical compositions and its botanical origin. *Evidence-Based Complementary and Alternative Medicine*,2013.

Tosi, B., Donini, A., Romagnoli, C., & Bruni, A. (1996). Antimicrobial activity of some commercial extracts of propolis prepared with different solvents. *Phytotherapy Research*, 10(4), 335-336.

Tosi, E. A., Ré, E., Lucero, H., & Bulacio, L. (2004). Effect of honey high-temperatureshort-time heating on parameters related to quality, crystallisation phenomenaand fungal inhibition. *LWT-Food Science and Technology*, 37(6), 669–678.

Tripathi, S., Mehrotra, G. K., & Dutta, P. K. (2009). Physicochemical and bioactivity of cross-linked chitosan–PVA film for food packaging applications.*International Journal of Biological Macromolecules*, *45*(4), 372-376.

Tsao, S. M., & Yin, M. C. (2001). In vitro activity of garlic oil and four diallyl sulphides against antibiotic-resistant Pseudomonas aeruginosa and Klebsiella pneumoniae. *Journal of Antimicrobial Chemotherap*y, 47(5), 665-670.

Twort, F. W. (1915). An investigation on the nature of ultra-microscopic viruses. *The Lancet*, *186*(4814), 1241-1243.

Unnithan, A. R., Barakat, N. A., Pichiah, P. T., Gnanasekaran, G., Nirmala, R., Cha, Y. S., ... & Kim, H. Y. (2012). Wound-dressing materials with antibacterial activity from electrospun polyurethane–dextran nanofiber mats containing ciprofloxacin HCl. *Carbohydrate polymers*, *90*(4), 1786-1793.

Uppal, R., Ramaswamy, G. N., Arnold, C., Goodband, R., & Wang, Y. (2011). Hyaluronic acid nanofiber wound dressing—production, characterization, and in vivo behavior. *Journal of Biomedical Materials Research Part B: Applied Biomaterials*, *97*(1), 20-29.

Urbancic-Rovan, V., & Gubina, M. (2000). Bacteria in superficial diabetic foot ulcers. *Diabetic Medicine*, *17*(11), 814-815.

Vandamme, L., Heyneman, A., Hoeksema, H., Verbelen, J., & Monstrey, S. (2013). Honey in modern wound care: A systematic review. *Burns*, 39(8), 1514-1525.

Vartiainen, J., Motion, R., Kulonen, H., Rättö, M., Skyttä, E., & Ahvenainen, R. (2004). Chitosan-coated paper: Effects of nisin and different acids on the antimicrobial activity. *Journal of applied polymer science*, *94*(3), 986-993.

Vowden, P., Vowden, K., & Carville, K. (2011). Antimicrobial dressings made easy. *Wounds International*, 2 (1).

Wagh, V. D. (2013). Propolis: a wonder bees product and its pharmacological potentials. *Advances in pharmacological sciences*, *2013*.

Wang, P., & He, J. H. (2013). Electrospun polyvinyl alcohol-honey nanofibers. *Thermal Science*, 17(5), 1549–1550.

Wang, T., Zhu, X. K., Xue, X. T., & Wu, D. Y. (2012). Hydrogel sheets of chitosan, honeyand gelatin as burn wound dressings. *Carbohydrate Polymers*, 88(1), 75–83.

Welle, A., Kröger, M., Döring, M., Niederer, K., Pindel, E., & Chronakis, I. S. (2007). Electrospun aliphatic polycarbonates as tailored tissue scaffold materials. *Biomaterials*, *28*(13), 2211-2219.

Werner, S., & Grose, R. (2003). Regulation of wound healing by growth factors and cytokines. *Physiological reviews*, *83*(3), 835-870.

White, J.W. Jr. (1978). Honey. *Advances in Food Research*, 24, 288.

WHO (2003), Diet, Nutrition and the Prevention of Chronic Diseases. Technical Report Series, 916. World Health Organization, Geneva

Xie, H., Jia, Z., Huang, J., & Zhang, C. (2011). Preparation of low molecular weightchitosan by complex enzymes hydrolysis. *International Journal of Chemistry*, 3(2),180.

Xie, Z., Paras, C. B., Weng, H., Punnakitikashem, P., Su, L. C., Vu, K., ... & Nguyen, K. T. (2013). Dual growth factor releasing multi-functional nanofibers for wound healing. *Acta biomaterialia*, 9(12), 9351-9359.

Xu, C., Xu, F., Wang, B., & Lu, T. (2011). Electrospinning of poly (ethylene-co-vinyl alcohol) nanofibres encapsulated with Ag nanoparticles for skin wound healing. *Journal of Nanomaterials*, *2011*, 3.

Xuan, H., Li, Z., Yan, H., Sang, Q., Wang, K., He, Q., ... & Hu, F. (2014). Antitumor activity of Chinese propolis in human breast cancer MCF-7 and MDA-MB-231 cells. *Evidence-Based Complementary and Alternative Medicine*, 2014.

Yan, E., Fan, S., Li, X., Wang, C., Sun, Z., Ni, L., & Zhang, D. (2012). Electrospun polyvinyl alcohol/chitosan composite nanofibers involving Au nanoparticles and their in vitro release properties. *Materials Science and Engineering: C*, *33*, 461–465.

Yarin, A. L., Kataphinan, W., & Reneker, D. H. (2005). Branching in electrospinning of nanofibers. *Journal of applied physics*, *98*(6), 064501.

Yuan, J., Geng, J., Xing, Z., Shim, K. J., Han, I., Kim, J. C., ... & Shen, J. (2015). Novel wound dressing based on nanofibrous PHBV–keratin mats. *Journal of tissue engineering and regenerative medicine*, *9*(9), 1027-1035.

Yunoki, S., Kohta, M., Ohyabu, Y., & Iwasaki, T. (2015). In Vitro Parallel Evaluation of Antibacterial Activity and Cytotoxicity of Commercially Available Silver-Containing Wound Dressings. *Plastic Surgical Nursing*,*35*(4), 203-211.

Zahedi P., Rezaeian I., Ranaei, Siadat S O., Jafari SH., Supaphol, P. (2010). A review on wound dressings with an emphasis on electrospun nanofibrous polymeric bandages. *Polymers for Advanced Technologies*, 21(2), 77-95

Zhang, C., Yuan, X., Wu, L., Han, Y., & Sheng, J. (2005). Study on morphology of electrospun poly (vinyl alcohol) mats. *European polymer journal*, 41(3), 423-432.

Zhang, Y., Huang, X., Duan, B., Wu, L., Li, S., & Yuan, X. (2007). Preparation of electrospun chitosan/poly (vinyl alcohol) membranes. *Colloid and Polymer Science*, *285*(8), 855-863.

Zhang, Y., Lim, C. T., Ramakrishna, S., & Huang, Z. M. (2005). Recent development of polymer nanofibers for biomedical and biotechnological applications. *Journal of Materials Science: Materials in Medicine*, *16*(10), 933-946.

Zhou, Y., Yang, D., Chen, X., Xu, Q., Lu, F., & Nie, J. (2007). Electrospun water-soluble carboxyethyl chitosan/poly (vinyl alcohol) nanofibrous membrane as potential wound dressing for skin regeneration. *Biomacromolecules*, *9*(1), 349-354.

Zong, X., Kim, K., Fang, D., Ran, S., Hsiao, B. S., & Chu, B. (2002). Structure and process relationship of electrospun bioabsorbable nanofiber membranes. *Polymer*, *43*(16), 4403-4412.

10. APPENDIX

.

Carbohydrate Polymers 122 (2015) 135–143

Contents lists available at ScienceDirect

Carbohydrate Polymers

journal homepage: www.elsevier.com/locate/carbpol

High concentration honey chitosan electrospun nanofibers: Biocompatibility and antibacterial effects

Wessam A. Sarhan, Hassan M.E. Azzazy*

Novel Diagnostics & Therapeutics Research Group, Department of Chemistry, School of Sciences & Engineering, The American University in Cairo, New Cairo 11835, Egypt

ARTICLE INFO

Article history:
Received 2 October 2014
Received in revised form
12 December 2014
Accepted 16 December 2014
Available online 2 January 2015

Keywords:
Chitosan
Honey
Wound dressing
Antibacterial
Nanofibers

Chemical compounds studied in this article:
Chitosan (PubChem CID: 71853)
PVA (PubChem CID: 11199)
Acetic acid (PubChem CID: 176)
Glutaraldehyde (CID: 3485)

ABSTRACT

Honey nanofibers represent an attractive formulation with unique medicinal and wound healing advantages. Nanofibers with honey concentrations of <10% were prepared, however, there is a need to prepare nanofibers with higher honey concentrations to increase the antibacterial and wound healing effects. In this work, chitosan and honey (H) were cospun with polyvinyl alcohol (P) allowing the fabrication of nanofibers with high honey concentrations up to 40% and high chitosan concentrations up to 5.5% of the total weight of the fibers using biocompatible solvents (1% acetic acid). The fabricated nanofibers were further chemically crosslinked, by exposure to glutaraldehyde vapor, and physically crosslinked by heating and freezing/thawing. The new HP–chitosan nanofibers showed pronounced antibacterial activity against *Staphylococcus aureus* but weak antibacterial activity against *Escherichia coli*. The developed HP–chitosan nanofibers revealed no cytotoxicity effects on cultured fibroblasts. In conclusion, biocompatible, antimicrobial crosslinked honey/polyvinyl alcohol/chitosan nanofibers were developed which hold potential as effective wound dressing.

1. Introduction

Electrospinning is recognized as an efficient method for producing nanofibers (Li & Xia, 2004). The electrospun fibers show the advantages of high porosity and large surface to volume ratio (Altstädt, Lovera, Schmidt, Schmidt, & Fery, 2008). Moreover, nanofibers resemble the natural extracellular matrix and were reported to promote proliferation and migration of cells (Bhardwaj & Kundu, 2010). Electrospun nanofibers represent an efficient formulation for drugs and natural remedies as they allow loading high concentration of combinations of natural and synthetic materials and controlled/sustained release (Meinel, Germershaus, Luhmann, Merkle, & Meinel, 2012).

Honey has profound medicinal and nutritional properties (Khan, Abadin, & Rauf, 2007). It exhibits antimicrobial activity, debriding and deodorising action as well as anti-inflammatory, antioxidant and wound healing activities (Lusby, Coombes, & Wilkinson, 2002). In 2013, Maleki et al. were able to fabricate honey/polyvinyl alcohol nanofibers. Unfortunately, the maximum concentration that could be incorporated within the electrospun nanofibers was 2.25% honey of the total weight of the nanofibrous mat (Maleki, Gharehaghaji, & Dijkstra, 2013). Recently, Wang and He (2013), worked on fabrication of high honey concentration nanofibers, however, the maximum concentration of included honey was 9% with 10% polyvinyl alcohol of the total weight of the nanofibrous mat (Wang & He, 2013). Thus, there is a need to fabricate nanofibers composed primarily of high honey concentrations. Such concentrations will maximize the therapeutic and nutritional benefits of honey nanofibrous formulations in smaller dosage forms.

Chitosan is a biodegradable, biocompatible polymer with antibacterial, aqueous adsorption and wound healing ability (Schiffman & Schauer, 2007). Also, it can promote tissue regeneration and achieve hemostasis (Busilacchi, Gigante, Mattioli-Belmonte, Manzotti, & Muzzarelli, 2013; Muzzarelli, Greco, Busilacchi, Sollazzo, & Gigante, 2012). Chitosan meets also the demands of several industrial and biomedical activities

* Corresponding author at: Department of Chemistry, School of Sciences & Engineering, SSE # 1184, The American University in Cairo, AUC Avenue, PO Box 74, New Cairo 11835, Egypt. Tel.: 202 2615 2559; fax: +202 2795 7565.
E-mail address: hazzazy@aucegypt.edu (H.M.E. Azzazy).

http://dx.doi.org/10.1016/j.carbpol.2014.12.051
0144-8617/

(Muzzarelli, 2010; Muzzarelli, Greco, Busilacchi, Sollazzo, & Gigante, 2012b; Muzzarelli, El Mehtedi, & Mattioli-Belmonte, 2014).

Because of the high viscosity of chitosan in solutions, electrospinning of chitosan was only possible by using toxic or highly concentrated acidic solvents (Geng, Kwon, & Jang, 2005; Homayoni, Ravandi, & Valizadeh, 2009; Su et al., 2011). Residues of such solvents are unfavorable especially in applications requiring biocompatible materials. Aqueous salts of chitosan were prepared, but the concentration of the incorporated chitosan did not exceed 1% (Charernsriwilaiwat, Opanasopit, Rojanarata, Ngawhirunpat, & Supaphol, 2010; Charernsriwilaiwat, Opanasopit, Rojanarata, & Ngawhirunpat, 2011). Another approach for electrospinning chitosan in more biocompatible solvents was via co-spinning with other readily spun polymers. Among them, co-spinning chitosan with polyvinyl alcohol is one of the most common composites (Liao et al., 2011; Yan et al., 2012; Zhou et al., 2007). Still, nanofibers prepared by this method could only incorporate limited chitosan concentrations.

It is the aim of the present work to co-spin high concentrations of chitosan and honey with polyvinyl alcohol using biocompatible solvents. This would maximize the benefit of these two important materials in the smallest dosage form.

2. Experimental

2.1. Materials

Chitosan (Mwt: 240 kDa, DDA: 84%; Chitoclear, cg110, TM 3728; Primex; Siglufjordur, Iceland). Polyvinyl alcohol (Mwt: 85,000; Sigma Aldrich, St. Louis, USA), acetic acid (glacial, 99–100%; Merck, Wadeville, South Africa), glutaraldehyde (25% in H_2O; Sigma Aldrich, St. Louis, USA). Nutrient broth & nutrient agar (Becton Dickinson and Company, USA). Trypsin (85450C-25G; Sigma Aldrich), RPMI_1640 with L-Glutamine (R8758; Life Science), fetal bovine serum (10270-106; Gibco), thiazolyl blue tetrazolium bromide–MTT (M2128-1G; Sigma Aldrich), PBS, trypan blue and triton X (Sigma Aldrich, St. Louis, USA). Clover honey was obtained from the faculty of Agriculture, Cairo University. The viscosity of the honey was 15,300 mpas and its total soluble solid content was 81%.

2.2. Preparation of the polyvinyl alcohol/chitosan (P-chitosan), honey/polyvinyl alcohol (HP) and honey/polyvinyl alcohol/chitosan (HP–chitosan) solutions

Different solutions composed of different weight ratios of P-chitosan and HP as well as HP–chitosan were prepared as follows: P-chitosan (7%:1.5%, 7%:2.5% and 7%:3.5%); HP (20%:10% and 30%:10%), and HP–chitosan (30%:7%:1.5%, 30%:7%:3.5%, 30%:5%:5.5%, 30%:5%:4.5%, 20%:7%:3.5% and 40%:7%:3.5%). Solutions were prepared in 1% acetic acid. Each of the as prepared solutions of HP–chitosan was aged at room temperature for different time intervals.

2.3. Viscosity measurements

The viscosity of the polyvinyl alcohol (7%), P-chitosan (7%:3.5%), HP (30%:7%), and HP–chitosan (30%:7%:3.5% and 10%:7%:3.5%) samples were determined using a viscometer (Myr; VR-3000, Viscotech Hispania, Tarragona, Spain). The solutions were aged at room temperature for a week. The viscosity of all samples was tested at different time intervals (0, 24, 48 h and 1 week). The average value of three measurements was reported as mean ± SD.

2.4. Electrospinning of polyvinyl alcohol/chitosan (P-chitosan), honey/polyvinyl alcohol (HP) and honey/polyvinyl alcohol/chitosan (HP–chitosan) nanofibers

Each of the as-prepared solutions of P-chitosan, HP and HP–chitosan with different weight blending ratios was electrospun into nanofibers via the electrospinner (E-spin, NanoTech, Kalyanpur, India). The solutions were loaded in a 5 ml plastic syringe that was attached to a stainless steel needle (22 gauge) as a nozzle. The electrospun polymer solutions were subjected to different voltages (Gamma High Voltage Power Supply, USA) for adjustment of the optimum voltage for each of the spun solutions. The flow rate of the solution was maintained at 10 μl/min and the distance between the nozzle and the collector was maintained at 15 cm. Collection of the samples was done on a ground collector wrapped with an aluminum sheet.

2.5. Cross-linking of fiber mats

Physical and chemical methods were used to crosslink the fiber mats of HP–chitosan. Glutaraldehyde (GA) was used for chemical crosslinking. The fiber mats were placed in a closed desiccator that was saturated with GA vapors (40 ml). Exposure of the nanofiber mats to the GA vapors was done for different time intervals (30, 60, 120 and 180 min as well as 48 h and 72 h). Subsequently, enhancement of the crosslinking reaction and removal of unreacted (GA) were done via heating the nanofiber mats in an oven under vacuum at 70 °C for 24 h as well as at 40 °C for 24 h. Physical crosslinking was performed by freezing/thawing and heating techniques. Freezing and thawing was performed via freezing the fiber mats for 15 min in liquid nitrogen followed by thawing at room temperature for 15 min for three successive cycles. Heating was carried out under vacuum in an oven (Jeiotech, OV-11, South Korea) at both 110 °C, 100 °C for 15 min and 80 °C for 25 min as well as at 70 °C for 24 h.

2.6. Characterization and measurements of the electrospun nanofibers

The morphologies of the electrospun nanofibers were observed using scanning electron microscopy (FESEM, Leo Supra 55, Zeiss Inc., Oberkochen, Germany). Fourier transform infrared spectroscopy (FTIR) was performed for the raw polyvinyl alcohol and chitosan and the HP–chitosan nanofibrous mats using FTIR (Thermo scientific, Nicolet 380, USA). The transmission mode with KBr pellets was used for bulk chitosan and polyvinyl alcohol as well as and HP–chitosan nanofibrous mats.

2.7. Degree of swelling and weight loss

The HP–chitosan nanofibrous mats were tested for the degree of swelling and weight loss that were calculated according to Eqs. (1) and (2), respectively. Both tests were carried out in phosphate buffered saline [PBS], pH (7.4) at 37 °C for 1, 4 and 24 h.

$$\text{Degree of swelling}\,(\%) = \left[\frac{M - Mi}{Mi}\right] \times 100 \quad (1)$$

Sharma, Dinda, & Mishra (2013)

$$\text{Weight loss}\,(\%) = \left[\frac{Mi - Md}{Mi}\right] \times 100 \quad (2)$$

where M is the swollen weight of the nanofibrous sample which was dried using a filter paper, Md is the dried mass of the nanofibrous sample after being immersed in buffer medium, measured by drying the swollen mats at 40 °C until constant weight was reached, and Mi is the initial dry mass of sample.

2.8. Assessment of antibacterial activity

Viable cell count technique was used to determine the antibacterial activity of the electrospun HP–chitosan nanofibrous mats with 30% honey/7% polyvinyl alcohol and increasing chitosan concentrations (1.5%, 3.5%, and 5.5%). The antibacterial activity was assessed against both *Staphylococcus aureus* and *Escherichia coli*. Each of the *S. aureus* and *E. coli* were added into 10 ml nutrient broth medium that was adjusted to an OD of 0.1 at 625 nm. Subsequently (0.1 g) of the HP–chitosan nanofibrous mats were added to each of the *S. aureus* and *E. coli* test tubes. All the nanofibrous mats were UV sterilized for 20 min prior to antibacterial testing. The *S. aureus* and *E. coli* tubes containing the nanofibrous mats and a control were then incubated at 37 °C with shaking at 100 rpm. Samples from the treated bacterial broth and the control were taken and serially diluted in nutrient broth at 24 and 48 h. Subsequently, 100 μL from each dilution were spread on nutrient agar plates that were then incubated at 37 °C for 24 h, after which the numbers of surviving colonies were counted.

The antibacterial activity was estimated according to Eq. (3):

$$\text{Antibacterial activity} = (\log \text{CFU} * t - \log \text{CFU} * 0) - (\log \text{CFU}t - \log \text{CFU}0) \quad (3)$$

where CFU0 and CFU*t* are the number of colony forming units at time zero and time *t* for the nanofibrous samples; CFU*0 and CFU**t* are the number of colony forming units at time zero and time t for the control (Amrit, Hendrix, Dutschik, & Warmoeskerken, 2012).

2.9. Cytotoxicity evaluation (MTT assay)

Primary skin fibroblast cells of neonatal mice origin were used to evaluate the toxicity of the HP–chitosan nanofibrous mats with increasing chitosan concentrations (1.5%, 3.5%, and 5.5%) and 30% honey/7% polyvinyl alcohol. Preparation of the primary cell culture was done according to the method of Seluanov, Vaidya, and Gorbunova (2010). Non crosslinked and crosslinked nanofibrous mats were tested for each concentration. Crosslinking was achieved via exposure to GA vapors for 180 min, followed by heating at 70 °C under vacuum. Cytotoxicity was evaluated via the addition of the extracts of the nanofiber scaffolds to cells cultured in a 24-well plate and the cytotoxicity was determined via MTT assay. The nanofibrous mats were extracted via soaking the scaffolds in culture media for 24 h at 37 °C. Subsequently the extracts were harvested for cytotoxicity testing. Normal cells without any treatment were used as the negative control whereas (1% Triton X) was used as the positive control. The cells were seeded in a 24 well plate at a density of 10^4 cells/well and incubated in a humidified incubator with 5% CO_2 for 24 h at 37 °C before treatment with the extracts to allow cell attachment. Subsequently, the extract for each scaffold was added to the cell monolayer and incubated for 48 h into CO_2 incubator at 37 °C and 5% CO_2. Triplicate wells were prepared for each sample. After 48 h, the difference in morphology between cell controls and scaffold extracts was observed by observing the cells under inverted microscope. Cell viability was assessed after 3 days via MTT assay. The absorbance was determined at 570 nm. And percent of cell survival was calculated according to the following equation:

$$\text{Survival\%} = \left[\frac{A_{\text{sample}} - A_b}{A_c - A_b}\right] \times 100 \quad (4)$$

where A_c is the negative control; A_b is the blank.

The average value of three measurements was reported as mean ± SD. Analysis of the data was done via analyses of variance (ANOVA) test. And results were considered statistically significant with a probability less than 0.05.

3. Results and discussion

3.1. Preparation of polyvinyl alcohol/chitosan (P-chitosan), honey/polyvinyl alcohol (HP)and honey/polyvinyl alcohol/chitosan (HP–chitosan) nanofibers

The solutions of P-chitosan, HP, and HP–chitosan were tested for viscosity at different time intervals as shown in Table 1. At zero time, the viscosity of (HP; 30%:7%) was very low (175 mpas) and the viscosity of the (P-chitosan; 7%:3.5%) was very high (85,440 mpas) making both solutions impossible to spin. Whereas, the combination of (HP–chitosan; 30%:7%:3.5%) exhibited 34,000 mpas at day zero. Such viscosity value, however, was still above the optimum viscosity required for spinning. Thus, the HP–chitosan solutions were allowed to age at room temperature for a week. Interestingly, the viscosity of the HP–chitosan solutions dropped noticeably upon aging. This was unlike the P-chitosan and the HP solutions that exhibited increased viscosities after aging for one week (Table 1).

The decrease in viscosity of the HP–chitosan solutions with time could be due to enzymatic degradation of chitosan via the enzymes present in the honey. Small amounts of enzymes occur naturally in honey, including enzymes that transform polysaccharides into smaller products as amylase. Chitosan is most likely to be affected by such enzymes (Xie, Jia, Huang, & Zhang, 2011). Moreover, hydrogen peroxide, which is an important component of honey, may have contributed to the enzymatic degradation of chitosan (Brudzynski, 2006). Interestingly, it was observed that the increase in the honey concentration within the HP–chitosan mixtures has resulted in further reduction in the viscosity of the solutions (Table 1).

3.2. Morphology of the polyvinyl alcohol/chitosan (P-chitosan), honey/polyvinyl alcohol (HP) and honey/polyvinyl alcohol/chitosan (HP–chitosan) nanofibers

Different concentrations of the P-chitosan, HP and HP–chitosan were electrospun. For P-chitosan combinations, the highest concentration of chitosan that could be electrospun with polyvinyl alcohol using 1% acetic acid, was 1.5%. For HP combinations the highest concentration of honey that could be electrospun with polyvinyl alcohol was 20% honey (Fig. 1a). However the electrospun fibers showed clusters, which are most probably clusters of honey that were not included within the polyvinyl alcohol nanofibers. Remarkably, upon addition of 3.5% chitosan to the same HP combination, uniform nanofibers were produced (Fig. 1b). This is due

Table 1
Change in the viscosity (mpas) of the polyvinyl alcohol (P), honey/P (HP), P-chitosan, and HP–chitosan solutions upon aging.

time	P (7%) (mpas)	HP (30%:7%) (mpas)	P-chitosan (7%:3.5%) (mpas)	HP–chitosan (10%:7%:3.5%) (mpas)	HP–chitosan (30%:7%:3.5%) (mpas)
0 h	300	175	85,440	48,010	34,000
24 h	328	214	162,830	9770	6520
48 h	385	245	152,020	6100	3830
168 h	404	319	122,180	2787	1851

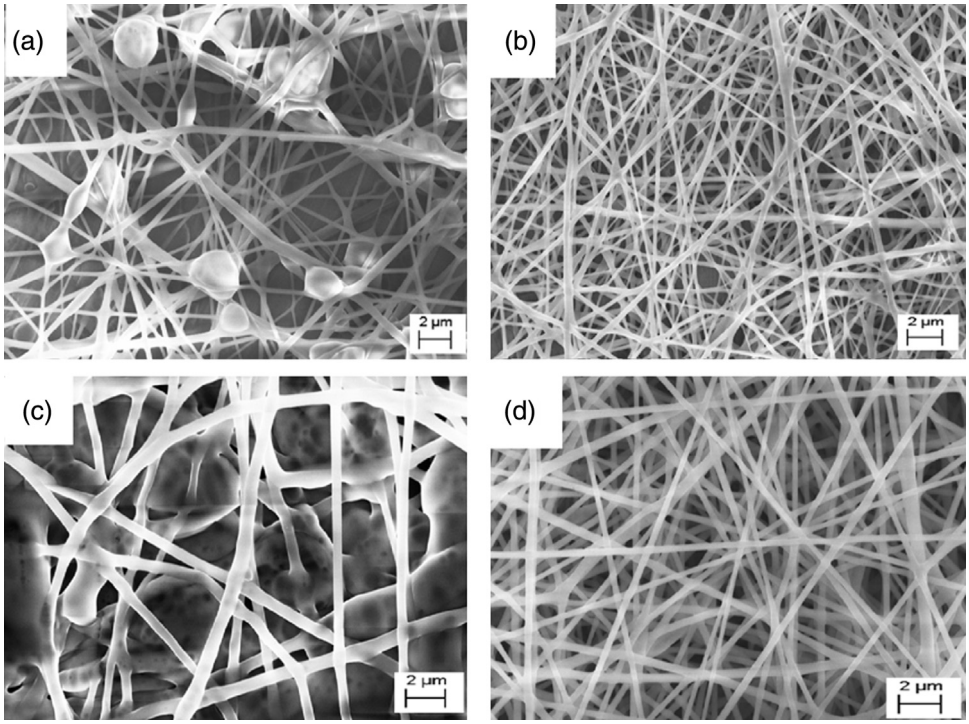

Fig. 1. SEM images of the electrospun nanofiber mats with the highest concentration (%) of honey within the honey/polyvinyl alcohol (HP) and the HP–chitosan nanofibers: (a) HP (20%:10%), (b) HP–chitosan (20%:7%:3.5%) (c) HP (30%:10%), (d) HP–chitosan (30%:7%:3.5%).

to the favorable effect of chitosan on the viscosity of the solution allowing it to reach to the optimum degree of chain entanglements required to form uniform nanofibers.

Upon increasing the honey concentration to 30% in the HP combination the honey clusters increased extensively (Fig. 1c) indicating the inability of the polyvinyl alcohol polymer to incorporate higher concentrations of honey even at higher concentrations of polyvinyl alcohol, where the decrease in viscosity imparted by honey on the HP combination could not be overcome by increasing the concentration of polyvinyl alcohol. On the other hand, increasing the chitosan concentration to 3.5% in the P-chitosan resulted in highly viscous solution that was impossible to spin (Table 1). Interestingly, the combination HP–chitosan (30%:7%:3.5%), upon aging for more than 2 days acquired the optimum viscosity required for easy spinning and formation of uniform nanofibers (Fig. 1d). Such combination of HP–chitosan allowed for the first time the production of biocompatible fibers via biocompatible solvents of high concentrations of both honey and chitosan.

Realizing the synergistic effect of both honey and chitosan on the viscosity of the HP–chitosan combinations, attempts were made to increase the concentration of the incorporated honey and chitosan. Spinning 35% and 40% honey within the combination of chitosan (3.5%)/polyvinyl alcohol (7%) was successful (Fig. 2a and b). Also, spinning 4.5% and 5.5% chitosan in the presence of 30% honey was achieved (Fig. 2c and d). However, due to the high viscosity of the increased concentration of chitosan, the concentration of PVA incorporated was decreased to 5%.

In previous attempts to prepare nanofibers containing high honey concentration, the maximum incorporated concentration that was electrospun with polyvinyl alcohol was 9% (Wang & He, 2013). This is because increasing the honey concentration results in remarkable decrease in viscosity of the solution, thus making it impossible to electropsin. This is the first report to prepare nanofibers with honey concentrations reaching to 40% of the actual weight of the nanofiberous mat. Furthermore, the favorable effect of honey on the viscosity of the chitosan solution upon aging allowed for the first time the incorporation of higher chitosan concentrations reaching to 5.5% while using biocompatible solvents.

The FTIR spectra of the polyvinyl alcohol CH and HP–chitosan nanofibers were analyzed. Chitosan exhibited characteristic bands at 3429 cm^{-1} and 1655 cm^{-1} corresponding to the OH and the amide O—C—NH_2 groups. The bands of the CH_3 and CH_3—O groups could be observed between 1000 and 2000 cm^{-1} (Paipitak, Pornpra, Mongkontalang, Techitdheer, & Pecharapa, 2011). The FT-IR spectra of polyvinyl alcohol showed bands at 3429 cm^{-1}, 2923 cm^{-1}, and 1444 cm^{-1} the characteristic bands for OH, CH_2, and CH—OH groups (Yan et al., 2012). The previous characteristic bands of both polyvinyl alcohol and chitosan were all preserved in the resulting hybrid fibers. However, it was observed that the absorption peak at about 3429 cm^{-1} and 1655 cm^{-1} concerned with OH and amide O—C—NH_2 groups shifted to a lower wave number in the composite HP–chitosan. At the same time, the characteristic peak in the hybrid HP–chitosan at 1058 cm^{-1} could be attributed to the C—O—C symmetric stretching and C—O—H bending vibrations of protein in honey. Whereas, the amide band of protein in honey could be observed at 1641 cm^{-1} (Philip, 2009). Moreover, the peaks between 900 cm^{-1} and 750 cm^{-1} were attributed to the anomeric region, which is a characteristic of saccharide configuration of honey (Jaganathan & Mandal, 2009; Philip, 2010).

3.3. Morphology before and after cross-linking treatment

It was observed that the nanofibrous scaffolds of HP–chitosan combinations lose their nanofibrous structure in aqueous media. Thus, efficient crosslinking was necessary to broaden the possible applications of the developed nanofibers.

Through the present work different crosslinking strategies were undertaken, to allow efficient crosslinking without jeopardizing the biocompatibility of the fibers. In chemical crosslinking the temperature of heating did not exceed 110 °C. This is because excessive heating above 140 °C can result in reduction of the honey quality and increase in the hydroxymethylfurfural content (Tosi, Ré,

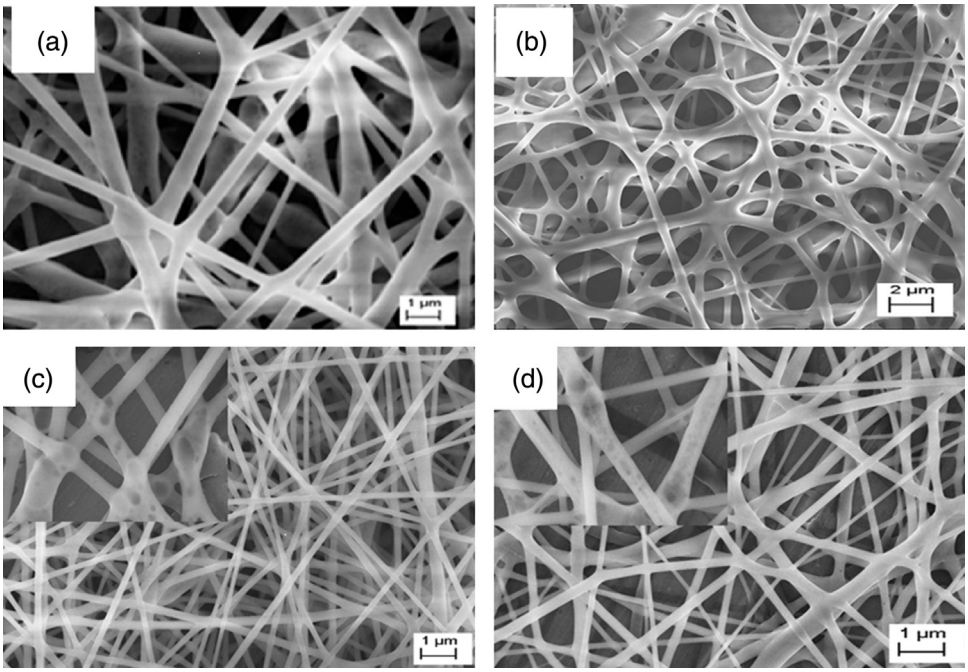

Fig. 2. SEM images of the electrospun nanofiber mats with the maximum concentration (%) of both honey and chitosan within the honey/polyvinyl alcohol/chitosan (HP–chitosan) nanofibers: (a) HP–chitosan (35%:7%:3.5%), (b) HP–chitosan (40%:7%:3.5%), (c) HP–chitosan (30%:5%:4.5%), (d) HP–chitosan (30%:5%:5.5%).

Lucero, & Bulacio, 2004). Fig. 3 shows the images of the chemically cross-linked nanofibers after immersion in PBS for 15 min.

The fibers that were subjected to GA vapors for three days showed superior crosslinking (Fig. 3a) and maintained their original shapes and no swelling was observed. Fibers subjected to GA vapors for 2 days showed similar results however slight swelling was observed (Fig. 3b). Interestingly, decreasing the exposure time to GA vapors to 3 h maintained their nanofibrous structure with some swelling (Fig. 3c). Meanwhile, decreasing the exposure time to 1 h (Fig. 3d) showed lower crosslinking efficiency, where partial degradation of the outer layers of the fibers began with noticeable swelling. However, crosslinking efficiency decreased noticeably upon decreasing the GA exposure time to 30 min, where the percentage of the degraded fibers increased and the nanofibrous structure in the outer layer was nearly lost. Subjecting the nanofibers to GA vapors for 1 h and 3 h, with subsequent heating for 24 h to promote crosslinking at 40 °C, showed the same crosslinking efficiency as nanofibers heated at 70 °C. It was reported that exposing honey to 40 °C for 96 h did not affect any of its biomolecules (Molan, 1992).

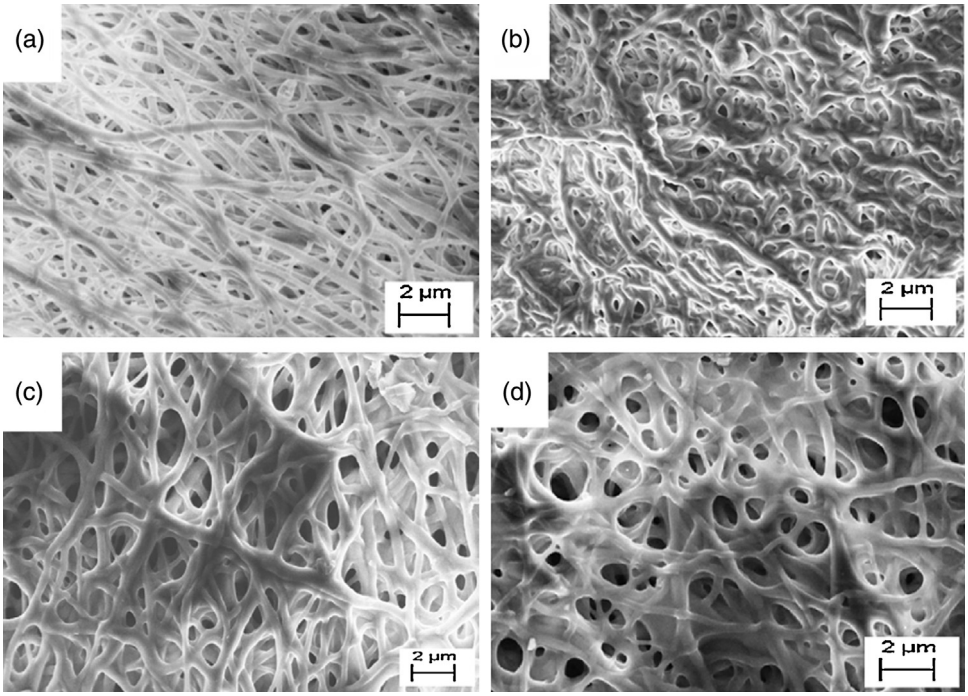

Fig. 3. SEM images of the chemically cross-linked Honey/polyvinyl alcohol/chitosan (HP–chitosan) (30%:7%:3.5%) nanofibrous mats. Cross-linking was performed by exposure to GA vapors and then heating at 70 °C under vacuum for 24 h. Different mats were exposed to GA for different time intervals (a) 3 days, (b) 2 days, (c) 3 h, and (d) 1 h.

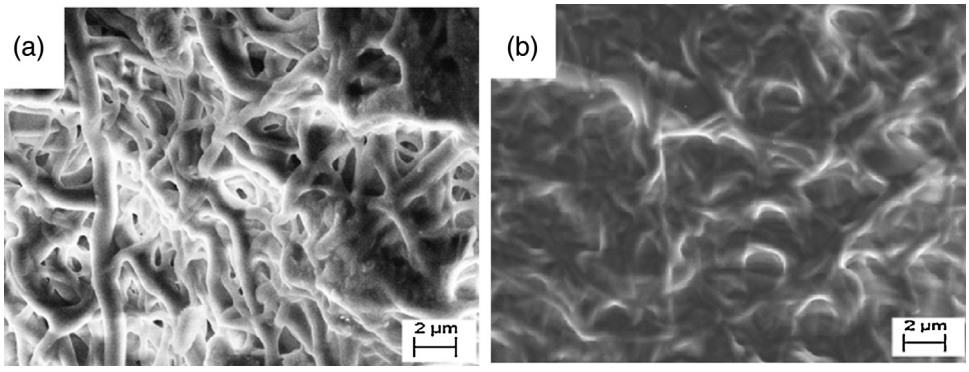

Fig. 4. SEM images of the honey/polyvinyl alcohol/chitosan (HP–chitosan) (30%:7%:3.5%) nanofiber mats that exhibited physical cross-linking by: (a) heating at 110 °C for 15 min under vacuum and (b) heating at 70 °C for 24 h under vacuum.

Among the different physical crosslinking procedures applied, cross-linked fibers could only be achieved by heating at 110 °C for 15 min (Fig. 4a), it could be observed also that such fibers exhibited noticeable swelling. Meanwhile, heating at 70 °C for 24 h showed partially degraded swollen fibers (Fig. 4b). Heating induces the crystallization of the incorporated polymers (Kang et al., 2010). Freezing and thawing in liquid nitrogen as well as heating at elevated temperatures made the nanofibrous scaffold brittle and liable to cracking.

It is worth noting, that upon physical cross-linking by heating, a change in the color of the nanofibers was observed from white to light brown. The same effect was observed upon aging of the nanofibers for several months. Such color change may indicate possible interactions between the sugar aldehyde groups and the chitosan amino groups.

3.4. Weight loss and water retention behavior

The water uptake capability and degree of weight loss of the electrospun fibers were investigated. As shown in Fig. 5, the non-crosslinked fibers exhibited swelling capabilities between 46% and 197%, with the highest swelling observed for the sample containing 3.5% chitosan and 20% honey (HP–chitosan: 20%:7%:3.5%) tested at 4 h. Although, polyvinyl alcohol, chitosan and honey enhance water uptake, the samples showed moderate swelling capabilities when compared to previously spun chitosan and polyvinyl alcohol fibers lacking honey. Jannesari, Varshosaz, Morshed, and Zamani (2011), reported that the swelling value of polyvinyl alcohol/chitosan nanofibers was 390% after 24 h compared to 135% for the HP–chitosan: 3.5%:20%:7% in the present work.

Such results may be attributed to the high water solubility of honey, where although honey increases the water uptake (MohdZohdi, Abu BakarZakaria, Yusof, Mohamed Mustapha, & Abdullah, 2011), its high water solubility leads to an increase in the degradation rate of the fibers. Similarly, Wang et al. observed the same effect upon inclusion of 20% honey in a gelatine/chitosan/honey hydrogel. Honey first promotes swelling due to its high osmolarity, however, upon water uptake the high water solubility of honey accelerates the degradation rate and thus results in low swelling due to the absence of a compact structure to retain the water (Wang, Zhu, Xue, & Wu, 2012). Thus, the highest swelling percent in all tested samples were observed at 4 h that decreased at 24 h. Moreover, upon comparing the HP–chitosan samples of 30%:7%:3.5% and 20%:7%:3.5% (Fig. 5a), it was observed that an increase in the water uptake capability is achieved upon decreasing the honey concentration.

On the other hand, chitosan with its decreased water solubility decreases the weight loss within the HP–chitosan nanofibrous mats, which is observed upon comparing the decrease in swelling and the increase of the weight loss of the (HP–chitosan; 30%:7%:1.5%) compared to (HP–chitosan; 30%:7%:3.5%) (Fig. 5a and b). However, upon increasing the chitosan concentration to 5.5% in the HP–chitosan nanofibers, a marked increase in the swelling percent was only observed at 24 h. This is because,

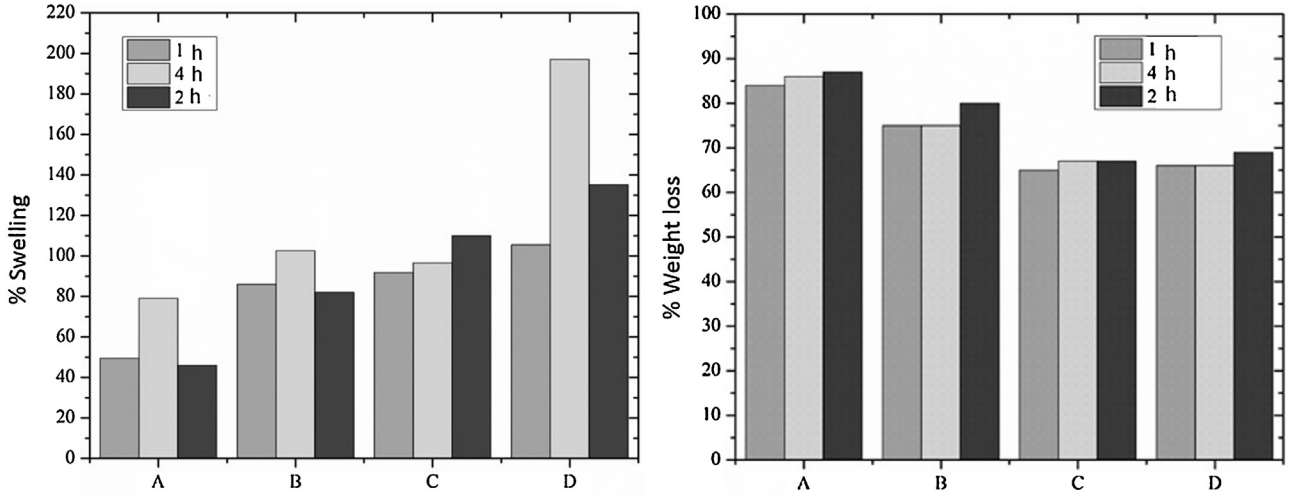

Fig. 5. % Swelling (a) and % weight loss (b) of the honey/polyvinyl alcohol/chitosan (HP–chitosan) nanofiber mats with different weight ratios of HP–chitosan after immersion in PBS (pH 7.4) for 1, 4, and 24 h. Different weight ratios of the tested HP–chitosan included: (A) 30%:7%:1.5%, (B) 30%:7%:3.5%, (C) 30%:7%:5.5%, and (D) 20%: 7%:3.5%.

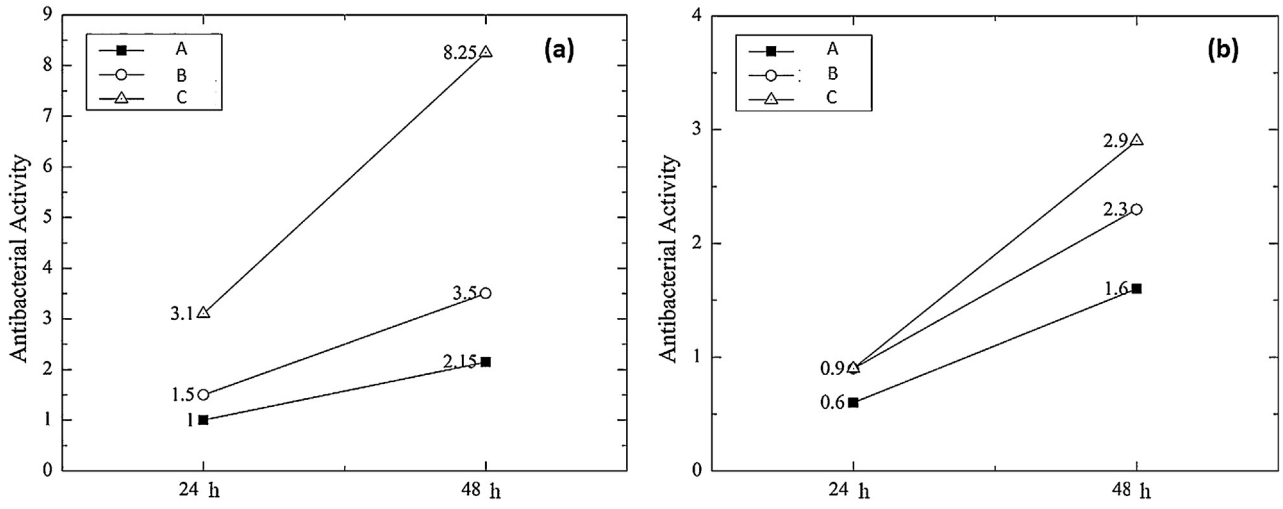

Fig. 6. The antibacterial activity of the electrospun honey/polyvinyl alcohol/chitosan (HP–chitosan) of mats against *S. aureus* (a) and *E. coli* (b) at 24 and 48 h on 7×10^8 CFU/ml bacteria. The weight blending ratios of the electrospun mats were 7% polyvinyl alcohol, 30% honey and increasing concentrations of chitosan; (A) 1.5%, (B) 3.5%, and (C) 5.5%.

although chitosan enhances water uptake, increasing the chitosan concentration above a certain level does produce the opposite effect. This was explained by Son et al., who observed that in the chitosan/polyvinyl alcohol nanofibrous scaffolds of low chitosan concentrations, the hydrophilic polyvinyl alcohol could easily form polymeric hydrogels in solutions thus allowing enhanced swelling. Whereas, above certain concentration of chitosan, the intermolecular forces between the chitosan side chains and the amine groups increase, thus leading to decreased swelling (Son, Yeom, Song, Lee, & Hwang, 2009).

3.5. Antibacterial evaluation

The antimicrobial activity of honey is due to its ability to produce hydrogen peroxide, its high sugar content, its acidity and its content of flavonoids (Vandamme, Heyneman, Hoeksema, Verbelen, & Monstrey, 2013). On the other hand, the antibacterial activity of chitosan is mainly due to the interaction between the chitosan polycations and the negatively charged surfaces of bacteria, which leads to loss of bacterial membrane permeability leading to cell leakage and death (Muzzarelli, Tarsi, Filippini, Giovanetti, Biagini, & Varaldo, 1990).

Considering its biodegradable nature, the antibacterial activity of the HP–chitosan nanofibrous mats is dependent on the concentration of its components in the media which increases with time. As shown in Fig. 6a, the antibacterial activity against *S. aureus* increased with increasing the chitosan concentration within the HP–chitosan nanofibers. Moreover, increasing the incubation time resulted in marked increase in antibacterial activity especially with the 3.5% and 5.5% incorporated chitosan concentrations. Complete bacterial inhibition was achieved at 48 h with the 5.5% chitosan. This may be attributed to the decreased solubility of chitosan, thus at longer incubation periods larger percentage of the nanofibers are degraded leading to increase in the concentration of available chitosan thus leading to increased antibacterial activity.

Testing the HP–chitosan nanofibrous mats on *E. coli* revealed weak antibacterial activity (Fig. 6b). Such results agree with the results of No, Young Park, Ho Lee, and Meyers (2002) who observed the weak antibacterial activity of chitosan against gram negative bacteria (No, Young Park, Ho Lee, & Meyers, 2002).

It is worth mentioning that the nanofibrous structure enhanced the antibacterial activity of the included components. The tested sample (0.1 g) contains less than 20 ppm chitosan and approximately 0.175% honey and produced pronounced antibacterial effects against *S. aureus* and weak antibacterial effects against *E. coli* compared to no antibacterial effect at such concentrations for both honey and chitosan alone (Goy, Britto, & Assis, 2009; Islam, Masum, Mahbub, & Haque, 2011I; Liu et al., 2006; Mandal & Mandal, 2011). Such results could be attributed to the dramatic increase in the surface to volume ratio of the nanofibers.

3.6. Cytotoxicity evaluation

Cells grown with the extracts of the HP–chitosan nanofibers showed similar morphologies to that of the negative control (data not shown). Primary skin fibroblast cells were cultured with the extract of the crosslinked and noncrosslinked HP–chitosan nanofibrous scaffolds having the concentrations of 30%:7%:1.5%, 30%:7%:3.5% and 30%:7%:5.5% for 3 days and their toxicities were evaluated using MTT assay as shown in Fig. 7.

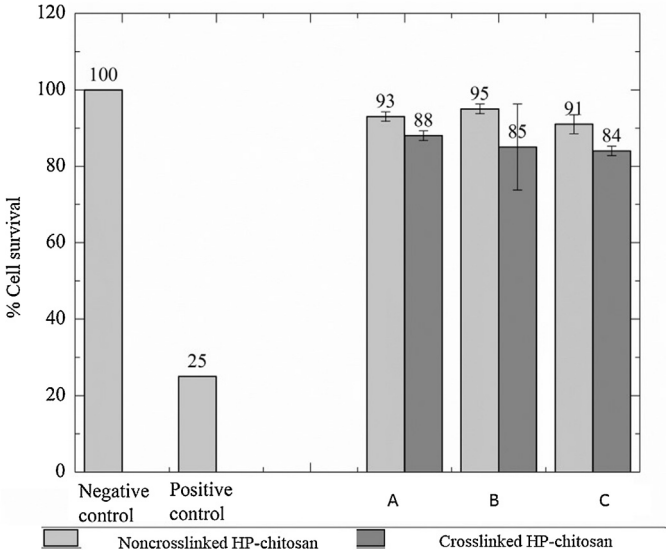

Fig. 7. Effect of electrospun honey/polyvinyl alcohol/chitosan (HP–chitosan) nanofibers on cultured fibroblasts investigated using MTT assay. Different HP–chitosan nanofibrous scaffolds with 30% honey, 7% polyvinyl alcohol, and different concentrations of chitosan: (A) 5.5%, (B) 3.5%, and (C) 1.5%, were tested. Both non-crosslinked and crosslinked HP–chitosan nanofibrous scaffolds were tested. The data represents the mean ± SD ($N = 3$).

Cells cultured with the HP–chitosan nanofibrous scaffolds exhibited no significant differences in cell viability to those of the negative control (cultured with no nanofibrous scaffolds) ($p < 0.05$) and significantly different and improved viability than the cells cultured with the positive control. Such results indicate the biocompatibility of the developed HP–chitosan nanofibrous scaffolds. It was realized, however, that the crosslinked nanofibers in all tested nanofibrous samples showed slight decrease in the viability of the cells compared to the noncrosslinked nanofibers. This may be due to the traces of GA remaining on the nanofibers. Still, the viability of the cells cultured with the crosslinked nanofibers after 3 days were similar to those of the negative control indicating good biocompatibility.

4. Conclusions

In this study, polyvinyl alcohol was co-spun with honey and chitosan resulting in HP–chitosan nanofibers with honey concentrations ranging from 20% to 40% and chitosan concentrations ranging from 1.5% to 5.5%. The combination of chitosan and honey had a synergistic effect on the viscosity of the solution allowing it to reach the optimum viscosity required for electrospinning. Such effect allowed for the first time for fabrication of nanofibers comprising 40% of their actual weight honey compared to 9% in previous attempts and up to 5.5% chitosan without the use of high concentrated acids or toxic solvents. Physical and chemical crosslinking of the developed HP–chitosan nanofibers resulted in different degrees of crosslinking which may extend their applications. The developed nanofibers (HP–chitosan; 30%:7%:3.5%) exhibited enhanced antibacterial activity against *S. aureus* but poor antibacterial activity against *E. coli*. The antibacterial activity increased by increasing the concentration of the incorporated chitosan within the nanofibers from 1.5% to 5.5%. Additionally, changing the concentrations of chitosan and honey resulted in different degrees of water uptake ranging from 46% to 197%. The degradation rate of the developed nanofibers was inversely related to the concentration of the chitosan within the nanofibers. Glutaraldehyde crosslinked and noncrosslinked nanofibers had no toxicity on cultured primary fibroblasts. The developed HP–chitosan nanofibers with high concentrations of honey and chitosan hold the potential as effective biocompatible wound dressings.

Acknowledgement

The authors would like to thank Dr. Mahmoud El. Syed Nour, Faculty of Agriculture, Cairo University, Giza, Egypt for his generous supply of the clover honey and its specifications.

References

Altstädt, V., Lovera, D., Schmidt, H., Schmidt, S., & Fery, A. (2008). Electrospun polymeric fine fibers. *Imaging & Microscopy*, *10*(2), 29–31.

Amrit, U. R., Hendrix, R., Dutschk, V., & Warmoeskerken, M. M. C. G. (2012). A study of the antibacterial activity of polyhexamethylenebigaunide on cotton substrate. In *12th AUTEX World Textile Conference – Innovative textile for high future demands* 13th to 15th June 2012, 13 June 2012, Zadar, Croatia.

Bhardwaj, N., & Kundu, S. C. (2010). Electrospinning: A fascinating fiber fabrication technique. *Biotechnology Advances*, *28*(3), 325–347.

Brudzynski, K. (2006). Effect of hydrogen peroxide on antibacterial activities of Canadian honeys. *Canadian Journal of Microbiology*, *52*(12), 1228–1237.

Busilacchi, A., Gigante, A., Mattioli-Belmonte, M., Manzotti, S., & Muzzarelli, R. A. A. (2013). Chitosan stabilizes platelet growth factors and modulates stem cell differentiation toward tissue regeneration. *Carbohydrate Polymers*, *98*(1), 665–676.

Charernsriwilaiwat, N., Opanasopit, P., Rojanarata, T., Ngawhirunpat, T., & Supaphol, P. (2010). Preparation and characterization of chitosan-hydroxybenzotriazole/polyvinyl alcohol blend nanofibers by the electrospinning technique. *Carbohydrate Polymers*, *81*(3), 675–680.

Charernsriwilaiwat, N., Opanasopit, P., Rojanarata, T., & Ngawhirunpat, T. (2011). Fabrication and characterization of chitosan-ethylenediaminetetraacetic acid/polyvinyl alcohol blend electrospun nanofibers. *Advanced Materials Research*, *194*, 648–651.

Geng, X., Kwon, O. H., & Jang, J. (2005). Electrospinning of chitosan dissolved in concentrated acetic acid solution. *Biomaterials*, *26*(27), 5427–5432.

Goy, R. C., Britto, D. D., & Assis, O. B. (2009). A review of the antimicrobial activity of chitosan. *Polímeros*, *19*(3), 241–247.

Homayoni, H., Ravandi, S. A. H., & Valizadeh, M. (2009). Electrospinning of chitosan nanofibers: Processing optimization. *Carbohydrate Polymers*, *77*(3), 656–661.

Islam, M., Masum, S. M., Mahbub, K. R., & Haque, M. (2011). Antibacterial activity of crab-chitosan against *Staphylococcus aureus* and *Escherichia coli*. *Journal of Advanced Scientific Research*, *2*(4).

Jaganathan, S. K., & Mandal, M. (2009). Antiproliferative effects of honey and of its polyphenols: A review. *Journal of Biomedicine and Biotechnology*, *2009*. Article ID: 830616, 13 pages.

Jannesari, M., Varshosaz, J., Morshed, M., & Zamani, M. (2011). Composite poly (vinyl alcohol)/poly (vinyl acetate) electrospun nanofibrous mats as a novel wound dressing matrix for controlled release of drugs. *International Journal of Nanomedicine*, *6*, 993–1003.

Kang, Y. O., Yoon, I. S., Lee, S. Y., Kim, D. D., Lee, S. J., Park, W. H., et al. (2010). Chitosan-coated poly (vinyl alcohol) nanofibers for wound dressings. *Journal of Biomedical Materials Research Part B: Applied Biomaterials*, *92*(2), 568–576.

Khan, F. R., Abadin, Z. U., & Rauf, N. (2007). Honey: Nutritional and medicinal value. *International Journal of Clinical Practice*, *61*(10), 1705–1707.

Li, D., & Xia, Y. (2004). Electrospinning of nanofibers: Reinventing the wheel? *Advanced Materials*, *16*(14), 1151–1170.

Liao, H., Qi, R., Shen, M., Cao, X., Guo, R., Zhang, Y., et al. (2011). Improved cellular response on multiwalled carbon nanotube-incorporated electrospun polyvinyl alcohol/chitosan nanofibrous scaffolds. *Colloids and Surfaces B: Biointerfaces*, *84*(2), 528–535.

Liu, N., Chen, X. G., Park, H. J., Liu, C. G., Liu, C. S., Meng, X. H., et al. (2006). Effect of MW and concentration of chitosan on antibacterial activity of *Escherichia coli*. *Carbohydrate Polymers*, *64*(1), 60–65.

Lusby, P. E., Coombes, A., & Wilkinson, J. M. (2002). Honey: A potent agent for wound healing? *Journal of Wound Ostomy & Continence Nursing*, *29*(6), 295–300.

Maleki, H., Gharehaghaji, A. A., & Dijkstra, P. J. (2013). A novel honey-based nanofibrous scaffold for wound dressing application. *Journal of Applied Polymer Science*, *127*(5), 4086–4092.

Mandal, M. D., & Mandal, S. (2011). Honey: Its medicinal property and antibacterial activity. *Asian Pacific Journal of Tropical Biomedicine*, *1*(2), 154–160.

Meinel, A. J., Germershaus, O., Luhmann, T., Merkle, H. P., & Meinel, L. (2012). Electrospun matrices for localized drug delivery: Current technologies and selected biomedical applications. *European Journal of Pharmaceutics and Biopharmaceutics*, *81*(1), 1–13.

MohdZohdi, R., Abu BakarZakaria, Z., Yusof, N., Mohamed Mustapha, N., & Abdullah, M. N. H. (2011). Gelam (*Melaleuca* spp.) honey-based hydrogel as burn wound dressing. *Evidence-Based Complementary and Alternative Medicine*, *2012*.

Molan, P. C. (1992). The antibacterial activity of honey. 2: Variation in the potency of the antibacterial activity. *Bee World*, *73*(2), 59–76.

Muzzarelli, R. A. A., Tarsi, R., Filippini, O., Giovanetti, E., Biagini, G., & Varaldo, P. E. (1990). Antimicrobial properties of *N*-carboxybutyl chitosan. *Antimicrobial Agents and Chemotherapy*, *34*, 2019–2023.

Muzzarelli, R. A. A. (2010). Chitins and chitosans as immune adjuvants and non-allergenic drug carriers. *Marine Drugs*, *8*(2), 292–312.

Muzzarelli, R. A. A., Boudrant, J., Meyer, D., Manno, N., DeMarchis, M., & Paoletti, M. G. (2012). Current views on fungal chitin/chitosan, human chitinases, food preservation, glucans, pectins and inulin: A tribute to Henri Braconnot, precursor of the carbohydrate polymers science, on the chitin bicentennial. *Carbohydrate Polymers*, *87*, 995–1012.

Muzzarelli, R. A. A., Greco, F., Busilacchi, A., Sollazzo, V., & Gigante, A. (2012). Chitosan, hyaluronan and chondroitin sulfate in tissue engineering for cartilage regeneration: A review. *Carbohydrate Polymers*, *89*, 723–739.

Muzzarelli, R. A. A., El Mehtedi, M., & Mattioli-Belmonte, M. (2014). Emerging biomedical applications of nano-chitins and nano-chitosans obtained via advanced eco-friendly technologies from marine resources. *Marine Drugs*, *12*, 5468–5502.

No, H. K., Young Park, N., Ho Lee, S., & Meyers, S. P. (2002). Antibacterial activity of chitosans and chitosan oligomers with different molecular weights. *International Journal of Food Microbiology*, *74*(1), 65–72.

Paipitak, K., Pornpra, T., Mongkontalang, P., Techitdheer, W., & Pecharapa, W. (2011). Characterization of PVA-chitosan nanofibers prepared by electrospinning. *Procedia Engineering*, *8*, 101–105.

Philip, D. (2009). Honey mediated green synthesis of gold nanoparticles. *Spectrochimica Acta Part A: Molecular and Biomolecular Spectroscopy*, *73*(4), 650–653.

Philip, D. (2010). Honey mediated green synthesis of silver nanoparticles. *Spectrochimica Acta Part A: Molecular and Biomolecular Spectroscopy*, *75*(3), 1078–1081.

Schiffman, J. D., & Schauer, C. L. (2007). Cross-linking chitosan nanofibers. *Biomacromolecules*, *8*(2), 594–601.

Seluanov, A., Vaidya, A., & Gorbunova, V. (2010). Establishing primary adult fibroblast cultures from rodents. *Journal of Visualized Experiments*, *44*.

Sharma, C., Dinda, A. K., & Mishra, N. C. (2013). Fabrication and characterization of natural origin chitosan–gelatin–alginate composite scaffold by foaming method without using surfactant. *Journal of Applied Polymer Science*, *127*, 3228–3241.

Son, B., Yeom, B. Y., Song, S. H., Lee, C. S., & Hwang, T. S. (2009). Antibacterial electrospun chitosan/poly (vinyl alcohol) nanofiberscontaining silver nitrate and titanium dioxide. *Journal of Applied Polymer Science*, *111*(6), 2892–2899.

Su, P., Wang, C., Yang, X., Chen, X., Gao, C., Feng, et al. (2011). Electrospinning of chitosan nanofibers: The favorable effect of metal ions. *Carbohydrate Polymers*, *84*(1), 239–246.

Tosi, E. A., Ré, E., Lucero, H., & Bulacio, L. (2004). Effect of honey high-temperature short-time heating on parameters related to quality, crystallisation phenomena and fungal inhibition. *LWT-Food Science and Technology*, *37*(6), 669–678.

Vandamme, L., Heyneman, A., Hoeksema, H., Verbelen, J., & Monstrey, S. (2013). Honey in modern wound care: A systematic review. *Burns*, *39*(8), 1514–1525.

Wang, P., & He, J. H. (2013). Electrospun polyvinyl alcohol-honey nanofibers. *Thermal Science*, *17*(5), 1549–1550.

Wang, T., Zhu, X. K., Xue, X. T., & Wu, D. Y. (2012). Hydrogel sheets of chitosan, honey and gelatin as burn wound dressings. *Carbohydrate Polymers*, *88*(1), 75–83.

Xie, H., Jia, Z., Huang, J., & Zhang, C. (2011). Preparation of low molecular weight chitosan by complex enzymes hydrolysis. *International Journal of Chemistry*, *3*(2), p180.

Yan, E., Fan, S., Li, X., Wang, C., Sun, Z., Ni, L., et al. (2012). Electrospun polyvinyl alcohol/chitosan composite nanofibers involving Au nanoparticles and their in vitro release properties. *Materials Science and Engineering C*, *33*, 461–465.

Zhou, Y., Yang, D., Chen, X., Xu, Q., Lu, F., & Nie, J. (2007). Electrospun water-soluble carboxyethyl chitosan/poly (vinyl alcohol) nanofibrous membrane as potential wound dressing for skin regeneration. *Biomacromolecules*, *9*(1), 349–354.

ACS APPLIED MATERIALS & INTERFACES

Research Article

www.acsami.org

Honey/Chitosan Nanofiber Wound Dressing Enriched with *Allium sativum* and *Cleome droserifolia*: Enhanced Antimicrobial and Wound Healing Activity

Wessam A. Sarhan,[†] Hassan M. E. Azzazy,*[,†] and Ibrahim M. El-Sherbiny[‡]

[†]Department of Chemistry, School of Sciences & Engineering, The American University in Cairo, New Cairo 11835, Egypt

[‡]Center for Materials Science, University of Science and Technology, Zewail City of Science and Technology, 6th October City, Giza 12588, Egypt

ABSTRACT: Two natural extracts were loaded within fabricated honey, poly(vinyl alcohol), chitosan nanofibers (HPCS) to develop biocompatible antimicrobial nanofibrous wound dressing. The dried aqueous extract of *Cleome droserifolia* (CE) and *Allium sativum* aqueous extract (AE) and their combination were loaded within the HPCS nanofibers in the HPCS-CE, HPCS-AE, and HPCS-AE/CE nanofiber mats, respectively. It was observed that the addition of AE resulted in the least fiber diameter (145 nm), whereas the addition of the AE and CE combination resulted in the least swelling ability and the highest weight loss. In vitro antibacterial testing against *Staphylococcus aureus*, *Escherichia coli*, Methicillin-resistant *S. aureus* (MRSA), and multidrug-resistant *Pseudomonas aeruginosa* was performed in comparison with the commercial dressing AquacelAg and revealed that the HPCS-AE and HPCS-AE/CE nanofiber mats allowed complete inhibition of *S. aureus* and the HPCS-AE/CE exhibited mild antibacterial activity against MRSA. A preliminary in vivo study revealed that the developed nanofiber mats enhanced the wound healing process as compared to the untreated control as proved by the enhanced wound closure rates in mice and by the histological examination of the wounds. Moreover, comparison with the commercial dressing Aquacel Ag, the HPCS, and HPCS-AE/CE demonstrated similar effects on the wound healing process, whereas the HPCS/AE allowed an enhanced wound closure rate. Cell culture studies proved the biocompatibility of the developed nanofiber mats in comparison with the commercial Aquacel Ag, which exhibited noticeable cytotoxicity. The developed natural nanofiber mats hold potential as promising biocompatible antibacterial wound dressing.

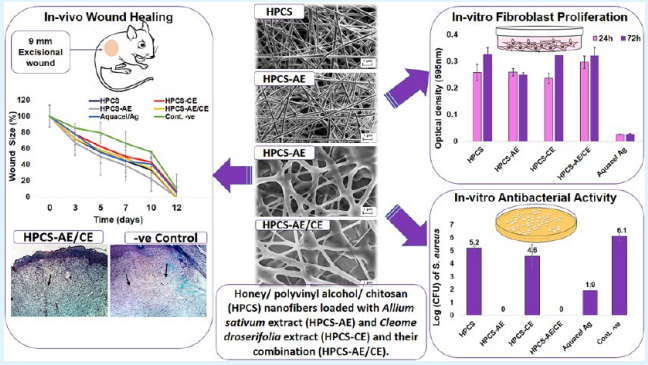

KEYWORDS: *honey chitosan nanofibers, natural extracts, antibacterial, wound healing, cell culture*

INTRODUCTION

Chronic nonhealing wounds have a major socioeconomic impact with more than 25 billion dollars as the cost of nonhealing wounds.[1] One of the main reasons that complicates and delays the wound healing process is bacterial infection. Thus, advanced antimicrobial wound dressings are witnessing increased demand within the wound care market. Such dressings allow the sustained release of the loaded antimicrobials, thus permitting the realization of their antibacterial activity while maintaining a healthy concentration to the healing tissues. Antimicrobials as silver, iodine, and chlorhexidine have a broad spectrum of antibacterial activity and are extensively used in wound treatment; however, they may damage healthy tissues.[2,3] Thus, investigation of additional antimicrobials is warranted.

Allium sativum (garlic) has been known historically for its use to treat infectious diseases.[4] *Allium sativum* exhibits well proven antibacterial activity against both Gram-positive and Gram-negative bacteria as well as resistant bacterial strains.[5−8] Such a therapeutic effect of *Allium sativum* is mainly attributed to its water-soluble and oil-soluble organosulfur compounds.

Cleome droserifolia (Forssk.), Del., a member of the *Cleomaceae* family, is another plant of striking medical importance.[9] *Cleome droserifolia* is still traditionally used by the Egyptian Bedouins in the treatment of diabetes and wounds. *Cleome droserifolia* is also used for treating rheumatism, scabies, and inflammation[10] that is in addition to its proven antioxidant activity.[11,12] The phytochemical studies revealed the enrichment of *Cleome* with different beneficial compounds including phenolics, flavonoids, terpenoids, and alkaloids.[13−15] Recently, the antibacterial effects of *Cleome droserifolia* have been observed and were linked to its content of different terpenes.[9] However, studies regarding the *Cleome*'s biological

Received: January 20, 2016
Accepted: February 24, 2016
Published: February 24, 2016

DOI: 10.1021/acsami.6b00739
ACS Appl. Mater. Interfaces 2016, 8, 6379−6390

activity as well as its phytochemistry are still far from being complete.[9]

It has been argued that the antimicrobial efficacy alone of an advanced dressing is insufficient and other properties that enhance the wound healing process are also required.[16] Thus, through the current research, a new series of electrospun nanofibrous wound dressings based on high concentrations of honey and chitosan, and enriched with *Allium sativum* and *Cleome droserifolia*, has been developed for enhanced antimicrobial and wound healing activity. Honey and chitosan are well-known for their wound healing and antibacterial properties.[17−20]Moreover, the nanofibrous structure resembles the extracellular matrix of the skin and thus enhances the healing process. In our previous research, the developed honey/chitosan-based nanofibrous mats were proved to have mild antibacterial activity.[21] Consequently, this study aims to enhance the antibacterial activity of honey chitosan nanofiber mats by adding natural extracts and test the combination of the natural extracts with honey and chitosan within the nanofibrous structure for their antibacterial and wound healing abilities.

EXPERIMENTAL SECTION

Materials. Fresh bulbs of *Allium sativum* (AE) were purchased from a local vendor, and honey (clover) was obtained from the faculty of Agriculture, Cairo University. *Cleome droserifolia* (CE) was collected from the mountains of Sinai, Egypt. Chitosan (M_w of 240 kDa and DDA of 84%, Chitoclear, cg110, TM 3728) was supplied from Primex (Siglufjordur, Iceland). Poly(vinyl alcohol) (M_w of 85 kDa), glutaraldehyde (25% in H_2O), and absolute ethanol (≥99.8%) were supplied from Sigma-Aldrich (St. Louis, MO). Glacial acetic acid (99−100% purity) was provided from Merck (Wadeville, South Africa). Muller Hinton broth, agar−agar, nutrient broth, and nutrient agar were purchased from Oxoid (Basingstocke, UK). AquacelAg (ConvaTec Inc.) was purchased from a local pharmacy in Egypt. Fetal bovine serum (FBS), thiazolyl blue tetrazolium bromide-MTT (M2128-1G), phosphate buffered saline (PBS), Dulbecco's modified eagle medium (DMEM), and triton X were supplied from Sigma-Aldrich (St. Louis, MO).

Preparation of Aqueous Extracts of *Allium sativum* (AE) and *Cleome droserifolia* (CE). Bulbs of fresh AE were extracted according to the method of ref 22. Fresh bulbs of AE (10 g) were peeled, washed with distilled water several times, and then the AE was homogenized aseptically using a sterile mortar and a pestle. Subsequently, Whatman No. 1 paper was used to filter the homogenized mixture. The obtained filtrate was then directly used in the preparation of the electrospinning solutions. On the other hand, dried leaves of CE were extracted according to established protocols.[23] The air-dried aerial parts of CE were powdered and extracted via boiling in distilled water for 2 min and then allowed to stand for 10 min before filtration. Whatman No. 1 paper was used to filter the boiled mixture. Subsequently, a rotary evaporator was used to remove the water, and the remaining extract was dried in a vacuum oven at 40 °C (Jeiotech, OV-11, South Korea) until a dry powder of CE extract was obtained. The powder was weighed and stored until further use.

Preparation of the Electrospun Solutions. Various blend solutions of honey/poly(vinyl alcohol)/chitosan (HPCS), honey/poly(vinyl alcohol)/chitosan/*Allium sativum* extract (HPCS-AE), honey/poly(vinyl alcohol)/chitosan/*Cleome droserifolia* extract (HPCS-CE), and honey/poly(vinyl alcohol)/chitosan/*Allium sativum* extract/*Cleome droserifolia* extract (HPCS-AE/CE) were prepared. In the preparation of the blend solution of (HPCS-AE), AE was used as 50% of the solvent in which honey (30 w/v), chitosan (3.5 w/v), and poly(vinyl alcohol) (7 w/v) were dissolved. Both of the blend solutions of HPCS and HPCS-AE were prepared in 1% of aqueous acetic acid. Both solutions were allowed to age at room temperature for 1 week. *Cleome droserifolia* dry powder extract (CE) (10 w/v) was added to both as-prepared HPCS and HPCS-AE blend solutions before electrospinning and stirred for 1 h to form the blend solutions of HPCS-CE (30:7:3.5:10 wt %) and HPCS-AE/CE (30:7:3.5:10 wt %) in 50% AE as the solvent, respectively. During preparation of all blend solutions, poly(vinyl alcohol) was dissolved separately in one-half the volume of the solvent at 100 °C with stirring followed by addition of the remaining volume of the solvent with the other constituents to the cooled solutions to avoid any degradation of the active constituents due to exposure to elevated temperatures.

Viscosity Measurements. The aqueous AE extract replaced 50% of the solvent of the HPCS blend solution; thus, its effect on the viscosity of the blend solution had to be examined. The viscosity of the HPCS-AE (30%:7%:3.5%:50%) blend solution was determined and compared to that of the HPCS (30%:7%:3.5%). The viscosity of the aged solutions was determined using a viscometer (Myr; VR-3000, Viscotech Hispania, Tarragona, Spain) at different time intervals (0, 24, 48 h, and 1 week). The average value of three measurements was reported as mean ± SD.

Electrospinning of the As-Prepared Blend Solution. The electrospinning of the HPCS, HPCS-AE, HPCS-CE, and HPCS-AE/CE solutions was performed using NANON-O1A electrospinner (MECC, Japan). The as-prepared solutions were loaded in a 5 mL plastic syringe attached to an 18 gauge stainless steel needle as the nozzle. Different voltages and flow rates were applied to each of the blend solutions, and the optimum values that allowed the most uniform nanofibers were selected for collection of the nanofibrous mats. The distance between the needle and the collector was kept at 13 cm. Samples were collected on ground collector that was wrapped in aluminum sheets and cotton gauze. During collection, a stationary collecting surface was used, but the spinneret moved transversely at a speed of 100 mm/s and a width of 100 mm.

Characterization and Measurements. The morphologies of the developed nanofibers were observed using scanning electron microscopy (FESEM, Leo Supra 55, Zeiss Inc., Oberkochen, Germany). Diameters of the fabricated nanofibers were measured using Image-J software. For each of the developed nanofibrous mats, 100 fibers were measured from three different images, and the average diameter was calculated.

Assessment of the Swelling and Weight Loss of the Cross-Linked Nanofibrous Mats. The developed HPCS, HPCS-AE, HPCS-CE, and HPCS-AE/CE nanofibrous mats were cross-linked via exposure to vapors of glutaraldehyde (GA) (40 mL) for 1 and 3 h. The cross-linked nanofibrous mats were subsequently heated at 40 °C in a vacuum oven to remove any traces of unreacted GA and to enhance the cross-linking. The swelling ability and weight loss of the cross-linked nanofibrous mats were evaluated via placing the mats in phosphate buffered saline, PBS (pH 7.4) at 37 °C. The following relationships were used for determination of the swelling ability of the nanofibrous mats at 1, 4, and 24 h, and their weight loss at 24 h:

$$\text{degree of swelling } (\%) = [M - M_i/M_i] \times 100 \quad (1)$$

$$\text{weight loss } (\%) = [M_i - M_d/M_i] \times 100 \quad (2)$$

where M is the weight of the swollen nanofibrous mats after plotting their surface with filter paper, and M_d is the weight of the dried nanofibrous mats after being removed from the phosphate buffer saline. The swollen nanofibrous mats were dried in an oven at 40 °C until constant weight was achieved. M_i is the initial dry weight of the electrospun nanofibrous mats.[24]

Antibacterial Evaluation. The developed HPCS, HPCS-AE, HPCS-CE, and HPCS-AE/CE were evaluated for their antibacterial activities using the viable cell count technique as compared to AquacelAg (ConvaTec Inc.) as the positive control. The antibacterial activities of the developed nanofibrous mats and the AquacelAg were tested against *Staphylococcus aureus*, *Escherichia coli*, multidrug-resistant (MDR) *Pseudomonas aeruginosa*, and methicillin-resistant *Staphylococcus aureus* (MRSA). The electrospun nanofibrous mats were UV sterilized for 20 min, then 0.05 g of each of the developed nanofibrous mats as well as AquacelAg were added to sterile tubes containing 3 mL of sterile Muller Hinton broth. Each of the tested bacterial strains was incubated overnight at 37 °C, and fresh colonies

DOI: 10.1021/acsami.6b00739
ACS Appl. Mater. Interfaces 2016, 8, 6379−6390

were used to prepare bacterial suspensions for each of them. The turbidity of the bacterial suspensions was adjusted to 0.5 McFarland standard (1×10^8 cfu/mL). Aliquots (30 uL) of each bacteria were added to the sterile tubes with the nanofibrous mats and the AquacelAg. The tubes as well as negative controls were subsequently incubated at 37 °C with shaking at 100 rpm. Following 24 h of incubation, 10 uL from each of the treated bacterial broth as well as the controls were taken, and serial dilution was performed. From each dilution, 50 uL was spread on nutrient agar plates that were incubated at 37 °C. After 24 h of incubation, the surviving colonies were counted. The plates that allowed counting from 10 to 150 CFU were used for counting. The experiment was repeated three times, and the mean value of CFU was recorded.

In Vivo Wound Healing Studies. In vivo wound healing studies were performed on male mice weighing 25 g. All animals were anaesthetized with a mixture of ketamin HCl (50 mg/kg) and xylene HCl (20 mg/kg), and then their backs were shaved. A 9 mm wound was created on the back of each mice with a biopsy puncher. The HPCS, HPCS-AE, HPCS-CE, and HPCS-AE/CE were UV sterilized for 20 min, and each of the nanofibrous mats was placed on the wound site. AquacelAg (ConvaTec Inc.) was used as the positive control, whereas the negative control remained untreated and was covered with a cotton gauze. The change in the wound area was measured at 3, 5, 7, 10, and 12 days. The extent of wound healing is expressed as the percentage of wound area that remained exposed. Each sample as well as the controls were tested on three mice, and the mean value of three measurements was recorded.

$$\text{wound size } (\%) = [W_{(3,5,7,10,12)}/W_{(0)}] \times 100$$

where $W_{(0)}$ and $W_{(3,5,7,10,12)}$ represent the exposed areas of the wounds on days 0 and 3, 5, 7, 10, and 12, respectively.[25]

Histological Examination and the Scoring System Used for the Histologic Outcomes. The wound site with the surrounding muscle and skin was cut and then fixed with 10% buffered formalin. The collected samples were then put in paraffin and sectioned. Each of the tissue samples was then subjected to Hematoxylin and Eosin (H&E) staining as well as Masson's trichrome (MT) staining. The H&E stained sections were evaluated and scored at days 3, 5, 7, 10, and 12, and the MT stained sections were evaluated and scored at day 10. The stained sections were evaluated for the following histologic outcomes: necrosis, amount and kind of inflammatory infiltrates, hemorrhage, granulation tissue, epithelization, thickness of the epidermis, and collagen deposition. A histologic scoring system was used to assess each parameter, and a score of 0−3 was assigned for each sample. Necrosis, hemorrhage, inflammatory infiltrates, collagen deposition, epithelization, and thickness of the epidermis were graded as 0 (none), 1 (scant), 2 (moderate), and 3 (abundant). Severity of inflammation was scored as follows: 0 (no inflammatory cells) no inflammation; 1 (presence of abundant macrophages and scarce neutrophils); 2 (presence of equal macrophages and neutrophils); and 3 (presence of abundant neutrophils and scarce macrophages). The maturation (thickness) of the granulation tissue was graded as 0 (immature), 1 (mild maturation), 2 (matured), and 3 (fully matured with collagen deposition). Collagen distribution (based on the collagen fibers distribution in the microscopic fields) was graded as 0 (no collagen distributed), 1 (nonuniform distribution), 2 (mild uniformity in distribution), and 3 (uniform distribution).

Cell Viability Assay. The HPCS, HPCS-AE, HPCS-CE, and HPCS-AE/CE as well as AquacelAg as a positive control were tested for their cytotoxicity. The nanofibrous samples were UV sterilized for 30 min, and then the extract solutions of each of the nanofibrous mats and the AquacelAg were prepared via immersion of the sterilized mats in DMEM with 1% PS and 10% heat-inactivated FBS and incubating them at 37 °C. The extract solutions of the tested samples were then filtered via sterile disposable filters (0.20 mm, Merck, Darmstadt, Germany). DMEM medium was then used to make several dilutions of the extract (0%, 25%, 50%, and 100%). Human fibroblast cells (HFD4, ATCC; crl-2522) (1×10^4 cells per well) were incubated for 24 h in a 96 well plate. The extract solutions were then added to the plate and incubated in a CO_2 incubator at 37 °C. After 24 h, the human fibroblast cells were incubated with the extract solution for 48 h. Subsequently, MTT solution (20 ul) was added to each well and then incubated for 4 h. The formed dark blue formazan crystals were dissolved in DMSO (200 uL), and their optical density was recorded at a wavelength of 595 nm to determine the viability of each sample. The obtained results were compared to the results obtained from an untreated control.[26]

Cell Proliferation. The cell proliferation ability of the developed HPCS, HPCS-AE, HPCS-CE, and HPCS-AE/CE as well as AquacelAg as a positive control was evaluated. The human fibroblast cells were seeded (1×10^4 cells/well) on the tested samples and incubated for 1 and 3 days. At each time point, the tested samples were removed from the original plate to a new 24 culture plate that contains fresh media (1 mL) and MTT solution (100 uL) per well, and then incubated for 4 h. The formed formazan crystals were dissolved in DMSO, and the optical density was measured at 595 nm.[26]

RESULTS AND DISCUSSION

Viscosity Measurements of the HPCS and HPCS-AE Blend Solutions. It was recently proven that electrospinning HPCS nanofibers with high honey and CS concentrations was made possible only via aging the solution of PVA/CS with the 30% honey for a week.[21,27] In the present work, AE substituted 50% of the solvent in which the HPCS solution was prepared. It was observed that the HPCS-AE solution exhibited very high viscosity at the time of preparation; thus the solution was allowed to age at room temperature for a week while monitoring its viscosity at different time intervals. As shown in Table 1, the addition of the aqueous AE to the HPCS solution resulted in a massive decrease in its viscosity as compared to the control HPCS solution. Such a decrease in viscosity could be attributed to the degradation of the CS backbone due to the addition of the aqueous extracts of AE.

Table 1. Change in the Viscosity (mPa·s) of the HPCS and HPCS-AE upon Aging

sample	2 h	24 h	48 h	168 h
HPCS	27 610	6990	3660	1980
HPCS-AE	1410	640	420	420

As can be noted from Table 1, the decrease in viscosity imparted via the addition of the aqueous AE was very sharp, and it was realized from the first 2 h (1410 mPa·s) and reached its maximum reduction in viscosity after 48 h, reaching to 420 mPa·s as compared to 3660 mPa·s for the HPCS solution lacking the aqueous AE. This illustrates that AE played an important role in the degradation of the CS chains with the subsequent decrease in viscosity of the solution.

Prior to electrospining and after both solutions of HPCS and HPCS-AE have reached the viscosity optimum for electrospinning, the CE (10%) dry powder extract was added and stirred for an hour. It is worth mentioning that the CE extract could not be added to both the HPCS and the HPCS-AE solutions before aging due to the very high viscosities of the solutions, which were difficult to stir. It was observed that the addition of CE dry powder extract did not affect the viscosity required for electrospinning even after aging.

Electrospinning of the (HPCS), (HPCS-AE), (HPCS-CE), and (HPCS-AE/CE) Solutions. Recently, we have managed to electrospin HPCS nanofibers, which contained up to 40% honey and 5.5% CS. The developed HPCS nanofibers represented the first successful report of preparing nanofibers

DOI: 10.1021/acsami.6b00739
ACS Appl. Mater. Interfaces 2016, 8, 6379−6390

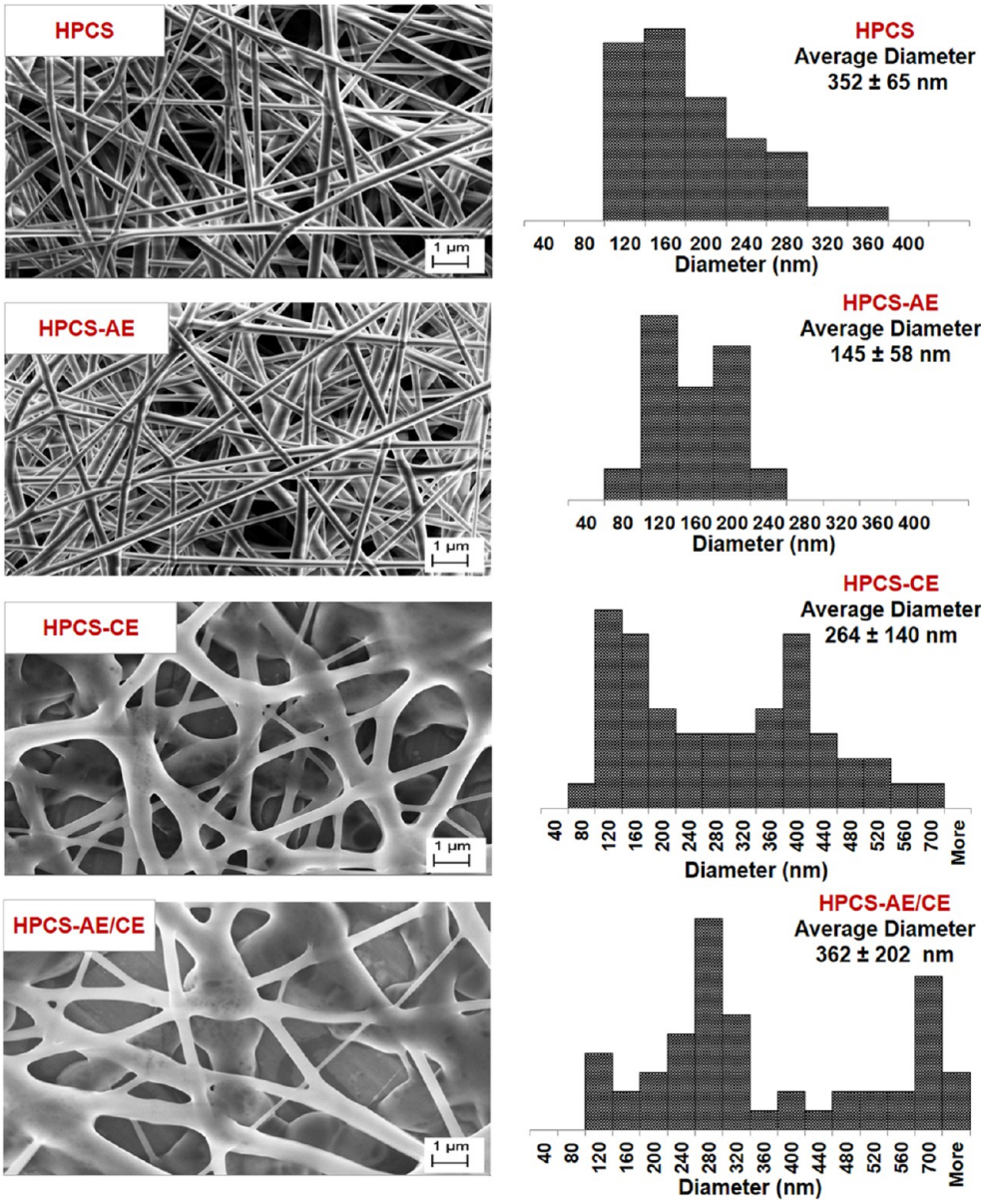

Figure 1. SEM images of the electrospun nanofibers and their diameter distribution illustrating variation in morphology and fiber diameter of the honey/poly(vinyl alcohol)/chitosan (HPCS) nanofibers due to the incorporation of the natural extracts: *Allium sativum* (AE), *Cleome droserifolia* (CE), and their combination (AE/CE).

including high concentrations of honey and chitosan using biocompatible solvents.[21]

Aqueous AE extract substituted 50% of the HPCS solvent, whereas the dry powder of CE (10% w/v) was added to both of the prepared solutions of the HPCS and HPCS-AE prior to electrospinning. The prepared solutions were then electrospun and collected as nanofibrous mats for subsequent examination.

The addition of the aqueous AE with its imparted effect on the viscosity of the solution has facilitated the electrospinning process. However, due to the massive reduction in viscosity, undesirable dripping has occurred during the electrospinning. The parameters that allowed a steady and continuous jet for the HPCS-AE solutions included a voltage of 27 kV, a flow rate of 0.5 mL/h, and the distance between the needle and the collector was kept at 13 cm. The nanofibers were collected for 4.5 h, and the surface morphology of the resulting nanofibrous mats was examined using SEM (Figure 1). The SEM micrographs of both of the nanofibers (HPCS and HPCS-AE) showed a dense, compact, smooth, and uniform bead-free morphology. Moreover, it was observed that the inclusion of the AE allowed for the least fiber diameter among the examined nanofibrous mats (145 ± 58 nm) as well as the most focused fiber diameter distribution. Upon the addition of the CE to both the HPCS and the HPCS-AE solutions, it became more difficult to electrospin the solutions until optimizing the electrospinning parameters to be 28 kV, 0.7 mL/h flow rate, while the distance between the needle and the collector was maintained at 14 cm. The nanofibers were collected for 3.5 h; however, achieving a uniform fiber deposition was still critical. This may be attributed to the sticky nature of the *Cleome droserifolia* (CE) where they exhibit glandular sticky leaves.[28] Figure 1 shows a bimodal diameter distribution of the HPCS-CE and HPCS-AE/CE nanofibers, due to the addition of a high concentration of the CE combined with its sticky nature.

DOI: 10.1021/acsami.6b00739
ACS Appl. Mater. Interfaces 2016, 8, 6379−6390

Additionally, noticeable branching of the fibers was observed with a noted formation of clusters at the branching point.[29] The observed branching is most probably due to spinning of a highly concentrated solution[30] using a high voltage in addition to the sticky nature of such a solution. Spinning of high concentrated solutions leads to a jet with relatively large diameter, which could lead to the formation of branches.[31] This in turn resulted in larger interfiber spaces, which was proved to be more useful in cell related applications such as wound healing and tissue engineering,[32,33] taking into consideration the density of the collected nanofibrous mat.

Assessment of the Swelling and Weight Loss Abilities. Determination of the swelling capability of the nanofibers allows prediction of their exudate management ability.[34] The developed nanofibers of HPCS, HPCS-AE, HPCS-CE, and HPCS-AE/CE were cross-linked and tested for their swelling abilities after immersion in PBS (pH 7.4) for 1, 4, and 24 h. Cross-linking of the developed nanofibers was performed via exposing the nanofibrous mats to the GA vapors for 1 and 3 h[21] followed by heating at 40 °C to enhance the cross-linking of nanofibers and remove any GA residues.

It was realized that at 1 h cross-linking, the HPCS, HPCS-AE, and HPCS-CE exhibited almost similar swelling abilities with a slight reduction in the swelling percent of both HPCS-AE and HPCS-CE especially after 24 h of immersion in the PBS (Figure 2a). At 3 h cross-linking the HPCS-CE exhibited noticeable reduction in its swelling ability, whereas the swelling percent of the HPCS-AE/CE nanofibrous mats was observed to be the lowest at both the 1 and the 3 h cross-linking times, showing values of less than 15% swelling as compared to approximately 90% of swelling in the case of both the HPCS and the HPCS-AE after 24 h of immersion in the PBS buffer (Figure 2b). Such results indicate that the addition of the CE to both the HPCS and the HPCS-AE nanofibers greatly decreased their swelling abilities. This may be due to the sticky nature of the CE, which hinders the intermolecular motion, and chain disentanglements of the developed nanofibers, and thus hinders their swelling capabilities.[28] As the swelling of the nanofibers can give some indication about their breathability, it seems that the breathability of both HPCS-CE and HPCS-AE/CE decreased, especially that of the HPCS-AE/CE.

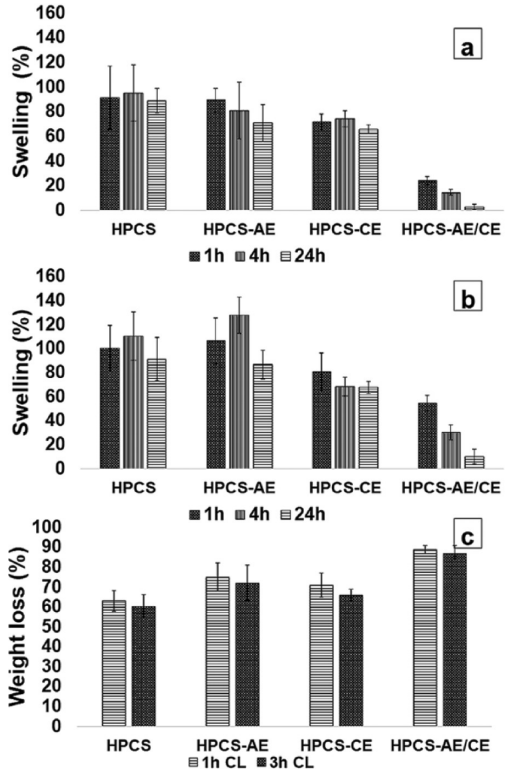

Figure 2. Swelling % (a and b) and weight loss % (c) of the (HPCS), (HPCS-AE), (HPCS-CE), and (HPCS-AE/CE). The swelling abilities of the fibers (a) 1 h cross-linked (1 h CL) and (b) 3 h cross-linked (3 h CL) were tested after immersion in PBS (pH 7.4) for 1, 4, and 24 h. The weight loss of the 1 and 3 h cross-linked nanofibers (c) was tested after immersion in PBS (pH 7.4) for 24 h.

Increasing the cross-linking time allows also maintaining a compact nanofibrous structure that permits the water uptake capability of the porous nanofibrous structure to be realized. At the same time, the cross-linking degree should not be increased to the point hindering the intermolecular motion and chain entanglements within the nanofibers.[35,36] Increasing the cross-linking time enhanced the swelling ability of HPCS-AE and HPCS-AE/CE at 3 h cross-linking but had nearly no effect on the HPCS and HPCS-CE nanofibers, which exhibited similar swelling values at both of the tested cross-linking times (1 and 3 h). Such results indicate that the slight increase in the cross-linking time affected only the nanofibers containing the aqueous AE. This may be attributed to the fact that the AE containing nanofibers exhibited increased weight loss as compared to the HPCS and HPCS-CE nanofibers (Figure 2c). Upon cross-linking of the AE containing nanofibers, a more compact nanofibrous structure could be maintained for a longer period of time, which resulted in the enhancement realized in their swelling abilities after 3 h cross-linking.

According to the results of the swelling study, it is expected that the HPCS-AE/CE nanofibers would exhibit nearly no ability for exudate management, whereas the HPCS, HPCS-AE, and HPCS-CE nanofiber wound dressings would exhibit moderate ability for exudate management. The HPCS, HPCS-AE, and HPCS-CE samples exhibited moderate swelling abilities as compared to previously spun CS/PVA nanofibers lacking honey.[24] This may be attributed to the high water solubility of honey, which leads to an increase in the weight loss of the nanofibers.[21] Moreover, despite that CS enhances the water uptake ability of the nanofibers, increasing the concentration of CS leads to an opposite effect. This was observed by Son et al., who demonstrated that in nanofibrous mats of CS/PVA of low CS concentration, polymeric hydrogels are readily formed by the hydrophilic PVA in solutions, thus resulting in enhanced swelling. However, upon increasing the CS concentration, the intermolecular forces between the amine groups and the CS side chains increase and reduced the swelling ability.[37]

Assessment of the Antibacterial Activity. Chronic, nonhealing wounds that suffer from resistant bacterial strains experience major complications as well as delayed healing. Thus, research into the development of effective antimicrobial wound dressings represents an increasing trend within the wound dressing market. Silver-based dressings stand as one of the most common and effective antimicrobial dressings used. However, development of resistance has unfortunately been reported together with some undesirable side effects of silver.[38] Recently, we have proven that the HPCS nanofiber mats exhibit mild antibacterial activity against *S. aureus* and weak antibacterial activity against *E. coli*.[21] To enhance the antibacterial activity of the HPCS nanofibers, AE and CE and

DOI: 10.1021/acsami.6b00739
ACS Appl. Mater. Interfaces 2016, 8, 6379−6390

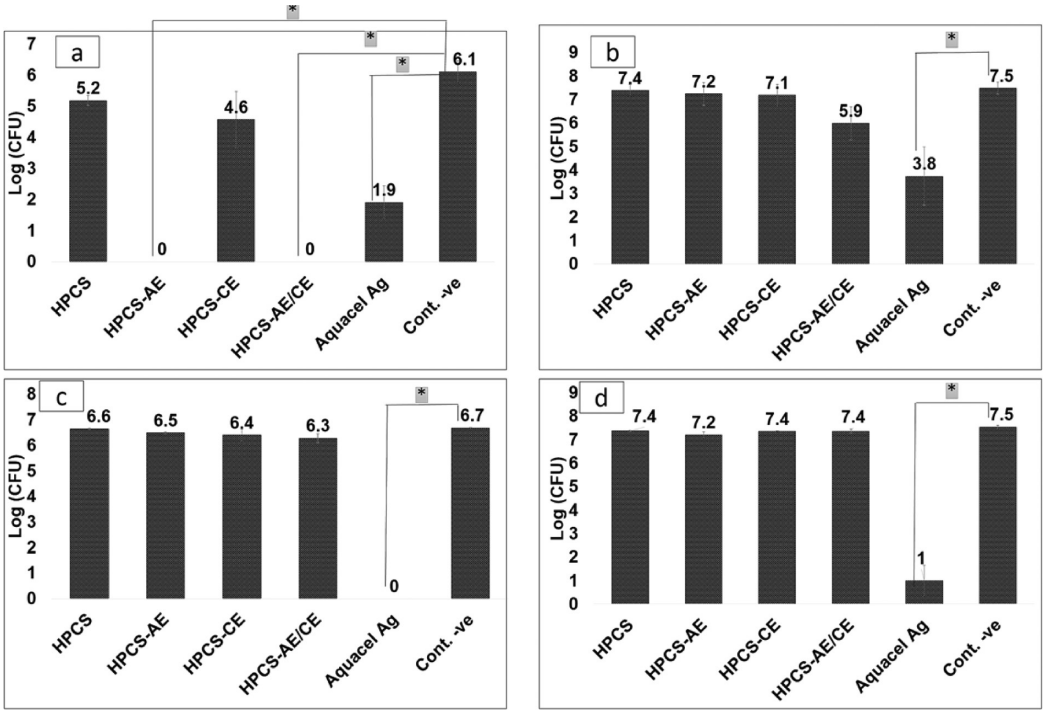

Figure 3. Antibacterial activity of the electrospun mats of (HPCS), (HPCS-AE), (HPCS-CE), and (HPCS-AE/CE) against *S. aureus* (a), MRSA (b), *E. coli* (c), and MDR *P. aeruginosa* (d) at 24 h on 7×10^8 CFU/mL bacteria. Data represent mean ± SD ($n = 3$, Student's t test, $^*p < 0.05$).

their combination were loaded within the HPCS nanofibers and tested for their antibacterial activity against *S. aureus* and *E. coli* as well as two resistant strains, MRSA and MDR *P. aeruginosa*. The antibacterial effect of the commercial wound dressing, AquacelAg, was tested and compared to the antibacterial effects of the developed nanofibrous wound dressings. Recently, Yunoki et al. reported that the AquacelAg showed the highest antibacterial activity among other silver-based dressings in the market.[39]

The antibacterial activity of honey has been attributed to its capability for hydrogen peroxide production, its increased sugar content, as well as its acidity in addition to its flavonoid content.[40] On the other hand, CS's antibacterial activity is mainly due to its polycationic nature, which leads to cell leakage and death upon its interaction with the negatively charged surfaces of the bacteria.[41] The thiosulfinates mainly including diallyl sulfide, diallyl disulfide, and allyl methyl sulfide have been linked to the antibacterial activity of the aqueous extracts of *Allium sativum* through their ability to disrupt cell components as well as blocking pathways of different bacterial enzymes.[42,43] *Cleome*'s antibacterial activity has been linked to its content of different terpenes including the sesquiterpenes carotol, β-eudesmol, and δ-cadinene.[9]

The antibacterial activities of *Allium sativum* aqueous extract and *Cleome droserifolia* dry extract have been screened via measuring the inhibition zone. The results demonstrated enhanced antibacterial activity of AE against *S. aureus*, and week antibacterial activity against *E. coli* and MRSA, whereas no antibacterial activity was noted against *P. aeruginosa*. *Cleome droserifolia*, on the other hand, demonstrated only weak antibacterial activity against MRSA and *S. aureus* (results not shown).

Figure 3 represents the antibacterial effects of the developed HPCS, HPCS-AE, HPCS-CE, and HPCS-AE/CE nanofibrous mats in comparison with the commercial wound dressing AquacelAg. It was observed that both the HPCS-AE and the HPCS-AE/CE nanofibrous mats exhibited complete bacterial inhibition against *S. aureus* as compared to noticeable bacterial reduction with the AquacelAg dressing (Figure 3a). Such effect is mainly due to the inclusion of the aqueous AE within the HPCS nanofibers. Moreover, it was observed that among the developed nanofibrous mats, only the HPCS-AE/CE exhibited some antibacterial activity against MRSA, thus indicating that the combined antibacterial effects of both the AE and the CE were required to achieve antibacterial activity against the MRSA-resistant strain (Figure 3b). Still, the achieved antibacterial activity against MRSA was not significant as compared to the negative control ($p < 0.05$) and less than that realized with the AquacelAg.

On the other hand, none of the developed nanofibers exhibited antibacterial activity against both the *E. coli* and the MDR *P. aeruginosa*, whereas the AquacelAg exhibited complete inhibition of *E. coli* and enhanced inhibition against MDR *P. aeruginosa* (Figure 3c and d).

The antibacterial activities of the honey, CS, *Allium sativum*, and *Cleome droseifolia* were reported against both Gram-positive and Gram-negative bacteria.[9,41,44] Moreover, enhanced antibacterial activity against *S. aureus* as compared to *E. coli* was reported for CS[45] and *Cleome droseifolia* oil[9] as well as the mixture of honey and *Allium sativum*.[46] This coincides with the results obtained here regarding the increased antibacterial activity observed against the tested *S. aureus* and MRSA strains.

Assessment of the Wound Healing Ability. The developed nanofiber dressings and the AquacelAg commercial dressing were applied on an excisional 9 mm wound on the dorsal back of mice. Photographs of the wound region were taken on days 3, 5, 7, 10, and 12 to determine the change in the wound size over time (Figure 4). To determine the wound healing ability of the tested dressings, the percentage of the wound size remaining exposed was determined via comparing

DOI: 10.1021/acsami.6b00739
ACS Appl. Mater. Interfaces 2016, 8, 6379−6390

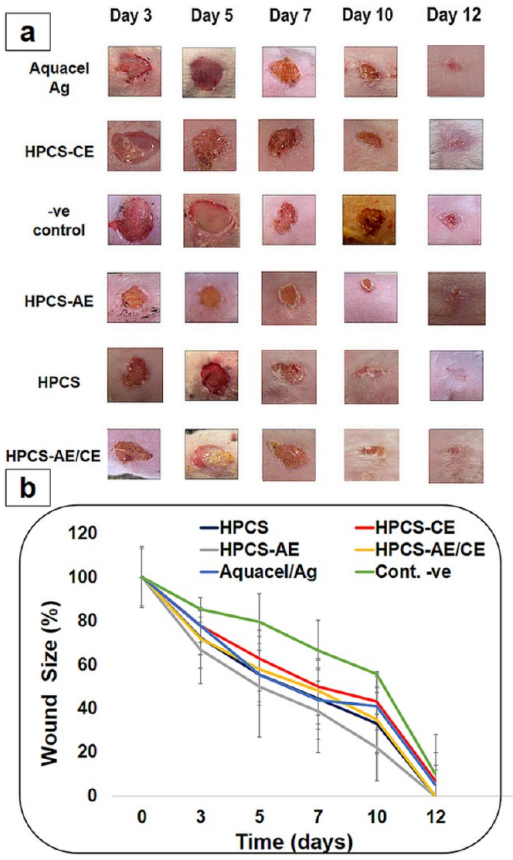

Figure 4. Photographic images of the extent of wound healing: (a) graphical illustration of the changes in wound size (b) on days 3, 5, 7, 10, and 12 for the developed nanofibrous dressings HPCS, HPCS-AE, HPCS-CE, and HPCS-AE/CE as well as the untreated negative control (-ve control) and the treated positive control with the commercial dressing AquacelAg.

the size of the wound at each time point with the size of the wound on day 0 (Figure 4).

Honey and CS have been reported to enhance wound healing.[47,48] Honey enhances the tissue repair process via stimulating the leukocytes to release cytokines and triggering an immune response against infection.[49] Moreover, honey allows fast autolytic debridement and suppression of inflammation.[50] CS has been reported to indirectly enhance cell proliferation in vivo.[51] Additionally, immediate migration of polymorphonuclear cells (PMN) and mononuclear cells (MN) was observed after application of CS. The PMN and MN degrade CS into its low molecular weight oligomers and monomers, which exhibit strong ability for promoting cell migration.[52] *Allium sativum* enhances the wound healing process via increasing the re-epithelialization as well as the profuse dose-dependent neovascularization.[53,54] *Cleome droserifolia*, on the other hand, has not yet been studied for its effect on wound healing; however, *Cleome* is known for its antioxidant activity,[11,55] and antioxidants have been correlated to the enhancement of the wound healing process via preventing the overexposure of the wound to oxidative stress, which delays the wound healing process.[56]

As observed in Figure 4, the wound size was noticeably reduced on day 3 with the HPCS, HPCS-AE, and HPCS-AE/CE nanofiber dressings as compared to the negative control wounds. Significant reduction in the wound size was observed with all of the tested dressings as well as the AquacelAg as compared to the negative control on days 5 and 7. At the same time, the negative control nearly exhibited no reduction in wound size in day 5 (Figure 4). It was observed that the wound closure was greatly enhanced with the HPCS nanofiber mats, and upon addition of AE in the HPCS-AE mats, the wound closure rate increased. On the other hand, the wound closure rate was reduced upon addition of the CE to the HPCS-CE nanofibrous mats, whereas the combination of both extracts within the HPCS-AE/CE nanofiber dressings showed wound closure rates similar to those of the HPCS dressing (Figure 4). Upon comparing the wound closure rate of the developed nanofibrous dressings to the commercial AquacelAg, it was observed that the HPCS and the HPCS-AE/CE showed similar effects, whereas the HPCS-AE showed enhanced wound closure rates.

It is also of note that all of the developed nanofibrous dressings attached easily to the wounds with no need for biological adhesives. This is due to the hydrophilic nature of the PVA, CS, and honey in addition to the high water solubility of the high concentration of honey incorporated. Thus, the developed dressings allow the wound to stay desirably hydrated.

Assessment of the Histological Outcomes. The wound tissues were H&E stained, and their histopathology was examined and scored at days 3, 5, 7, 10, and 12 and were also MT stained and evaluated for collagen deposition at day 10 (Figures 5 and 6, and Table 2). The histological data demonstrated that all of the developed nanofibrous dressings together with the AquacelAg reduced the necrosis as compared to the negative control with the HPCS-CE showing the most enhanced reduction since day 5 (Figure 5 and Table 2). Moreover, the application of the developed dressings to the wound site has reduced the number of inflammatory cells as compared to the control where they were completely diminished at day 10 in the case of HPCS-AE/CE nanofibrous dressing. Additionally, it was observed that the number of macrophage cells was greater than the neutrophils in all of the treated wounds. As compared to the negative control, it was observed that the developed dressings as well as the AquacelAg allowed early epithelization with the AquacelAg, HPCS, and HPCS-AE/CE showing the earliest epithelization as well as thicker observed epidermis (Figure 5 and Table 2). Moreover, it was observed that the HPCS-AE/CE and the AquacelAg allowed earlier granulation tissue formation. Additionally, the tested nanofibrous dressings and the AquacelAg have allowed mature granulation tissue formation with dense collagen deposition (Figure 5 and Table 2). This was confirmed via Masson's trichome staining of the wounds on day 10, which demonstrated that the collagen regenerated in the treated wounds was denser than the negative control, and that both AquacelAg and the HPCS showed the most dense collagen deposition. Moreover, the AquacelAg, HPCS, HPCS-AE/CE, and HPCS-AE demonstrated the most uniform collagen distribution (Figure 6 and Table 2).

Overall, the scoring of the histologic data indicated that among the tested nanofiber dressings, the HPCS-AE/CE has demonstrated the most enhanced effect on wound healing followed by the HPCS dressing with scores very similar to those of AquacelAg. Both nanofiber dressings allowed reduction in the inflammatory phase, and earlier granulation tissue formation as well as earlier epithelization and formation

DOI: 10.1021/acsami.6b00739
ACS Appl. Mater. Interfaces 2016, 8, 6379−6390

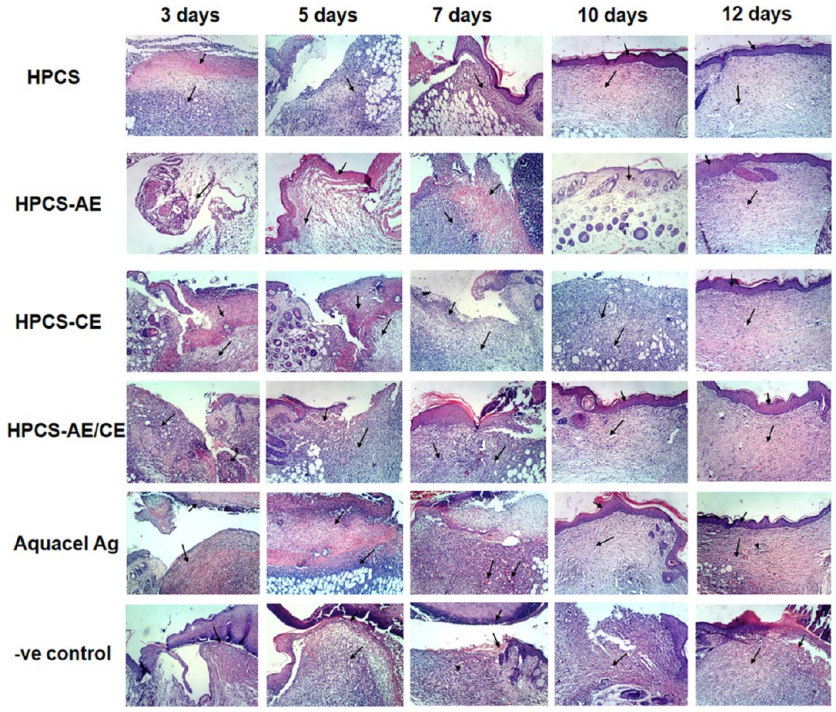

Figure 5. Histopathological evaluation of skin sections. Micrographs of H&E stained tissues of wounds treated with the developed nanofiber dressings and the AquacelAg as well as untreated negative control at different time intervals (3, 5, 7, 10, and 12 days) (original magnification 100). HPCS: Micrographs of the central wound area in mice treated with the HPCS nanofiber wound dressing. Note the massive infiltration of inflammatory cells at days 3 and 5 and the matured granulation tissue with well oriented collagen deposition as well as thick epidermal layer in days 10 and 12 and that the number of inflammatory cells is greatly diminished. HPCS-AE: Micrographs of the central wound area in mice treated with the HPCS-AE nanofibrous wound dressing. Note the massive infiltration of inflammatory cells at days 3, 5, and 7 with observed exudation on days 5 and 7. Mature well vascularized granulation tissue with well oriented collagen deposition was observed on day 12. HPCS-CE: Micrographs of the central wound area in mice treated with the HPCS-CE nanofibrous wound dressing. Note the massive inflammatory cell infiltration in days 3, 5, and 7 and the well vascularized (note the newly formed blood capillaries) mature granulation tissue formation with well oriented collagen deposition since day 10. HPCS-AE/CE: Micrographs of the central wound area in mice treated with the HPCS-AE/CE nanofiber wound dressing. Note the massive infiltration of inflammatory cells in days 3, 5, and 7 and the formation of mature well vascularized granulation tissue with well oriented collagen deposition since day 10. Notice the formation of thick epidermal layer since day 10 and that the number of inflammatory cells is greatly diminished. AquacelAg: Micrographs of the central wound area in mice treated with the AquacelAg wound dressing. Note the massive infiltration of inflammatory cells in days 3 and 5 and the formation of highly vascularized mature granulation tissue with collagen deposition since day 7. Notice the formation of thick epidermal layer since day 10 and that the number of inflammatory cells is greatly diminished. -ve control: Micrographs of central area of wound in untreated controls. Note the massive infiltration of inflammatory cells and the hemorrhage in days 7 and 12 and the disorganized granulation tissue. Notice the absence of epithelial layer in day 10 and the thin epidermis on day 12.

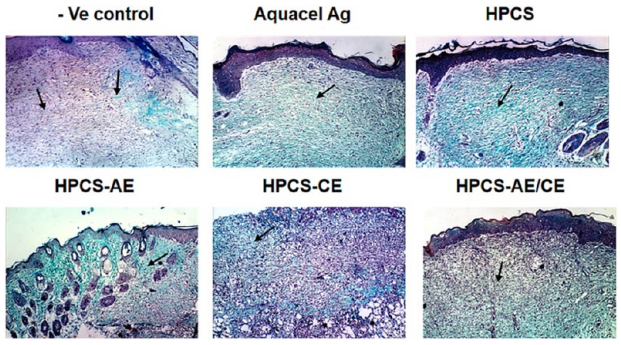

Figure 6. Histopathological evaluation of skin sections. Micrographs of Masson's trichome stained tissues of wounds treated with the developed nanofibrous dressings and the AquacelAg as well as untreated negative control at day 10 (original magnification 100). Notice the dense collagen deposition in the AquacelAg, HPCS, HPCS-AE/CE, HPCS-AE, and HPCS-CE nanofibrous dressings as compared to the negative control (-ve control).

of thicker epidermis. Additionally, both dressings induced dense and uniform collagen deposition.

Assessment of the Cell Viability and Proliferation. The cytotoxicity of the developed HPCS, HPCS-AE, HPCS-CE, and HPCS-AE/CE nanofiber mats as well as the commercial wound dressing, AquacelAg, were investigated using MTT assay. Soluble MTT is metabolized into the insoluble purple formazan salt via the enzymes found inside the mitochondria of the viable cells. The fibroblast cells were cultured in different concentrations of the extract solutions of the tested nanofiber mats (100%, 75%, 50%, and 25%), and the cytotoxicity was estimated via determining the viable cell densities after 48 h (Figure 7a). It was observed that the HPCS and the HPCS-CE mats exhibited the highest cell viability of 90% and 87%, respectively, in the 100% extract solution, whereas the HPCS-AE exhibited significant decreased cell viability of 68% ($p < 0.05$) that increased to 75% upon addition of the CE in the HPCS-AE/CE nanofibers in the 100% extract solution (Figure 7a). On the other hand, it was realized that the AquacelAg exhibited significant cytotoxicity to the cultured fibroblasts at all tested dilutions ($p < 0.05$) and demonstrated viable cell counts of ~9% similar to the results of the positive cytotoxic control (Figure 7a).

DOI: 10.1021/acsami.6b00739
ACS Appl. Mater. Interfaces 2016, 8, 6379−6390

Table 2. Histological Scoring System for the H&E and Masson's Trichome Stained Skin Sections in the Control and Experimental Groups[a]

histopathological lesions	control group				Aquacel Ag				HPCS				HPCS-AE				HPCS-AE/CE				HPCS-CE			
	3	5	7	10	12	3	5	7	10	12	3	5	7	10	12	3	5	7	10	12	3	5	7	10	12
necrosis	+++	+++	++	+	−	++	++	+	−	−	++	++	+	−	−	++	++	+	−	−	++	++	−	−	−
inflammatory cells	+++	+++	++	++	++	+++	+++	+++	+	+	+++	+++	++	−	−	+++	++	++	−	−	++	++	++	+	+
hemorrhage	++	++	++	+	−	−	−	−	−	−	−	−	−	−	−	−	−	−	+	−	−	−	−	−	−
granulation tissue maturation	−	−	++	++	++	−	++	++	++	+++	−	−	++	++	+++	−	−	+++	+++	+++	−	−	+	+	+++
epithelization	−	−	−	−	+++	−	−	+	+++	+++	−	−	−	++	+++	−	−	−	+++	+++	−	−	−	+	+++
epidermis thickness	−	−	−	−	++	−	−	−	++	+	−	−	−	−	++	−	−	−	+	++	−	−	−	−	+
collagen deposition					+					+++					++					++					++
collagen distribution					+					+++					+++					+++					++

[a]The number of the histopathological scores: 0, −; 1, +; 2, ++; 3, +++.

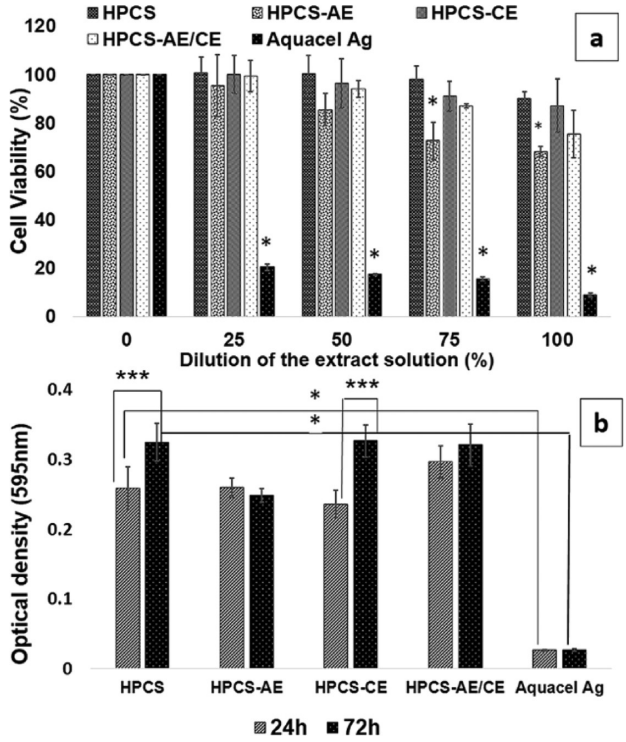

Figure 7. Cell viability (a) and cell proliferation (b) determined by the MTT assay for the developed nanofibrous mats: HPCS, HPCS-AE, HPCS-CE, and HPCS-AE/CE. AquacelAg served as a positive control in both assays. Data represent mean ± SD (n = 3, Student's t test, *p < 0.05 versus the HPCS mats, ***p < 0.05 versus culture times 24 h).

Fibroblast cell proliferation was evaluated via incubation of the fibroblast cells on the HPCS, HPCS-AE, HPCS-CE, HPCS-AE/CE, and AquacelAg dressings for 1 and 3 days. Figure 7b illustrates the analysis results of the fibroblast cell proliferation as determined by the MTT assay. The OD values of the HPCS, HPCS-CE, and HPCS-AE/CE nanofibrous mats increased with culture time. The HPCS and the HPCS-CE illustrated the most significant enhancement (p < 0.05) in proliferation at 3 days of incubation (Figure 7b), whereas the HPCS-AE mats demonstrated nearly the same OD values at both 1 and 3 days. The AquacelAg, on the other hand, demonstrated a significant cytotoxic effect on the fibroblast cell proliferation as observed from its low OD values (Figure 7b). Such results confirm the cytotoxicity previously realized for the AquacelAg dressing in the cytotoxicity evaluation (Figure 7a). The realized cytotoxicity of the AquacelAg was previously observed via different studies.[39,57]

Generally, the HPCS and the HPCS-CE demonstrated the highest levels of cell viability and proliferation within the tested nanofibrous mats. The addition of the CE extract to the HPCS-AE nanofibers has enhanced their viability and cell proliferation results. Interestingly, all of the developed nanofibrous dressings demonstrated major enhancement in cell viability and proliferation as compared to the commercial AquacelAg (Figure 7a and b).

It is worth mentioning that swelling abilities of the nanofibrous mats as well as their abilities to enhance cell viability and proliferation could be enhanced via increasing the pore diameter. This could be achieved via manipulation of the processing parameters during electrospinning[58] or via inclusion of certain treatments as carbon nanotubes prior to electro-

DOI: 10.1021/acsami.6b00739
ACS Appl. Mater. Interfaces 2016, 8, 6379−6390

spinning.[59] Moreover, the density of the nanofibrous mats must be taken into consideration as increased density will lead to reduction in the breathability of the developed mats, which will consequently lead to restriction of cell viability and transportation of nutrients and metabolic wastes as well as reduction in the swelling ability of the developed nanofibrous mats. Within this context, it was reported that ultrasonication of the developed nanofibrous mats could overcome such limitation.[32,60] Moreover, collecting low density nanofibrous mats on a substrate could be another approach to overcome such limitation. Consequently, future work on the HPCS, HPCS-AE, HPCS-CE, and HPCS-AE/CE developed nanofibrous mats will consider optimizing the nanofibrous mats' breathability via different approaches followed by testing the effect of each approach on the cell viability and proliferation as well as the swelling ability of the developed nanofibers.

CONCLUSIONS

Honey, chitosan, and poly(vinyl alcohol) nanofibers (HPCS) and HPCS nanofibers with 50% of the solvent substituted with *Allium sativum* extract (HPCS-AE) as well as HPCS and HPCS-AE nanofibers loaded with 10% of *Cleome droserifolia* extract in the (HPCS-CE) and (HPCS-AE/CE) were fabricated via electrospinning, characterized, and tested for their swelling, weight loss, antibacterial, cytotoxicity, and wound healing abilities, as well as their effect on fibroblast cell proliferation. It was observed that substituting 50% of the solvent with *Allium sativum* extract resulted in a massive decrease in the viscosity of the HPCS solution. The HPCS-AE/CE nanofibrous scaffolds exhibited the lowest swelling abilities and the highest weight loss among the developed nanofibers at the two tested cross-linking degrees, showing values of less than 15% swelling and 90% weight loss as compared to approximately 90% swelling and 60−70% weight loss in the case of both HPCS and HPCS-AE after 24 h of immersion in PBS buffer. While none of the developed nanofibers produced noticeable antibacterial effects against *E. coli* and MDR *Pseudomonas aeruginosa*, the HPCS-AE/CE and the HPCS-AE nanofibrous scaffolds exhibited complete bacterial inhibition of *S. aureus* better than that produced with the commercial dressing AquacelAg. Moreover, the bacterial count of MRSA resistant strain was reduced by 1.5 log with the HPCS-AE/CE as compared to a 3.5 log reduction with the AquacelAg. On testing the wound healing abilities of the developed nanofiber dressings as compared to the AquacelAg, it was observed that the HPCS and the HPCS-AE/CE produced similar wound closure rates, whereas the HPCS-AE has allowed enhanced wound closure. The scoring of the histologic data demonstrated that the HPCS-AE/CE and the HPCS nanofibrous dressings exhibited the most enhanced effects on the wound healing process with scores very similar to those of AquacelAg. Additionally, it was observed that HPCS, HPCS-CE, and HPCS-AE/CE demonstrated the highest levels of cell viability and proliferation, while the commercial AquacelAg has exhibited noticeable cytotoxicity. Therefore, the antibacterial and wound healing properties of the developed nanofiber mats, as well as their minimal side effects, make them competitive candidates for use as effective wound dressings.

AUTHOR INFORMATION

Corresponding Author

*Tel.: +2 02 2615 2559. Fax: +2 02 2795 7565. E-mail: hazzazy@aucegypt.edu.

Notes

The authors declare the following competing financial interest(s): Dr. Hassan Azzazy and Mrs. Wesam Sarhan are authors of patent application on use of honey/chitosan nanofiber loaded with biological and medicinal plants as wound dressing.

ACKNOWLEDGMENTS

We appreciate the technical support offered by Assistant Professor Rehab El-Sokkary in the Medical Microbiology and Immunology Department, Faculty of Medicine, Zagazig University, for her help with testing bacterial isolates. This work was funded by a grant from the American University in Cairo to Prof. Hassan Azzazy.

REFERENCES

(1) Sen, C.; Gordillo, G.; Roy, S.; Kirsner, R.; Lambert, L.; Hunt, T.; Gottrup, F.; Gurtner, G.; Michael, T.; Longaker, M. Human Skin Wounds: A Major and Snowballing Threat to Public Health and The Economy. *Wound Repair Reg.* **2009**, *17*, 763−771.

(2) Vowden, P.; Vowden, K.; Carville, K. Antimicrobial Dressings Made Easy. *Wounds International*, 2011; p 2, available from http://www.woundsinternational.com.

(3) Seaman, S. Dressing Selection in Chronic Wound Management. *J. Am. Podiatr. Med. Assoc.* **2002**, *92*, 24−33.

(4) Durairaj, S.; Srinivasan, S.; Lakshmanaperumalsamy, P. In Vitro Antibacterial Activity and Stability of Garlic Extract at Different pH and Temperature. *Electr. J. Biol.* **2009**, *5*, 5−10.

(5) Cutler, R.; Wilson, P. Antibacterial Activity of a New, Stable, Aqueous Extract of Allicin against Methicillin-Resistant *Staphylococcus aureus*. *Br. J. Biomed. Sci.* **2004**, *6*, 71−74.

(6) Tsao, S.; Yin, M. In Vitro Activity of Garlic Oil and Four Diallyl Sulphides against Antibiotic-Resistant *Pseudomonas aeruginosa* and *Klebsiella pneumoniae*. *J. Antimicrob. Chemother.* **2001**, *47*, 665−670.

(7) Bakri, I.; Douglas, C. Inhibitory Effect of Garlic Extract on Oral Bacteria. *Arch. Oral Biol.* **2005**, *50*, 645−651.

(8) Iwalokun, B.; Ogunledun, A.; Ogbolu, D.; Bamiro, S.; Jimi-Omojola, J. In Vitro Antimicrobial Properties of Aqueous Garlic Extract against Multidrug-Resistant Bacteria And Candida Species from Nigeria. *J. Med. Food* **2004**, *7*, 327−333.

(9) Muhaidat, R.; Al-Qudah, M.; Samir, O.; Jacob, J.; Hussein, E.; Al-Tarawneh, I.; Bsoul, E.; Orabi, S. Phytochemical Investigation and In Vitro Antibacterial Activity of Essential Oils from *Cleome droserifolia (Forssk.) Delile* and *C. Trinervia fresen (Cleomaceae)*. *S. Afr. J. Bot.* **2015**, *99*, 21−28.

(10) Hussein, N.; Ahmed, A.; Darwish, F. Sesquiterpenes from *Cleome droserifolia*. *Pharmazie* **1994**, *49*, 76−77.

(11) El-Shenawy, N.; Abdel-Nabi, I. Comparative Analysis of the Protective Effect of Melatonin and *Cleome droserifolia* Extract on Antioxidant Status of Diabetic Rats. *Egypt. J. Hosp. Med.* **2004**, *14*, 11−25.

(12) El-Shenawy, N.; Soliman, M.; Abdel-Nabi, I. Does *Cleome droserifolia* Have Anti-Schistosomiasis Mansoni Activity? *Rev. Inst. Med. Trop. Sao Paulo* **2006**, *48*, 223−228.

(13) Aboushoer, M.; Fathy, M.; Abdel-Kader, S.; Goetz, G.; Omar, A. Terpenes and Flavonoids from an Egyptian Collection of *Cleome droserifolia*. *Nat. Prod. Res.* **2010**, *24*, 687−696.

(14) Abdel-Monem, A. New Alkaloid and a New Diterpene from *Cleome paradoxa* B.Br. (Cleomaceae). *Nat. Prod. Res.* **2012**, *26*, 264−269.

(15) Jane, R.; Patil, S. *Cleome viscosa*: An Effective Medicinal Herb for Otitis Media. *Int. J. Sci. Nat.* **2012**, *3*, 153−158.

(16) Cooper, R. A Review of the Evidence For the Use of Topical Antimicrobial Agents in Wound Care. *Worldwide Wounds* **2004**, 1−11.

(17) Dai, T.; Tanaka, M.; Huang, Y.; Hamblin, M. Chitosan Preparations for Wounds and Burns: Antimicrobial and Wound-Healing Effects. *Expert Rev. Anti-Infect. Ther.* **2011**, *9*, 875−879.

DOI: 10.1021/acsami.6b00739
ACS Appl. Mater. Interfaces 2016, 8, 6379−6390

(18) Ong, S.; Wu, J.; Moochhala, S.; Tan, M.; Lu, J. Development of a Chitosan-Based Wound Dressing with Improved Hemostatic and Antimicrobial Properties. *Biomaterials* **2008**, *29*, 4323−4332.
(19) Lusby, P.; Coombes, A.; Wilkinson, J. Honey: a Potent Agent for Wound Healing? *J. Wound Ostomy Continence Nurs.* **2002**, *29*, 295−300.
(20) Al-Waili, N.; Saloom, K. Effects of Topical Honey on Post-Operative Wound Infections Due to Gram Positive and Gram Negative Bacteria Following Caesarean Sections And Hysterectomies. *Eur. J. Med. Res.* **1999**, *4*, 126−130.
(21) Sarhan, W.; Azzazy, H. High Concentration Honey Chitosan Electrospun Nanofibers: Biocompatibility and Antibacterial Effects. *Carbohydr. Polym.* **2015**, *122*, 135−143.
(22) Al-Astal, Z. Effect of Storage and Temperature of Aqueous Garlic Extract on the Growth of Certain Pathogenic Bacteria. *J. Al Azhar Univ.* **2003**, *6*, 11−20.
(23) Ezzat, S.; Motaal, A. Isolation of New Cytotoxic Metabolites From *Cleome droserifolia* Growing in Egypt. *Z. Naturforsch., C: J. Biosci.* **2012**, *67*, 266−274.
(24) Jannesari, M.; Varshosaz, J.; Morshed, M.; Zamani, M. Composite Poly(vinyl alcohol)/Poly (vinyl acetate) Electrospun Nanofibrous Mats as A Novel Wound Dressing Matrix for Controlled Release of Drugs. *Int. J. Nanomed.* **2011**, *6*, 993−1003.
(25) Gil, E.; Panilaitis, B.; Bellas, E.; Kaplan, D. Functionalized Silk Biomaterials for Wound Healing. *Adv. Healthcare Mater.* **2013**, *2*, 206−217.
(26) Son, S.; Linh, N.; Yang, H.; Lee, B. In Vitro and In Vivo Evaluation of Electrospun PCL/PMMA Fibrous Scaffolds for Bone Regeneration. *Sci. Technol. Adv. Mater.* **2013**, *14*, 015009.
(27) Xie, H.; Jia, Z.; Huang, J.; Zhang, C. Preparation of Low Molecular Weight Chitosan by Complex Enzymes Hydrolysis. *Int. J. Chem.* **2011**, *3*, 180.
(28) Płachno, B.; Adamec, L.; Huet, H. Mineral Nutrient Uptake from Prey and Glandular Phosphatase Activity As a Dual Test of Carnivory in Semi-Desert Plants with Glandular Leaves Suspected of Carnivory. *Ann. Bot.* **2009**, *104*, 649−654.
(29) Xu, C.; Xu, F.; Wang, B.; Lu, T. Electrospinning of Poly (ethylene-co-vinyl alcohol) Nanofibres Encapsulated with Ag Nanoparticles for Skin Wound Healing. *J. Nanomater.* **2011**, *3*, 1−7.
(30) Reneker, D.; Yarin, A. Electrospinning Jets and Polymer Nanofibers. *Polymer* **2008**, *49*, 2387−2425.
(31) Yarin, A.; Kataphinan, W.; Reneker, D. Branching in Electrospinning Nanofibers. *J. Appl. Phys.* **2005**, *98*, 064501 http://ideaexchange.uakron.edu/polymer_ideas/81,.
(32) Gu, B.; Park, J.; Kim, M.; Kang, C.; Kim, J.; Kim, C. Fabrication of Sonicated Chitosan Nanofiber Mat with Enlarged Porosity for Use as Hemostatic Materials. *Carbohydr. Polym.* **2013**, *97*, 65−73.
(33) Shokrgozar, M.; Mottaghitalab, F.; Mottaghitalab, V.; Farokhi, M. Fabrication of Porous Chitosan/Poly (vinyl alcohol) Reinforced Single-walled Carbon Nanotube Nanocomposites for Neural Tissue Engineering. *J. Biomed. Nanotechnol.* **2011**, *7*, 276−284.
(34) Li, B.; Shan, C.; Zhou, Q.; Fang, Y.; Wang, Y.; Xu, F.; Sun, G. Synthesis, Characterization, and Antibacterial Activity of Cross-Linked Chitosan-Glutaraldehyde. *Mar. Drugs* **2013**, *11*, 1534−1552.
(35) Li, C.; Fu, R.; Yu, C.; Li, Z.; Guan, H.; Hu, D.; Zhao, D.; Lu, L. Silver Nanoparticle/Chitosan Oligosaccharide/Poly (vinyl alcohol) Nanofibers as Wound Dressings: A Preclinical Study. *Int. J. Nanomed.* **2013**, *8*, 4131.
(36) Kim, J.; Kim, J.; Lee, Y.; Kim, K. Properties and Swelling Characteristics of Cross-Linked Poly (vinyl alcohol)/Chitosan Blend Membrane. *J. Appl. Polym. Sci.* **1992**, *45*, 1711−1717.
(37) Son, B.; Yeom, B.; Song, S.; Lee, C.; Hwang, T. Antibacterial Electrospun Chitosan/Poly (vinyl alcohol) Nanofibers Containing Silver Nitrate And Titanium Dioxide. *J. Appl. Polym. Sci.* **2009**, *111*, 2892−2899.
(38) Lansdown, A. Silver. 2: Toxicity in Mammals and How its Products Aid Wound Repair. *J. Wound Care.* **2002**, *11*, 173−7.
(39) Yunoki, S.; Kohta, M.; Ohyabu, Y.; Iwasaki, T. In Vitro Parallel Evaluation of Antibacterial Activity and Cytotoxicity of Commercially Available Silver-Containing Wound Dressings. *Plast. Surg. Nurs.* **2015**, *35*, 203−211.
(40) Vandamme, L.; Heyneman, A.; Hoeksema, H.; Verbelen, J.; Monstrey, S. Honey in Modern Wound Care: A Systematic Review. *Burns* **2013**, *39*, 1514−1525.
(41) Muzzarelli, R.; Tarsi, R.; Filippini, O.; Giovanetti, E.; Biagini, G.; Varaldo, P. Antimicrobial Properties of N-Carboxybutyl Chitosan. *Antimicrob. Agents Chemother.* **1990**, *34*, 2019−2023.
(42) Elsom, G.; Denis, H.; David, M. An Antibacterial Assay of Aqueous Extract of Garlic Against Anaerobic/Microaerophilic and Aerobic Bacteria. *Microb. Ecol. Health Dis.* **2000**, *12*, 81−84.
(43) Chen, G.; Chung, J.; Ho, H.; Lin, J. Effects of the Garlic Compounds Diallyl Sulphide and Diallyl Disulphide on Aryamine N-Acetyltransferase Activity in *Klebsiella Pneumoniae*. *J. Appl. Toxicol.* **1999**, *19*, 75−81.
(44) Gaherwal, S.; Johar, F.; Wast, N.; Prakash, M. Anti-Bacterial Activities of *Allium sativum* Against *Escherichia Coli*, *Salmonella* Ser. typhi and *Staphylococcus aureus*. *Int. J. Microbiol. Res.* **2004**, *5*, 19−22.
(45) No, H.; Park, N.; Lee, S.; Meyers, S. Antibacterial Activity of Chitosan and Chitosan Oligomers with Different Molecular Weights. *Int. J. Food Microbiol.* **2002**, *74*, 65−72.
(46) Andualem, B. Combined Antibacterial Activity of Stingless Bee (Apis Mellipodae) Honey and Garlic (*Allium Sativum*) Extracts against Standard and Clinical Pathogenic Bacteria. *Asian Pac. J. Trop. Biomed.* **2013**, *3*, 725−731.
(47) Seckam, A.; Cooper, R. Understanding How Honey Impacts on Wounds: An Update on Recent Research Findings. *Wounds Int.* **2013**, *4*, 20−24.
(48) Dai, T.; Tanaka, M.; Huang, Y.; Hamblin, M. Chitosan Preparations for Wounds and Burns: Antimicrobial and Wound-Healing Effects. *Expert Rev. Anti-Infect. Ther.* **2011**, *9*, 857−879.
(49) Yaghoobi, R.; Kazerouni, A. Evidence for Clinical Use of Honey in Wound Healing as an Anti-Bacterial, Anti-Inflammatory Anti-Oxidant and Anti-Viral Agent: A Review. *Jundishapur J. Nat. Pharm. Prod* **2013**, *8*, 100−104.
(50) Molan, P.; Rhodes, T. Honey: A Biologic Wound Dressing. *Wounds* **2015**, *27*, 141−151.
(51) Azuma, K.; Izumi, R.; Osaki, T.; Ifuku, S.; Morimoto, M.; Saimoto, H.; Minami, S.; Okamoto, Y. Chitin, Chitosan, and its Derivatives for Wound Healing: Old and New Materials. *J. Funct. Biomater.* **2015**, *6*, 104−142.
(52) Minami, S. Mechanism of Wound Healing Acceleration By Chitin and Chitosan. *Jpn. J. Vet. Res.* **1997**, *44*, 218−219.
(53) Pazyar, N.; Feily, A. (2011). Garlic in Dermatology. *Dermatol. Rep.* **2011**, *3*, 51−55.
(54) Sidik, K.; Mahmood, A.; Salmah, I. Acceleration of Wound Healing by Aqueous Extract of *Allium sativum* in Combination with Honey on Cutaneous Wound Healing in Rats. Int. J. *Mol. Med. Adv. Sci.* **2006**, *2*, 231−5.
(55) El-Khawaga, O.; Abou-Seif, M.; El-Waseef, A.; Negm, A. Hypoglycemic, Hypolipidemic and Antioxidant Activities of *Cleome droserifolia* in Streptozotocin-Diabetic Rats. *J. Stress Physiol. Biochem.* **2010**, *6*, 28−41.
(56) Fitzmaurice, S.; Sivamani, R.; Isseroff, R. Antioxidant Therapies for Wound Healing: a Clinical Guide to Currently Commercially Available Products. *Skin Pharmacol. Physiol.*. **2011**, *24*, 113−126.
(57) Burd, A.; Kwok, C.; Hung, S.; Chan, H.; Gu, H.; Lam, W.; Huang, L. A Comparative Study of the Cytotoxicity of Silver-based Dressings in Monolayer Cell, Tissue explant, and Animal Models. *Wound repair reg.* **2007**, *15*, 94−104.
(58) Pilehrood, M.; Dilamian, M.; Mirian, M.; Sadeghi-Aliabadi, H.; Maleknia, L.; Nousiainen, P.; Harlin, A. Nanofiberous Chitosan-Polyethylene Oxide Engineered Scaffolds: A Comparative Study between Simulated Structural Characteristics and Cells Viability. *BioMed Res. Int.* **2014**, *2014*, No. ID 438065.
(59) Shokrgozar, M.; Mottaghitalab, F.; Mottaghitalab, V.; Farokhi, M. Fabrication of Porous Chitosan/Poly (vinyl alcohol) Reinforced Single-walled Carbon Nanotube Nanocomposites for Neural Tissue Engineering. *J. Biomed. Nanotechnol.* **2011**, *7*, 276−284.

DOI: 10.1021/acsami.6b00739
ACS Appl. Mater. Interfaces 2016, 8, 6379−6390

(60) Lee, J.; Jeong, S.; Bae, M.; Yang, D.; Heo, D.; Kim, C.; Alsberg, C.; Kwon, I. Highly Porous Electrospun Nanofibers Enhanced by Ultrasonication for Improved Cellular Infiltration. *Tissue Eng., Part A* **2011**, *17*, 2695−2702.

DOI: 10.1021/acsami.6b00739
ACS Appl. Mater. Interfaces 2016, 8, 6379−6390

Materials Science and Engineering C 67 (2016) 276–284

Contents lists available at ScienceDirect

Materials Science and Engineering C

journal homepage: www.elsevier.com/locate/msec

The effect of increasing honey concentration on the properties of the honey/polyvinyl alcohol/chitosan nanofibers

Wessam A. Sarhan [a], Hassan M.E. Azzazy [a,*], Ibrahim M. El-Sherbiny [b]

[a] Department of Chemistry, School of Sciences and Engineering, The American University in Cairo, New Cairo 11835, Egypt
[b] Center for Materials Science, University of Science and Technology, Zewail City of Science and Technology, 6th October City, 12588 Giza, Egypt

ARTICLE INFO

Article history:
Received 21 October 2015
Received in revised form 6 April 2016
Accepted 2 May 2016
Available online 04 May 2016

Keywords:
Honey chitosan nanofibers
Biomaterials
Antibacterial activity
Swelling
Porosity

ABSTRACT

The effect of increasing honey concentrations from 10% to 30% within the Honey (H)/polyvinyl alcohol (P)/chitosan (CS) nanofibers was investigated. Changes in the electrospun nanofiber diameters, crystallinity, thermal behavior, porosity and antibacterial activity have been assessed using SEM, XRD, DSC, TGA, mercury porosimeter and viable cell count technique. The HPCS nanofibers were cross-linked and tested for their swelling abilities and degradation behavior. The mean diameter of HPCS nanofibers increased from 284 ± 97 nm to 464 ± 185 nm upon increasing the honey concentration from 10% to 30%. Irrespective the honey concentrations, the nanofibers have demonstrated enhanced porosity. Increasing the honey concentration resulted in a reduction in the swelling of the 1 h cross-linked HPCS nanofibers containing 10% and 30% H from 520% to 100%; respectively. Degradation after 30 days was reduced in the 3 h cross-linked HPCS nanofibers compared to the non-crosslinked HPCS nanofibers. Enhanced antibacterial activity was achieved against both *Staphylococcus aureus* and *Escherichia coli* upon increasing the honey concentration. Changing the honey concentration and the extent of nanofiber crosslinking can be used to adjust different parameters of the HPCS nanofibers to suit their applications in wound healing and tissue engineering.

1. Introduction

Electrospinning is a feasible and simple technique for production of nanofibers [1–4]. The electrospun nanofibers exhibit increased surface to volume ratio with improved and controlled porosity allowing their use in various applications including tissue engineering, [5,6] drug delivery [7,8] wound healing, [9,10] filtration, energy storage, defense, and security [11–13]. Among the different materials spun into nanofibers, chitosan stands as one of the most advantageous biopolymers due to its enhanced properties. Chitosan is well known for its biocompatibility, biodegradability, nontoxicity and non-immunogenicity [14]. Chitosan is also characterized by its cost-effectiveness as it is derived from chitin the second most abundant polymer after cellulose [15]. This has also allowed chitosan to be an important candidate in a large number of applications [16,17]. However, electrospinning of chitosan into nanofibers is not an easy process particularly due to its high charge and viscosity, in addition to the need to use toxic or highly acidic solvents [18,19]. Residues of such solvents are not favorable in biomedical applications. The optimum strategy to avoid this drawback is through co-spinning of chitosan with other easily spun polymers such as polyvinyl alcohol and poly ethylene oxide [20–22]. Such strategy, however allows the electrospinning of only small concentrations of chitosan.

Honey, a carbohydrate rich syrup has been used since ancient times and is now rediscovered for its antibacterial and wound healing activity [23–26]. Honey nanofibers are gaining increasing interest due to the enhanced activity realized upon combining the advantages of the nanofibrous structure especially the increased surface to volume ratio with the advantageous properties of honey. However, due to its low viscosity honey was only electrospun in small concentrations [27,28]. Recently, we have managed to electrospun honey/polyvinyl alcohol/chitosan combinations (HPCS) into nanofibers with high concentrations of chitosan (up to 5.5% *w*/w) and honey (up to 40% w/) via nontoxic solvent (1% acetic acid) and the resulting HPCS nanofibers demonstrated an enhanced nontoxicity and biocompatibility [29].

High concentration HPCS nanofibers represent promising candidates for various biomedical applications due to their biodegradability, biocompatibility and antibacterial effects [30,31]. However, such high concentrations of honey included within the nanofibers is expected to affect the crystallinity, porosity, thermal properties, and degradation behavior of the nanofibers, thus the effect of changing the honey concentration on such properties will be evaluated in the present study along

* Corresponding author at: School of Sciences and Engineering, The American University in Cairo, AUC Avenue, SSE # 1184, P.O. Box 74, New Cairo 11835, Egypt.
E-mail address: hazzazy@aucegypt.edu (H.M.E. Azzazy).
URL: http://www.aucegypt.edu/fac/hassanazzazy (H.M.E. Azzazy).

http://dx.doi.org/10.1016/j.msec.2016.05.006
0928-4931/

with the change in swelling and weight loss extents and antibacterial abilities of the developed HPCS nanofibers.

2. Materials and methods

2.1. Materials

Chitosan (Mw, 240 kDa and DDA of 84%, Chitoclear, cg110, TM 3728) was provided by Primex, Siglufjordur, Iceland. Polyvinyl alcohol of Mw, 85 kDa, and glutaraldehyde (25% in H_2O) were obtained from Sigma Aldrich (St. Louis, USA). Glacial acetic acid of 99–100% purity was purchased from Merck (Wadeville, South Africa). Nutrient broth and Nutrient agar were obtained from Becton Dickinson and Company (USA).

2.2. Electrospinning of honey/polyvinyl alcohol/chitosan (HPCS) mixtures

Various honey/polyvinyl alcohol/chitosan (HPCS) solutions with increasing honey concentrations were prepared using the following weight% ratios; 10:7:3.5, 20:7:3.5, and 30:7:3.5 of honey, polyvinyl alcohol, and chitosan, respectively dissolved in 1% acetic acid. Then, the as-prepared solutions were allowed to age at room temperature for a week. Afterwards, the conductivity of the as-prepared solutions were measured using a conductivity meter (Ysi 3200). Subsequently, the aged solutions were electrospun with the aid of an electrospinner (*E*-spin, NanoTech, Kalyan-pur, India). In brief, a 5 ml plastic syringe was loaded with the different solutions and was attached to the nozzle that has outside and inner diameters of 1.3 and 0.7 mm respectively. Then, different voltages (Gamma High Voltage Power Supply, USA) were applied to the electrospun solutions, and the voltage required for optimum collection of the nanofibers was selected. The distance between the collector and the tip of the nozzle was maintained at 15 cm and the flow rate was maintained at 10 μl/min. All the samples were collected on ground collector covered with an aluminum sheet. The humidity and temperature were maintained at 30–35% and 32 °C, respectively during electrospinning.

2.3. Characterization and measurements

The surface morphologies of the electrospun nanofibers were observed using scanning electron microscopy (FESEM, Leo Supra 55, Zeiss Inc., Oberkochen, Germany) and transmission electron microscopy (Jeol, Musashino, Akishima, Tokyo, Japan). Image-J software was used for measurement of the diameters of the collected nanofibers. From three different images 100 fibers were measured for each of the developed nanofibrous mats. Subsequently, the average diameter and diameter distribution were determined. The X-ray diffraction patterns of the HPCS nanofibers with increasing honey concentrations were obtained using an XRD diffractometer (Bruker 4040, Karlsruhe, Germany) with a wavelength, $\lambda = 0.154$ nm at 40 kV, 150 mA, and at a scan speed of 4° per minute in the 2θ range of 5°–80°. Porosity measurements and pore size distribution of each of the electrospun HPCS nanofibers were obtained using mercury porosimetry (PoreMaster® mercury intrusion porosimeter, Quantachrome, Florida, USA). Thermal behavior of the nanofibers was investigated using differential scanning calorimetry (DSC 4000, PerkinElmer, Inc., Massachusetts, USA). The nanofibrous mats were weighed and sealed in aluminum pans. Then, the temperature was elevated from room temperature to 200 °C followed by cooling to room temperature and then heating again to 200 °C with a heating rate of 10 °C/min. Moreover, thermogravimetric analysis (TGA) of the nanofibers was performed (TGA Q50, TA Instruments). Samples were heated in a platinum pan under nitrogen atmosphere (60 ml/min) up to 700 °C, at a heating rate of 10 °C/min.

2.4. Assessment of swelling of the cross-linked HPCS nanofibers

The developed HPCS nanofibrous mats with increasing honey concentrations; 10:7:3.5, 20:7:3.5, and 30:7:3.5 (w%) were cross-linked through exposure to glutaraldehyde (GA) vapours for 1 h and 3 h followed by heating at 40 °C to enhance the crosslinking and remove any unreacted GA. The cross-linked nanofibrous mats were then evaluated for their swelling ability. The mats were placed in phosphate buffered saline, PBS of a pH 7.4 at 37 °C, and their swelling ability was determined at 1, 4 and 24 h with the aid of the following relationship:

$$Swellingdegree\ (\%) = [M - M_i/M_i] \times 100$$

Where *Mi* is the initial dry weight of the nanofibrous mats, and *M* is the swollen weight of the nanofibrous mats after surface blotting with a filter paper.

2.5. Degradation rate of the cross-linked HPCS nanofibers

The degradation behavior of the developed HPCS nanofibers with increasing honey concentrations 10:7:3.5, 20:7:3.5, and 30:7:3.5 (w%) was determined in PBS (pH 7.4) at 37 °C and 100 rpm after 30 days. The degradation behavior of both the non-cross-linked (non CL) and cross-linked samples via exposure to glutaraldehyde (GA) vapours for 3 h (3 h CL) followed by heating at 40 °C was determined. The degradation index (D_i) was determined based on the mass loss according to the following equation:

$$D_i = (W_0 - W_t)/W_0 \times 100$$

where W_0 is the initial weight of the electrospun nanofibers, and W_t is the weight of the dried fibers after 30 days.

2.6. Antibacterial activity

The antibacterial activities for the obtained HPCS nanofibrous mats with increasing honey concentrations; 10:7:3.5, 20:7:3.5, and 30:7:3.5 (w%) of honey, polyvinyl alcohol, and chitosan, respectively were determined against *Staphylococcus aureus* and *Escherichia coli*. The nanofibrous mats (0.05 g) after UV sterilization for 20 min were placed in sterile vials containing 3 ml of Muller Hinton broth. A bacterial suspension of each of the bacterial strains was prepared from fresh colonies after overnight incubation at 37 °C and the turbidity was adjusted to 0.5 McFarland standard (1×10^8 CFU/ml). A 10 μl of that suspension was diluted in 9 ml Muller Hinton broth to prepare (1×10^7 CFU/ml) bacterial suspension. A 30 μl aliquot of each organism and from each bacterial dilution was added to each vial containing the nanofibrous mats. Then, the tubes containing the bacterial strains and the nanofibrous mats as well as the controls were incubated at 37 °C with shaking at 100 rpm. After 24 h, samples of 10 μl were taken from the treated bacterial broth and the controls. Serial dilution in nutrient broth was performed for each sample from which 50 μl were spread on nutrient agar plates that were subsequently incubated for 24 h at 37 °C. Following the 24 h incubation, surviving colonies were counted. The dilution that allowed counting 10 to 150 CFU were counted. The experiment was repeated three times and the mean value of CFU was recorded.

3. Results and discussion

3.1. Electrospinning of increasing concentrations of honey within the HPCS nanofibers

Prior to electrospinning, the conductivity of the aged polyvinyl alcohol/chitosan solutions (7:3.5 w%) with increasing honey concentrations (10, 20, and 30 w%) was determined. It was observed that the change in the honey concentration within the polyvinyl alcohol/

chitosan solutions resulted in a small variation in the conductivity of the solutions from 1510 uS with the PCS solutions containing 30% H to 1480 and 1400 uS with the 20%H and 10% H, respectively. The conductivity of a solution is related to its amount of ions. Thus, the decrease in the honey concentration results in a decrease in the amount of ions present in the solution and consequently led to a reduction in its conductivity. Subsequently, the aged HPCS solutions with increasing honey concentrations were electrospun into nanofibers at a feed rate of 10 μl/min and distance of 15 cm between the nozzle and the collector. Different voltages ranging from 10 kV to 29 kV were applied to obtain the optimum value which corresponds the lowest voltage that allowed collection of uniform nanofibers that were free of any beads, sticking or clusters. For each applied voltage, a sample of nanofibers was collected after five minutes of electrospinning followed by examining its morphology under the SEM (data not shown). It was observed that 24 kV is the minimum voltage that allowed for a uniform nanofiber deposition. As apparent from Fig. 1, it was noted that increasing the honey concentration led to increasing the diameter of the nanofibers. For instance, the HPCS nanofibers with 10% honey exhibited a mean fiber diameter of 284 ± 97 nm (Fig. 1a & b) which increased to 371 ± 110 nm, and 464 ± 185 nm upon increasing the honey concentration to 20% (Fig. 1c & d), and 30% (Fig. 1e & f), respectively. Although the increase in conductivity of a solution results in a reduction in the diameter size of electrospun nanofibers, the main parameter affecting the diameter of the nanofibers is the solution concentration [32]. And because of the high concentrations of the honey loaded within the developed HPCS nanofibers, the increase in the fiber diameter is a direct consequence for increasing the amount of honey loaded within the nanofibers as can be observed from Fig. 2a & b, where it is apparent that honey is embedded within the chitosan/polyvinyl alcohol nanofibers. It was also observed that the amount of honey loaded within the nanofibers influences the fiber diameter distribution. As seen in Fig. 1d, addition of 20% honey to the chitosan/polyvinyl alcohol nanofibers allowed for the most focused fiber diameter distribution, as most of the nanofibers exhibited diameters between 300 nm and 450 nm. Whereas, the addition of 10% and 30% honey to the chitosan/polyvinyl alcohol nanofibers resulted in broad distribution of the diameters of the fibers (Fig. 1b & f).

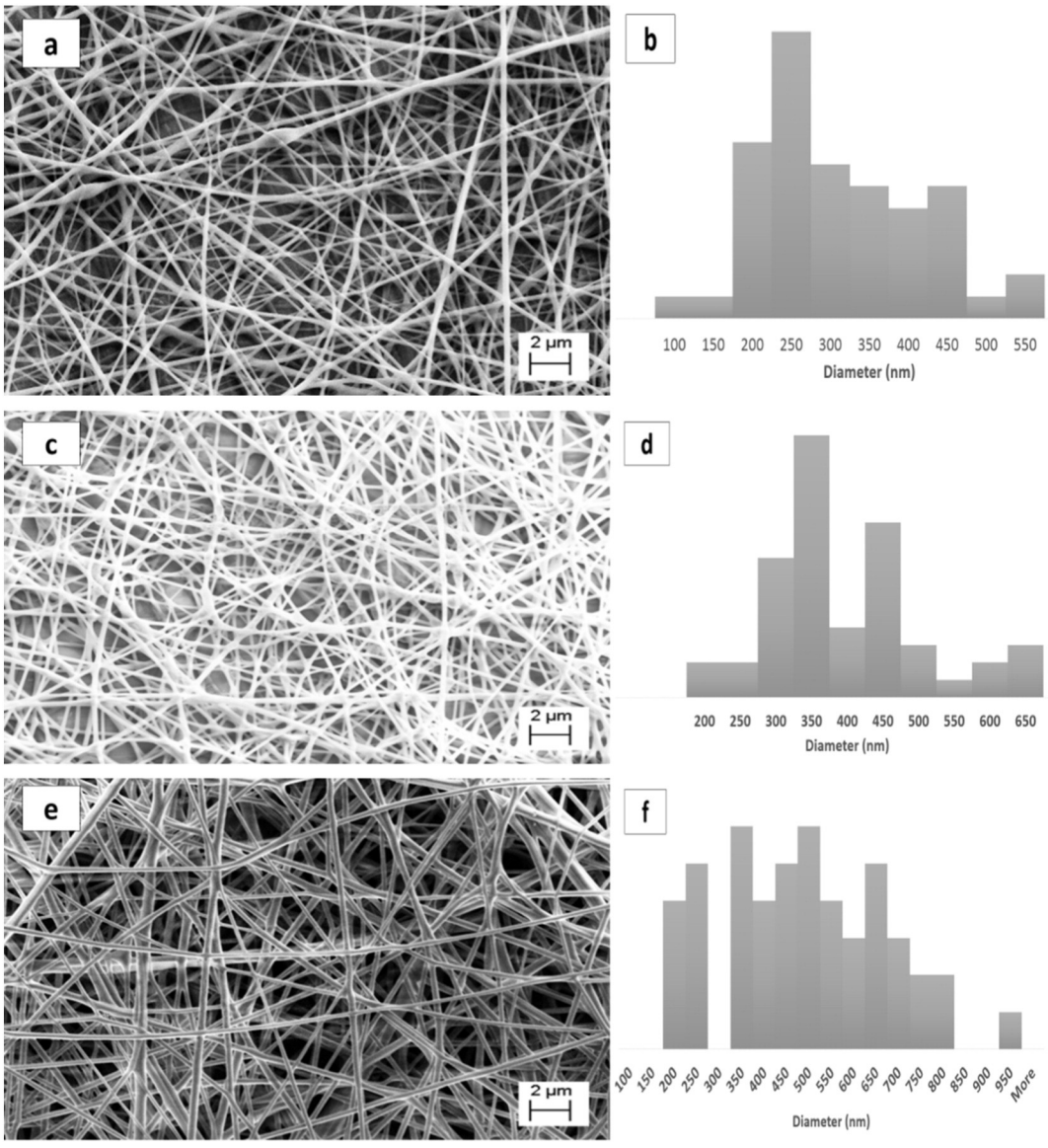

Fig. 1. SEM images of the electrospun honey/polyvinyl alcohol/chitosan (HPCS) nanofibrous mats with increasing concentrations of honey (a, c, e) and their diameter distribution (b, d, f): (a, b) HPCS (10%:7%:3.5%), (c, d) HPCS (20%:7%:3.5%), and (e, f) HPCS (30%:7%:3.5%).

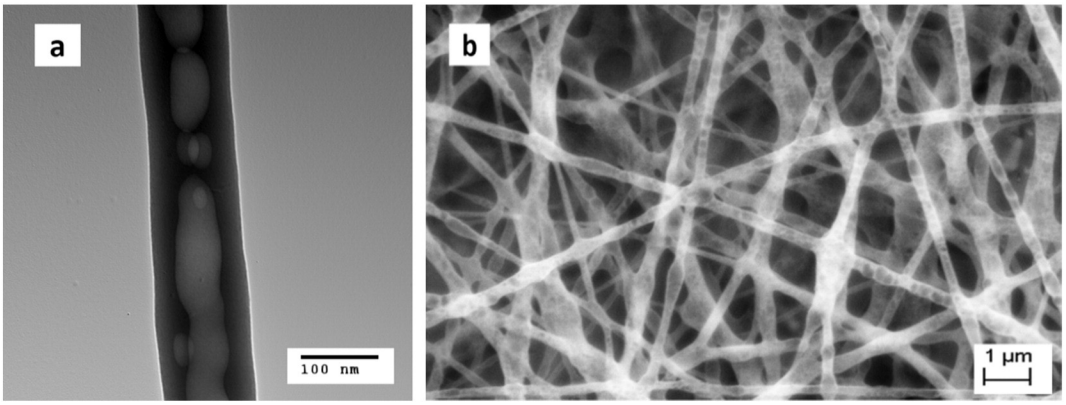

Fig. 2. TEM (a) & SEM (b) images of honey/polyvinyl alcohol/chitosan (HPCS) nanofibers (30:7:3.5 w%) illustrating the inclusion of honey within the nanofibers.

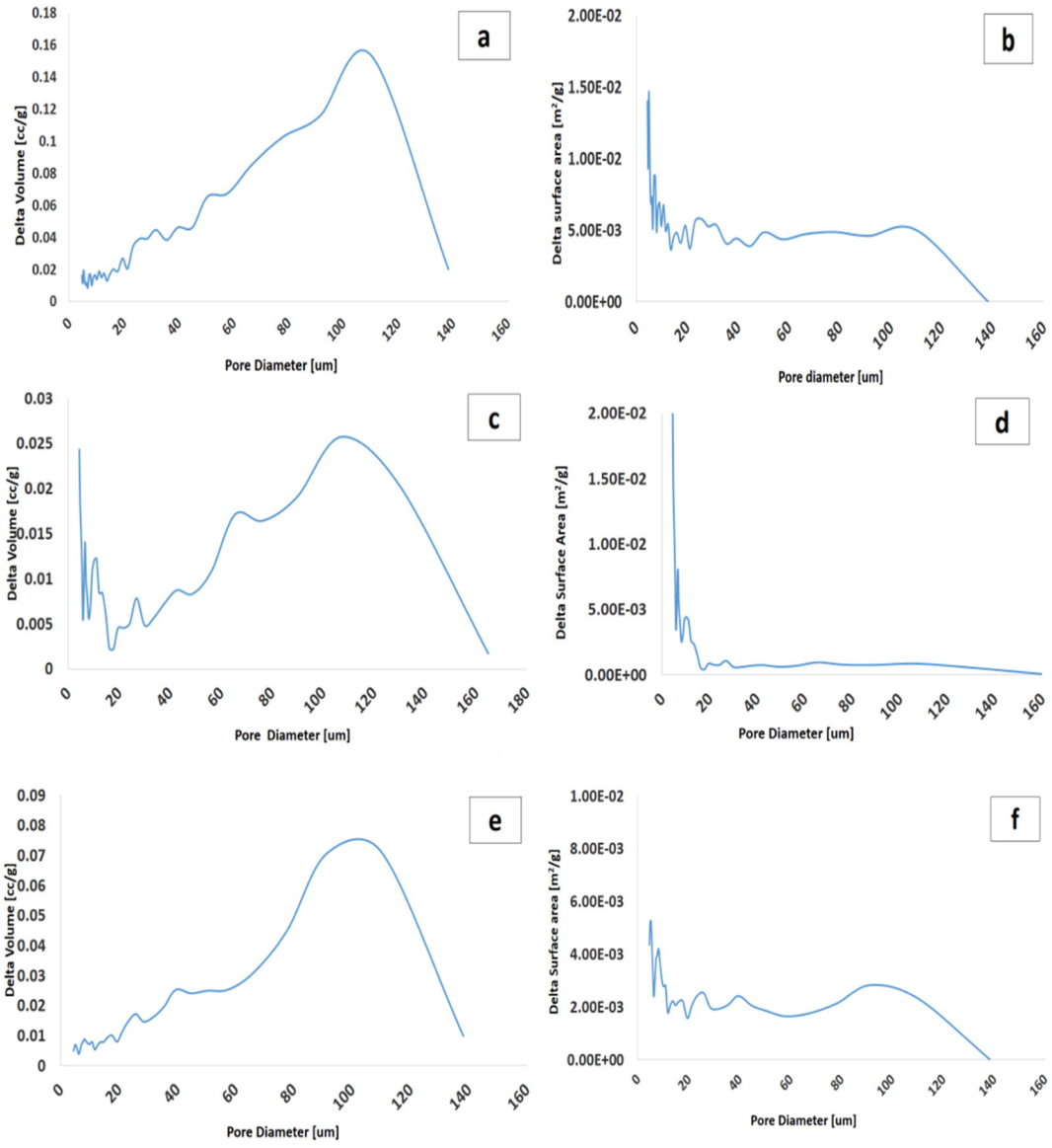

Fig. 3. Mercury porosimetry results of pore diameter versus delta volume of intruded mercury (a1, c, e), and pore diameter versus delta surface area (b, d, f) of the honey/polyvinyl alcohol/chitosan (HPCS) nanofibrous mats with increasing honey concentrations; (a, b) HPCS (10%:7%:3.5%), (c, d) HPCS (20%:7%:3.5%) (e, f), and HPCS (30%:7%:3.5%).

3.2. Effect of increasing the honey concentration on the porosity of the HPCS nanofibers

In both tissue engineering and wound healing applications, the porosity of the nanofibrous scaffolds will affect the migration and proliferation of cells, growth of the blood vessels and the exchange of the waste products and nutrients between the cells and their surrounding microenvironment [33]. Mercury porosimetry is a well-known method for measuring porosity of materials, and it is based on the fact that mercury does not wet solid surfaces. The sample is completely surrounded with mercury that does not intrude through the pores except after applying pressure. As the pressure increases, mercury intrudes through the large pores first, and by further increase in pressure, the mercury intrudes into the fine pores. After the pressure reaches to the maximum the porosity and pore volume are calculated. It is of note that, mercury porosimetry measures pore sizes between 0.0018 and 400 μm, however pore sizes smaller than 0.0018 μm cannot be measured via mercury porosimetry thus presenting a source of error in the mercury porosimetry results [34,35]. As shown in Fig. 3, mercury porosimetry was used for quantitative assessment of the pore size distribution and porosity of the HPCS nanofibers with increasing honey concentrations (10%, 20% and 30%). Increasing the honey concentration resulted in a slight decrease in the overall porosity. In addition, it was noted that the porosity of all the HPCS nanofibers developed in this study, irrespective the honey concentrations, have demonstrated enhanced porosity compared to previously spun chitosan and chitosan/polyvinyl alcohol nanofibers [36,37]. The developed HPCS nanofibers with 10% and 20%, 30% honey have demonstrated porosity of 97.8% and 95.1% respectively, compared to 79.9% in previously spun non-sonicated chitosan nanofibers [36].

Recently, it was reported that the increase in the overall porosity due to increase in the pore size and fiber diameters enhances the viability of cells. Whereas, increasing the overall porosity due to the simultaneous reduction in fiber diameter and pore diameter could reduce the cell viability [38]. In our study, it was observed that the pore diameter was greatly influenced by the change in the honey concentration within the HPCS nanofibers. The HPCS nanofibers with 10% and 30% honey exhibited wider distribution of pore diameter and most importantly exhibited increased number of pores having large pore diameter reaching to 140 μm (Fig. 3b & f). This was also observed in the volume of mercury intruded through the fibers where most of the volume intruded was through pores having pore diameters between 35 μm and 138 μm (Fig. 3a & b). These results could be attributed to the relatively large fiber diameter as well as the wide distribution of the diameters of the nanofibers of the 10% and 30% honey HPCS nanofibers, respectively. Similar results were observed by Ryu et al., who observed that by increasing the polymer concentration from 15 to 30%, the fiber diameter increased from 90 to 480 nm and subsequently the porosity as determined by mercury porosimetry increased from 25% to 80% [39]. Moreover, Ko et al., have demonstrated that the porosity of SiO2-ZrO2 composite nanofibers ranged from 81.3% to 91.7% by increasing the amount of ZrO_2 from 10 to 20% due to an increase in the fiber diameter with an increase in the ZrO2 content. Thus, a direct relation between the increase in the fiber diameter and pore diameter and porosity was verified via different previous studies [40]. Such increased pore diameter achieved in the 10% and 30% honey nanofibers is favorable in cell related applications such as tissue engineering and wound healing [37]. Although the 20% honey HPCS nanofibers showed large fiber diameter of 371 ± 110 nm but they also exhibited a focused diameter distribution (Fig. 1d), this in turn resulted in a more focused pore diameter distribution at less than 20 μm (Fig. 3d). However, a large volume of mercury can still be seen intruded from the pores with pore diameters between 40 μm and 160 μm (Fig. 3c). This could be attributed to the fact that they can allow much greater volume to be intruded through them due to their larger surface area compared to the pores with small diameters as less than 20 μm.

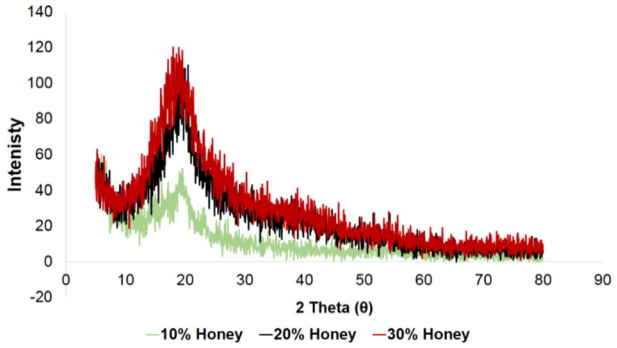

Fig. 4. XRD diffraction patterns of the honey/polyvinyl alcohol/chitosan (HPCS) nanofibers with increasing honey concentrations. The weight blending ratios of the electrospun mats were 7% polyvinyl alcohol (P), 3.5% chitosan (CS), and increasing concentrations of honey (H): 10%, 20%, and 30%.

3.3. Effect of increasing the honey concentration on crystallization and thermal properties of the HPCS nanofibers

The XRD diffraction patterns of pure polyvinyl alcohol and chitosan have been previously reported [41,42]. Moreover, the XRD patterns of polyvinyl alcohol/chitosan (PCS) nanofibers and films were reported by Jia et al., who observed that nanofibers of the PCS exhibited deteriorated crystalline structure compared to the films [43].

Fig. 4, illustrates the XRD diffraction patterns of the prepared HPCS nanofibers with increasing honey concentrations. The HPCS nanofibers exhibited an amorphous microstructure with a single broad peek around $2\theta = 20°$. Such XRD patterns are in coherence with those observed for the previously prepared polyvinyl alcohol/chitosan nanofibers [43]. Thus the addition of honey did not affect the diffraction model of the polyvinyl alcohol/chitosan nanofibers and consequently the increase in the honey concentration within the HPCS nanofibers had no effect on their diffraction pattern.

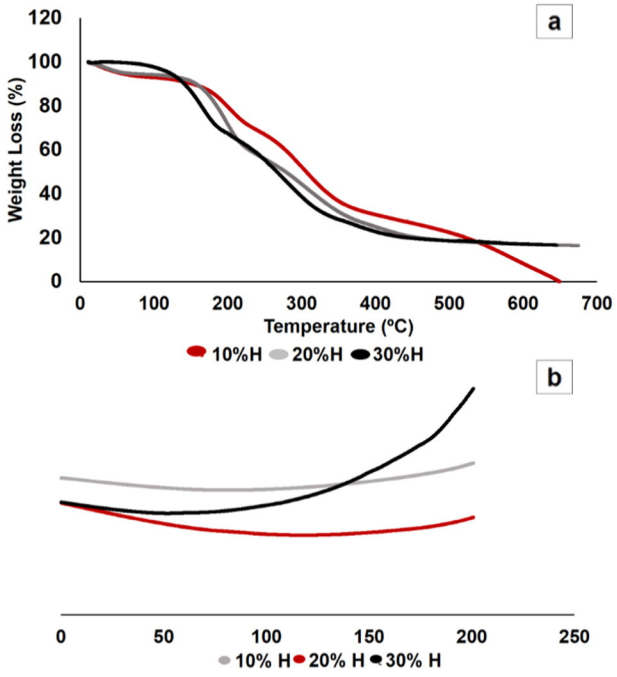

Fig. 5. TGA (a) DSC (b) thermograms of the honey/polyvinyl alcohol/chitosan (HPCS) nanofibers with increasing honey concentrations. The weight blending ratios of the electrospun mats were 7% polyvinyl alcohol (P), 3.5% chitosan (CS), and increasing concentrations of honey (H): 10%, 20%, and 30%.

The deterioration of the crystalline structure of the electrospun nanofibers was previously reported [44,45]. Such deterioration could be attributed to the fast deposition and drying of the elongated electrospun nanofibers thus hindering the crystallization [43].

TGA of the HPCS nanofibers with increasing honey concentrations (10%, 20% and 30%) was performed. As observed in Fig. 5a, the examined samples demonstrated similar thermal degradation process that takes place in several steps. The first step of weight loss is attributed to moisture elimination which resulted in loss of less than 10% of the weight of the examined nanofibers below 120 °C.

It is of note that at 120 °C the HPCS nanofibers having 10% honey exhibited the highest weight loss of ~8% whereas the weight loss decreased by increasing the amount of honey within the HPCS nanofibers to ~6% and ~3% with the 20% and 30% honey, respectively. This indicates that the HPCS nanofibers with higher honey concentrations exhibited higher initial moisture content, which is a result of the hygroscopic nature of honey. The second and major weight loss of approximately 50% of the weight occurred after 120 °C till 400 °C and is mainly attributed to the thermal decomposition of the polymer structure as well as the degradation of the honey components followed by carbonization of the honey contents. In the final step of the thermal decomposition at temperatures above 500 °C, the polymer backbone has been ruptured in addition to the oxidation of the organic matter found in honey. These observations are in agreement with what has been previously reported [46,47]. TGA clearly demonstrates that the fabricated HPCS nanofibers with different honey concentrations exhibit good thermal stability below 120 °C.

The DSC thermograms of the HPCS nanofibers with increasing concentrations of honey (10, 20, and 30 w%) are illustrated in Fig. 5b. The three DSC thermograms showed no peaks. This further proves the deteriorated crystalline structure of the developed HPCS nanofibers. Moreover, it was previously proven that increasing the chitosan content within the PCS nanofibers to ~1% resulted in further deterioration of the crystallinity of the fibers [43,48]. Thus, in the present work the increase in the chitosan concentrations to 3.5% within the developed HPCS nanofibers combined with the nanofibrous structure and the honey loaded within the nanofibers resulted in a significant deterioration in the crystalline structure and development of the nanofibers in amorphous form resulting in absence of any peaks in the DSC thermogram. Obviously, increasing the honey concentration loaded within the nanofibers did not affect the DSC thermograms of the obtained HPCS nanofibers.

3.4. Effect of increasing the honey concentration on the swelling of the HPCS nanofibers

Honey and chitosan nanofibrous mats represent top candidates for wound dressing applications and determining their swelling capabilities would allow prediction of their exudate management ability [49].

Recently we have illustrated that the swelling capabilities of the noncrosslinked HPCS nanofibrous mats with varying degrees of chitosan and honey ranged from 46% to 197% [29]. Such values illustrate the low swelling capability of the noncrosslinked HPCS nanofibrous mats. In the present study the swelling capability of the crosslinked fibers with increasing honey concentrations was investigated.

Crosslinking allows maintaining the nanofibrous structure of the developed HPCS nanofibrous mats in aqueous media, thus, allowing for improved porosity. However, increasing the crosslinking degree will decrease the swelling ability of the nanofibers due to the increased rigidity of the network as a result of increasing both the inter- and intramolecular interactions [50]. Consequently, the effect of changing the honey concentration was studied at two mild crosslinking degrees. These include exposing the nanofibers to GA vapours for 1 h and 3 h with subsequent heating at 40 °C to enhance crosslinking and remove any residual GA. Such crosslinking treatments were selected as they represent the shortest possible exposure to GA vapours that allowed crosslinking, thus avoiding deteriorating the nontoxicity and biocompatibility of the developed nanofibers upon excessive exposure to the GA vapours. Moreover, the HPCS nanofibers that were crosslinked via exposure to GA vapours for 3 h with subsequent heating were proved nontoxic and biocompatible via MTT cytotoxicity evaluation [29].

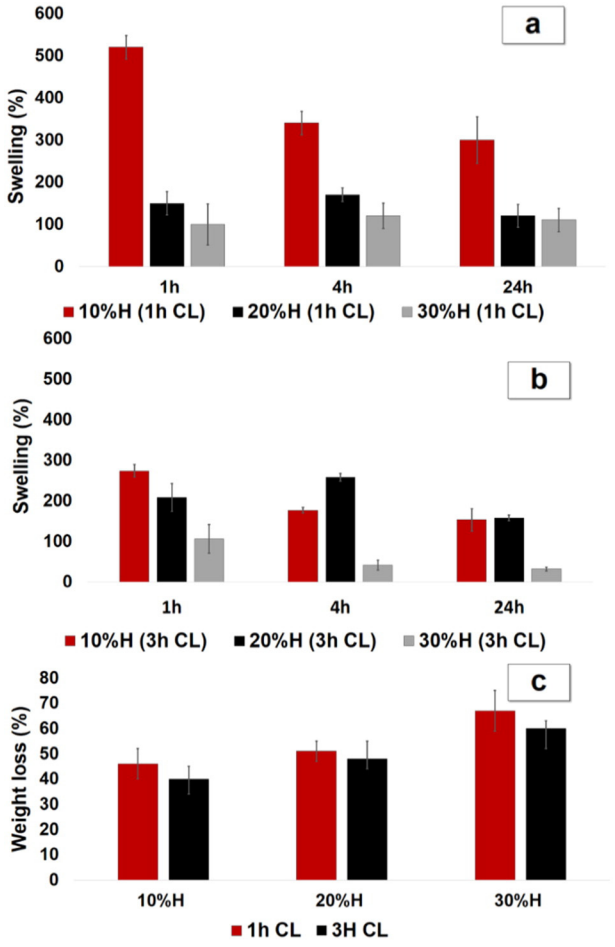

Fig. 6. % Swelling of the (a) 1 h cross-linked (CL) (b) 3 h cross-linked (CL), honey/polyvinyl alcohol/chitosan (HPCS) nanofibers mats with increasing honey concentrations after immersion in PBS (pH 7.4) for 1, 4, and 24 h. The weight blending ratios of the electrospun mats were 7% polyvinyl alcohol (P), 3.5% chitosan (CS), and increasing concentrations of honey (H) 10%, 20%, and 30%.

Increasing the honey concentration within the nanofibers decreased its swelling ability at both the tested crosslinking degrees (Fig. 6a & b). It could be observed from the figures that the HPCS nanofibers with 10% honey and 1 h of crosslinking with the GA vapours exhibited superior swelling capabilities reaching to 520% at 1 h and 300% after 24 h (Fig. 6a). On the other hand, the effect of the crosslinking time on the swelling capabilities of the HPCS nanofibers varied according to their incorporated honey concentration. For the HPCS nanofibers with 10% honey, increasing the crosslinking time from 1 h to 3 h decreased their swelling capabilities noticeably from 520% to 273%. Whereas, HPCS nanofibers with 20% honey exhibited increased swelling ability with the increase in the crosslinking time from 1 h to 3 h. Noticeably, the HPCS nanofibers with 30% honey demonstrated the lowest swelling ability at both crosslinking times.

Although honey is known for its high water uptake ability [51], it also has high water solubility. Such high water solubility results in increasing the degradation rates of the nanofibers and consequently losing their compact porous structure that can hold in water [52]. Thus, this eventually results in massive decrease in swelling ability. This was observed by the very low swelling abilities of the HPCS nanofibers with 30% honey.

Interestingly, the increase in the crosslinking efficiency by increasing the exposure time to the GA vapours allows the nanofibers to maintain a more compact nanofibrous structure [53,54] thus, the percent of released and solubilized honey decreases. This allows the honey to be maintained within the nanofibers for longer periods of time, and thus its water uptake capabilities could be realized. On the other hand, the increase in the crosslinking degree decreases the swelling ability as it hinders the intermolecular motion and chain disentanglements within the nanofibrous scaffold. These two opposite effects on the swelling abilities of the nanofibrous scaffolds could be observed in the results presented in Fig. 6a & b. In the HPCS nanofibers with 10% honey, the amount of honey within the nanofibers is small thus the effect of the swelling hindering due to crosslinking was more pronounced than the water uptake ability of the maintained honey. Whereas, when the concentration of honey increased to 20%, the water uptake ability of the maintained honey in this case exceeded the hindering effect of crosslinking on swelling which allowed the HPCS nanofibers with 20% honey to exhibit a noticeable increase in swelling ability even at 24 h by increasing the crosslinking time to 3h. The HPCS nanofibers with 30% honey however showed slight decrease in the swelling ability at 24h with increasing the crosslinking time. This is because at such high concentration of honey such crosslinking treatments could not overcome the increased solubility of the HPCS nanofibers with 30% honey which affects the compact structure of the nanofibrous scaffold. These results reveal the importance of optimization of the crosslinking degree as well as the honey concentrations within the developed HPCS nanofibers to adjust the water uptake ability according to the desired application.

3.5. Effect of increasing the honey concentration on the degradation rates of the HPCS nanofibers

The effect of increasing the honey concentration within the HPCS nanofibers on the degradation behavior of both the noncrosslinked and crosslinked nanofibers via exposure to GA vapours for 3 h followed by heating at 40 °C for 24 h was studied.

As illustrated in Fig. 7, increasing the honey concentration within the HPCS nanofibers increased the degradation ability of the nanofibers after 30 days of incubation in PBS at 37 °C and 100 rpm. This could be attributed to the high water solubility of honey. Thus, in the HPCS nanofibers with higher honey concentrations such effect could be realized with an increase in the degradation behavior of the nanofibers.

Meanwhile, the crosslinked HPCS nanofibers at all honey concentrations showed decreased degradation ability compared to the noncrosslinked fibers. This is mainly because crosslinking the HPCS nanofibers via exposure to GA for 3 h allows maintaining the nanofibrous structure as was previously proven [29]. Exposure of the HPCS nanofibers to GA allows chemical crosslinking of chitosan either through formation of Michael-type adducts or Schiff's base structures [55] and thus decreases their degradation rate.

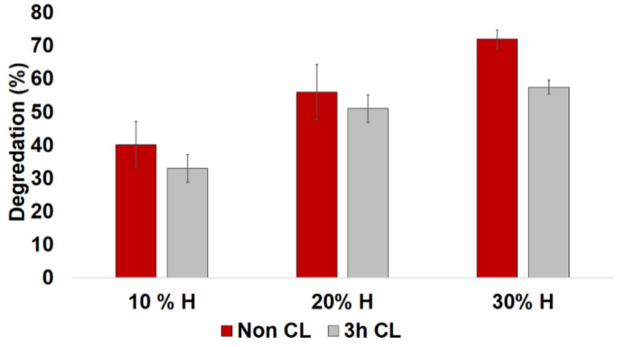

Fig. 7. % Degradation of the Non-cross-linked (Non CL) & 3 h cross-linked (CL), honey/polyvinyl alcohol/chitosan (HPCS) nanofibers mats with increasing honey concentrations after immersion in PBS (pH 7.4) for 30 days at 37 °C. The weight blending ratios of the electrospun mats were 7% polyvinyl alcohol (P), 3.5% chitosan (CS), and increasing concentrations of honey (H) 10%, 20%, and 30%.

3.6. Effect of increasing the honey concentration on the antibacterial activity of the developed HPCS nanofibers

Both honey and chitosan exhibit antibacterial activity. Honey exerts its antibacterial activity via its acidity, high sugar content as well as its ability for hydrogen peroxide production [56]. Whereas, the polycationic nature of chitosan allows it to interact with the negatively charged membranes of bacteria leading to loss in the permeability of the membrane with subsequent cell leakage and death [57].

Electrospun nanofibers allow enhancement of the antibacterial activity of both chitosan and honey within the developed HPCS nanofibers, mainly due to the increase in the surface to volume ratio [29].

It was previously shown that the antibacterial effect of HPCS nanofibers with 30% honey are significantly affected by the change in the chitosan concentrations within the nanofibers [29]. In the present work the effect of changing the honey concentration within the HPCS nanofibers was investigated as shown in Fig. 8. The increase in the honey concentration within the HPCS nanofibers enhanced their antibacterial activities against both *S. aureus* and *E. coli* at 1×10^7 CFU/ml (Fig. 8a & b). However, upon increasing the bacterial count to 1×10^8 CFU/ml the increase in the honey concentration resulted in an increase in the antibacterial activity against *S. aureus*, whereas nearly no antibacterial effect was realized against *E.coli*. These results agree with the previously reported results of the HPCS nanofibers that demonstrated enhanced antibacterial activity against gram positive *S. aureus* over the gram negative *E.coli* [29].

4. Conclusions

Different honey concentrations (10%, 20% and 30%) have been electrospun within chitosan (3.5%)/polyvinyl alcohol (7%) nanofibers.

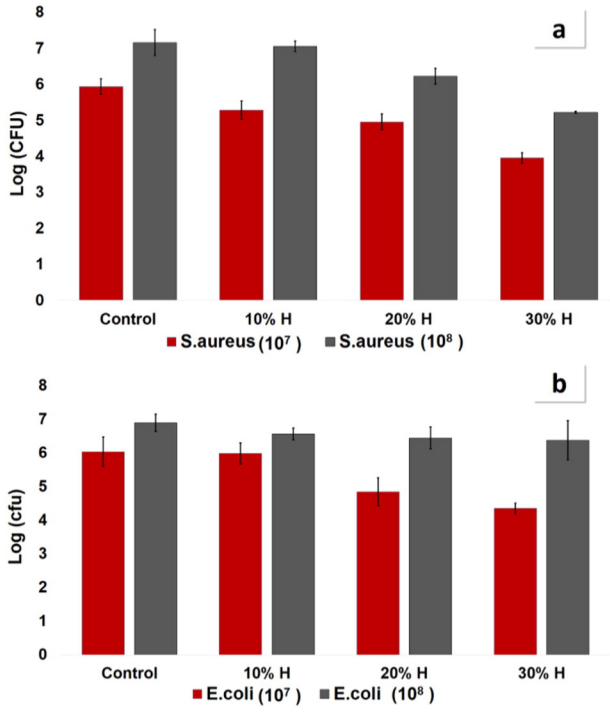

Fig. 8. The antibacterial activity of the electrospun honey/polyvinyl alcohol/chitosan (HPCS) nanofibrous mats against 1×10^8 CFU/ml and 1×10^7 CFU/ml of *E. coli* (a) and *S. aureus* (b) represented by reduction in the log (CFU) after h. The weight blending ratios of the electrospun mats were 7% polyvinyl alcohol (P), 3.5% chitosan (CS), and increasing concentrations of honey (H); 10%, 20%, and 30%.

The effect of increasing the honey concentration on the different properties of the electrospun nanofibers has been investigated. Increasing the honey concentration resulted in an increase in the fiber diameter from 284 ± 97 nm with 10% honey to 464 ± 185 nm with 30% honey, whereas the porosity was slightly decreased from 97.8% with 10% honey to 95.1% in the case of the nanofibers incorporating 20% and 30% honey. Interestingly, it was observed that both the HPCS combinations with 10% honey and 30% honey exhibited an increased number of pores with large pore diameter reaching to 140 μm which is advantageous for tissue engineering and wound healing applications. The swelling of the nanofibers was greatly influenced by the concentration of incorporated honey and the degree of crosslinking. Highest swelling extent was observed with HPCS nanofibers having 10% honey, and the least swelling was noted in the HPCS nanofibers having 30% honey. However, the swelling ability of the nanofibers containing 20% honey was noticeably enhanced with increasing the crosslinking degree. The degradation ability of the nanofibers increased with increasing the honey concentration within the HPCS nanofibers and decreased with crosslinking of the fiber mats. The crystallization and thermal behavior of the nanofibers on the other hand were not affected by changing the honey concentration within the developed HPCS nanofibers, Increasing the honey concentration within the HPCS nanofibers enhanced their antibacterial activity against both *S. aureus* and *E.coli* at 7×10^7 CFU/ml. Whereas, at 7×10^8 CFU/ml nearly no antibacterial effect was realized against *E.coli* at all honey concentrations included within the HPCS nanofibers.

Acknowledgements

This research has been funded by a research grant from the American University in Cairo. The authors appreciate the technical support offered by Ms. Worood A. El-Mehalmey, Center of Materials Science, Zewail City for her help with the thermogravimetric analysis.

References

[1] I.S. Chronakis, Novel nanocomposites and nanoceramics based on polymer nanofibers using electrospinning process—a review, J. Mater. Process. Technol. 167 (2005) 283–293.
[2] Z.M. Huang, Y.Z. Zhang, M. Kotaki, et al., A review on polymer nanofibers by electrospinning and their applications in nanocomposites, Compos. Sci. Technol. 63 (2003) 2223–2253.
[3] H. Jia, G. Zhu, B. Vugrinovich, et al., Enzyme-carrying polymeric nanofibers prepared via electrospinning for use as unique biocatalysts, Biotechnol. Prog. 18 (2002) 1027–1032.
[4] B.M. Min, G. Lee, S.H. Kim, et al., Electrospinning of silk fibroin nanofibers and its effect on the adhesion and spreading of normal human keratinocytes and fibroblasts in vitro, Biomaterials 25 (2004) 1289–1297.
[5] Q.P. Pham, U. Sharma, A.G. Mikos, Electrospinning of polymeric nanofibers for tissue engineering applications: a review, Tissue Eng. 12 (2006) 1197–1211.
[6] L. Ghasemi-Mobarakeh, M.P. Prabhakaran, M. Morshed, et al., Electrospun poly (ε-caprolactone)/gelatin nanofibrous scaffolds for nerve tissue engineering, Biomaterials 29 (2008) 4532–4539.
[7] G. Verreck, I. Chun, J. Rosenblatt, et al., Incorporation of drugs in an amorphous state into electrospun nanofibers composed of a water-insoluble, nonbiodegradable polymer, J. Control. Release 92 (2003) 349–360.
[8] H. Jiang, Y. Hu, Y. Li, et al., A facile technique to prepare biodegradable coaxial electrospun nanofibers for controlled release of bioactive agents, J. Control. Release 108 (2005) 237–243.
[9] P. Zahedi, I. Rezaeian, S.O. Ranaei-Siadat, et al., A review on wound dressings with an emphasis on electrospun nanofibrous polymeric bandages, Polym. Adv. Technol. 21 (2010) 77–95.
[10] P.O. Rujitanaroj, N. Pimpha, P. Supaphol, Wound-dressing materials with antibacterial activity from electrospun gelatin fiber mats containing silver nanoparticles, Polymer 49 (2008) 4723–4732.
[11] S. Ramakrishna, K. Fujihara, W.E. Teo, et al., Electrospun nanofibers: solving global issues, Mater. Today 9 (2006) 40–50.
[12] L. Persano, A. Camposeo, C. Tekmen, et al., Industrial upscaling of electrospinning and applications of polymer nanofibers: a review, Macromol. Mater. Eng. 298 (2013) 504–520.
[13] V. Thavasi, G. Singh, S. Ramakrishna, Electrospun nanofibers in energy and environmental applications, Energy Environ. Sci. 1 (2008) 205–221.
[14] K. Sun, Z.H. Li, Preparations, properties and applications of chitosan based nanofibers fabricated by electrospinning, Express Polym Lett 5 (2011) 342–361.
[15] H. Homayoni, S.A.H. Ravandi, M. Valizadeh, Electrospinning of chitosan nanofibers: processing optimization, Carbohydr. Polym. 77 (2009) 656–661.
[16] R.A.A. Muzzarelli, Chitins and chitosans as immune adjuvants and non-allergenic drug carriers, Mar. Drugs 8 (2010) 292–312.
[17] R.A.A. Muzzarelli, M. El Mehtedi, M. Mattioli-Belmonte, Emerging biomedical applications of nano-chitins and nano-chitosans obtained via advanced eco-friendly technologies from marine resources, Mar. Drugs 12 (2014) 5468–5502.
[18] X. Geng, O.H. Kwon, J. Jang, Electrospinning of chitosan dissolved in concentrated acetic acid solution, Biomaterials 26 (2005) 5427–5432.
[19] P. Su, C. Wang, X. Yang, et al., Electrospinning of chitosan nanofibers: the favorable effect of metal ions, Carbohydr. Polym. 84 (2011) 239–246.
[20] H. Liao, R. Qi, M. Shen, et al., Improved cellular response on multiwalled carbon nanotube-incorporated electrospun polyvinylalcohol/chitosan nanofibrous scaffolds, Colloids Surf. B: Biointerfaces 84 (2011) 528–535.
[21] E. Yan, S. Fan, X. Li, et al., Electrospun polyvinyl alcohol/chitosan composite nanofibers involving Au nanoparticles and their in vitro release properties, Mater. Sci. Eng. C 33 (2012) 461–465.
[22] Y. Zhou, D. Yang, X. Chen, et al., Electrospun water-soluble carboxyethyl chitosan/poly (vinyl alcohol) nanofibrous membrane as potential wound dressing for skin regeneration, Biomacromolecules 9 (2007) 349–354.
[23] P.C. Molan, The antibacterial activity of honey: 1. The nature of the antibacterial activity, Bee World 73 (1992) 5–28.
[24] M. Subrahmanyam, Topical application of honey in treatment of burns, Br. J. Surg. 78 (1991) 497–498.
[25] M.D. Mandal, S. Mandal, Honey: its medicinal property and antibacterial activity, Asian Pac. J. Trop. Biomed. 1 (2011) 154–160.
[26] P. Molan, Clinical usage of honey as a wound dressing: an update, J. Wound Care 13 (2004) 353–356.
[27] H. Maleki, A.A. Gharehaghaji, P.J. Dijkstra, A novel honey-based nanofibrous scaffold for wound dressing application, J. Appl. Polym. Sci. 127 (2013) 4086–4092.
[28] P. Wang, J.H. He, Electrospun polyvinyl alcohol-honey nanofibers, Therm. Sci. 17 (2013) 1549–1550.
[29] W.A. Sarhan, H.M. Azzazy, High concentration honey chitosan electrospun nanofibers: biocompatibility and antibacterial effects, Carbohydr. Polym. 122 (2015) 135–143.
[30] Z.G. Chen, P.W. Wang, B. Wei, et al., Electrospun collagen–chitosan nanofiber: a biomimetic extracellular matrix for endothelial cell and smooth muscle cell, Acta Biomater. 6 (2010) 372–382.
[31] R. Jayakumar, M. Prabaharan, S.V. Nair, et al., Novel chitin and chitosan nanofibers in biomedical applications, Biotechnol. Adv. 28 (2010) 142–150.
[32] K. Garg, G.L. Bowlin, Electrospinning jets and nanofibrous structures, Biomicrofluidics 5 (2012) 013403.
[33] S.N. Alhosseini, M. Fathollah, M. Masoud, et al., Synthesis and characterization of electrospun polyvinyl alcohol nanofibrous scaffolds modified by blending with chitosan for neural tissue engineering, Int. J. Nanomedicine 7 (2012) 25.
[34] A.K. Haghi (Ed.), Electrospinning of Nanofibers in Textiles, CRC Press, 2011.
[35] J. Širc, R. Hobzová, N. Kostina, M., et al., Morphological characterization of nanofibers: methods and application in practice, J. Nanomater. 2012 (2012) 121.
[36] B.K. Gu, S.J. Park, M.S. Kim, et al., Fabrication of sonicated chitosan nanofiber mat with enlarged porosity for use as hemostatic materials, Carbohydr. Polym. 97 (2013) 65–73.
[37] M.A. Shokrgozar, F. Mottaghitalab, V. Mottaghitalab, et al., Fabrication of porous chitosan/poly (vinyl alcohol) reinforced single-walled carbon nanotube nanocomposites for neural tissue engineering, J. Biomed. Nanotechnol. 7 (2011) 276–284.
[38] M. KazemiPilehrood, M. Dilamian, M. Mirian, et al., Nanofibrous chitosan-polyethylene oxide engineered scaffolds: a comparative study between simulated structural characteristics and cells viability, BioMed. Res. Int. 2014 (2014), ID 438065.
[39] Y.J. Ryu, H.Y. Kim, K.H. Lee, et al., Transport properties of electrospun nylon 6 nonwoven mats, Eur. Polym. J. 39 (2003) (2003) 1883–1889.
[40] J.B. Ko, S.W. Lee, D.E. Kim, et al., Fabrication of SiO2-ZrO2 composite fiber mats via electrospinning, J. Porous. Mater. 13 (2006) 325–330.
[41] K. Nakane, T. Yamashita, K. Iwakura, et al., Properties and structure of poly(vinyl alcohol)/silica composites, J. Appl. Polym. Sci. 74 (1999) 133–138.
[42] R.J. Samuels, Solid state characterization of the structure of chitosan films, J. Polym. Sci. Polym. Phys. 19 (1981) 1081–1105.
[43] Y.T. Jia, J. Gong, X.H. Gu, et al., Fabrication and characterization of poly (vinyl alcohol)/chitosan blend nanofibers produced by electrospinning method, Carbohydr. Polym. 67 (2007) 403–409.
[44] J.M. Deitzel, J.D. Kleinmeyer, D. Harris, et al., The effect of processing variables on the morphology of electrospun nanofibers and textiles, Polymer 42 (2001) 261–272.
[45] X.H. Zong, K.S. Kim, D.F. Fang, et al., Structure and process relationship of electrospun bioabsorbable nanofiber membranes, Polymer 43 (2002) 4403–4412.
[46] D. Chauhan, J. Dwivedi, N. Sankararamakrishnan, Novel chitosan/PVA/zerovalent iron biopolymeric nanofibers with enhanced arsenic removal applications, Environ. Sci. Pollut. Res. 21 (2014) 9430–9442.
[47] M.L. Felsner, C.B. Cano, J.R. Matos, et al., Optimization of thermogravimetric analysis of ash content in honey, J. Braz. Chem. Soc. 15 (2004) 797–802.
[48] I. Uslu, H. Çelikkan, O. Atakol, et al., Preparation of PVA/chitosan doped with boron composite fibers and their characterization, Hacet. J. Biol. Chem. 36 (2008) 117–122.
[49] B. Li, C.L. Shan, Q. Zhou, et al., Synthesis, characterization, and antibacterial activity of cross-linked chitosan-glutaraldehyde, Mar. Drugs 11 (2013) 1534–1552.
[50] Y. Jin, D. Yang, Y. Zhou, et al., Photocrosslinked electrospun chitosan-based biocompatible nanofibers, J. Appl. Polym. Sci. 109 (2008) 3337–3343.
[51] R. MohdZohdi, Z. Abu BakarZakaria, N. Yusof, et al., Gelam (*Melaleuca* spp.) honey-based hydrogel as burn wound dressing, J. Evid. Based Complement. Alternat. Med. 2012 (2011), ID 843025.

[52] T. Wang, X.K. Zhu, X.T. Xue, et al., Hydrogel sheets of chitosan, honey and gelatin as burn wound dressings, Carbohydr. Polym. 88 (2012) 75–83.
[53] C. Li, R. Fu, C. Yu, et al., Silver nanoparticle/chitosan oligosaccharide/poly (vinyl alcohol) nanofibers as wound dressings: a preclinical study, Int. J. Nanomedicine 8 (2013) 4131.
[54] J.H. Kim, J.Y. Kim, Y.M. Lee, et al., Properties and swelling characteristics of cross-linked poly (vinyl alcohol)/chitosan blend membrane, J. Appl. Polym. Sci. 45 (1992) 1711–1717.
[55] J.D. Schiffman, C.L. Schauer, Cross-linking chitosan nanofibers, Biomacromolecules 8 (2007) 594–601.
[56] L. Vandamme, A. Heyneman, H. Hoeksema, et al., Honey in modern wound care: a systematic review, Burns 8 (2013) 1514–1525.
[57] R.A.A. Muzzarelli, R. Tarsi, O. Filippini, et al., Antimicrobial properties of *N*-carboxybutyl chitosan, Antimicrob. Agents Chemother. 34 (1990) 2019–2023.

EXPERT REVIEWS

Phage approved in food, why not as a therapeutic?

Expert Rev. Anti Infect. Ther. 13(1), 91–101 (2015)

Wessam A Sarhan and Hassan ME Azzazy*

Novel Diagnostics and Therapeutics Research Group, YJ-Science and Technology Research Centre, School of Sciences and Engineering, The American University in Cairo, AUC Avenue, SSE 1184, P.O. Box 74, New Cairo, 11835, Egypt.
**Author for correspondence:*
Tel.: +20 2 2615 2559
Fax: +20 2 2795 7565
hazzazy@aucegypt.edu

Bacterial resistance is not only restricted to human infections but is also a major problem in food. With the marked decrease in produced antimicrobials, the world is now reassessing bacteriophages. In 2006, ListShield™ received the US FDA approval for using phage in food. Nevertheless, regulatory approval of phage-based therapeutics is still facing many challenges. This review highlights the use of bacteriophages as biocontrol agents in the food industry. It also focuses on the challenges still facing the regulatory approval of phage-based therapeutics and the proposed approaches to overcome such challenges.

KEYWORDS: bacterial resistance • bacteriophages • food biocontrol products • phage therapy

In 1917, the term bacteriophage was first introduced by Felix d'Herelle who was also the first to test phage therapy. d'Herelle applied bacteriophages against livestock infections and even tested them on himself. It was then recognized that the same phenomenon was described by Twort in 1915 and by Hankin in 1896 in the Ganges River against *Vibrio cholerae* [1–3]. It was in the 1920s, when d'Herelle used bacteriophages for fighting different bacterial infections around the world that the discipline known as 'phage therapy' was introduced. Phage therapy rapidly developed globally and was used as the major antibacterial in many countries. Moreover, phage therapy also attracted the attention of many pharmaceutical companies including E.R. Squibb & Sons (Princeton, NJ, USA), Eli Lilly (Indianapolis, IN, USA) and Swan-Myers/Abbott laboratories, which produced commercial phage preparations [4]. However, because phage properties were poorly understood and well purified and characterized preparations were lacking, phage therapy resulted in variable outcomes and many specialists questioned its efficacy. With the introduction of antibiotics in the 1940s, bacteriophages were unable to stand against the miracle antibiotics [4]. However, during the past two decades, which witnessed the continuous rise in bacterial resistance together with alarming decrease in the production of new antibiotics, the Western world is actively revisiting the world of bacteriophages in different practical applications. An interest that has resulted in several companies developing phage-based products for food, agriculture, diagnostics and therapeutics (TABLE 1).

Bacteriophages: brilliant antibacterials

Bacteriophages are the most abundant microorganisms with an estimated number of 10^{30}–10^{32} phage particles. Humans are regularly exposed to bacteriophages in water and unprocessed food. Moreover, phages are present in the intestinal tract, saliva and in dental plaque. One milliliter of unpolluted water contains 2×10^8 phage particles [5,6].

Bacteriophages infect bacteria *via* two possible lifecycles: the lysogenic and the lytic. The infection begins with the adsorption of the bacteriophage onto the surface of the bacteria then the viral genetic material is injected into the cytoplasm. Lytic bacteriophages take immediate control of the biochemical machinery of the host cell to make new virions and the growth cycle ends by killing the host cell [7]. In contrast, temperate bacteriophages insert their genome into the chromosome of the host cell and remain in the dormant state until the bacteria is exposed to certain stimuli, which lead to initiation of the lytic cycle.

TABLE 2 illustrates attributes of bacteriophages that make them attractive antibacterial therapeutics [8,9]. It is relatively easy and inexpensive to find new phages against bacterial resistance compared with years and billions of dollars in case of antibiotic. Moreover, the ability of bacteriophages to kill pathogenic bacterial strains

 10.1586/14787210.2015.990383 ISSN 1478-7210

Table 1. List of some bacteriophage-based companies.

Company	Established	Ref.
Omnilytics (USA)	1954	[98]
Exponential Biotherapies (USA)	1994	[99]
Biophage Pharma (Canada)	1995	[100]
PhageTech (Canada)	1997	[101]
Intralytix (USA)	1998	[102]
Hexal Gentech (Germany)	1998	[103]
Phage Biotech (Israel)	2000	[104]
GangaGen (Bangalore, India; San Francisco, CA; Ottawa, Canada)	2000	[105]
PhageGen (Las Vegas, NV; previously Regma Bio Technologies of London)	2000	[106]
Phico Therapeutics (UK)	2000	[107]
Phage-Therapy (Tbilisi, Georgia)	2002	[108]
Ampliphi biosciences (Australia)	2002	[109]
Novolytics (UK)	2002	[110]
Technophage (Portugal)	2002	[111]
Enzobiotics/New Horizons Diagnostics (USA)	2003	[112]
Pherecydespharma (France)	2006	[113]

in situ through exponential growth of phage is significant for the treatment of chronic bacterial infections [8,10].

Rediscovering bacteriophages

Since the discovery of penicillin, antibiotic production is estimated at US$25 billion per year. The widespread and sometimes inappropriate use of antibiotics has contributed to the increased incidence of bacterial resistance. The overuse of antibiotics in animal feed has also contributed to antibiotic resistance. Many of the 17 antibiotic classes are used in animal feed. Although Europe has banned the use of antibiotics for promoting animal growth, it is still allowed in the USA [5].

In the USA, bacterial resistance costs the health-care system over US$20 billion every year, leading to over 8 million extra hospital days. Moreover, the social costs are over US$35 billion every year. In the EU, multidrug-resistant bacteria result in the death of nearly 25,000 patients annually and the associated economical burdens are postulated to be nearly 1.5 billion Euros annually [11].

Several antibiotic-resistant bacteria have been identified including methicillin-resistant *Staphylococcus aureus*, vancomycin-resistant *S. aureus* [8] and vancomycin-resistant *Enterococcus faecium* [11]. In 2010, a serious *Escherichia coli*-resistant strain was reported in India which carried a gene called NDM1 (New Delhi metallo-β-lactamase). This was the first report on spread of resistant strains in a community, as such incidences were restricted to hospitals [12]. The problem of bacterial resistance is further complicated with the marked decrease in introducing new antimicrobials. Major decrease in antibiotic development occurred over the past 25 years. From 2008 to 2012, only two antibiotics were under development [13,14], and from 2003 to 2007, only five antibiotics were underdevelopment compared with over 14 antibiotics back between 1983 and 1987 [14].

Applications of bacteriophages

Although the focus of Western countries on bacteriophages as an antibacterial has almost faded with the introduction of antibiotics, countries as the former Soviet Union with Georgia as the epicenter continued their studies on bacteriophages to treat serious and chronic infections [14].

In the 1980s, Smith and coworkers carried out several studies to assess the effectiveness of phage therapeutics against *E. coli* infections [15–17]. Many other reports evaluated bacteriophage therapeutic efficacy against different bacterial infections as *E. coli* [18], *Pseudomonas aeruginosa* [19], *Acinetobacter baumanii* [20], *Klebsiella pneumoniae* [21], *Vibrio vulnificus* [22], as well as Salmonella [23] in animal models. Other studies revealed phage therapeutic effectiveness against drug-resistant strains of bacteria, such as vancomycin-resistant *E. faecium* [24] and methicillin-resistant *S. aureus* [25]. More remarkably, phages were able to reach intracellular bacteria, such as *Mycobacterium tuberculosis* [26].

Another important property of bacteriophages is their ability to disperse biofilms, although it was observed that antibiotic use at subminimal concentrations could end in induction of biofilm formation [27,28]. Biofilms represent aggregation of cells either eukaryotic or prokaryotic. Such cells are surrounded by a matrix of extracellular polymeric substance. Bacteria found within biofilms possess increased resistance to antibiotics and biocides, where it may require 1000-times more of such agents to eradicate biofilm bacteria compared with free-living bacteria [28]. Bacteriophages, however, have proven ability to infect bacteria within biofilms [28]. Phage replication within the bacterial cells results in localized amplification in phage numbers. Phages then spread within the biofilm eradicating the bacteria producing the extracellular polymeric substance. Moreover, some bacteriophages have the ability to express or carry depolymerizing enzymes that can degrade extracellular polymeric substance [28]. Unfortunately, the chance of isolating a natural phage that shows both advantages is low. Thus, researchers are now engineering phages to express biofilm degrading enzymes [29]. Phage dispersing biofilms show strong potential not only on the therapeutic front but also at the industrial scale, where biofilms represent a continuous source of bacteria on different surfaces. It was shown also that phages and antibiotics are not mutually exclusive instead they could be synergistic, especially for managing biofilm infections [30,31].

Table 2. Comparison between phages and antibiotics as antibacterials.

Bacteriophages	Antibiotics
Very specific affecting only the targeted bacterial species with no disruption of normal flora therefore minimizing the possibility of secondary infections	Target both pathogenic microorganisms and normal microflora which may lead to serious secondary infections
Autodosing through replication at the site of infection (repeated administration may not be needed)	Metabolized and eliminated and do not accumulate at the site of infection
No serious side effects have been described Minor side effects may be due to the liberation of endotoxins from bacteria lysed *in vivo* by the phages	Multiple side effects, including allergies, intestinal disorders, secondary infections, adverse effects on the kidney and the liver
Phage-resistant bacteria are not resistant to other phages having a similar target range	Resistance to antibiotics extends over targeted bacteria
Finding new phages against developed bacterial resistance can be achieved in days	Developing a new antibiotic against antibiotic-resistant bacteria is a very lengthy and expensive process
Ability to clear biofilms	Limited ability of biofilm clearance

Many studies were done on the use of phage as a microbial control in food, including meat, poultry, fish, fruits and vegetables, both in the preharvest and postharvest (fresh and packaged foods) stages. Studies have been conducted on different stages in the food production chain, including also livestock decontamination, and sanitation of contact surfaces and equipment to control some of the most persistent foodborne pathogens in poultry including *Campylobacter jejuni* [32] and *Salmonella typhimurium* [33]. Phage was also applied in cattle and sheep against *E. coli* O157:H7 [34]. However, more studies are required to enhance the *in vivo* biotherapeutic effects of phages, including better understanding of the interactions between phage and bacteria in the gut and alimentary system of live animals [35].

Since the regulatory approval of ListShield™ as the first phage-based product for control of *Listeria* in products of meat and poultry, studies for phages targeting food (meat, fruits, vegetables, processed ready to eat [RTE] food, cheese, pasteurized milk, powdered infant formulas, etc.) in the postharvest stage have increased [36]. Guenther *et al.* (2009 and 2012) studied the effect of bacteriophages against *Listeria monocytogenes* and *S. typhimurium* in RTE foods, respectively [37,38]. Kim *et al.* (2007) reported the use of a phage cocktail against *Cronobacter sakazakii* in reconstituted infant formula [39]. Anany *et al.* (2011) immobilized anionic heads of phages on cationic cellulose membranes leaving the tails to catch and kill both *L. monocytogenes* and *E. coli* O157:H7 in RTE and raw meat [40].

Bacteriophages were also used as biocontrol agents in vegetables and fruits. Leverentz *et al.* (2001) used phage alone or in combination with bacteriocin to reduce *Salmonella* contamination in fresh cut fruits [41]. Whereas, Viazis *et al.* (2010) showed complete inactivation of *E. coli* O157:H7 strains in lettuce and spinach using a combination of phage mixture and trans-cinnamaldehyde oil [42]. In 2013, the combined use of bacteriophages with modified atmosphere packaging improved the effect of bacteriophages [43].

Several reviews have addressed successful bacteriophage applications in human therapy [44–46] and in food either in the preharvest or postharvest stages [47].

Phages approved as biocontrol agents in the food industry

The market of food and beverage was valued at US$5.7 trillion worldwide in 2008 and is expected to reach US$7 trillion in 2014 [5]. Food poisoning and spoilage due to bacterial contamination represent a major burden on health and food industry. The Centers for Disease Control estimated about 9.4 million cases of foodborne illnesses in addition to about 56,000 hospitalizations, and over 1350 deaths in the USA annually [48]. Moreover, microbial contamination is the major cause of food spoilage, which results in loss of 25% of food produced each year [49].

Due to the increase in bacterial resistance, together with the progress achieved in understanding phage biology and its applications, numerous companies worldwide are currently investing in developing phage-based products as food biocontrol agents, decontamination, sanitation and diagnostics.

In 2005, the US Environmental Protection Agency approved Agriphage™ (OmniLytics Inc., Sandy, UT) [50] for treating bacterial spots in different crops. In 2006, the FDA approved ListShield™ to be applied directly on RTE meat and poultry to control *L. monocytogenes* [51]. Thus, bacteriophages were for the first time considered generally recognized as safe (GRAS) [29]. Table 3 presents selected examples of using approved phage products in food.

In 2007, FDA approved phage-based preparations produced by Omnilytics to decontaminate live animals from *E. coli* and *Salmonella* [52]. Now, several products are commercially available including Finalyse spray against *E. coli* O157:H7 in cattle and Armament against *Salmonella* in poultry [47].

The future of phage-based products in the food industry shows tremendous promise, especially with the number of companies as well as research institutes actively engaged in phage

Table 3. FDA approved phage-based products for use in ready to eat food.

Product	Regulatory approval	Applications	Ref.
ListShield™ Intralytix, Inc. USA	US FDA (2006) and USDA for direct application onto foods (21 CFR 172.785.) EPA (EPA registration 74234-1)	– Ready to eat food: salami, sausage, basterami, etc. – Sea food – Food contact surfaces and enviroments	[114]
EcoShield Intralytix, Inc. USA	FDA (2011) cleared as 'Food Contact Notification' or FCN, (FCN No. 1018). FSIS Directive 7120.1 (safe and suitable antimicrobial)	– Red meat parts and trim intended to be ground	[115]
SalmoFresh Intralytix, Inc. USA	FDA (GRAS Notice No. GRN 000435), FSIS Directive the Star K-certified Kosher and IFANCA-certified Halal product. OMRI-listed suitable in the production of organic foods	– Poultry – Fish and shellfish – Fresh and processed fruits and vegetables	[116]
LISTEX™ Micreos EBI Food Safety Netherlands	In 2006 approved by the FDA as GRAS, and by the USDA in 2007 and by the EFSA, Health Canada, BAG (Switzerland) and FSANZ (Food Standards Australia New Zealand)	– Meat – Ready to eat meat – Fish – Cheese	[117]
Agriphage Omnilytics USA	EPA 2005 for use in agriculture	– In agriculture on fruits and vegetables	[118]

research. However, this is not the case for phage therapy in humans, where a number of challenges still impede its approval.

Phages not approved as therapeutics; challenges still in the way

Despite the long history of phage therapy in addition to its safety record, phages are still not approved by the FDA to be used as therapeutics. Back in the 1970s, 1980s and 1990s, the FDA revised the usage of phage preparations as therapeutics in human. At the time, phage phiX174 was applied *via* intravenous administration to patients with immunodeficiency such as those infected with HIV. In the 1970s, after the inclusion of phages in several vaccines, the FDA performed a safety review on phages and concluded that bacteriophages are safe and allowed the continued usage of the vaccines [7].

In 2008, the first phage Phase I clinical trial was approved by the FDA. The study evaluated the use of a phage preparation of eight phages against venous leg ulcers. The trial verified the safety of the phage cocktail preparation [53].

Despite the documented safety of bacteriophages, however, regulatory bodies have not approved its use as a therapeutic, although recently approving it in food. Such approval confirms that phage is safe for human consumption and thus represents a major step towards its approval as a therapeutic. Challenges that currently hinder regulatory approval of phage as human therapeutics as well as possible approaches to overcome them will be discussed (Figure 1).

Immunogenicity

Phage immunogenicity is a major challenge facing phage therapy, mainly because of its effects on phage pharmacokinetics and also because of the possible side effects, such as anaphylactic shocks. Phages are recognized as foreign antigens by mammalian hosts [54].

It was initially reported that the reticulo-endothelial system was responsible for the decrease in the concentrations of bacteriophages in the blood of mice [55]. Decades later it was proven that the liver played the major role in phage elimination with over 99% of the phages present in the circulatory system were phagocytosed by the liver [56]. Such elimination of phage by the reticulo-endothelial system, coinciding with lack of information on phage pharmacokinetics, has resulted in majority of phage applications being administered orally [57]. Consequently, despite the advantageous therapeutic effects of phages on systemic diseases, most studies to date were concerned with the treatment of non-systemic diseases, such as gastrointestinal, ear and wound infections [58]. Merril *et al.* [59] serially passed phages in animals to isolate mutants that were capable of staying longer in circulation and allowing enhanced systemic administration [59].

In addition to the interaction with the innate immune system, bacteriophages also stimulate the adaptive immune system and consequently the production of antibodies [60]. Less antigenic bacteriophages may be developed through phage displaying certain peptide ligands; Sokoloff and coworkers injected a T7-phage peptide display library in rats, and observed that phage displaying peptides with arginine or carboxy-terminal lysine residues protected against the complement-mediated inactivation of the bacteriophage by binding C-reactive protein, whereas human serum phages that displayed C-terminal tyrosine residues were resistant to inactivation [61].

Within this context, Kim *et al.* were the first to introduce PEGylation to bacteriophages to increase bacteriophages survival and efficacy [62]. Consistent with this, Molenaar *et al.* have shown that the incorporation of targeting ligands

increased the efficient delivery and specificity of the M13 phage to liver Kupffer and parenchymal cells [63]. S-radiolabeled M13 bacteriophage was chemically modified by conjugation of either succinate groups or galactose to the phage coat protein to facilitate the uptake of the phages by scavenger receptors and hepatic receptors, respectively. Although the main purpose of this study was to increase efficiency of *in vivo* panning of phage libraries, the same principle could be used for targeting other organs for therapeutic purposes [63].

Pharmacokinetics

The pharmacokinetic behavior of phages was only weakly addressed. Efficient pharmacokinetic data are required to support phage delivery *via* the bloodstream to achieve systemic effects. Phages replicate exponentially, interact and show different phenomena completely different from the chemical kinetics of conventional drugs [64]. Consequently, studying the pharmacokinetics of bacteriophages as antibacterial therapeutics necessitates knowledge of the infected host, the bacteriophage and the infecting bacteria as well as their complex interactions. Interestingly, through the process of infection and phage therapy, the growth of bacteria would lead to exponential growth of phages, unlike the conventional use of antibiotics [64]. Along this line, Dubos and coworkers treated mice that were infected intracerebrally with *Shigella dysenteriae* by administering phage into the peritoneal cavity [65]. Similar studies by Smith and Huggins demonstrated that mice infected either intracerebrally or intramuscularly with *E. coli* were rescued with phages *via* intramuscular administration [15]. In both the studies, the levels of the bacteriophages were highest in the infected tissues but then decreased as the bacterial levels decreased. On the other hand, phage levels in the blood of the control animals were in accordance with the phage dilution in the total blood of the animal. These data were used as the basis for mathematical models predicting the kinetic behavior of phages [64,66]. Several parameters should be considered to achieve effective phage therapeutics. These include the route and timing of administration and the required dose [64].

Systemic side effects

Lytic phages are the only phages that are used in therapy. First because they are more potent than the temperate phages, and second because temperate phages have the risk of transferring fragments of the DNA of the host to other bacterial species, thus posing the risk of producing virulent strains if such fragments were toxin encoding or antibiotic-resistant genes.

No reports have been recorded of serious complications accompanying phage therapy. Moreover, humans are in continuous exposure to bacteriophages, as they are so common in the environment. For example, unpolluted water contains ca. 2×10^8 (phage/ml), and phages are continuously consumed in foods [44].

Safety of bacteriophages was proved through different studies where bacteriophage did not cause adverse effects in humans [67,68]. However, there are concerns that any lytic bacterial treatment will generate endotoxins and superantigens that may be released during the massive and fast destruction of bacteria *in vivo* [58]. Although this possibility may be low, engineered phages that are either lysis deficient or non-replicative have been developed. For example, filamentous phages were engineered to express certain toxic genes in *E. coli* leading to bacterial toxicity but not their lysis, thus overcoming the problem of endotoxins [69]. Non-lytic and non-replicative phages were also designed against *P. aeruginosa* [70]. Interestingly, in both the studies, it was observed that the non-lytic phages increased the survival of treated infected mice compared with lytic phages, which may have been caused by reduced inflammation.

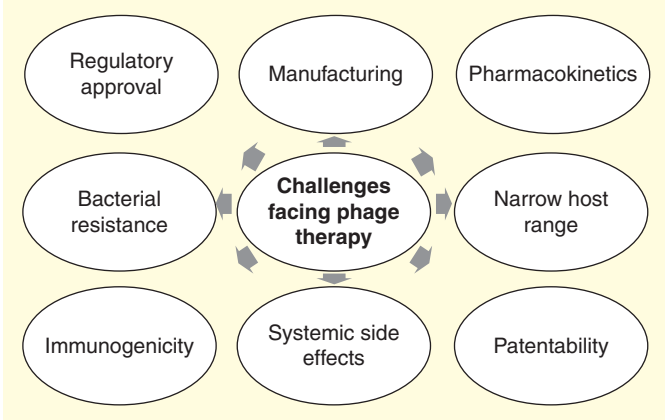

Figure 1. Challenges facing phage therapy.

It is also important to ensure that bacteriophages for therapy do not carry gene sequences that possess significant similarity with antibiotic-resistance genes, genes for other bacterial virulence factors and genes for phage-encoded toxins. Moreover, phages should be also incapable of generalized transduction [47]. A number of quality assurance and quality control measures to consider are described in Merabishvili *et al.* (2009) [71].

Narrow host range

Each phage strain infects only one type of bacteria. The downside of such narrow host range is the limited applicability in cases where the identification of the specific bacterial host cannot be achieved [7]. However, with the tremendous developments of rapid diagnostics, identifying the specific bacterial host is easily achieved. In most situations, however, bacteriophage cocktails are used to broaden the host range and increase the overall therapeutic efficiency. It is unlikely, however, to achieve 100% therapeutic efficiency [7,58]. Thus, the use of single phages versus cocktails of phages has to be further studied and optimized as both regimens may lead to the development of resistance [72]. Nevertheless, as will be discussed later, approval of phage cocktails is problematic, thus other methods have also to be developed. Using broad host spectrum bacteriophages, such as *Listeria* P100 or *S. aureus* phi812 was proposed [73,74]. Also, broad host range could be achieved *via*

grafting the g3p phage protein of one filamentous bacteriophage to another [75,76]. Such an approach, however, although would broaden the host range of the engineered bacteriophage and would facilitate its patentability, may also complicate its regulatory approval. Moreover, safety of such engineered phages has not been thoroughly studied, especially that such engineered phages may increase the probability of phage-mediated transfer of genetic sequences among bacterial species [77].

Developing clinical diagnostics to allow rapid identification of the infective bacterial pathogen as well as their phage susceptibility may be necessary to allow the use of the required phage instead of phage cocktails. These phage-based diagnostics should be fast and reliable [78].

Along this line, Loessner and coworkers [78] developed luciferase reporter bacteriophages for the sensitive and fast detection of viable cells of *Listeria*. In addition, diagnostic tests that utilized phage enzyme lysins have been developed allowing rapid bacterial identification and have resulted in commercialized products (Enzobiotics; Columbia, MD, USA) [9].

Bacterial resistance

Bacteriophages are the most abundant and diverse microorganisms on the planet. Such diversity is due to the continuous adaptation to different pressures. Bacteriophages have evolved different mechanisms that enable it to avoid, withstand and get over different mechanisms of bacterial resistance [79]. It was found that in monoculture studies performed *in vitro*, phage resistance can evolve within hours or days [58]. However, it was observed that bacteria develop phage resistance *in vitro* more rapidly than *in vivo* [80]. Thus, the correlation between the rate of resistance development *in vivo* and *in vitro* is an area that requires further study.

The exposure of a certain bacterial strain to a single bacteriophage is suggested to aid in the emergence of phage-resistant strains of the bacteria. On the other hand, several studies report that phage cocktails help control or delay the evolution of phage-resistant strains [72,81,82]. Reduction of appearance of resistant bacterial strains can be achieved using new techniques, such as using combinations of bacteriophages with other antimicrobials (such as antibiotics or antimicrobial herbal extracts), cycling bacteria through mixtures of different phages and targeting phage-resistance mechanism by genetically engineered bacteriophages [58].

In this context, additional studies are needed to identify phage receptors and understanding the interaction of bacteriophages with the receptors on the host surface. Until now, except for *E. coli,* very few phage receptors have been identified [79]. Moreover, the evolution of phages in response to the mutations in the host surface receptors needs to be investigated. Finally, the environment in which phage-resistance mechanisms are studied need to be translated from a closed laboratory environment with single phage at a time to a more real complex environment containing multiple anti-phage barriers [79].

Manufacturing; (safety & efficacy)

In the past, and in Russia until now, phages have been administered to humans: orally, either in tablets or liquid formulations (10^5 to 10^{11} PFU/dose); locally to the skin, ear or eye in the form of creams, tampons and rinses; rectally; as aerosols; as intrapleural injections; and intravenously [45]. Still, there are two critical factors that need to be standardized during bacteriophage manufacturing, which are safety and efficacy. Inability to optimize these factors may have been responsible for the recorded negative results of phage therapy. Efficacy of the phage preparation reflects the presence of sufficient virulent phages, especially against the target bacteria [83]. Poor viability and/or stability of phage preparations may result from improper manufacturing techniques. Therefore, in some early commercial phage preparations, mercurials and oxidizing agents as well as heat treatments were used to ensure bacterial sterility. Nevertheless, such treatments may result in ineffective preparations due to phage inactivation. However, advanced manufacturing techniques are now utilized for phage purification. Moreover, determination of the phage titer and viability is essential [83].

Safety on the other hand is a very important parameter, as issues related to the presence of exotoxins and pyrogens released during bacterial lysis by bacteriophages have always raised serious safety concerns. Consequently, bacteriophage manufacturing for clinical use must be optimized to eliminate bacterial exotoxins and pyrogens [60]. Early therapeutic phage preparations suffered from inefficient purification resulting in crude lysates of the host bacteria in the preparation [84]. Efficient purification can be achieved by ammonium sulfate precipitation and also by CsCl gradient centrifugation [84]. Ultrafiltration and two-step chromatography were also used [84]. However, the purification procedures have witnessed considerable evolution in the past few years. Recently, Kramberger and coworkers [85] utilized methacrylate monoliths columns in *S. aureus* phage purification from a lysate of bacterial cells. This method resulted in recovery of 60% of viable phages in a single purification step [85]. In this context, Gill and Haymen, published an interesting review exploring the different available methods for bacteriophage purification as well as the different levels of purification required for different applications together with the current protocols utilized in the commercial production of different products of phage therapy [83]. Standard purification techniques should be developed to achieve clinical grade bacteriophage preparations.

Regulatory approval

Despite the successful application of phage therapy for decades in some eastern countries such as Poland and the former Soviet republics, especially Georgia and Russia [86], their clinical data failed to gain regulatory approval because such data were not developed under the regulatory authorities frameworks.

A major hurdle in the way of phage becoming part of the mainstream medicine is the absence of well-defined guidelines for regulatory approval of phage. Instead, phage is regulated according to existing guidelines developed for typical

antibacterials [7], meaning that every component of the therapeutic cocktail of phages must undergo individual clinical trials and that the composition of the approved phage cocktail cannot be changed without re-approval. Such regulations do not take into consideration the differences between phages and antibiotics. Fortunately, there exists a regulatory framework that could be applied for phage therapy, which is that of the influenza live-virus vaccine. Such a vaccine is formulated from a cocktail of three or four influenza strains that the FDA has approved to be reformulated annually according to the circulating flu strain [7].

However, with the recent approval of different phage preparations in food and agriculture together with the approval of some clinical trials, the situation may be improving. Recently some Phase I studies have been carried out and published [87], whereas others are being conducted but to date have not been published [53]. In 2009, Biocontrol Ltd Company (Nottingham, UK) has completed randomized, double-blind, placebo-controlled, fully regulated Phase II clinical trial for phage therapy against *Pseudomonas* infections in the western world [54]. Another FDA-approved Phase I clinical trial in 2008 used phage to target *P. aeruginosa, E. coli*, and *S. aureus* in venous ulcers [87].

An important approach that should be considered by the regulatory authorities is regulating phages for the 'pharmacy approach'. The approach allows phage cocktails to be custom made by licensed hospital pharmacists from current Good Manufacturing Practice phage preparations instead of all hospitals using the same preparations [7].

In Europe, and pending resolution of regulatory issues, phage therapy is used under the supervision and responsibility of medical ethical committees within the approval of the World Medical Association Declaration of Helsinki [88,89]. This is only a temporary solution that will not result in efficient introduction of phage therapy into the western or the rest of the world [53].

Patentability

Recently, a patent by Heo and coworkers was granted and was based on bacteriophage MPK6, a novel bacteriophage belonging to the order Caudovirales, and its pharmaceutical composition for treating *P. aeruginosa* [90,91]. The issue of phage patentability resembles that of patenting monoclonal antibodies, where in both cases a wide array of potential targets exist and the methodology for their discovery is common knowledge. Individual bacteriophages are patentable where they can be put under the Budapest treaty in an approved collection [92]. However, in both the cases, there are always other agents (either antibodies or phages) that can be discovered, isolated and optimized to formulate even more efficient bacteriophage preparations [53]. The European patent laws allow patenting of known phages provided that the use of these phages has not been disclosed [93]. Moreover, the new phage formula can be patented [53]. The European patent office necessitates a certain technical intervention for isolating phage from its natural environment, as well as proper characterization of the isolated phage. For the US Patent and Trademark Office, however, only genetically engineered bacteriophages can meet the patent regulations. Several patents, however, have been granted by the US patent office, including a patent for reduction of sepsis with a pharmaceutical preparation including bacteriophages, as well as other patents approved for using phage in the food sector. A detailed discussion of patent issues related to therapeutic use of phage is described elsewhere [93–95].

Expert review

The regulatory approval of phage consumption in food provides a validation for its safety for humans. Thus, the main hurdles still facing the regulatory approval of phage as therapeutics include the need for more clinical evidence for its therapeutic efficacy as well as new or modified regulatory guidelines. Such clinical evidence must be supported by detailed data on phage immunogenicity, pharmacokinetics and formulations.'

Some approaches for overcoming the challenges that hinder the approval of such an important therapeutic are discussed below.

- Bacteriophages act as exogenous antigens inducing a humoral reaction due to the presence of immunogenic epitopes in phage proteins [64]. Masking or modifying these recognition epitopes is needed to improve phage blood circulation and decrease immunogenic response. Chemical modification through PEGylation of the bacteriophages and/or addition of biocompatible moieties can be used to improve phage pharmacokinetics and decrease its immunogenicity [61,63].
- Phage pharmacokinetics. The basic kinetic principles of self-replicating phages have been recently addressed in a number of important studies [7,64] which will allow better experimental design and data interpretation. There is still a need to develop kinetic models describing the density dependent bacteria–phage interactions [8].
- Optimization of the formulation and long-term stability. A small-scale quality controlled production of defined bacteriophage cocktail for use in human was developed and resulted in approved clinical trials [71].
- The approval of phage in food (Table 1) should motivate researchers and the pharmaceutical industry to pursue more clinical evidence for its therapeutic efficacy and to work with the regulatory agencies to develop new guidelines for phage therapy. This is now important with the alarming rise of bacterial resistance and the low number of new antibiotics introduced [86].

Five-year view

The application of bacteriophages in different food sectors is expected to increase supported by the regulatory approval of different phage products (Table 1).

With the alarming increase in bacterial resistance together with the decreased number of new antibiotics, the current regulatory guidelines may be modified in favor of phage therapy.

Developing specific and simple tests that allow rapid identification of the causative bacterial strain as well as their phage

susceptibility is one of the major areas that will aid in phage adoption as therapeutics. Along this line, nano-based tests will be one of the fast developing areas in the upcoming years [96]. It is expected that stable phage formulations alone or with other antibiotics or natural antibacterials may be developed with the aid of novel nanomaterials [97].

Financial & competing interests disclosure

W Sarhan and H Azzazy are authors of a patent application describing the use of nanofibers and phage for wound healing. The authors have no other relevant affiliations or financial involvement with any organization or entity with a financial interest in or financial conflict with the subject matter or materials discussed in the manuscript apart from those disclosed.

Key issues

- In 2011, the WHO has made the call 'No action today, no cure tomorrow' raising the need for immediate solutions against the serious problem of bacterial resistance.
- Phage holds a substantial antibacterial potential as a therapeutic and a bio-control agent in food.
- In 2006, US FDA approved the first phage product to be applied directly to ready-to-eat meat.
- Different challenges are still in the way for approval of phage therapy, such as: immunogenicity, pharmacokinetics, systemic side effects, narrow host range, bacterial resistance, manufacturing safety and efficacy, regulatory approval and patentability.
- The regulatory approval for phage consumption in food should motivate the pharmaceutical industry and scientific community for developing bacteriophage therapeutics.

References

Papers of special note have been highlighted as:
• of interest
•• of considerable interest

1. Hankin M. L'action bactericide des eaux de la Jumna et du Gangesur le vibrion du cholera. Ann Inst Pasteur 1896;10:511-23
2. Twort F. An investigation on the nature of ultra microscopic viruses. Lancet 1915;186: 1241-3
3. D'Herelle F. Sur un microbe invisible antagoniste des bacillus dysenteriques. ComptesRendus Acad Sci 1917;165:373-5
4. Monk A, Rees C, Barrow P, et al. Bacteriophage applications: where are we now? Lett Appl Microbiol 2010;51:363-9
5. Endersen L, O'Mahony J, Hill C, et al. Phage Therapy in the Food Industry. Ann Rev food sci. & technol 2014;5:327-49

•• **An important review, illustrating the use of whole and modified phages as well as their derivatives in both the preharvest and postharvest stages of the food production. The review also highlights some safety concerns required to ensure the safety and efficacy of phage preparations.**

6. Barr JJ, Auro R, Furlan M, et al. Bacteriophage adhering to mucus provide a non-host-derived immunity. Proc Natl Acad Sci USA 2013;110:10771-6
7. Sulakvelidze A. The challenges of bacteriophage therapy. Eur Ind Pharm 2011;10:14-18
8. Ryan E, Gorman S, Donnelly R, Gilmore BF. Recent advances in bacteriophage therapy: how delivery routes, formulation, concentration and timing influence the success of phage therapy. J pharm pharmacol 2011;63:1253-64
9. Thiel K. Old dogma, new tricks—21st Century phage therapy. Nature Biotechnol 2004;22:31-6

• **A very interesting paper, in simple language describing phage, the challenges it is still facing as well as good illustration of the key market players in phage therapy.**

10. Merabishvili M, De Vos D, Verbeken G, et al. Selection and characterization of a candidate therapeutic bacteriophage that lyses the Escherichia coli O104:H4 strain from the 2011 outbreak in Germany. PLoS One 2012;7:e52709
11. Leung E, Weil D, Raviglione M, Nakatani EH. The WHO policy package to combat antimicrobial resistance. Bull World Health Organ 2011;89:390-2
12. Brain T. Race against time to develop new antibiotics. Bull World Health Organ 2011;89:88-9
13. Gravitz L. Turning a new phage. Nature Med 2012;18:1318-20
14. Spellberg B, Guidos R, Gilbert D, et al. The epidemic of antibiotic-resistant infections: a call to action for the medical community from the Infectious Diseases Society of America. Clin Infect Dis 2008;46:155-64
15. Pirnay JP, Verbeken G, Rose T, et al. Introducing yesterday's phage therapy in today's medicine. Future Virol 2012;7: 379-90
16. Smith H, Huggins M. Effectiveness of phages in treating experimental Escherichia coli diarrhoea in calves, piglets, and lambs. J Gen Microbiol 1983;129:2659-75
17. Smith H, Huggins M, Shaw K. Factors influencing the survival and multiplication of bacteriophages in calves and in their environment. J Gen Microbiol 1987;133: 1127-35
18. Chibani-Chennoufi S, Sidoti J, Bruttin A, et al. In vitro and in vivo bacteriolytic activities of Escherichia coli phages: implications for phage therapy. Antimicrob Agents Chemother 2004;48:2558-69
19. Ahmad S. Treatment of post-burns bacterial infections by bacteriophages, specifically ubiquitous Pseudomonas spp. notoriously resistant to antibiotics. Med Hypotheses 2002;58:327-31
20. Soothill J. Treatment of experimental infections of mice with bacteriophages. J Med Microbiol 1992;37:258-61
21. Bogovazova G, Voroshilova N, Bondarenko V. Immuno-biological properties and therapeutic effectiveness of preparations from Klebsiella bacteriophages. Zh Mikrobiol Epidemiol Immunobiol 1992;3.30-3
22. Cerveny K, DePaola A. Duckworth D, Gulig PA. Phage therapy of local and systemic disease caused by Vibrio vulnificusin iron-dextran-treated mice. Infect Immun 2002;70:6251-62
23. Toro H, Price S, McKee A, et al. Use of bacteriophages in combination with competitive exclusion to reduce Salmonella from infected chickens. Avian Dis 2005;49: 118-24

24. Biswas B, Adhya S, Washart P, et al. Bacteriophage therapy rescues mice bacteremic from a clinical isolate of vancomycin-resistant Enterococcus faecium. Infect Immun 2002;70:204-10

25. Matsuzaki S, Yasuda M, Nishikawa H, et al. Experimental protection of mice against lethal Staphylococcus aureus infection by novel bacteriophage. J Infect Dis 2003;187: 613-24

26. Broxmeyer L, Sosnowska D, Miltner E, et al. Killing of Myco-bacterium avium and Mycobacterium tuberculosis by a Mycobacteriophage Delivered by a Nonvirulent Mycobacterium: a Model for Phage Therapy of Intracellular Bacterial Pathogens. The J Infec. Dis 2002;186: 1155-60

27. Kaplan JB. Antibiotic-induced biofilm formation. Int J Artif Organs 2011;34: 737-51

28. Harper DR, Parracho HM, Walker J, et al. Bacteriophages and Biofilms. Antibiotics 2014;3:270-84

29. Lu T, Collins J. Engineered Bacteriophage Targeting Gene Networks as Adjuvants for Antibiotic Therapy. Proc Natl. Acad Sci 2009;106:4629-34

30. Comeau AM, Tetart F, Trojet SN, et al. Phage-antibiotic synergy (PAS): beta-lactam and quinolone antibiotics stimulate virulent phage growth. PLoS One 2007;2:e799

31. Ryan EM, Alkawareek MY, Donnelly RF, et al. Synergistic phage–antibiotic combinations for the control of Escherichia coli biofilms in vitro. FEMS Immunol. Med Microbiol 2012;65:395-8

32. El-Shibiny A, Scott A, Timms A, et al. Application of a group II Campylobacter bacteriophages to reduce strains of Campylobacter jejuni and Campylobacter coli colonizing broiler chickens. J Food Prot 2009;72:733-40

33. Bardina C, Spricigo DA, Cortes P, Llagostera M. Significance of the bacteriophage treatment schedule in reducing Salmonella colonization in poultry. Appl Environ Microbiol 2012;78:6600-7

34. Raya RR, Oot RA, Moore-Maley B, et al. Naturally resident and exogenously applied T4-like and T5-like bacteriophages can reduce Escherichia coli O157:H7 levels in sheep guts. Bacteriophage 2011;1:15-24

35. Mills S, Shanahan F, Stanton C, et al. Movers and shakers: influence of bacteriophages in shaping the mammalian gut microbiota. Gut Microbes 2013;4:4-16

36. Zhang H, Wang R, Hongduo B. Phage inactivation of foodborne Shigella on ready-to-eat spiced chicken. Poult Sci 2013;92:211-17

37. Guenther S, Huwyler D, Richard S, Loessner MJ. Virulent bacteriophage for efficient biocontrol of Listeria monocytogenes in ready-to-eat foods. Appl Environ Microbial 2009;75:93-100

38. Guenther S, Herzig O, Fieseler L, et al. Biocontrol of Salmonella typhimurium in RTE foods with the virulent bacteriophage FO1-E2. Int J Microbiol 2012;154:66-72

39. Kim KP, Klumpp J, Loessner MJ. Enterobacter sakazakii bacteriophages can prevent bacterial growth in reconstituted infant formula. Int J Food Microbiol 2007;11:195-203

40. Anany H, Chen W, Pelton R, Griffiths MW. Biocontrol of Listeria monocytogenes and Escherichia coli O157: H7 in meat by using phages immobilized on modified cellulose membranes. Appl Environ.Microbiol 2011;77:6379-87

41. Leverentz B, Conway WS, Camp MJ, et al. Biocontrol of Listeria monocytogenes on fresh-cut produce by treatment with lytic bacteriophages and a bacteriocin. Appl Environ Microbiol 2011;69:4519-26

42. Viazis S, Akhtar M, Feirtag J, Diez-Gonzalez F. Reduction of Escherichia coli O157:H7 viability on leafy green vegetables by treatment with a bacteriophage mixture and trans-cinnamaldehyde. Food Microbiol 2010;28:149-57

43. Boyacioglu O, Sharma M, Sulakvelidze A, Goktepe I. Biocontrol of Escherichia coli O157:H7 on fresh cut leafy greens: using a bacteriophage cocktail in combination with modified atmosphere packaging. Bacteriophage 2013;3:e24620

44. Sulakvelidze A, Alavidze Z, Morris J. Bacteriophage Therapy. Antimicrob Agents And Chemot 2001;45:649-59

• **Mini review of phage therapy published literature in Eastern bloc countries from the early 1920s, including preclinical studies in animals as well as early problems of phage therapy research.**

45. Slopek S, Weber-Dabrowska B, Dabrowski M, Kucharewicz-Krukowska A. Results of bacteriophage treatment of suppurative bacterial infections in the years 1981–1986. Arch Immunol Ther Exp 1987;35:569-83

• **Summary of six papers of reports on phage therapy in humans from the period 1981–1986.**

46. Abedon ST, Kuhl SJ, Kutter EM. Phage treatment of human infections. Bacteriophage 2011;1:66-85

•• **An important review on early phage therapeutic trials in France along with the Polish, US, Georgian and Russian historical experiences. Also the review covers more recent therapeutic phage trials differentiated in terms of disease.**

47. Goodridge LD, Bisha B. Phage-based biocontrol strategies to reduce foodborne pathogens in foods. Bacteriophage 2011;1: 130-7

• **The review presents the current literature concerning the use of phage in bacterial decontamination of food as well as the food production environment.**

48. Scallan E, Hoekstra RM, Angulo FJ, et al. Foodborne illness acquired in the United States-major pathogens. Emerg Infect Dis 2011;17(1):7-15

49. Razzaghi-Abyaneh M, Shams-Ghahfarokhi M. Natural Antimicrobials in Food Safety and Quality, CABI Publ, Wallingford, UK; 2011

50. US Environ Prot Agency. Xanthomonas campestris pv. vesicatoria and Pseudomonas syringae pv. tomato specific bacteriophages; exemption from the requirement of a tolerance. Fed Regist 2005.70:16700-4. Available from: www.epa.gov/EPA-PEST/ 2005/December/Day-28/p24540.pdf [Last accessed on 5 Nov 2014]

51. Bren L. Bacteria-eating virus approved as food additive. FDA Consum 2007;41:20-2

52. Garcia P, Rodriguez L, Rodriguez A, Martinez B. Food biopreservation: promising strategies usingbacteriocins, bacteriophages and endolysins. Trends Food Sci Technol 2010;21:373-82

53. Parracho H, Burrowes B, Enright M, et al. The role of regulated clinical trials in the development of bacteriophage therapeutics. J mol genet med 2012;6:279-86

•• **An important review discussing the potential for the development of successful and acceptable bacteriophage therapy through optimizing research according to the critical aspects of modern, regulated clinical trials.**

54. Kaur T, Nafissi N, Wasfi O, et al. Immunocompatibility of Bacteriophages as Nanomedicines. J Nanotech 2012;2012:13. Article ID 247427, http://dx.doi.org/ 10.1155/2012/247427

55. Nungester W, Watrous R. Accumulation of bacteriophage in spleen and liver following

its intravenous inoculation. Proc Soc Exper Biol Med 1934;31:901-5

56. Inchley C J. The activity of mouse Kupffer cells following intravenous injection of T4 bacteriophage. Clin Exp Immunol 1969;5:173-87
57. Merril C, Scholl D, Adhya S. The prospect for bacteriophage therapy in Western medicine. Nat Rev Drug Dis 2003;2:489-97
58. Lu T, Koeris M. The next generation of bacteriophage therapy. Current Opinion in Microb 2011;14:524-31
59. Merril CR, Biswas B, Carlton R, et al. Long-circulating bacteriophage as antibacterial agents. Proc Natl Acad Sci USA 1996;93:3188-92
60. Miedzybrodzki R, Fortuna W, Weber-Dabrowska B, et al. A retrospective analysis of changes in inflammatory markers in patients treated with bacterial virus. Clin Exp Med 2009;9:303-12
61. Sokoloff A, Bock I, Zhang G, et al. The interactions of peptides with the innate immune system studied with use of T7 phage peptide display. Molec Ther 2000;2:131-9
62. Kim K, Cha J, Jang E, et al. PEGylation of bacteriophages increases blood circulation time and reduces T-helper type 1 immune response. Microb Biotechn 2008;1:247-57
63. Molenaar T, Michon I, de Haas S, et al. Uptake and processing of modified bacteriophage M13 in mice: implications for phage display. Virology 2000;293:182-91
64. Payne R, Jansen V. Pharmacokinetic principles of bacteriophage therapy. Clin Pharmacok 2003;42:315-25

- **An important paper explaining the pharmacokinetic behavior of phage therapy and the important parameters to be optimized for achieving phage therapy with known and improved pharmacokinetics.**

65. Dubos R, Straus J, Pierce C. The multiplication of bacteriophage in vivo and its protective effects against experimental infection with Shigella dysenteria. J Exp Med 1943;20:161-8
66. Levin B, Bull J. Phage therapy revisited: the population biology of a bacterial infection and its treatment with bacteriophage and antibiotics. Am Nat 1996;147:881-98
67. Sarker S A, McCallin S, Barretto C, et al. Oral T4-like phage cocktail application to healthy adult volunteers from Bangladesh. Virology 2012;434:222-32
68. Bruttin A, Brussow H. Human volunteers receiving Escherichia coli phage T4 orally: a safety test of phage therapy. Antimicrob Agents and Chemother 2005;49:2874-8
69. Hagens S, Blasi U. Genetically modified filamentous phage as bactericidal agents: a pilot study. Lett Appl Microbiol 2003;37: 318-23
70. Hagens S, Habel A, von Ahsen U, et al. Therapy of experimental pseudomonas infections with a nonreplicating genetically modified phage. Antimicrob Agents Chemother 2004;48:3817-22
71. Merabishvili M, Pirnay J-P, Verbeken G, et al. Quality-controlled small-scale production of a well-defined bacteriophage cocktail for use in human clinical trials. PLoS One 2009;4:e4944
72. Hall AR, De Vos D, Friman VP, et al. Effects of sequential and simultaneous applications of bacteriophages on populations of Pseudomonas aeruginosa in vitro and in Wax Moth larvae. Appl Environment Microbiol 2012;78:5646-52
73. Pantucek R, Rosypalova A, Doskar J. The polyvalent staphylococcal phage phi 812: its host-range mutants and related phages. Virology 1998;246:241-52
74. Carlton R, Noordman W, Biswas B, et al. Bacteriophage P100 for control of Listeria monocytogenes in foods: genome sequence, bioinformatic analyses, oral toxicity study, and application. Regul Toxicol Pharmacol 2005;43:301-12
75. Marzari R, Sblattero D, Righi M, Bradbury A. Extending filamentous phage host range by the grafting of a heterologous receptor binding domain. Gene 1997;185: 27-33
76. Scholl D, Adhya S, Merril C. Escherichia coli K1's capsule is a barrier to bacteriophage T7. Appl Environ Microbiol 2005;71:4872-4
77. Moradpour Z, Ghasemian A. Modified phages: novel antimicrobial agents to combat infectious diseases. Biotechnol Adv 2011;29:732-8
78. Loessner M J, Rees CE, Stewart GS. SchererS. Construction of luciferase reporter bacteriophage A511:luxAB for rapid and sensitive detection of viable Listeria cells. Appl environ microbial 1996;62:1133-40
79. Labrie S, Samson J, Moineau S. Bacteriophage resistance mechanisms. Nature Rev Microb 2010;8:317-27
80. Capparelli R, Nocerino N, Lanzetta R, et al. Bacteriophage-Resistant Staphylococcus aureus Mutant Confers Broad Immunity against Staphylococcal Infection in Mice. PLoS One 2010;5:11720
81. Abuladze T, Li M, Menetrez M, et al. Bacteriophages reduce experimental contamination of hard surfaces, tomato, spinach, broccoli, and ground beef by Escherichia coli O157:H7. Appl Environ Microbiol 2008;74:6230-8
82. Kunisaki H, Tanji Y. Intercrossing of phage genomes in a phage cocktail and stable coexistence with Escherichia coli O157: H7 in anaerobic continuous culture. Appl Microbiol Biotechnol 2010;85:1533-40
83. Gill J, Hyman P. Phage choice, isolation, and preparation for phage therapy. Curr Pharm Biotechnol 2010;11:2-14
84. Skurnik M, Pajunen M, Kiljunen S. Biotechnological challenges of phage therapy. Biotechnol Lett 2007;29:995-1003
85. Kramberger P, Honour R, Herman R, et al. Purification of the Staphylococcus aureus bacteriophages VDX- 10 on methacrylate monoliths. J Virol Methods 2010;166:60-4
86. Kutter E, De Vos D, Gvasalia G, et al. Phage therapy in clinical practice: treatment of human infection. Curr Pharm Biotechnol 2010;11:69-86
87. Rhoads D, Wolcott R, Kuskowski M, et al. Bacteriophage therapy of venous leg ulcers in humans: results of a Phase I safety trial. J Wound Care 2009;18:237-8
88. Verbeken G, De Vos D, Vaneechoutte M, et al. European regulatory conundrum of phagetherapy. Future Microbiol 2007;2: 485-91
89. WMA Declaration of Helsinki. Ethical principles for medical research involving human subjects. Adopted by the18th WMA General Assembly, Helsinki, Finland, June 1964 and amended by the: 59th WMA General Assembly, Seoul, Korea, paragraph 32 October 2008
90. Heo YJ, Lee YJ, Jung HH, et al. Antibacterial efficacy of phages against Pseudomonas aeruginosa infections in mice and Drosophila melanogaster. Antimicrob Agents Chemoth 2009;53:2469-74
91. Heo Y J, Lee YR, Jung HH, Cho YH. Phage Therapy Against Pseudomonas Aeruginosa. US8282920; 2012
92. WIPO. Available from: www.wipo.int/ portal/en/index.html
93. Pirnay JP, Verbeken G, Rose T, et al. Introducing yesterday's phage therapy in today's medicine. Future Virology 2012;7: 379-90
94. Miedzybrodski B. Phage therapy current Research and Applications. Caister Academic Press 2014

95. Verbeken G, Pirnay J-P, De Vos D, et al. Optimizing the European regulatory framework for sustainable bacteriophage therapy in human medicine. Arch. Immunol Ther Exp 2012;60:161-72
96. Larguinho M, Baptista PV. Gold and silver nanoparticles for clinical diagnostics: from genomics to proteomics. J Proteomics 2012;75:2811-23
97. Dai M, Senecal A, Nugen SR. Electrospun water-soluble polymer nanofibers for the dehydration and storage of sensitive reagents. Nanotechnol 2014;25:225101; 8pp
98. Omnilytics. Available from: www.omnilytics.com/
99. Exponential Biotherapies. Available from: www.expobio.com/
100. Biophage Pharma. http:/www.biophagepharma.net/
101. PhageTech. Available from: www.phagetech.com
102. Intralytix. Available from: www.mtfalyt(X.com/
103. Hexal Gentech. Available from: www.hexal gentech.com
104. Phage Biotech. Available from: www.phagebiotech.com/
105. GangaGen. Available from: www,gangagen.com/
106. PhageGen. Available from: www.phagegen.com/
107. Phico Therapeutics. Available from: www.phicotfierapeutics.co.uk/
108. Phage-Therapy. Available from: www.phage-1herapy.com/
109. Ampliphi biosciences. Available from: www.ampliphibio.com/
110. Novolytics. Available from: www.novolytics.co.uk/
111. Technophage. Available from: www.technophage.pt
112. Enzobiotics/New Horizons Diagnostics. Available from: www.nhdiag.com/
113. Pherecydespharma. Available from: www.pherecydes-pharma.com
114. ListShield™ Intralytix, Inc. Available from: www.intralytix.com/Intral_Products_ListShield.htm
115. EcoShield Intralytix, Inc. Available from: www.intralytix.com/Intral_Products_EcoShield.htm
116. SalmoFresh Intralytix, Inc. Available from: www.intralytix.com/Intral_Products_SalmoFresh.htm
117. LISTEX™ Micreos EBI Food Safety. Available from: www.micreosfoodsafety.com/en/profile-mission.aspx
118. Agriphage Omnilytics. Available from: www.omnilytics.com/